BULLETIN OF THE EARTHQUAKE RESEARCH INSTITUTE,
UNIVERSITY OF TOKYO. Vol. 38, Part 1. March, 1960.

東京大学
地震研究所彙報

第 38 号　第 1 册

昭和 35 年 3 月

目　次

論文及報告

			頁
1.	非定常ダイナモ (1) (英文)	行武毅	1
2.	地震波のスペクトル構造—マグニチユードと卓越周期の関係—(英文)	松本利松	13
3.	電磁式地震計の理論的実験的研究 その1　電圧感度について (英文)	嶋悦三	29
4.	プロトン磁力計による箱根火山の磁気測量 (英文)	行武毅・棚岡巖	41
5.	北海道，十勝岳火山の泥流について (英文)	村井勇	55
6.	紀伊半島の局地地震 (第4報) — 臨時観測網による震源位置の決定 — (邦文)	宮村摂三	71
7.	紀伊半島南端部附近の地殻変動について (邦文)	岡田惇	113
8.	プロトン磁力計の試作研究 (続報) (邦文)	文部省科学試験研究費研究班 (代表者 力武常次)	125
9.	大地震前後の平均海水面変化について (英文)	山口生知	145

(The titles in occidental languages are given on the back cover.)

地震研究所彙報は，年4回定期に（ただし，第1号より第6号までは不定期に，第7号は3冊として刊行された），彙報別冊は不定期に刊行される．

この彙報に載せられた論文及び報告についての責任は，すべてその著者のみにある．

この彙報についての照会通信は，すべて東京大学地震研究所長にあてられたい．

The Bulletin is published quarterly. (Vols. 1–6 were published at irregular intervals and Vol. 7 consisted of three parts.)
Supplementary Volume is published at irregular interval.

The authors of the papers alone are responsible for the statements and opinions contained in their respective papers.

All communications relating to this Bulletin should be addressed to the Director of the Earthquake Research Institute, University of Tokyo, Japan.

Earthquake Research Institute, University of Tokyo
Address:
No. 1, Motofuji-cho, Bunkyo-ku,
Tokyo Metropolis, Japan.
Telephone: 921-3161-Extension 6506
Cable address: ZISINKEN, TOKYO.

東京大学地震研究所
所在地
東京都文京区本富士町一番地
電話 小石川 921—3161 (代) 構内 6506
電略 ブンケウ トウダイ ヂシン

BULLETIN OF THE EARTHQUAKE
RESEARCH INSTITUTE
Vol. 38 (1960), pp. 1-12

1. *Stability and Non-Steady State of Self-Exciting Dynamos. I.*

By Takesi YUKUTAKE,*

Graduate School, University of Tokyo.

(Read Nov. 24, 1959.—Received Dec. 24, 1959.)

Summary

Time-dependent behaviours of two conducting spheres rotating in an infinitely extended conductor are studied. Although it has been proved by Herzenberg that such a system works as a self-exciting dynamo, the steady state of it turns out to be unstable for small disturbances. In some special cases, a paradoxical result that the magnetic field continues its growth in spite of non-rotation of the spheres is obtained by the numerical integration of the non-linear simultaneous differential equations with the aid of a relay computer. This difficulty is caused by the crudeness of approximation for the electromagnetic coupling between the two spheres. If we improve this point, it seems likely that oscillatory fields and velocities could be found. It is intended to apply this study to investigations of the magneto-hydrodynamic actions which are supposed to be in the earth's core.

1. Introduction

The possibility of reversals of the earth's magnetic field is one of the most conspicuous suggestions from palaeomagnetic studies which have been flourishingly developing of late. In order to illustrate such reversals, a few theories have been put forward on the basis of homogeneous disk dynamo models. Bullard[1] studied a single homopolar dynamo and found particular oscillations of electric current and angular velocity but no reversal of the current. Rikitake[2] examined two disk dynamos that were coupled with one another and showed by numerical integration that the current could change its sign at the initial stage. Using a digital computer, Allan[3] confirmed such a reversal for a more extended

* Communicated by T. Rikitake.

1) E. C. BULLARD, *Proc. Camb. Phil. Soc.*, **51** (1955), 744.

2) T. RIKITAKE, *Proc. Camb. Phil. Soc.*, **54** (1958), 89.

3) D. W. ALLAN, *Nature*, **182** (1958), 469.

period of time. Since possible reversals of the earth's magnetic field have been demonstrated even by these simple systems of disk dynamos, it is desirable to study a more complicated model in order to have a better understanding of the dynamo action which is supposed to be prevailing in the earth's core.

Recently Herzenberg[4] has proved in a rigorous way that a system composed of two conducting spheres rotating in a large sphere, which is also conducting, works as a steady dynamo. Dr. Rikitake has suggested to the writer that it would be of importance and interest to study non-steady states of such a dynamo because Herzenberg's model would be more realistic than the disk dynamo models as far as its application to the magneto-hydrodynamic actions supposed in the earth's core is concerned.

In this paper the stability of a steady state of Herzenberg's model is examined and, in some particular cases, time-dependent behaviours of the system are traced by numerical calculation.

2. Equations

Suppose that two eddies, which are regarded as two conducting spheres of equal radius in this paper, are located in some favourable way, then it is possible for them to compose a system of self-exciting dynamo in an infinitely extended conductor which is assumed to stand still, the influence of the motion of eddies being ignored. It is intended here to study how these two eddies are connected electromagnetically with one another.

In the first place, induction due to the rotation of one sphere placed in a uniform magnetic field will be examined. The magnetic field induced by the rotation of a conducting sphere about an axis agreeing with the direction of the external uniform field (H) is of the toroidal type or T_2-type. The r, θ and φ components of such a field are written as

$$\boldsymbol{h}=\begin{bmatrix} 0 \\ 0 \\ -A(kr)^{-1/2}J_{5/2}(kr)\dfrac{dP_2(\theta)}{d\theta} \end{bmatrix}, \qquad r<a$$

$$=\begin{bmatrix} 0 \\ 0 \\ -B(kr)^{-1/2}Y_{5/2}(kr)\dfrac{dP_2(\theta)}{d\theta} \end{bmatrix}, \qquad r>a$$

4) A. HERZENBERG, *Phil. Trans. Roy. Soc. London*, **A**, **250** (1958), 543.

respectively for the inside and outside of the sphere, where $k^2=4\pi\sigma p$. The origin of the spherical coordinates (r, θ, φ) is taken at the centre of the sphere. σ denotes the electrical conductivity both inside and outside the sphere and p is the operational representation of $\partial/\partial t$.

On the other hand, we have the electric field induced by this field as follows,

$$\frac{1}{\sigma}\mathrm{rot}\,\boldsymbol{h}=\frac{1}{\sigma}\begin{bmatrix} 6Ar^{-1}(kr)^{-1/2}J_{5/2}(kr)P_2(\theta) \\ A\dfrac{1}{r}\dfrac{d}{dr}[r(kr)^{-1/2}J_{5/2}(kr)]\dfrac{dP_2(\theta)}{d\theta} \\ 0 \end{bmatrix}, \qquad r<a$$

$$=\frac{1}{\sigma}\begin{bmatrix} 6Br^{-1}(kr)^{-1/2}Y_{5/2}(kr)P_2(\theta) \\ A\dfrac{1}{r}\dfrac{d}{dr}[r(kr)^{-1/2}Y_{5/2}(kr)]\dfrac{dP_2(\theta)}{d\theta} \\ 0 \end{bmatrix}. \qquad r>a$$

At the boundary-surface of the sphere or $r=a$, the normal component of the magnetic flux density and the tangential component of the electric field should be continuous. Thus we have

$$AJ_{5/2}(ka)=BY_{5/2}(ka)\,,$$

$$\left[-3A\frac{1}{r}\frac{d}{dr}\{r(kr)^{-1/2}J_{5/2}(kr)\}\right]_{r=a}-4\pi\sigma\Omega Ha$$

$$=\left[-3B\frac{1}{r}\frac{d}{dr}\{r(kr)^{-1/2}Y_{5/2}(kr)\}\right]_{r=a},$$

where Ω represents the angular velocity of the sphere.

From these equations, we can determine the free constants A and B, so that the maximum component of the magnetic field (h_e) outside the sphere is easily obtained as

$$h_e=-\frac{2}{3}\pi^2\sigma\Omega Ha^2(ka)^{1/2}(kr)^{-1/2}J_{5/2}(ka)Y_{5/2}(kr)\,. \qquad (1)$$

In the case of a relatively slow change, ka and kr take small values, so that the Bessel functions involved can be replaced by a few terms of their ascending power series expressions. If we assume a sphere, 1000 *km* in radius, with a conductivity amounting to 10^{-6} *e.m.u.*, for example, the following may approximate (1) well so long as changes having a period larger than 2×10^4 *years* are considered.

$$h_e=\frac{2}{5}\pi\sigma a^5r^{-3}\left[1-\frac{4\pi\sigma a^2}{14}p+\frac{4\pi\sigma r^2}{6}p\right]\Omega H\,. \qquad (2)$$

The magnetic field thus produced is the strongest on the circle of $\theta=\pi/4$ on the sphere and penetrates into the outside of the sphere with its intensity weakening.

Let us next study the coupling between two spheres. Far away from one sphere (I), where the magnetic field (H_1) produced by its rotation may be regarded as uniform enough, the other sphere (II) is revolving as can be seen in Fig. 1. Its axis of rotation, which is nearly parallel to the field H_1, can be directed so as to let the direction of the field H_2 induced alike by sphere (II) almost coincide with the axis of sphere (I) and reinforce the original field assigned parallel to its rotational axis. If mechanical energy that makes the spheres rotate is supplied by some external force against the dissipation of energy due to Joule heat, the magnetic fields of each sphere are maintained by the above process. It should be noted, however, that if the field H_1 is completely parallel to the axis of sphere II, sphere I comes to be placed on the equatorial plane of sphere II where no field of H_2 can be induced, and *vice versa*. Therefore the axis of rotation should be slightly inclined against the direction of the field. In that case, some other components of magnetic field necessarily come out. According to the studies[5)6)] of electromagnetic induction by a rotating sphere, it has been proved that the fields induced in an asymmetric field do not grow infinitely however large the rotation speed is. It is then obvious that, by making the distance between the two spheres fairly large, only the fields induced in the field symmetric about the rotation axes become important, the other fields being possible to be ignored in an approximate study.

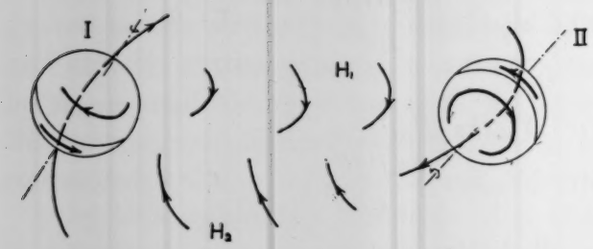

Fig. 1. A system of self-exciting dynamo.

In the light of the above discussion, it may be allowed to describe the behaviour of this system, using equation (2), as follows,

$$H_2(t)=-\frac{2}{5}\pi\sigma a^5 r^{-3}\left[\Omega_1(t)H_1(t)+4\pi\sigma\left(\frac{r^2}{6}-\frac{a^2}{14}\right)\frac{d}{dt}\{\Omega_1(t)H_1(t)\}\right], \quad (3)$$

$$H_1(t)=-\frac{2}{5}\pi\sigma a^5 r^{-3}\left[\Omega_2(t)H_2(t)+4\pi\sigma\left(\frac{r^2}{6}-\frac{a^2}{14}\right)\frac{d}{dt}\{\Omega_2(t)H_2(t)\}\right]. \quad (4)$$

5) E. C. BULLARD, *Proc. Roy. Soc.*, **A**, **199** (1949), 413.
6) A. HERZENBERG & F. J. LOWES, *Phil. Trans. Roy. Soc. London*, **A**, **249** (1957), 507.

Attention should be paid to the fact, however, that (3) and (4) are somewhat idealized. In an actual case, the righthand members should be multiplied by some factors less than unity according to the geometrical arrangement. We may therefore consider (3) and (4) as the relationship for the extreme case only.

When external torques G_1 and G_2 are being given to the spheres, we have the following equations of motion for this system,

$$C_1\frac{d\Omega_1}{dt}=G_1-\frac{8\pi}{75}\sigma a^5\Omega_1 H_1^2\,, \tag{5}$$

$$C_2\frac{d\Omega_2}{dt}=G_2-\frac{8\pi}{75}\sigma a^5\Omega_2 H_2^2\,, \tag{6}$$

where C_1 and C_2 represent the moments of inertia of the spheres I and II respectively. The second terms of the righthand side are the torques due to electro-magnetic coupling. Solving the above four equations (3), (4), (5) and (6) simultaneously, we may thoroughly observe how this system behaves.

Since it is too difficult to solve these non-linear simultaneous equations analytically, the only way to tackle them seems to make use of numerical calculation. In order to make variables dimensionless the following transformations are carried out.

$$\Omega=\mathfrak{O}\Omega'\,,\qquad t=\mathfrak{T}t'\,,\qquad H=\mathfrak{H}H'\,,$$

where $\mathfrak{O}=(\pi\sigma a^2)^{-1}$, $\mathfrak{T}=\pi\sigma a^2$, $\mathfrak{H}^2=G/a^3=C/\pi^2\sigma^2a^7$. Substituting these into the equations (3), (4), (5) and (6), and dropping primes, we have

$$\frac{dH_1}{dt}=-\left(\frac{3}{2}\varepsilon^2+\frac{1}{\Omega_1}\frac{d\Omega_1}{dt}\right)H_1-\frac{1}{\varepsilon}\frac{15}{4}\frac{H_2}{\Omega_1}\,, \tag{7}$$

$$\frac{dH_2}{dt}=-\frac{1}{\varepsilon}\frac{15}{4}\frac{H_1}{\Omega_2}-\left(\frac{3}{2}\varepsilon^2+\frac{1}{\Omega_2}\frac{d\Omega_2}{dt}\right)H_2\,, \tag{8}$$

$$\frac{d\Omega_1}{dt}=1-\frac{8}{75}H_1^2\Omega_1\,, \tag{9}$$

$$\frac{d\Omega_2}{dt}=1-\frac{8}{75}H_2^2\Omega_2\,, \tag{10}$$

where $\varepsilon=a/r$. For simplicity, it has been assumed that $C_1=C_2$ and $G_1=G_2$ in the above calculation. A set of solutions in the steady state is easily obtained as follows,

$$\left.\begin{aligned} \Omega_{10}&=-\frac{5}{2}\frac{1}{\varepsilon^3 q}\,, & H_{10}^2&=-\frac{15}{4}\varepsilon^3 q\,, \\ \Omega_{20}&=-\frac{5}{2}\frac{q}{\varepsilon^3}\,, & H_{20}^2&=-\frac{15}{4}\frac{\varepsilon^3}{q}\,, \end{aligned}\right\} \tag{11}$$

where q is defined by the equation

$$\left(\frac{H_1}{H_2}\right)^2=\frac{\Omega_2}{\Omega_1}=q^2\,.$$

3. Stability of the steady state

If the initial state is taken to be $H_2=-H_1$ and $\Omega_1=\Omega_2$, that is $q=-1$, the behaviours of the system I and II are quite the same, and therefore the steady state is given by

$$\Omega_0=\Omega_{10}=\Omega_{20}=\frac{5}{2}\frac{1}{\varepsilon^3}\,, \qquad H_0^2=H_{10}^2=H_{20}^2=\frac{15}{4}\varepsilon^3\,. \tag{12}$$

In this special case, equations (7), (8), (9) and (10) are reduced to the following,

$$\Omega\frac{dH}{dt}=-\left\{\frac{3}{2}\varepsilon^2(\Omega-\Omega_0)+\frac{d\Omega}{dt}\right\}H\,, \tag{13}$$

$$\frac{d\Omega}{dt}=1-\frac{H^2\Omega}{H_0^2\Omega_0}\,. \tag{14}$$

On the assumption that the magnetic field and the angular velocity deviates a little from the steady state, let us first examine whether those deviations will grow or decay. Let the magnetic field and angular velocity be

$$H=H_0+h\,, \qquad \Omega=\Omega_0+\omega\,,$$

where h and ω are small departures from the steady state. Substituting these into equations (13) and (14) and ignoring the products of these small quantities, we have,

$$\frac{dh}{dt}=\frac{2}{\Omega_0}h-\frac{H_0}{\Omega_0}\left(\frac{3}{2}\varepsilon^2-\frac{1}{\Omega_0}\right)\omega\,,$$

$$\frac{d\omega}{dt}=-\frac{2}{H_0}h-\frac{1}{\Omega_0}\omega\,.$$

Provided h and ω are proportional to $e^{\lambda t}$, two roots of λ are easily obtained from the above equations,

$$\lambda=\frac{1}{2\Omega_0}\{1\pm\sqrt{1+12\varepsilon^2\Omega_0}\}\ , \tag{15}$$

of which one is positive real and the other negative real. The existence of a positive real root indicates that the steady state expressed by (12) is unstable for small disturbances. It is therefore doubtful that the steady state of the dynamo investigated by Herzenberg[4] lasts over a long period.

When a departure from the steady state is considerable, we cannot examine the behaviour of this system by the above small perturbation method. It may readily be understood that the initial state of the system will play an important role in the determination of the variation in the magnetic field and the change in the angular velocity. Let the deviations from the steady state, regarded as appreciable at the initial stage, be H_i and Ω_i, then the magnetic field and the angular velocity are written as

$$H=H_0+H_i+h\ , \qquad \Omega=\Omega_0+\Omega_i+\omega\ ,$$

where h and ω are small quantities of the first order which vary with time. Substituting these into equations (13) and (14), we have the following equations by ignoring the products of h and ω,

$$\begin{aligned}\frac{dh}{dt}&=A+Bh+C\omega\ ,\\ \frac{d\omega}{dt}&=D+Eh+F\omega\ ,\end{aligned} \tag{16}$$

where

$$A=-\frac{H_0+H_i}{\Omega_0}\left\{\frac{3}{2}\varepsilon^2\Omega_0(1-y)+y-x^2\right\}\ ,$$

$$B=-\frac{1}{\Omega_0}\left\{\frac{3}{2}\varepsilon^2\Omega_0(1-y)+y-3x^2\right\}\ ,$$

$$C=-\frac{H_0+H_i}{\Omega_0}\left(\frac{3}{2}\varepsilon^2-\frac{1}{\Omega_0}\right)y^2\ ,$$

$$D=\frac{1}{y}(y-x^2)\ ,$$

$$E=-\frac{2}{H_0+H_i}\frac{x^2}{y}\ ,$$

$$F=-\frac{x^2}{\Omega_0}\ ,$$

$$x^2=\frac{(H_0+H_i)^2}{H_0^2}\,,$$

$$y=\frac{\Omega_0}{\Omega_0+\Omega_i}\,.$$

From these the following equations are obtained.

$$\begin{aligned}&\frac{d^2h}{dt^2}-(B+F)\frac{dh}{dt}+(BF-CE)h+AF-CD=0\,,\\&\frac{d^2\omega}{dt^2}-(B+F)\frac{d\omega}{dt}+(BF-CE)\omega+BD-AE=0\,,\end{aligned}\tag{17}$$

where

$$B+F=-\left(\frac{3}{2}\varepsilon^2-\frac{2x^2}{\Omega_0}\right)+\left(\frac{3}{2}\varepsilon^2-\frac{1}{\Omega_0}\right)y\,,$$

$$BF-CE=\frac{3x^2}{\Omega_0}\left\{\left(\frac{3}{2}\varepsilon^2-\frac{3x^2}{\Omega_0}\right)-\left(\frac{3}{2}\varepsilon^2-\frac{1}{\Omega_0}\right)y\right\}\,,$$

$$AF-CD=\frac{H_0+H_i}{\Omega_0}\left\{\left(\frac{3}{2}\varepsilon^2-\frac{1}{\Omega_0}\right)(y-x^2)^2-\frac{3}{2}\varepsilon^2x^2(x^2-1)\right\}\,,$$

$$BD-AE=-\frac{3}{2}\varepsilon^2(1-y)\left(1+\frac{x^2}{y}\right)-\frac{y}{\Omega_0}\left(1-\frac{x^2}{y}\right)^2\,.$$

It should be noticed that the last terms in the equations (17) do not appear in the case of the previous small perturbation method. These depend only on the initial state of the system and have effects of a kind of an external force exerting the system as in the case of a forced oscillation. This may be understood when we consider that at such a state the couples produced electromagnetically by the magnetic field do not balance themselves with the external torque accelerating the sphere, which consequences to reinforce or diminish the magnetic field and the angular velocity.

The solutions of the equations (17) are,

$$h=h_s+Me^{\xi t}+Ne^{\eta t}\,,$$

$$\omega=\omega_s+Pe^{\xi t}+Qe^{\eta t}\,,$$

where ξ and η denote the solution of homogeneous equations of (17) and

$$h_s=\frac{H_0+H_i}{\Omega_0}\left\{\frac{3}{2}\varepsilon^2x^2(x^2-1)-\left(\frac{3}{2}\varepsilon^2-\frac{1}{\Omega_0}\right)(y-x^2)^2\right\}\,,$$

$$\omega_s=\frac{3}{2}\varepsilon^2(1-y)\left(1+\frac{x^2}{y}\right)+\frac{y}{\Omega_0}\left(1-\frac{x^2}{y}\right)^2\,.$$

When both of ξ and η have negative real part, h and ω approach the values h_s and ω_s respectively. Therefore if h_s and ω_s are equal to zero, the state in question is one of the stable steady states. Or otherwise, it may be regarded as unstable, so long as h_s and ω_s take some definite values even if real parts of ξ and η are negative.

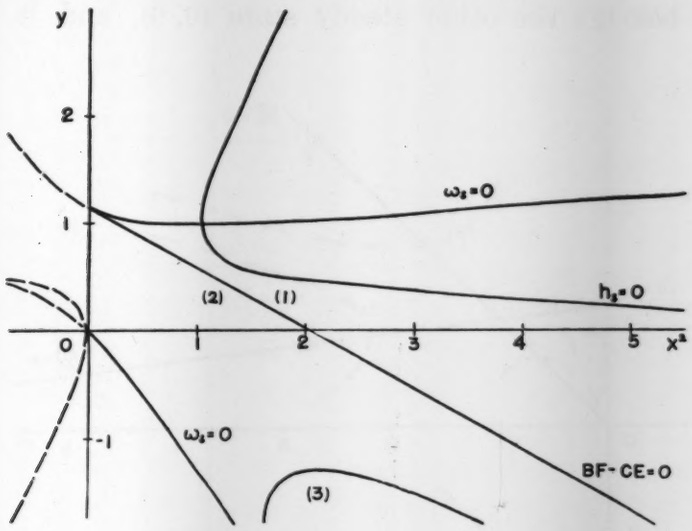

Fig. 2. Ordinate: $y=\frac{\Omega_0}{\Omega_0+\Omega_i}$, Abscissa: $x^2=\left(\frac{H_0+H_i}{H_0}\right)^2$
$\varepsilon=1/10^{\frac{1}{3}}$,
Region 1: $\xi>0$, $\eta<0$.
Region 2: $\xi<0$, $\eta<0$.
Region 3: ξ and η are complex.

In Fig. 2 curves of zero lines of h_s and ω_s are shown. The steady states are represented by the intersection points of these curves, *i.e.*, $x^2=1$, $y=1$ and $x^2=0$, $y=0$.

Provided that

$$\left\{\left(\frac{3}{2}\varepsilon^2-\frac{4x^2}{\Omega_0}\right)-\left(\frac{3}{2}\varepsilon^2-\frac{1}{\Omega_0}\right)y\right\}^2+\frac{8x^2}{\Omega_0}\left(\frac{3}{2}\varepsilon^2-\frac{1}{\Omega_0}\right)y<0\,,$$

which is shown in Fig. 2 as the inner range of a hyperbola (3), ξ and η become complex. In this range h and ω are oscillatory with diminishing amplitudes and tend to h_s and ω_s. When

$$\left\{\left(\frac{3}{2}\varepsilon^2-\frac{4x^2}{\Omega_0}\right)-\left(\frac{3}{2}\varepsilon^2-\frac{1}{\Omega_0}\right)y\right\}^2+\frac{8x^2}{\Omega_0}\left(\frac{3}{2}\varepsilon^2-\frac{1}{\Omega_0}\right)y>0\,,$$

ξ and η are real. According as $BF-CE\lesseqgtr 0$, that is,

$$y \gtrless -\frac{3x^2/\Omega_0-(3/2)\varepsilon^2}{(3/2)\varepsilon^2-1/\Omega_0},$$

one of the roots has the positive sign and the other negative, or both of them are negative. To the former case does the first steady state (1,1) belong, and therefore it is looked upon as an unstable saddle point. To the latter belongs the other steady state (0, 0), and it is the only stable node.

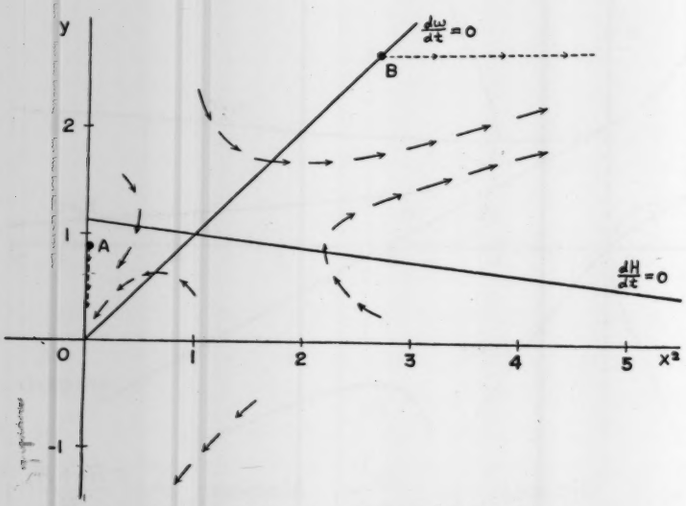

Fig. 3. Trajectories of representative points
$\varepsilon=1/10^{\frac{1}{3}}$,
A: $H_1=0.1$, $H_2=-0.1$, $\Omega_1=\Omega_2=25$.
B: $H_1=1.0$, $H_2=-1.0$, $\Omega_1=\Omega_2=9.375$.

Taking equations (13) and (14) into account too, the trajectories of the representative points on x^2-y plane are schematically drawn in Fig. 3. As for some particular cases, equations (7), (8), (9) and (10) are integrated numerically, using the relay computer FACOM-128B. For examples, three of them are shown in Fig. 4, trajectories of which are also depicted in Fig. 3 with dotted lines. From these we see that, if the magnetic field and the angular velocity whose values belong region (2) are given initially x^2 and y approach themselves to zero, namely the angular velocity increases indefinitely while the magnetic field decreases monotonously. The sphere will be infinitely accelerated by the external force that has nothing to do with the generation of magnetic field while the magnetic field dissipates its energy as Joule heat. Perplexity occurs when values of the magnetic field and the angular velocity belong to region (1). The growth of the magnetic field is accompanied by the decrease in the angular velocity because the electromagnetic coupling is

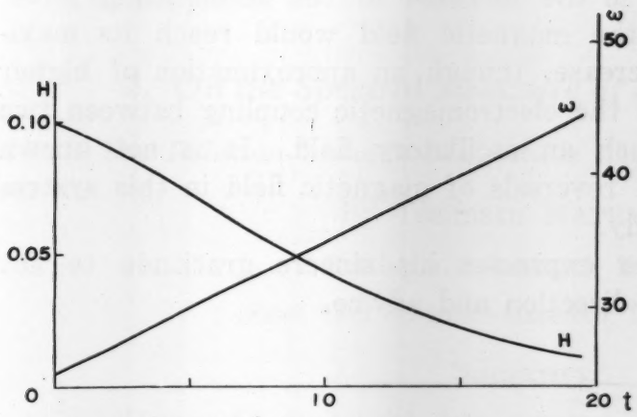

Fig. 4–1. $\varepsilon=1/10^{\frac{1}{3}}$,
Initial values: $H_1=0.1$, $H_2=-0.1$, $\Omega_1=\Omega_2=25$.

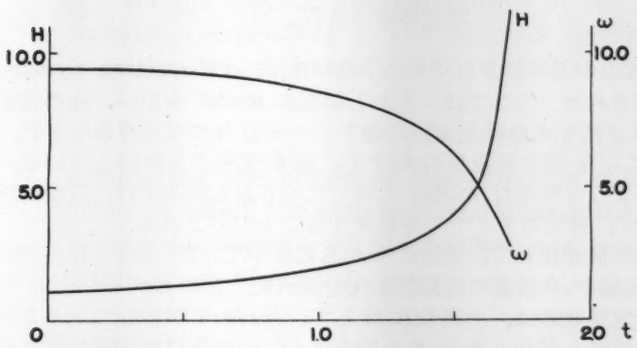

Fig. 4–2. $\varepsilon=1/10^{\frac{1}{3}}$,
Initial values: $H_1=1.0$, $H_2=-1.0$, $\Omega_1=\Omega_2=9.375$.

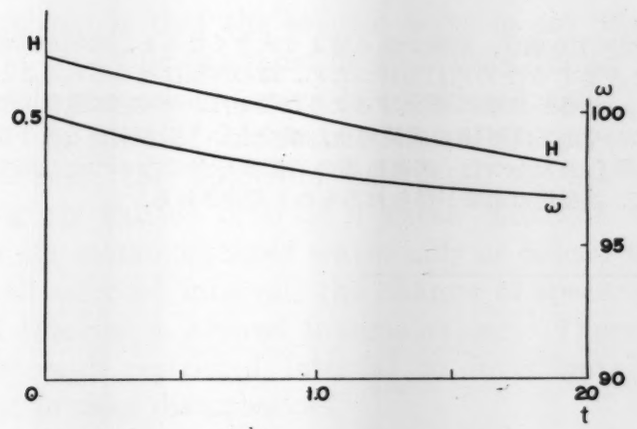

Fig. 4–3. $\varepsilon=1/10^{\frac{1}{3}}$,
Initial values: $H_1=\sqrt{3/8}$, $H_2=-\sqrt{3/8}$,
$\Omega_1=\Omega_2=100$

strengthened by the increase in the field and the decelerating torque will come to overwhelm the driving force. It is incomprehensible, however, from the physical point of view, that the diminution of the speed of rotation continues endlessly, as is shown in Fig. 3 and 4. It is probable that this difficulty might be originated in the crude approximation such as (2), where the second order terms of p are ignored. A better approximation of the magnetic field might exclude this unreasonableness.

4. Concluding remarks

It is clarified in this paper that a steady state of the dynamo with two rotating spheres in an infinitely extending conductor cannot be stable for small disturbances. If the magnetic field decreases by chance below a certain value, the coupling torque is weakened and the spheres come to rotate with infinitely rapid speed. If the field is strengthened, the speed

of rotation diminishes owing to the increase in the decelerating force. It is also anticipated that the magnetic field would reach its maximum value and begin to decrease, though an approximation of higher degree is needed to describe the electromagnetic coupling between two spheres in order to attain such an oscillatory field. It is not known whether or not we observe reversals of magnetic field in this system until we perform such a study.

In conclusion, the writer expresses his sincere gratitude to Dr. Rikitake who gave him kind direction and advice.

---

1. 非定常ダイナモ (1)

東京大学大学院
地球物理学課程 行　武　　毅

最近，Herzenberg によつて，導体球の中で回転する 2ケの小導体球が，self-exciting dynamo 系として，磁場を維持できることが証明された．ここでは，それと類似の model を用い，その安定性と時間的変化を調べた．従来，非定常ダイナモの研究は，円盤ダイナモを使つてなされてきた．力武は，2ケの円盤ダイナモを結合させて，電流や角速度の向きが，逆転することを示している．電流あるいは磁場の逆転の可能性がこのような簡単な model に対して示された現在では，近似の度をたかめ，より現実的な model を用いて，非定常ダイナモを研究することが望まれる．

ここでは，地球核内の流体運動を極端に理想化して，無限に拡がる導体中で，2ケの導体球が回転している場合を考え，そこに誘導される磁場や，角速度の時間的変化を調べた．この model に対して，定常状態は容易に求まるが，そのような定常状態は，小擾乱に対して，きわめて不安定であることが示される．電動計算機を用いて，数値的にも確められたことであるが，この系は初期値の与え方によつて，2 通りの変動をする．

1) 磁場は単調に減少し，角速度が一様に増加する場合．これは磁場が減少して，運動を抑制しようとする電磁的結合力が弱まると，球の回転が早くなり，外部から供給されたエネルギーが，全部運動エネルギーに転換される場合である．

2) 角速度が減少し，磁場が単調に増加する場合．磁場がある値より大きくなると，回転を抑制しようとする電磁的結合力が，運動を促進する外力に打ち勝つため，球の回転は遅められることになる．しかし，角速度は次第に減少し，磁場が無限に増大するような現象は，物理的に説明困難である．おそらく，角速度の減少と共に，やがては磁場の成長停止，減少という過程が起ると予測されるが，ここではそのような結果は得られなかつた．誘導磁場の近似が十分でなかつたためであろう．近似の度を高めることによつて，振動性の磁場が得られるものと期待される．

BULLETIN OF THE EARTHQUAKE
RESEARCH INSTITUTE
Vol. 38 (1960), pp. 13-27

2. On the Spectral Structure of Earthquake Waves.

—The Relation between Magnitude and Predominant Period—

By Tosimatu MATUMOTO,

Earthquake Research Institute.

(Read, Dec. 22, 1959.—Received, Dec. 28, 1959.)

Summary

Using the digitalized data processing apparatus, the velocity spectra of *P*-wave part and *S*-wave part were studied for the shocks occurred in the narrow region off shore of north east Honshû, Japan.

As the results, several groups of the predominant period were found corresponding to the maxima appeared in each velocity spectrum, and these periods were related to the magnitude of the shocks as

$$M=\alpha_i+\beta_i \log T_i \ .$$

Comparing the period of the vibration of a spherical shell, the possibility of which the groups of the predominant period were explained as the oscillations of the fundamental and the higher mode of the origin were discussed.

§ 1. Introduction

To attack the nature of earthquake waves, it is very important to know their spectral structure. However, an essential difficulty for this problem is that the seismic wave is not stationary. In such analysis, the time function must be stationary during the time interval of analysis, while the seismic wave is considered not to have such character.

In spite of this restriction, it is found that there are little differences between the spectrum calculated at the finite interval and that of slightly shifted interval if these intervals contain a single wave group or its metamorphosed waves only as described in a later section. In such well selected interval, the change of spectrum is small even if the range of interval is altered to some extent. Therefore Fourier analysis is valid for scuh restricted interval to investigate the spectral structures of earthquake disturbances.

In this paper, Fourier analysis is applied for *P*-wave part and *S*-wave part of shocks which occured in the narrow region off the *E* coast Kinkazan, of off shore of north east Honshû Japan.

§ 2. Tracer and Relay Computer used in this analysis

A few years ago, we made a relay computer designed for correlogram analysis as reported in our previous paper.[1]

When we use this computer the data must be digitalized and punched on the tape in advance. However, it is a troublesome work to measure the disturbance in the seismogram, to obtain the numerical values and then to punch them on the paper tape. To get rid of this work we made a tracer which directly converts the optically recorded seismic disturbance into a digital one.

Since it was not reported in our previous paper we will give a brief description of this instrument.

In this instrument, at first we choose the converting rate of the amplitude between the digital tape and the optical recorded seismogram by the amplitude adjuster according to the amplitude of the original seismic disturbance.

The next step is to put the cross wire of the microscope upon the trace of the record shifting the cross wire by rotating the handle attached at the right side of the instrument. By this operation the amplitude of the record is converted into the angle of rotation of the commutator, and the amplitude is read off in the cyclic-code. Through the cyclic-binary converter, the signal which is propotional to the amplitude of the original disturbance is ready to be sent to the perforator. When the switch is closed, the perforator is operated, and at the same time, the drum on which the seismogram is mounted is driven stepwise by the stepping ratchet.

The time interval of readings on the original seismogram is 0.2 or 1.0 sec, one of which being choosen according to the period involved in the disturbance.

The whole process of the conversion and the calculation is schematically shown in Fig. 2. For the purpuse of Fourier analysis, digitalized Fourier tapes, namely the tapes of sine and cosine functions, are provided. Both the Fourier tape and the digitalized tape are applied to the inputs of the relay computer, and their correlation is calculated.

To get the velocity spectrum of the seismic disturbance, the inverse of the velocity sensitivity of the seismograph are multiplied, and we can get the velocity spectrum of the seismic disturbance.

---

1) Y. SATÔ and T. MATUMOTO, *Bull. Earthq. Res. Inst.*, **34**(1956), 279–281

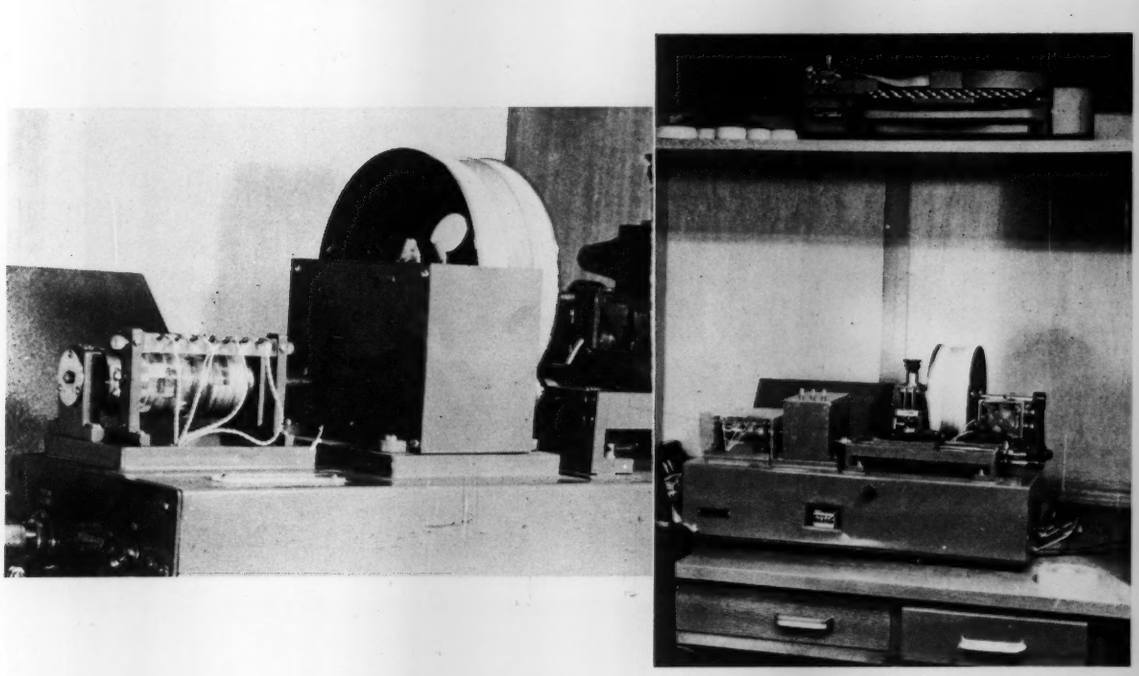

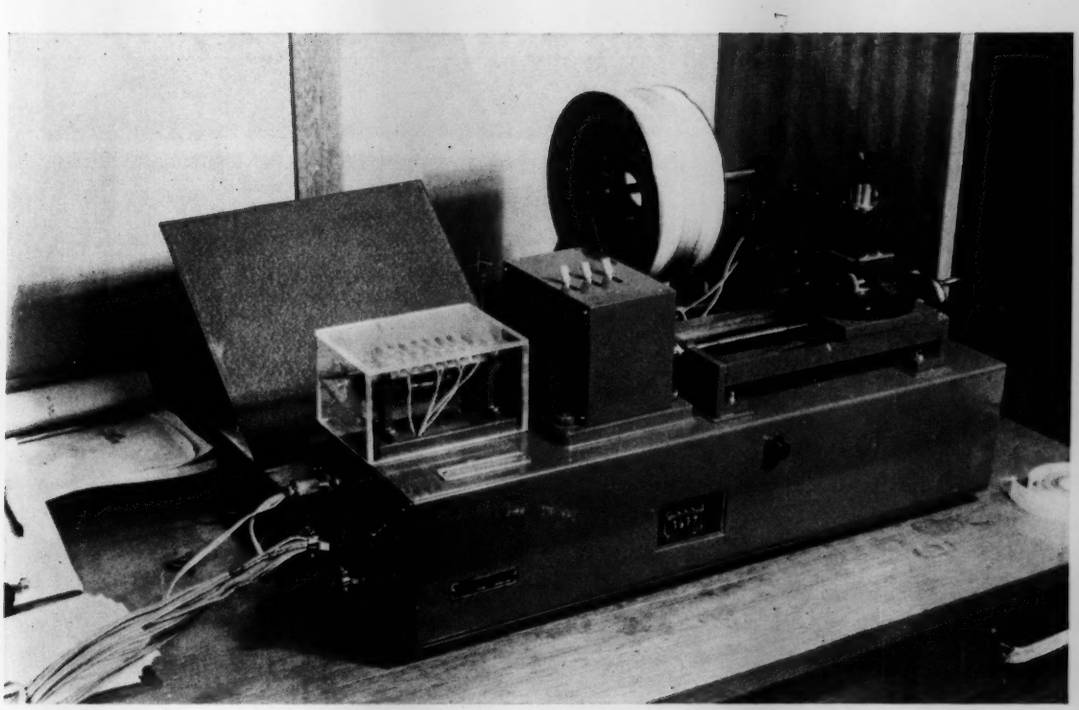

Fig. 1. The tracer by which an analogue seismogram is converted into the digital one.

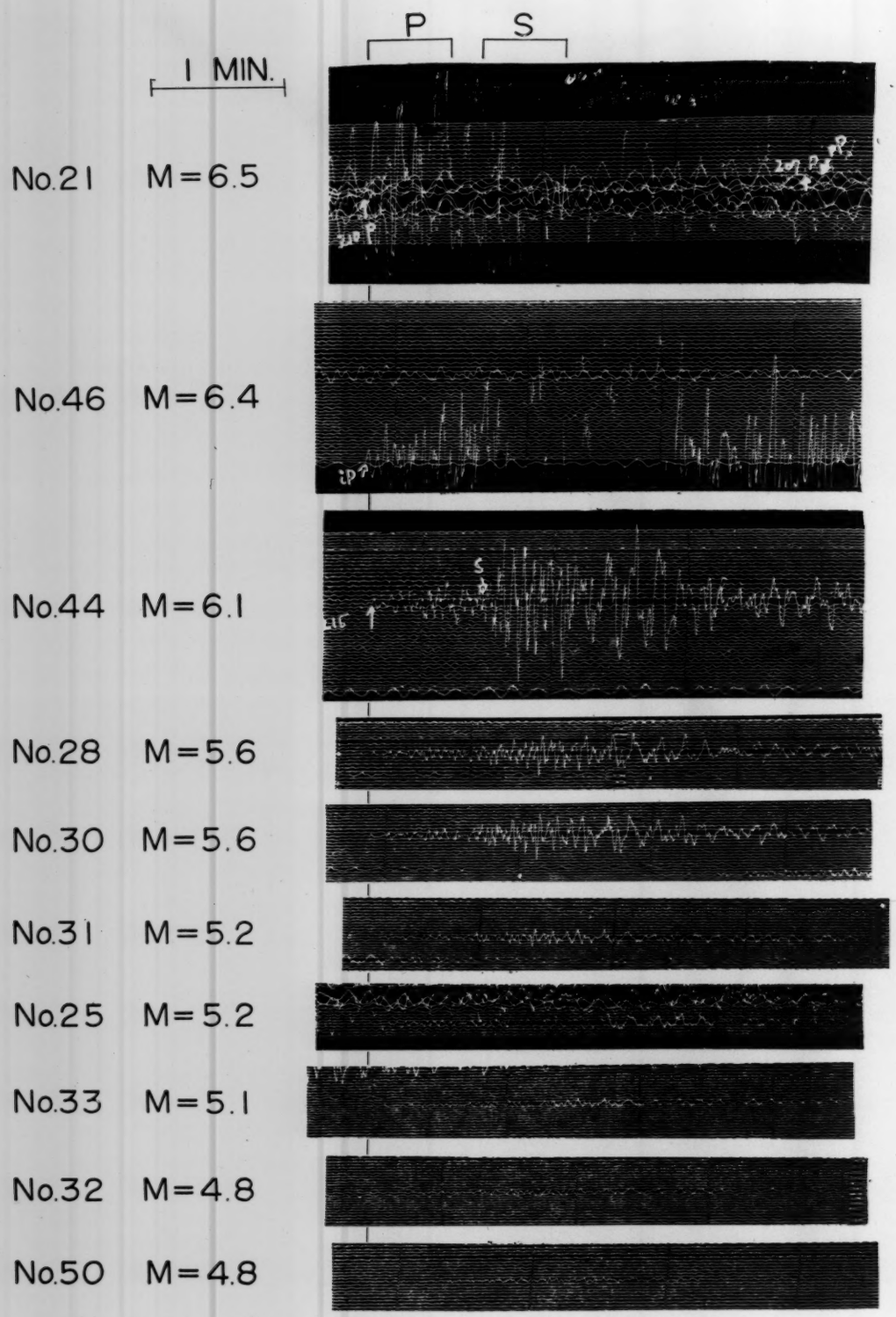

Fig. 3. Seismic Disturbances recorded by vertical HES 1–20 Instrument.

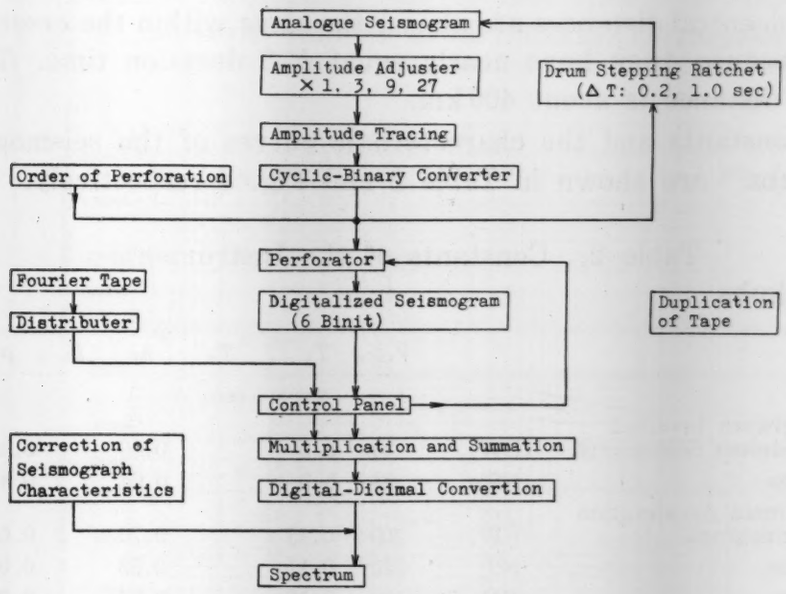

Fig 2. Schematic Illustration of Calculating Process of Spectra.

§ 3. Seismogram used in this Study

The seismograms used in this analysis were obtained at our seismological station located at Mt. Tsukuba.[2]

The serial number, date, location and magnitude of earthquakes are shown in Table 1. Some of these epicenters were determined by J.M.A.

Table 1. The List of Earthquakes Off *E* Coast of Kinkazan

No.	Date			Location	Depth	Magnitude
	April, 1958				km.	
21	07 d	18 h	05 m	38 1/4 *E*, 143 3/4 *N*	20 ca.	6.5
25	07	23	18			5.2
28	08	07	11	38 1/4, 143 3/4	Shallow	5.6
30	08	10	01	38 1/4, 143 3/4	20 ca.	5.6
31	08	15	27			5.2
32	08	16	39			4.8
33	08	17	03			5.1
44	10	11	50	38 1/4, 143 3/4	20 ca.	6.1
46	11	00	58	38 1/2, 1444	20 ca.	6.4
50	11	12	50			4.8

(Japan Meteorological Agency). For smaller earthquakes, however, the epicenters were not given by J.M.A., but it may be reasonable to assume

2) 140° 06′ 36″ E, 36° 12′ 39″ N.

that the epicentral distances are almost the same within the error of a few percent because they have nearly equal P–S duration time. The mean epicentral distance is about 400 km.

The constants and the characteristic curves of the seismographs at Mt. Tsukuba[3] are shown in Table 2 and Fig. 4 respectively.

Table 2. Constants of the Instruments

Mt. Tsukuba

No.		V_{max}	T_1	T_2	h_1	h_2	ρ	σ
			sec	sec.				
1. Hagiwara Inverted Pendulum Seismogrph	(EW)	34	5.0		0.60		0.45	
2. Ditto.	(NS)	34	5.0		0.64		0.47	
3. Ishimoto Acceleration Seismograph	(EW)	200	0.12		0.70		0.05	
4. Ditto.	(NS)	220	0.11		0.58		0.04	
5. Ditto.	(UD)	190	0.10		0.57		0.05	
6.* HES 1–1**	(EW)	29000	1.00	1.16	1.0	1.0	0.1	
7.* Ditto.	(NS)	29000	0.98	1.10	1.0	1.0		0.1
8.* Ditto.	(UD)	37000	0.97	1.26	0.8	1.0		0.1
9.* Anderson-Wood Type Torsion Seismograph	(EW)	2000	0.80		0.8		0.00	
10.* Ditto.	(NS)	2400	0.80		0.8		0.00	
11.* HES 1–20**	(EW)	1740	1.0	22.4	3.1	1.0		0.74
12.* Ditto.	(NS)	1880	1.0	20.7	3.0	1.0		0.73
13.* Ditto.	(UD)	2330	1.0	21.6	2.3	1.0		0.66
14. Columbia Long-Period Seismograph	(EW)	697	15.1	77.	3.1	1.2		0.25
15. Ditto.	(NS)	432	15.1	91.	3.1	1.0		0.26
16. Ditto.	(UD)	627	15.1	104.	1.5	1.1		0.12
17.* HES 1–0.2**	(EW)	144000	1.0	0.24	1.0	0.5		1.0
18.* Ditto.	(NS)	144000	1.0	0.24	1.0	0.5		1.0
19.* Ditto.	(UD)	150000	1.0	0.24	1.0	1.0		0.5

T_1: Period of pendulum.
T_2: Period of galvanometer.
h_1: Damping constant of pendulum when the galvanometer is clamped.
h_2: Damping constant of galvanometer when the pendulum is clamped.
ρ: Solid friction.
σ: Coupling factor.
*: Precise film recording system is adopted.
**: Hagiwara Electromagnetic Seismograph.
Annexed numbers indicate the approximate period in second of pendulum and galvanometer.

3) T. HAGIWARA and T. MATUMOTO, *Monthly Meeting of the Earth Research Institute*, (July, 1959).

The seismograms recorded by the vertical HES 1–20 instrument are shown in Fig. 3, the serial number of earthquakes corresponded to that of Table 1.

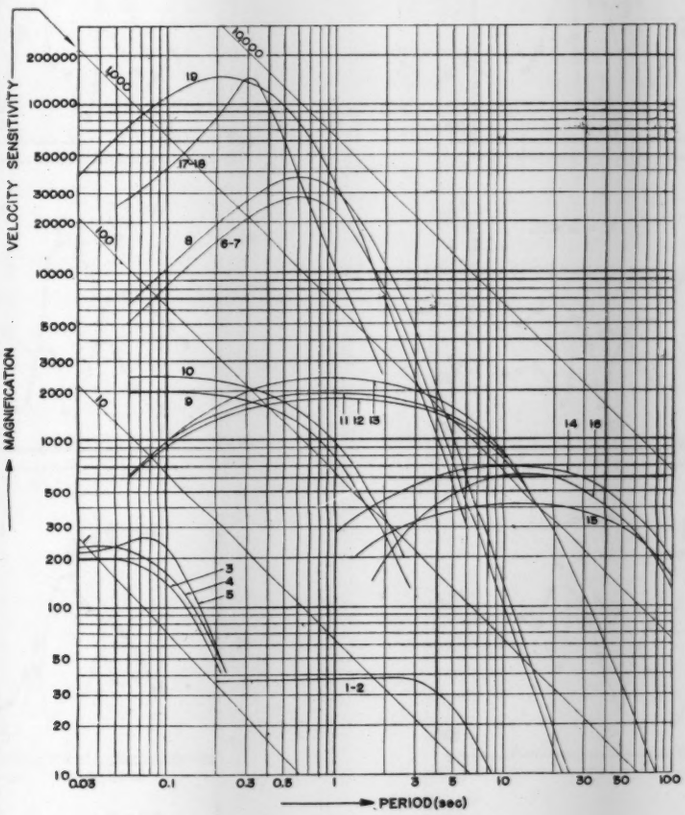

Fig. 4. Characteristic Curves of Seismographs observed at Mt. Tsukuba.

The analysis is performed both for *P*-wave part and *S*-wave part. Starting from the arrival of *P* and *S* phase, 180 sample points are selected on the original seismogram, in which the time interval of succeeding sample points is 0.2 sec each. Thus the range of the analysis in which Fourier coefficients are determined is $0.2\,\text{sec} \times 180 = 36\,\text{sec}$. In these ranges, only *P* (or *S*) wave and its metamorphosed waves are involved. Therefore we call them *P*-wave part and *S*-wave part.

§ 4. The Spectra or P-Wave and S-Wave Parts

Preceding our study, the analyses were performed for some different intervals which were shifted by several seconds to check the change of Fourier coefficients according to these intervals. The *S*-wave part of No. 44 earthquake, for instance, is analysed for the range of 36 sec from

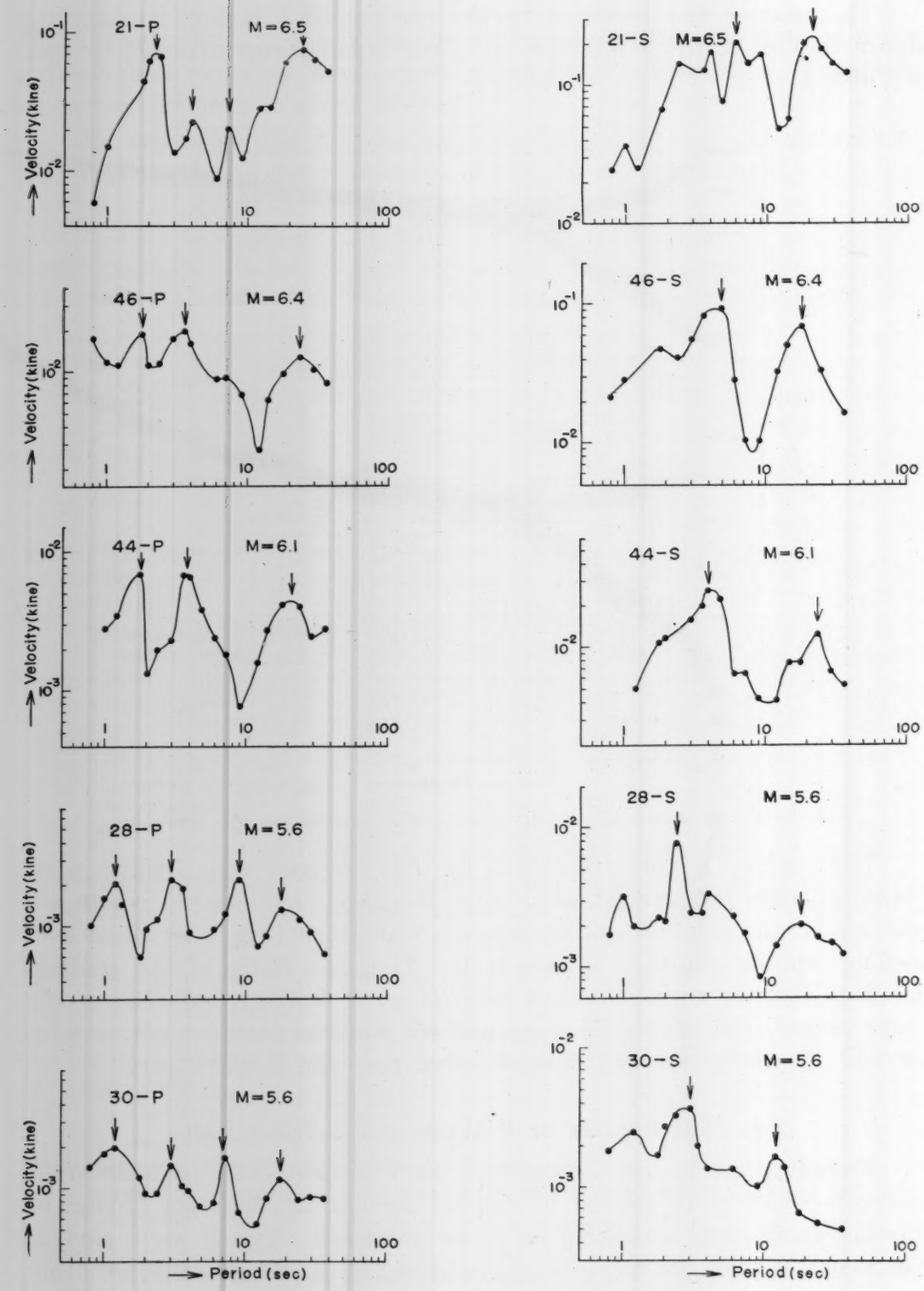

Fig. 7a. Spectra of *P*- and *S*-Wave Parts.

The number of each spectrum is corresponding to the serial number of Earthquakes shown in Table 1.

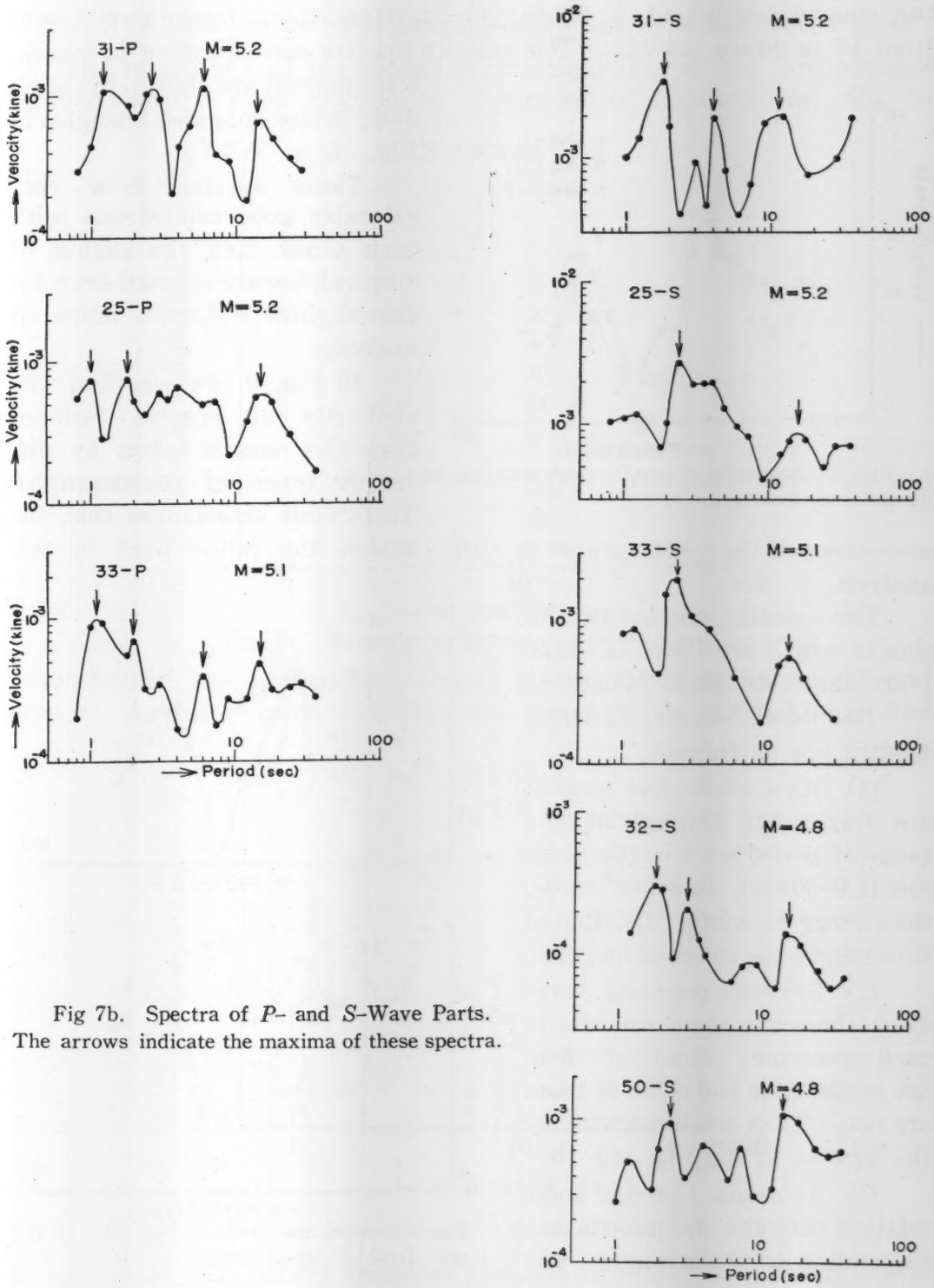

Fig 7b. Spectra of *P*- and *S*-Wave Parts. The arrows indicate the maxima of these spectra.

the commencement of S phase (44–S), from 5 to 41 sec (44–S1), and from 10 to 46 sec (44–S2). The volocity spectra corresponding to respective interval are shown by black dots, white dots and triangles in Fig. 5.

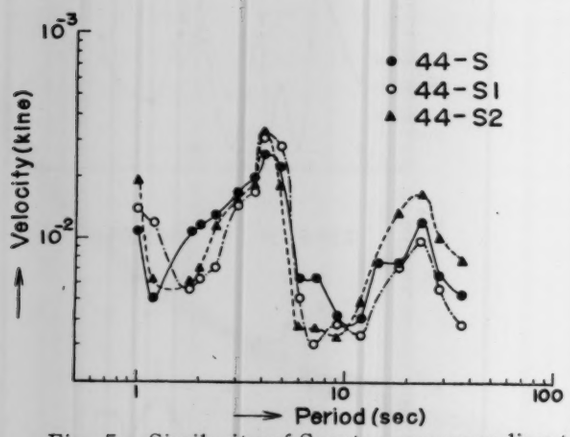

Fig. 5. Similarity of Spectra corresponding to the different Intervals.

These spectra show considerably good coincidence with each other, and the change of spectral feature is small even for the slightly different range of analysis.

In Fig. 6, we can find the similarity of spectra reduced from the records taken by different types of seismographs. This result also proves that the correction of the seismograph is valid within the range used in this analysis.

The velocity spectra of the shocks which are listed in Table 1 are shown in Figs. 7a and 7b.

The main features of these spectra are as follows:

(1) As a whole, the spectra are fairly flat throughout the range of period used in this analysis (1.0–36 sec). In other words, the energy is widely distributed throughout the range of analysis.

(2) To speak precisely, however, there are some maxima in each spectrum. Some of them are remarkable and some of them are not. They are illustrated by the arrows in Fig. 7a and 7b.

(3) It seems there is some relation between the periods corresponding to these maxima and magnitude of the shock, which will be described in the next paragraph.

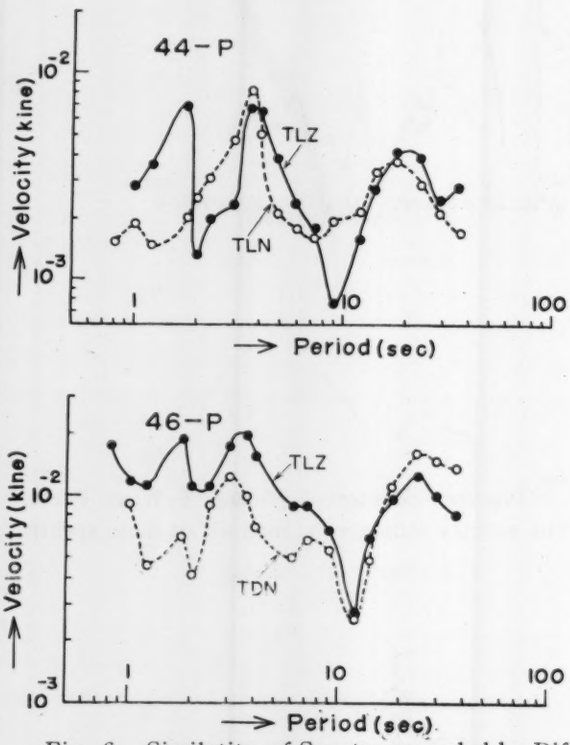

Fig. 6. Similatity of Spectra recorded by Different Type of Seismograph.

§ 5. The Relation between Magnitude and the Predominant Period

The magnitude of the shocks versus logarithm of the predominant periods shows a close relation as illustrated in Figs. 8a and 8b. In

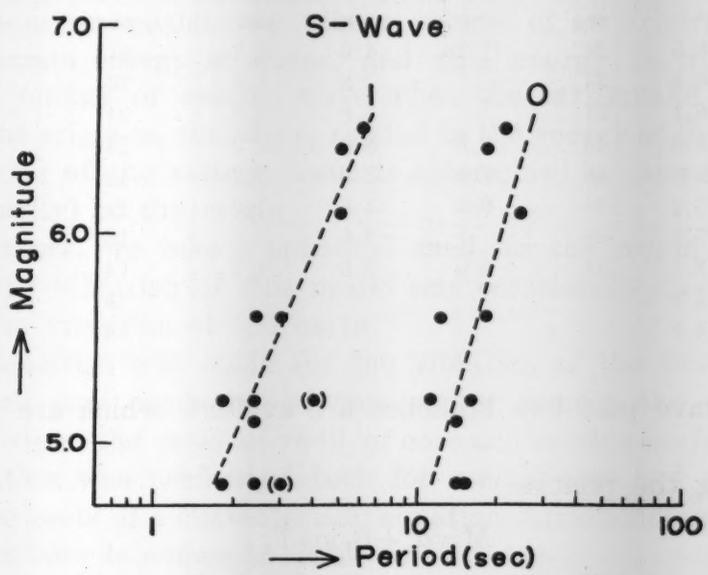

Fig. 8a. Predominant Periods of *S*-Wave Part.

these figures, the predominant periods are clearey separated into several groups. As for *P*-wave part they are separated to three groups and

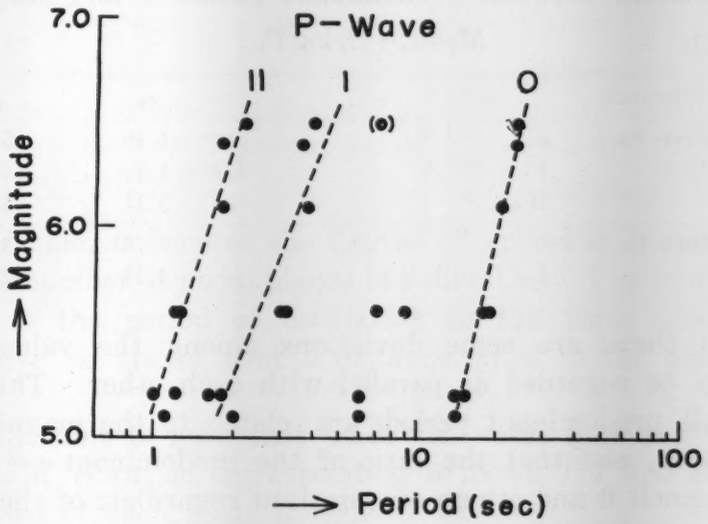

Fig. 8b. Predominant Periods of *P*-Wave Part.

an additional one. These branches are symbolized by the notation 0, I and II as shown in Table 3.

Table 3. Predominant Periods of Spectra

No.	M	P-Wave 0		I.	II.	S-Wave 0.		II
		sec	sec	sec	sec	sec	sec	sec
21	6.5	24.	(7.2)	4.0	2.2	21.		6.0
46	6.4	24.		3.6	1.8	18.		5.0
44	6.1	21.		3.8	1.8	24.		5.0
28	5.6	18.	9.0	3.0	1.2	18.		2.5
30	5.6	18.	7.0	3.0	1.2	12.		3.0
31	5.2	14.	6.0	1.6	1.2	11.	(4.0)	1.8
25	5.2	15.		1.8	1.0	16.		2.4
33	5.1	14.	6.0	2.0	1.1	14.		2.4
32	4.8					15.	(3.0)	1.8
50	4.8					14.		2.4

Also for S-wave part two branches are evident, which are noted by 0 and I.

Assuming the relation

$$M=\alpha_i+\beta_i \log T_i \ , \qquad (1)$$

the values of α_i and β_i are determined by the method of least squares.

The values of the respective branch are shown in Table 4.

Table 4. Relation between Predominant Period T and Magnitude M.
$M=\alpha_i+\beta_i \log T_i$.

Branch		α_i	β_i
P-Wave Part	0	−1.45	5.70
	I	4.31	3.25
	II	5.11	4.27
S-Wave Part	0	0.76	3.97
	I	4.11	3.03

Although there are some deviations among the values of β_i, all branches may be regarded as parallel with each other. This fact suggests that all predominant periods are related to the magnitude of the respective shock, and that the ratio of the predominont periods belonging to the branch 0 and others are constant regardless of the magnitude. It is natural to think that these characteristics of the predominant period are due to the nature of the origin, or in other words, to the mechanism of the occurrence of the earthquake, rather than to the nature of the ray path.

§ 6. Discussion

In the previous section, the nature of the velocity spectra is described. In this section, we want to make some discussion of them.

As the origin model, we take a volume of an arbitrary shape, in which the strain energy is stored, and this energy is transformed to the kinetic energy of seismic wave when the earthquake occurs. The volume of the origin is, therefore, related to the energy of the earthquake, and the period of the seismic wave is determined by the radius (or some related quantity) of the origin.

For instance, we take a spherical shell as the origin model. The period of the vibration of this model was occasionally calculated by us to attack the vibration of the earth.[3]

The calculation was made for the vibration of the first class of this model, which was composed of two parts, namely the core and the mantle. We put the ratio of radii of core and earth's surface as 0.5469. The calculation was performed both for a rigid core and a liquid core, but only the roots of a characteristic equation corresponding to the model of the liquid core is shown in Table 5.

Table 5. The Periods of Vibration of Spherical Shell.
($b/a=0.5469$, Liquid Core, $1/\xi_{n,N}=T_{n,N}V_s/2\pi a$)

	$1/\xi_{n,N}$		
n \ N	0	I	II
0	—	0.1358	0.0709
1	—	0.131	0.0704
2	0.414	0.122	0.0690

In this Table, n denotes the degree of spherical harmonics, and N indicates the number of nodal planes in r-direction. The number $T_{n,N}V_s/a$ is the ratio of the period of oscillation to the time taken by a distortional wave to travel over a distance equal to the diameter of the sphere.

It is important to note that when the value of n is given there are many modes of vibration corresponding to $N=0, 1, 2$ and so on.

The period of each mode is decided by

$$T_{n,N}=\frac{2\pi a}{V_s\xi_{n,N}} \qquad (6)$$

3) T. MATUMOTO and Y. SATÔ, *Bull. Earthq. Res. Inst.*, **32**(1954), 247–258.

In case of $n=2$, for instance, the periods are calculated against the various value of the radius as a shown in Table 6.

Table 6. Radius of Origin and Calculated Periods of Distortional Vibration

Radius a	Period of Distortional Vibration $N=0$	$N=1$	$N=2$
km.	sec.	sec.	sec.
1	0.650	0.192	0.108
2	1.30	0.383	0.217
4	2.60	0.766	0.433
6	3.90	1.15	0.650
10	6.50	1.92	1.08
20	13.0	3.83	2.17
40	26.0	7.66	4.33
60	39.0	11.5	6.50
100	65.0	19.2	10.8

The velocity of the distortional wave is assumed to be 4 km/sec in this calculation. Comparing the observed periods of Table 2 and the values of Table 6, it may be suggested that the periods which belong to the branch I are explained by the vibration of the higher mode ($N=1$). As these periods are deeply affected by the nature of origin, there is a possibility to attack the nature of origin by means of the investigation of the higher mode vibration as well as the fundamental one. In case of P-wave, the branch 0, I and II will be explained by the dilatational vibration of fundamental mode and of higher mode respectively.

Inserting the relation (2) into (1), we get

$$M=\alpha_{n,N}-\beta_{n,N}\log\left(\frac{2\pi}{V_s\xi_{n,N}}\right) \qquad (3)$$

When the values $\alpha_{n,N}\beta_{n,N}$ and $\xi_{n,N}$ corresponding to the fundamental mode are given, the relation between magnitude and the radius of origin is estimated.

In case of $n=2$ and $N=0$, the values are as follows as shown in Table 4 and Table 5:

$$\alpha_{2,0}=0.76\ ,\quad \beta_{2,0}=3.97\ ,\quad \xi_{2,0}=0.414\ .$$

Assuming $V_s=4$ km/sec, we get the following results:

$$M=0.02+3.97\log a\,(\mathrm{km}) \qquad (4)$$

Based on this equation, the relation between M and a is estimated as shown in Table 7.

Table 7. Relation between Magnitude and Radius of Origin.

M	4.0	4.5	5.0	5.5	6.0
$\log a$	1.003	1.129	1.255	1.381	1.507
a (km)	10.1	13.5	18.0	24.1	32.2
M	6.5	7.0	7.5	8.0	8.5
$\log a$	1.633	1.759	1.885	2.011	2.137
a (km)	43.0	57.4	76.8	103.	137.

In conclusion, author expresses his hearty thanks to Prof. T. Hagiwara and Asist. Prof. Y. Satô who gave him useful advices and revised this paper with goodwill.

---

2. 地震波のスペクトル構造
—マグニチュードと卓越周期の関係—

地震研究所　松　本　利　松

光学的に記録された地震記象を 2 進化したテープに変換する変換装置を新に製作した．この進化した記録を以前に報告したリレー式相関計算器にかけ，フーリエ解析を行つた．

1958 年 4 月，金華山沖に群発した地震を筑波山において観測した記録を使い，P 波部分および S 波部分の速度スペクトルを 1 秒から 36 秒の帯域について計算した．解析時間は 36 秒，標本化の時間間隔は 0.2 秒である．

主な結果は次の通りである．

(1) 速度スペクトルは全体としては比較的平均した強度分布を持つている．

(2) 精密に見ると，スペクトルには数個の極大が認められる．これらの極大値は P 波部分については 3 群に，S 波部分については 2 群にわけられる．極大値に対する周期の対数をマグニチュードについてプロットすると，かなり見事に直線上にのり，これらの直線は互に平行している．

(3) 震源を球殻のモデルに置きかえ，第 1 種の振動について固有周期を計算した結果と比較すると，これらの周期の比は $n=2$, $N=0$ および 1 に対応する振動周期の比と一致する．ただし n, N の値は θ および半径の方向に対する節平面の数を表わす．

(4) マグニチュード卓越周期の観測結果および，卓越周期震源模型の半径の計算結果を組合わせて，マグニチュード震源模型の半径の関係が求められた．すなわち

$$M=0.02+3.97 \log a(\mathrm{km})$$

これは従来の地震体積などの計算と一致する．

(5) 基本周期および高調波の周期は震源模型の仮定によつてかなり影響されるので，発震機構の研究などにもこの高調波の解析は有効であろう．

BULLETIN OF THE EARTHQUAKE
RESEARCH INSTITUTE
Vol. 38 (1960), pp. 29-39

3. *Theoretical and Experimental Approach to the Designs and Calibrations of Electro-magnetic Seismograph: I. Voltage Sensitivity of the Moving-coil Type Seismometer.*

By Etsuzo SHIMA,

Earthquake Research Institute.

(Read Sept. 22, 1959.—Received Dec. 1, 1959).

1. Introduction

Generally speaking, three types of electro-magnetic vibration-meters have been introduced, at least theoretically. They are the moving-coil type, the changing-flux type and the magneto-striction type. But from the practical point of view in earthquake measurement, no seismometers of the last type have hitherto been used, while the second type of instruments, which have boasted the highest sensitivity, are used only in the observation of minute earthquakes and distant earthquakes because of their non-linear response to stronger earth movements. On the other hand, the first type of instruments, which were introduced prior to the other types, have a wider range of linear response to the ground movement. Moreover, recent development in the material for the permanent magnet has made it possible to design smaller seismometers of higher sensitivity with much smaller permanent magnets.

On account of these advantages, almost all the seismometers of recent designs belong to the moving-coil type (with a fixed magnet) or to the moving-magnet type (with a fixed coil or coils), both of these types being the same theoretically: (essential difference of the above two types lies in the possibility of obtaining higher sensititity of the moving-magnet type without increasing the total weight of the seismometer when the magnet and the coil are given.) We may, therefore, say that seismometers of the moving-coil (or magnet) type are representative of the electro-magnetic seismometers at present. The writer is now engaged in theoretical and experimental studies of the design and calibration of this type of instrument based on the electro-acoustical theory. A part of these studies is hereby reported. In the following, an equivalent

four-terminal network of this type of seismometer is deduced, and is also given a simple method of determining the voltage sensitivity which is one of the most important parameters (instrumental constants) of this equivalent network.

2. Equivalent circuit of a moving-coil type seismometer

From the electro-acoustical point of view, an electro-magnetic seismometer can be seen as a kind of electro-mechanical transducer. The input of this transducer is the ground motion while the output of the same is the electric current. If we make use of the current concept of the mechanical impedance as used in the electro-acoustic theory, the mechanical quantities pertaining to the dynamics of the transducer are converted into the equivalent electro-magnetic quantities, and the equation of motion of the transducer is derived and solved by the analogous circuit theory. For the present purpose, the usual electrical mechanical analogy of mass-inductance is not relevant, but the mass-capacitance analogy is very apposite. The mechanical entities and their electrical equivalents to the purpose are listed in Table 1.

Table 1.

Mechanical element	Symbol used	Electrical element	Symbol used
Force	F	Current	I
Velocity	v	Voltage	E
Mass	M	Capacitance	C
Compliance	$1/k$	Inductance	L
Mechanical Resistance	r_m	Conductance	$1/R$

Now let us deduce the equations of motion of the seismometer in the electro-acoustic manner. The electro-magnetic seismometer converts the input ground motion into the output electric current. Therefore, this electro-mechanical transducer is to be considered as a four-terminal network. Let us denote the electric quantities in the mechanical input side by a suffix 1 and those in the output side by a suffix 2. Let the air-gap flux density of the magnet be B, and the total effective length of the wire forming the coil be l. Responding, then, to a current I_2 entering into the coil through the output terminal, a vibro-motive force BlI_2 is generated at the coil. Under additional external force F, the

total force exerted on the mass of the seismometer (which is here considered, for simplicity's sake, to be a one mass system) is $F+BlI_2$. This resultant force has to balance with the mechanical reaction consisting of the inertia force, the mechanical resistance and the spring force of the seismometer. We may think of this mechanical reaction as proportional to the velocity v of the seismometer mass. If we denote the proportionality constant by z_m the equation of motion governing the mechanical side is obtained as follows.

$$z_m v=F+AI_2 \qquad (1)$$

where $A\equiv Bl$. And A, which is the same as force factor in the treatment of electro-acoustic problems, is a voltage sensitivity[1] of the seismometer.

Since the coil moves in the magnetic field, electro-motive force $-Blv$ is generated in the moving coil. If we also take an exciting voltage E_2 into account, the total electro-motive force becomes E_2-Blv. Denote now the electric impedance by Z, then the current I_2 flowing through the coil is given by Kirchhoff's theorem as follows.

$$ZI_2=E_2-Blv=E_2-Av \qquad (2)$$

Making use of the mechanical electrical analogy shown in Table 1, we introduce here the following transformations.

$$F=AI_1 \qquad (3)$$

$$v=E_1/A \qquad (4)$$

Then (1) and (2) reduce to

$$ZI_2=-E_1+E_2 \qquad (5)$$

$$I_1+I_2=z_m E_1/A^2 \qquad (6)$$

To see clearly the meaning of the quantities in these equations, we shall examine the case when the external force F is absent, that is

$$F=AI_1=0 \qquad (7)$$

Then we have

$$E_1=A^2 I_2/z_m \qquad (8)$$

1) K. TAZIME, *Zisin*, **6** (1953), 43–44; **7** (1954), 96–115 (in Japanese).

$$E_2=(Z+A^2/z_m)I_2 \qquad (9)$$

From the equations (8) and (9) we can see that A^2/z_m has the dimension of electrical impedance, and is interpreted as the increment of the impedance due to the motion of seismometer. Thus A^2/z_m is called the motional impedance.[2] Introducing, therefore, the notation Z_m for A^2/z_m and solving I_1 and I_2 from (5) and (6), we have

$$\begin{pmatrix} I_1 \\ I_2 \end{pmatrix}=\begin{pmatrix} Y_{11} & Y_{12} \\ Y_{21} & Y_{22} \end{pmatrix}\begin{pmatrix} E_1 \\ E_2 \end{pmatrix} \qquad (10)$$

where Y_{ij}'s are

$$\left.\begin{aligned} Y_{11}&=1/Z_m+1/Z \\ Y_{12}&=Y_{21}=-Y_{22}=-1/Z \end{aligned}\right\} \qquad (11)$$

respectively. Equations (10) represent the characteristic relations of a physically realizable four-terminal network, because the matrix of Y_{ij} which may be called admittance matrix is symmetrical. Y_{ij}'s are admittance parameters.

Now let us examine Z_m and z_m in a little more detail. As we have assumed that the seismometer is one mass system, the equation of motion of the system when no current I_2 enters into the coil from the outside, is given by

$$Mpv+r_mv+kv/p=F \qquad (12)$$

in which $p=d/dt$ and M, r_m, $1/k$ denotes the mass, damping coefficient and compliance respectively. By the definitions already stated,

$$Z_m=A^2/z_m\,, \quad \text{and} \quad z_m=F/v=Mp+r_m+k/p$$

so that

$$Z_m=A^2/(Mp+r_m+k/p) \qquad (13)$$

If we transform M, r_m and k by the electrical equivalents shown in Table 1, we have

$$\begin{aligned} Z_m&=A^2/(Cp+1/R+1/Lp) \\ &=1/(Cp/A^2+1/A^2R+1/A^2Lp) \end{aligned} \qquad (14)$$

2) A. E. KENNELLY and G. W. PIERCE, *Proc. Am. Ac. Arts and Sc.*, **48** (1912).

Hence the equivalent circuits which give rise to the same impedance with Z_m are the parallel connection of L, C and R, magnitudes of which being A^2/k, M/A^2 and A^2/r_m. The wiring diagram of the L, C and R is shown in Fig. 1. The same circuit has first been suggested by Scherbatskoy and Neufeld[3] in 1937.

It is also to be remarked here that impedance Z, usually believed to be a series connection of a resistance r and a inductance L, is not so simple because of the existence of a iron core along the central axis of the moving coil of the seismometer. Effects of the hysteresis and eddy current losses are to be taken into consideration. But no adequate theoretical treatment of them is yet possible. The only practical approach to it is made on an experimental basis by the introduction of additional equivalent impedance in parallel as shown in Fig. 3a. If frequency f is known, Fig. 3a can be expressed as Fig. 3b, where $R'=R/\{1+(R/2\pi fL)^2\}$ and $L'=L/\{1+(2\pi fL/R)^2\}$. In the case when f is sufficiently small, then R and L in Fig. 3a or R' and L' in Fig. 3b become so small that these additional impedances may be neglected.

3. A simple method for determining the voltage sensitivity

Through these discussions we came to the conclusion that, if the voltage sensitivity A is known, the constants of the seismometer may be determined by measuring the electrical impedances. As A is the factor of transformations between mechanical and electrical elements, we cannot determine it by electrical measurements only. And so, to study the characteristics of a seismometer the measurement of A is inevitable.

Now, let us state a simple method for determining the voltage sensitivity A. When the current I passes through a coil, force AI is generated. So, if we can measure the force and the current, the voltage sensitivity will be determined. In Fig. 4 a simple apparatus for this purpose is shown. This apparatus consists of a lamp-and-scale, a balance and an ammeter. The balance has a mirror at the end of its rider-beam as shown in the figure, and it reflects the light-spot from the lamp to the scale. By this apparatus we can easily measure the small deflection of the balance from its equilibrium position.

Now, the measurement of the voltage sensitivity is carried out in the following sequence:

---

3) S. A. SHERBATSKOY and J. NEUFELD, *Geophysics*, **2** (1937), 213–242.

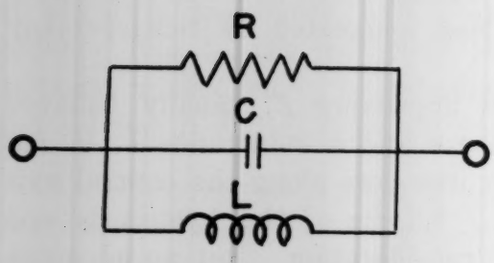

Fig. 1. Equivalent circuit of the motional Impedance.

$C=M/A^2$, $R=A^2/r_m$, $L=A^2/k$.

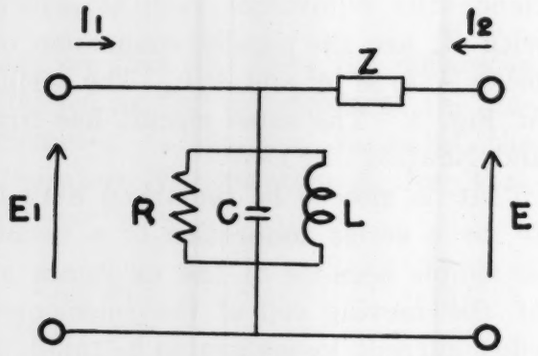

Fig 2. Equivalent circuit of the moving coil type electro-mechanical transducer.

$I_1=F/A$, $E_1=Av$

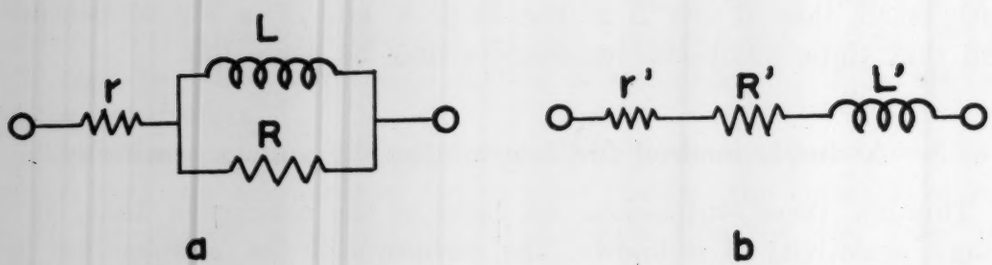

Fig. 3. Equivalent circuit of the impedance of moving coil. r: DC resistance.

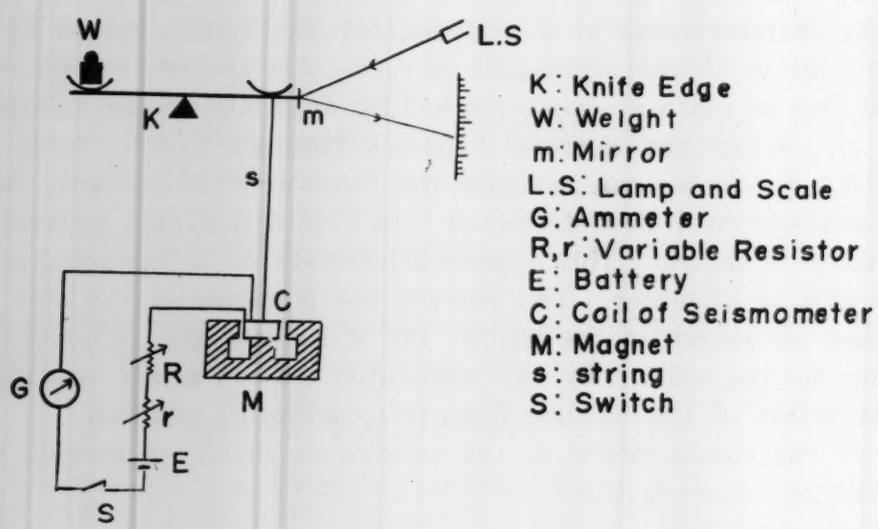

Fig. 4.

i) Connect the centre of the coil and the rider-beam with a string, and adjust the relative position of the balance and the coil so as the string is streched vertically.

ii) Appropriate weights are placed on the balance to bring the coil into the normal position of equilibrium when it is used actually. Remember the position of the light-spot on the scale at this equilibrium

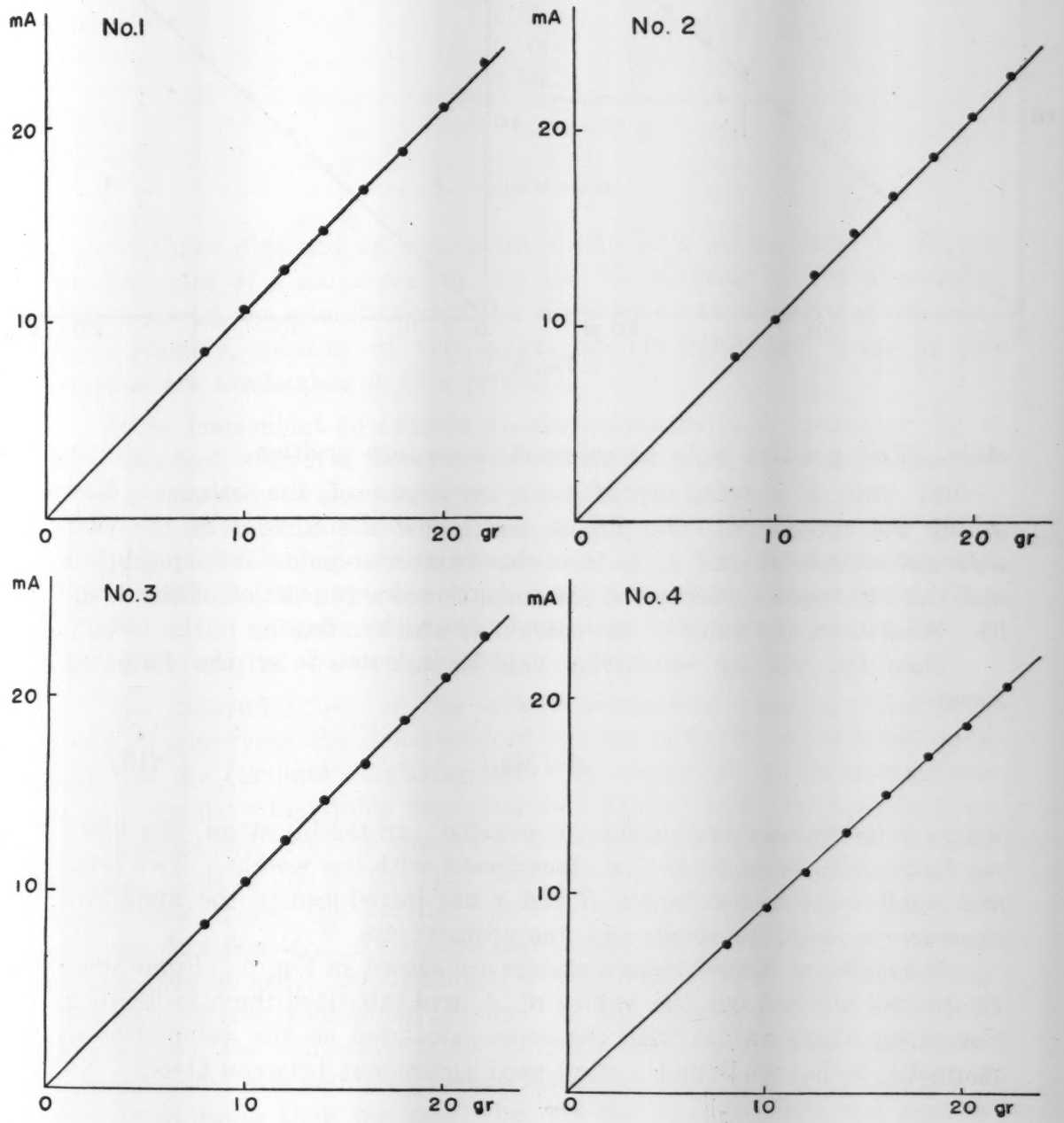

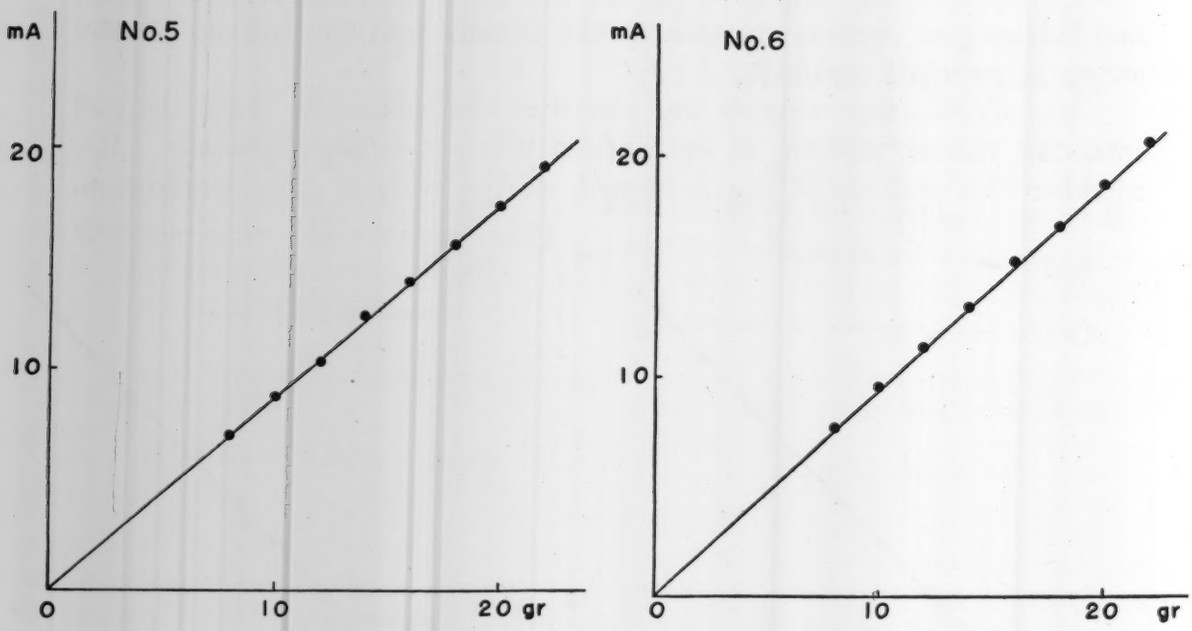

Fig. 5.

state. This position is to be referred to as zero position.

iii) Add a weight, say M gram, on a pan of the balance. Now switch the current into the circuit, and adjust the current by the variable resistances R and r, so that the balance regains its equilibrium and the light-spot comes to the abovementioned zero position of the stage ii). Read then the value of the current i, which is flowing in the circuit.

Then the voltage sensitivity can be calculated by the following formula,

$$A=Mg/i \tag{15}$$

where g is the acceleration due to gravity. In the iii) stage, the electric force pulls downwards to equiponderate with the weight. Two large and small variable resistances R and r are introduced in the apparatus in order to facilitate rough and fine adjustments.

Examples of actual measurements are shown in Fig. 5. From these figures we worked out the values of A, and tabulated them in Table 2. Comparing these values with the same calculated on the assumption of magnetic paths, we found a very good agreement between them.

Table 2.

Seismometer	Measured A in volt/kine	Calculated A in volt/kine
1	0.093	
2	0.095	
3	0.094	0.101
4	0.104	
5	0.112	
6	0.105	

4. Discussions

We have obtained an equivalent circuit of a seismometer in section 2. The case of a galvanometer can also be inferred by the abovementioned circuit by interchanging the direction of the input and the output. Namely, entities of the inputs are electrical and those of the outputs are mechanical in this problem.

It is convenient to express an electro-magnetic seismometer by a four-terminal network, because the characteristics of a galvanometer directly coupled to a seismometer are at once deduced by mere multiplications of the admittance matrices, as the given problem is the series connection of the four-terminal networks. And the above consideration can be extended to any case which contains an amplifier or some other circuits in the network of seismic apparatus. Doubtless to say, this is one of the merits of our equivalent circuit.

The determinations of the voltage sensitivity have, so far, been made by observing the deflections of a mass from the equilibrium position and the currents simultaneously. But in carring out these measurements, we have inevitably experienced that the larger the current flowing through the coil, the smaller is the apparent voltage sensitivity that results. This is due to the fact that the flux density decreases its intensity the more, the further the coil protrudes from the region of uniform flux density. As the voltage sensitivity is linearly proportional to the flux density, the reduction of the flux density turns into the reduction of the voltage sensitivity. In our measurement, which is a zero-method, the coil stays in its optimum position, and the proportionality of the force and the current intensity holds in a wider range of their magnitudes than the case when the coil moves. This fact enables

us to extend our measurement to a wider range, so that the accuracy of measurement may appreciably be improved.

Hitherto we have considered the voltage sensitivity as a constant. But, if we consider the influences of eddy current and the hysteresis losses of an apparatus, the voltage sensitivity does not remain a constant, and shows frequency characteristics. The same is true, also, for the impedance of the coil, and its magnitude increases when the driving frequency becomes higher.

When the seismometer inclines from the vertical—we can consider that such a circumstance may occur when we set a bore-hole-seismometer[4] at the bottom of a bore-hole—the coil may protrude out from the uniform magnetic field. And the apparent voltage sensitivity becomes smaller.

An example is given in Fig. 6, showing how the voltage sensitivity of a bore-hole seismometer changes its magnitude according to the deflection of the coil from the centre of its equilibrium. So, if we want precision in measurements, we have to consider these influences according to their actual conditions.

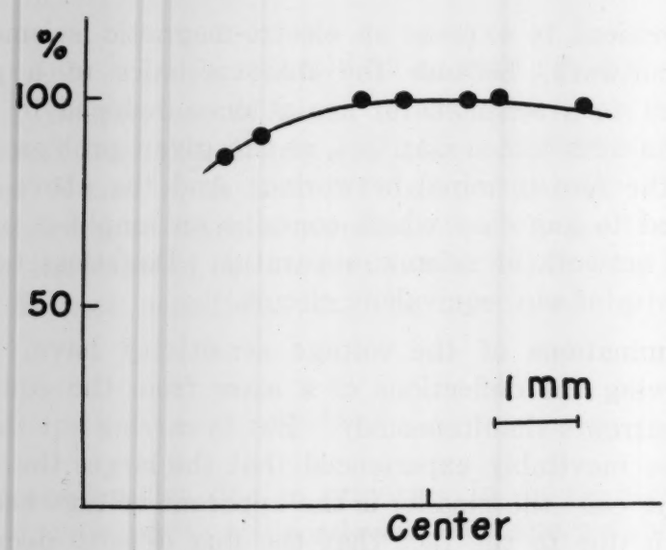

Fig. 6.

5. Concluding remarks

We have studied the moving coil type electro-magnetic seismometer as a four-terminal transducer, and deduced an equivalent circuit of the

4) H. KAWASUMI, E. SHIMA and M. SIBANO, *Annual Meeting of the Seismological Society of Japan* (April, 1955).

seismometer. This equivalent circuit agrees with the one which was first suggested by Sherbatskoy and Neufeld. By the use of this equivalent circuit, we can easily determine the instrumental constants of a seismometer simply by measuring the motional impedance electrically, when the voltage sensitivity is known. We can also use this equivalent circuit in the consideration of a galvanometer by reversing the input and the output. Thus, it has become possible to obtain the expressions of seismic apparata by the four-terminal networks conveniently and easily to infer the over-all characteristics of the apparata, and the characteristics are calculated by the mere multiplications of the admittance matrices.

We then designed a simple device for the measurement of the voltage sensitivity. By this device we could measure the voltage sensitivity more precisely than previously possible. Motional aspects of the voltage sensitivity are not dealt with in this paper, but we shall study them as the next problem.

In conclusion, author expresses his hearty thanks to Professor H. Kawasumi who gave him valuable discussions and perpetual encouragement.

---

3. 電磁式地震計の理論的実験的研究
その 1 電圧感度について

地震研究所 嶋 悦三

Moving coil type の電磁式地震計を，動電型変換器という立場から見れば，四端子の等価回路で，その働きを表現することが出来る．そして，この等価回路から，もし電圧感度が知れている場合には，電気端子側から，電気的 Impedance を測定すれば，地震計の常数はすべて決定し得ることがわかる．

この等価回路は，Galvanometer についても，地震計と全く同様な考え方から，入力端子と出力端子を入れかえることにより，そのまま利用出来るのである．なぜならば，電気端子側から見れば，地震計と Galvanometer は全く同等であると考えられるからである．

電圧感度を決めるためには，電気的測定のみからは出来ず，同時に機械的量を測定しなければならない．そして，これはなるべく手軽に行うことが望ましい．そのために，電圧感度を簡単に測定する一つの方法を考案した．装置は，coil に流れる電流のために生ずる力を，天秤をつかつて直接はかろうとするものである．この方法は，zero-method であるために，従前の方法と較べると，比較的大きな電流を coil に流すことが出来るので，精度をあげることが出来る．

電圧感度の動的測定は，今回は行わなかつたが，振動数が高くなれば，当然その影響を考えなければいけない，いいかえれば，電圧感度はもはや constant でなく周波数特性をもつだろうということが予想される．

BULLETIN OF THE EARTHQUAKE
RESEARCH INSTITUTE
Vol. 38 (1960), pp. 41-54

4. *Magnetic Survey on Hakone Volcano by Use of a Proton Magnetometer.*

By Takesi YUKUTAKE,*

Graduate School, University of Tokyo;
and
Iwao TANAOKA,

Earthquake Research Institute.

(Read Nov. 24, 1959.—Received Dec. 24, 1959.)

Summary

In connection with the seismic activity that occurred beneath the central cones of Hakone Volcano since the beginning of September, 1959, a magnetic survey with a proton magnetometer was carried out from Oct. 26 to 29, 1959.

It is made clear that the central area in the caldera can be divided magnetically into several areas. They are Kamiyama lavas, Komagatake lavas, Futagoyama lavas and the basalt lapilli and ash called Kanto ash. The differences in anomaly between these areas are obviously caused by the magnetization contrast of the formations. The intensity of magnetization of the central cone, Mt. Kamiyama, for example, seems unexpectedly large for an andesitic volcano, even though the topographic effect is taken into account.

Now that the distribution of the present magnetic field in the caldera has been obtained, repetition of a magnetic survey of this kind would elucidate the volcanic activity in relation to the change in the earth's magnetic field.

1. Introduction

A seismic activity with felt shocks of small magnitude started underneath the central cones of Hakone Volcano in the beginning of September, 1959. The activity lasted a few months. Seismographs installed by Prof. Minakami around the seismic area recorded a few hundred shocks every day during the most active period. In the hope of detecting changes in the earth's magnetic field, which might be accom-

*) Communicated by T. RIKITAKE.

panied by the activity, the writers undertook a magnetic work over the volcano.

It has been established that the magnetic method is very useful for studying volcanoes. Local magnetic anomalies that are closely related to the structure of volcanoes have been found on many volcanoes. The local anomalous changes in the earth's magnetic field as have been observed on Ooshima Island are even more important. Repeated magnetic surveys and continuous observations with variometers made there revealed geomagnetic changes which were likely caused by demagnetization and magnetization associated with rise and fall of the activities of Miharayama Volcano[1]. Since then, observation of changes in the geomagnetic field on volcanoes has been regarded as one of the most promising methods of foretelling the activity.

The first magnetic survey was carried out within the caldera surrounded by the old somma of Hakone Volcano with a portable proton magnetometer from Oct. 26 to Oct. 29. The magnetometer, all transistorized, was specially designed for field-use by the Research Group for Proton Magnetometer. The details of the magnetometer are reported elsewhere[2].

The portable proton magnetometer enables us to make absolute measurements of total geomagnetic force quite easily. A good many measurements can be performed in a short time. Preceding this survey, the writers calibrated the magnetometer at Aburatsubo station. According to the results of the comparison with the variometers, the instrumental error never exceeded 5 γ, which assured sufficient accuracy for the present survey.

In the northern part of Mt. Kamiyama, one of the central cones, there are engraved valleys with many sulphurous fumaroles, Oowakidani and Sôunzan valleys. In the latter there occurred a great landslide on July 26, 1953. It was reported[3] that the end of the slid area reached as far as 2 *km* from its source. As can be seen in Fig. 1, measuring points of this time are distributed, in the main, around Mt. Kamiyama, where the seismic activity was inferred to be most marked from the seismometric observations.

---

1) For instance,
T. RIKITAKE and I. YOKOYAMA, *Jour. Geophys. Res.*, **60** (1955), 165.
I. YOKOYAMA, *Bull. Earthq. Res. Inst.*, **33** (1955), 251.
I. YOKOYAMA, *Bull. Earthq. Res. Inst.*, **35** (1957), 567.

2) The RESEARCH GROUP for PROTON MAGNETOMETER, *Bull. Earthq. Res. Inst.*, in press.

3) F. KISHINOUYE and J. OSSAKA, *Bull. Earthq. Res. Inst.*, **33** (1955), 153.

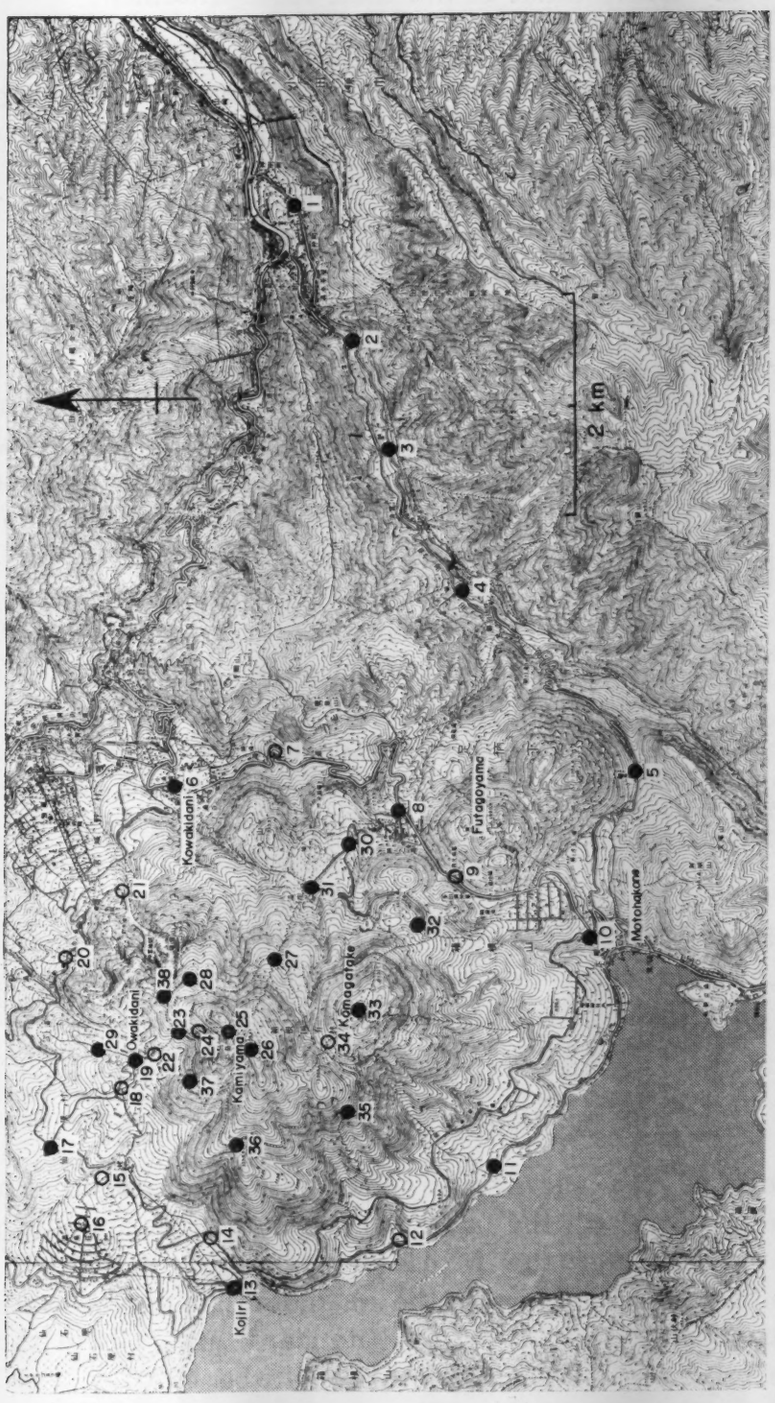

Fig. 1. Distribution of measuring points.
Full circles: Brass bars are buried as bench marks.
Hollow circles: Only wooden bars are buried.

2. Distribution of the total force intensity

Since three components of geomagnetic field or dip have been usually measured over volcanoes, no general representation of geomagnetic anomalies in the total force intensity has been obtained yet. In order to have an idea of the distribution of total force, we may study a somewhat idealized case in the following. When a circular cone with a radius of 5 *km* and a height of 0.8 *km*, which may well represent the mean topography of Ooshima Island, is uniformly magnetized in the direction of the geomagnetic field, the magnetic field caused by the natural remanent magnetization of rocks has been calculated by Rikitake[4]. As the results were expressed in the way of the distributions of three geomagnetic components, the writers have calculated the distribution of the total force intensity from them. Fig. 2 shows this result when the intensity of magnetization is taken to be unity and the normal dip at the cone is assumed to be 48°. It is noticeable that the maximum anomaly of the total force intensity is found at a point slightly south of the summit and that the regions of small anomaly appear on the east-west line, which results in the depression of the iso-anomaly lines towards the summit on that line.

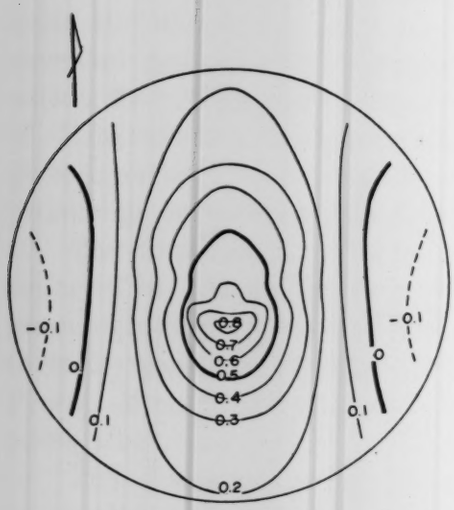

Fig. 2. The total force intensity of the magnetic field on the surface of the cone, when $J=1$ *e.m.u./cc.* (unit in gauss).

3. Results of the survey

The results of the survey are shown in Table 1 together with the height above sea level of the measuring points. Surroundings of the stations are sketched for the future measurements in Fig. 8. Corrections for the diurnal variations in the magnetic field have been made by adopting Aburatsubo station as the standard one, where the normal value of the total force intensity is taken to be 45707 γ, the value at 0^h00^m(J.S.T.) on Oct. 30, 1959. Thus corrected values are also shown

4) T. RIKITAKE, *Bull. Earthq. Res. Inst.*, **29** (1951), 161.

Table 1. The results of the survey.

No.	Locality		Height above sea level	Date	Total force intensity	Corrected total force intensity*)
1	湯本幼稚園	Yumoto Kindergarten	120m	Oct. 26th 14h51m	46000.7γ	46034.7γ
2	須雲園バンガロー	Sugumoen	165	15 20	45131.7	45165.3
3	初　花　荘	Hatuhana-sô	255	15 46	45648.4	45688.8
4	発電所上	Electric powerhouse	335	16 09	46418.7	46470.2
5	甘酒茶屋	Amazake-tyaya	700	16 40	45552.1	45594.1
6	翠松園ホール前(小涌園)	Suisyô-en Hall	595	Oct. 27th 10 25	45939.6	45984.1
7	恵明学園	Keimei-gakuen	670	10 45	46846.2	46878.1
8	芦　ノ　湯	Asinoyu	870	11 11	46782.8	46818.9
9	曾我兄弟の墓	Graves of the Sogas	870	11 27	45627.2	45662.6
10	元　箱　根	Motohakone	805	11 56	46317.7	46358.1
11	元箱根キャンプ場	Wood for camping	740	13 28	46313.0	46341.0
12	九頭竜明神	Kutôryû-myôzin	735	13 42	47045.8	47076.2
13	湖　　尻	Koziri	725	14 01	46073.5	46108.8
14	自動車専用道路入口	Gate to the toll road	780	14 20	46266.1	46306.9
15	姥　　子	Ubako	875	14 57	46437.5	46437.2
16	上温泉荘バス停留所前	Kami-Onsen-sô	840	15 12	46223.8	46252.7
17	大涌谷下十字路	Oowakidani T-shape joint	930	15 31	47142.1	47164.9
18	大涌谷下	Wayside of the toll road to Oowakidani	1010	15 45	47074.0	47100.3
19	大涌谷登山口	Oowakidani	1045	15 58	46498.6	46528.9
20	上湯一強羅間	Side of the toll road between Kaminoyu and Sôunzan	800	16 27	46630.1	46658.4
21	早雲山見晴台下	Sôunzan	750	16 45	46639.5	46684.1
22	大涌谷登山道	Above fumaroles of Oowakidani	1080	Oct. 28th 9 15	46484.5	46504.2
23	神山一早雲山別れ道	Cross-way of northern flank of Mt. Kamiyama	1180	9 59	46256.7	46281.0
24	神山登山道	Wayside to Kamiyama	1245	10 32	47825.6	47851.3
25	冠ケ岳下	At the foot of Kanmuri-ga-take	1350	11 10	47315.9	47338.6
26	神山頂上三角点	Summit of Mt. Kamiyama	1438	11 44	47539.0	47552.1
27	湯ノ花沢下り口	Cross-way of eastern flank of Mt. Kamiyama	1140	13 35	46702.9	46703.6
28	早雲山別れ道	Fork point	1205	14 19	46893.1	46895.1
29	大涌谷一上湯間	Wayside at the north of Oowakidani	980	15 46	47149.1	47152.2
30	湯ノ花沢ケーブル岐点	Fork point at Yunohanazawa	910	Oct. 29th 9 15	47485.0	47504.4
31	湯ノ花沢駐車場	Yunohanazawa	925	9 37	46047.6	46068.8
32	駒ケ岳ケーブル(登り口)	At the foot of Komagatake	1025	9 53	46132.2	46154.7
33	駒ケ岳頂上	Summit of Komagatake	1360	10 37	46578.4	46595.2
34	駒ケ岳北西山麓	North-western flank of Mt. Komagatake	1230	11 42	46190.9	46215.3
35	坊ケ沢下り口	Fork point above Bôgasawa	1190	12 15	46707.6	46724.8
36	神山西北西麓	On the western flank of Mt. Kamiyama	1195	13 44	46686.5	46695.2
37	冠ケ岳麓	North-western slope of Mt. Kanmuri-ga-take	1190	14 27	46569.0	46577.7
38	早雲山上方	Wayside above Sôunzan	1230	15 28	47489.7	47502.2

*) Corrected values for the diurnal variation.

Fig. 3. Distribution of the total force intensity.
(Unit in gammas)

in Table 1. On the basis of these data, isodynamic lines are drawn as can be seen in Fig. 3.

The normal values of the total force intensity in the neighbourhood of Hakone Volcano is obtained to be 46040 γ from the magnetic chart for 1950.0. Therefore the area surveyed this time has anomalies more than 500 γ as a whole. Besides this large scale anomaly, local anomalies of narrow extent are remarkable. We can see, from Fig. 3, several foci of large intensity are scattered within the caldera corresponding to the distribution of central cones. The region around Mt. Kamiyama is specified by a large anomaly of the total force intensity, while anomalies

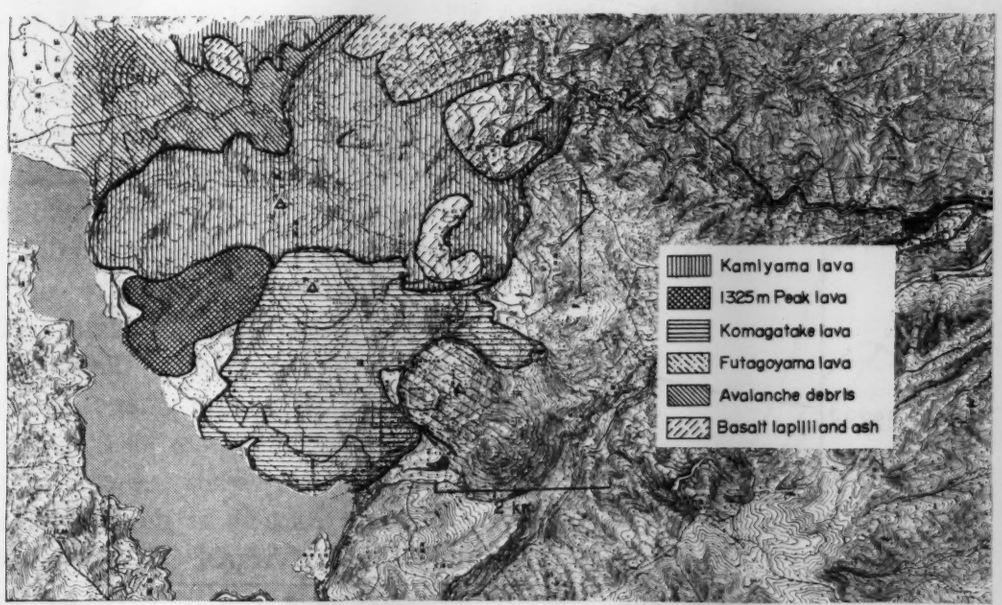

Fig. 4. The geological map in the central parts of the caldera. (After H. Kuno)

in the vicinity of Mt. Futagoyama seem rather small. Measurements on Mt. Komagatake have shown that the cone is magnetized with an intermediate intensity between Mt. Kamiyama's and Mt. Futagoyama's. In these territories bounded by central cones, there exist a few patches of great intensity that seem to have no apparent correspondence to the topography. This suggests that the magnetic field on the ground is more seriously affected by the magnetic properties of materials near the surface of the earth than by the togography. A geological chart[5] that is shown in Fig. 4 will ascertain it more clearly. The above stated anomaly characterized by every central cone can be illustrated by the difference in the magnetization of lavas mainly composed of andesite that

5) H. KUNO, *Explanetory Text Geol. Map in Japan, Atami* (1952).

flowed out from these cones. Although the distribution of the patches of great intensity does not seem to depend on the topography, it may be understood from Fig. 4 that these extraordinarily anomalous regions are formed by sedimentation of basalt lapilli and ash from Huzi Volcano.

4. Magnetization of Mt. Kamiyama

In this section, the anomalous distribution of magnetic field around Mt. Kamiyama, which is the largest among the central cones, will be studied in detail. We see that the total force intensity increases in

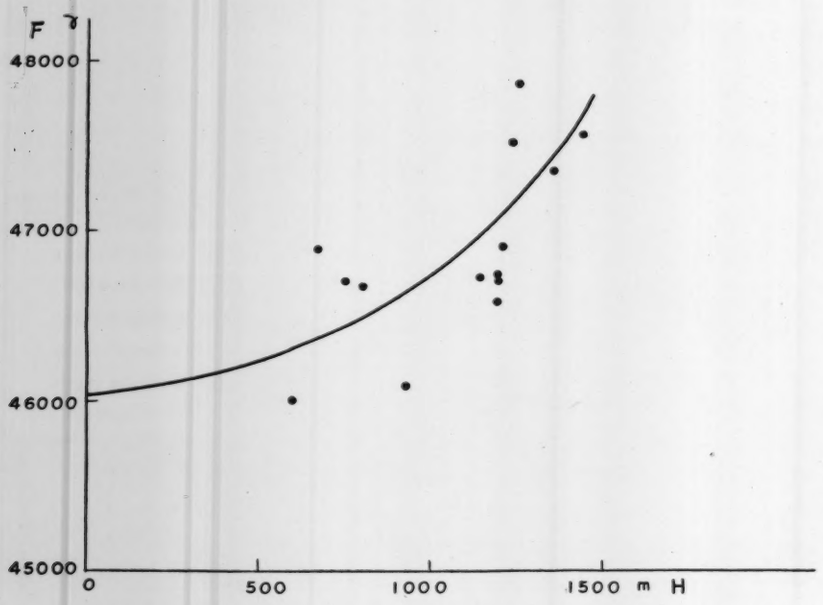

Fig. 5. Changes in the total force intensity with the altitude on Mt. Kamiyama.

general as the height above sea level increases. Fig. 5 shows how the magnetic field increases with the height.

It is also of interest to note that there exists an area of remarkably small anomaly in the north-western part of Mt. Kamiyama, whose topography shows as if the slope were engraved away just along the small anomalous region. The cross section along this valley is shown in Fig. 6. After Kuno[5], an explosion occurred in this part and the pyrocrastics due to this destruction were scattered widely over the north-western area of Mt. Kamiyama. The results of our magnetic survey seem to support the statement, because firstly it should be natural to consider that the small anomaly in that particular region may be caused

by the defect of magnetized materials which should have composed an ideal circular cone and secondly by the weakening effect of the magnetization due to the random orientation of magnetization of pyrocrastics. If the cone retained its complete form, judging from the present magnetic field, the distribution of total force intensity would be quite alike as that in Fig. 2.

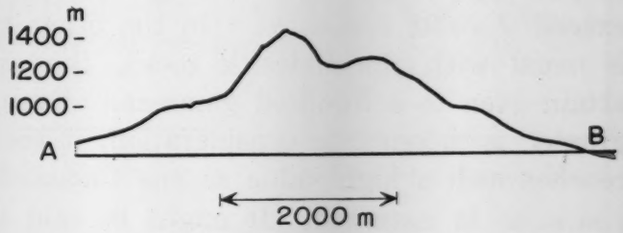

Fig. 6. Profile of Mt. Kamiyama along the line A–B in Fig. 3.

When the 700 m height above the sea level, which is the approximate height at the bottom of the caldera, is taken to be the base plane of Mt. Kamiyama, it may be allowed to approximate itself by a simple cone of 740 m in height and with a radius of 3 km. Assuming the values on the foot of the mountain to be 46000 γ, the anomaly of total force intensity on the top amounts to about 1500 γ. This anomaly is much larger than that of Mt. Asama, which is also an andesitic volcano as Mt. Kamiyama is. The anomaly related to Mt. Asama, however, amounts to a few hundred gammas at most[6].

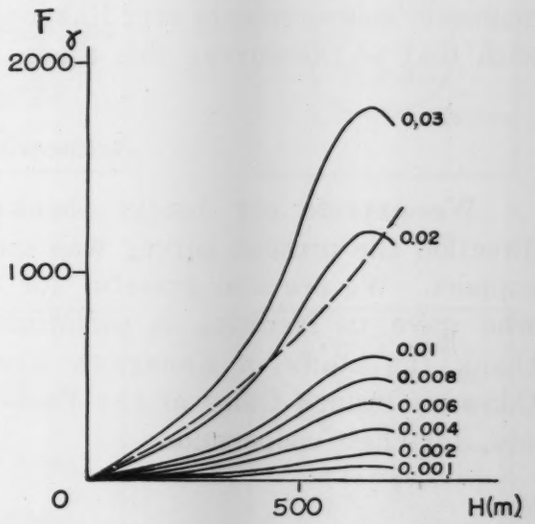

Fig. 7. The mean dependence of the total force intensity on the height, when a circular cone is uniformly magnetized. The intensity of magnetization J (in the unit of *e.m.u.*) is taken as a parameter. The broken line curve is obtained from measurements on Mt. Kamiyama.

If the mountain shape were regarded as the same as in the case of Fig. 2, where the altitude and radius are 800 m and 5 km respectively, the mean dependence of total force intensity upon the height would be shown as in Fig. 7, taking the intensity of magnetization J as a parameter. The result obtained by this survey is shown together by a broken line in Fig. 7. We cannot apply the results of the calculation to the case of Mt. Kamiyama as it is, because the mountain shape used in the calculation does not

6) T. MINAKAMI, *Bull. Earthq. Res. Inst.*, **18** (1940), 178.

agree with that of Mt. Kamiyama. If the calculation with regard to the mountain of the same shape as Mt. Kamiyama is carried out, the anomaly will become more marked than that in Fig. 7. Therefore it may be said from Fig. 7 that the magnetization of Mt. Kamiyama will never exceed $J=0.02$ *e.m.u./cc*. On the other hand if $J=0.001$ *e.m.u./cc*[7] as is usual with the andesitic rocks, the anomaly at the top does not attain even to a hundred gammas. Even if the correction for the topography is taken into consideration, it seems unlikely that the anomaly reaches such a high value as one thousand gammas, as far as $J=0.001$ *e.m.u./cc* is assumed. It might be said that the magnetization of Mt. Kamiyama is unexpectedly strong for an andesitic volcano.

In order to find geomagnetic changes that might be accompanied by the seismic activity of Hakone Volcano, it is of necessity to repeat the magnetic measurements over Hakone Volcano and to compare the results with that of the survey this time.

Acknowledgments

We express our hearty thanks to Dr. T. Rikitake, under whose direction the present survey was conducted, for his valuable advice and support. We are also grateful for his kind help to Prof. T. Minakami who gave us facilities in performing the measurements. The writers thank the staffs of Kanagawa Prefectural Office and the members of Odawara Branch Office of the Public Work Section, Kanagawa Prefecture, for their cooperation.

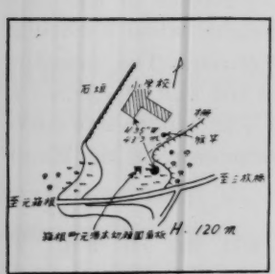

Fig. 8–1. Station No. 1.

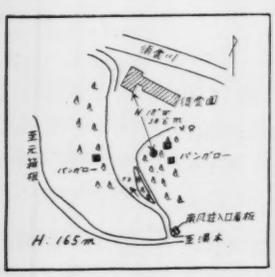

Fig. 8–2. Station No. 2.

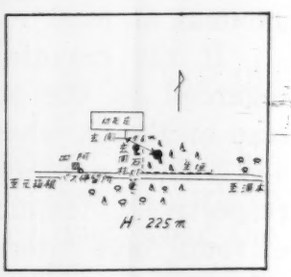

Fig. 8–3. Station No. 3.

7) T. NAGATA, S. AKIMOTO, S. UYEDA, Y. SHIMIZU, M. OZIMA and K. KOBAYASHI, *Phil. Mag. Suppl., Adv. Phys.*, **6** (1957), 225.

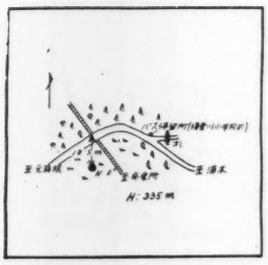

Fig. 8–4. Station No. 4.

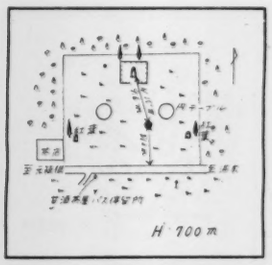

Fig. 8–5. Station No. 5.

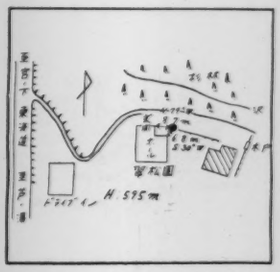

Fig. 8–6. Station No. 6.

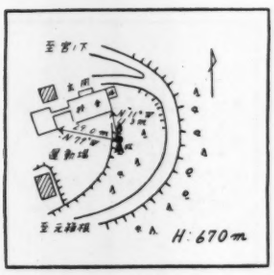

Fig. 8–7. Station No. 7.

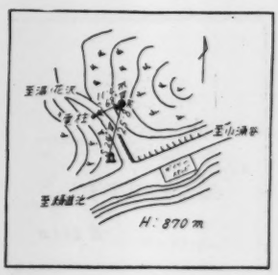

Fig. 8–8. Station No. 8.

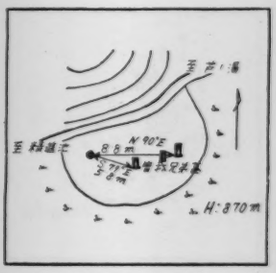

Fig. 8–9. Station No. 9.

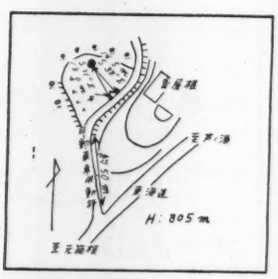

Fig. 8–10. Station No. 10.

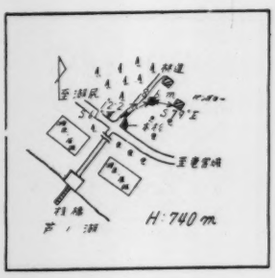

Fig. 8–11. Station No. 11.

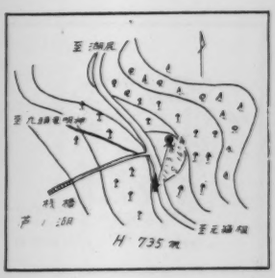

Fig. 8–12. Station No. 12.

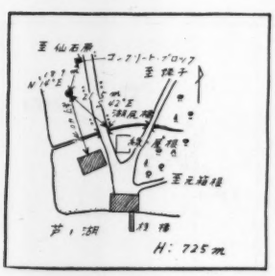

Fig. 8–13. Station No. 13.

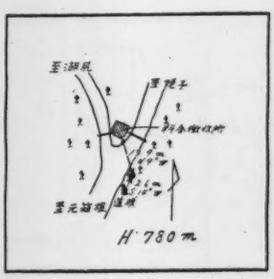

Fig. 8–14. Station No. 14.

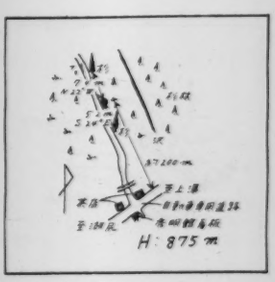

Fig. 8–15. Station No. 15.

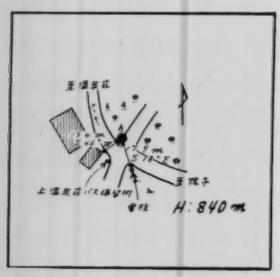

Fig. 8–16. Station No. 16.

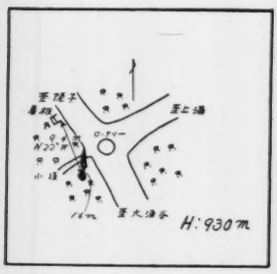

Fig. 8–17. Station No. 17.

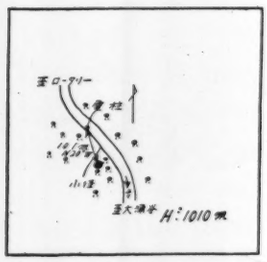

Fig. 8–18. Station No. 18.

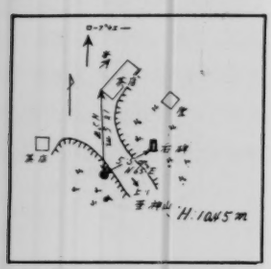

Fig. 8–19. Station No. 19.

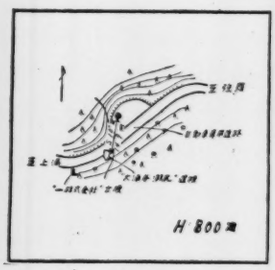

Fig. 8–20. Station No. 20.

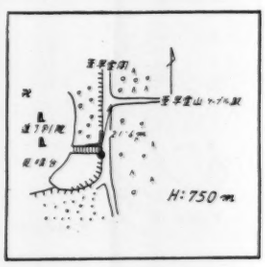

Fig. 8–21. Station No. 21.

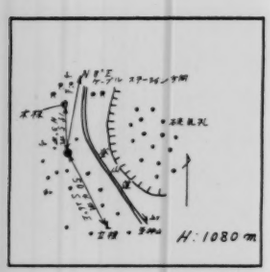

Fig. 8–22. Station No. 22.

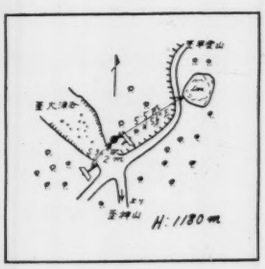

Fig. 8–23. Station No. 23.

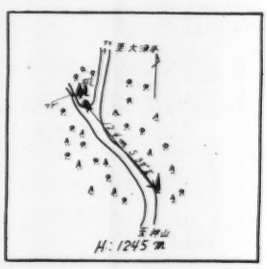

Fig. 8–24. Station No. 24.

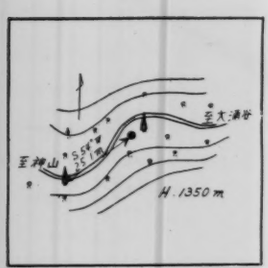

Fig. 8–25. Station No. 25.

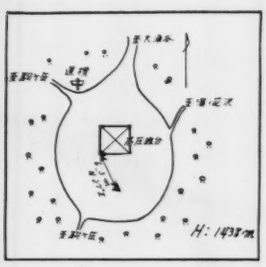

Fig. 8–26. Station No. 26.

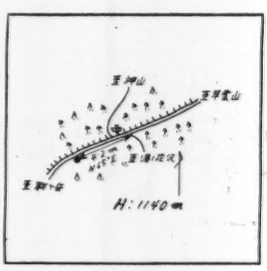

Fig. 8–27. Station No. 27.

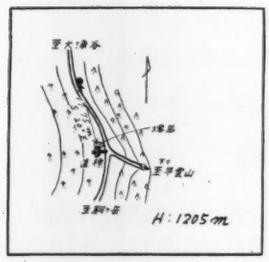

Fig. 8–28. Station No. 28.

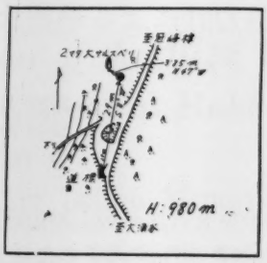

Fig. 8–29. Station No. 29.

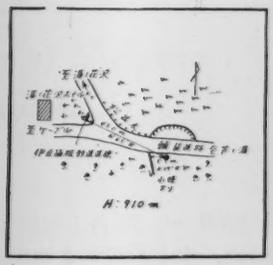

Fig. 8–30. Station No. 30.

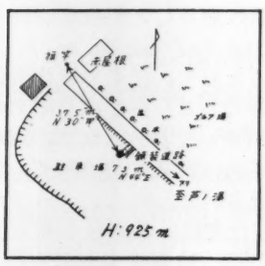

Fig. 8–31. Station No. 31.

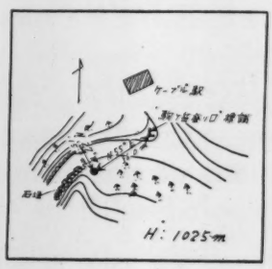

Fig. 8–32. Station No. 32.

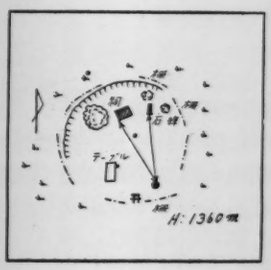

Fig. 8–33. Station No. 33.

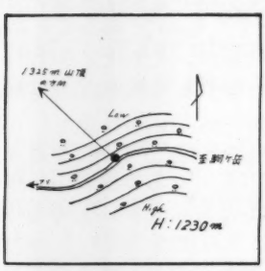

Fig. 8–34. Station No. 34.

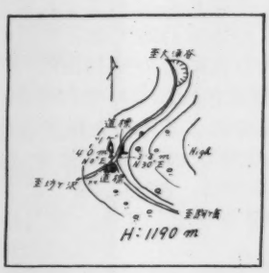

Fig. 8–35. Station No. 35.

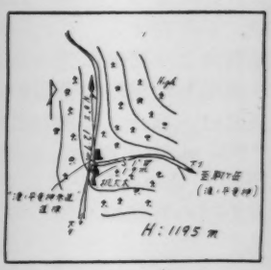

Fig. 8–36. Station No. 36.

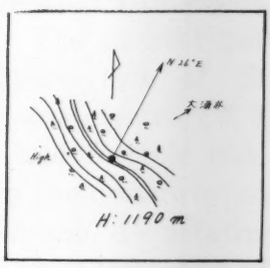

Fig. 8–37. Station No. 37.

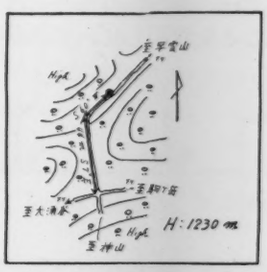

Fig. 8–38. Station No. 38.

4. プロトン磁力計による箱根火山の磁気測量

東京大学大学院 地球物理学課程 行武毅
地震研究所 棚岡巖

1959 年，9 月上旬以来，箱根火山中央火口丘の神山周辺に，有感地震を伴う地震活動が活潑となつた．水上教授によつてカルデラ内の数カ所に設置された地震計は，活動最盛期には，連日 200～300ケの地震を記録し，活動開始以来 3ケ月後に至つても，まだその終熄を見ていない．筆者等は，火山活動に伴つて期待される地磁気変化を検出しようと，箱根火山カルデラ内で，10 月 26 日から 29 日までの 4 日間プロトン磁力計を用いて，第 1 回目の磁気測量を行なつた．

火山地域では，火山の構造に関連して，磁気異常が観察される．大島三原山における地磁気偏角の連続観測より，現在では，火山活動と地磁気の変化との間に密接な関係のあることが推定されている．磁気測量を繰り返せば，箱根火山においても，同様のことが期待されるわけである．

使用したプロトン磁力計は，文部省科学試験研究費研究班の試作になるもので，従来の観測所固定用のものを，トランジスターを用いて小型化し，携帯に便利にしたものである．測定は全磁力だけに限られるが，携帯用プロトン磁力計の出現により，地磁気絶対測定が著しく容易になり，短時間内に数多くの測点で測定することが可能になつた．器械の精度については，測量に先立つて，油壺において地磁気変化計の記録と比較し，5γ 以上の誤差はないことが確認された．

測定の結果は，第 1 表，第 3 図に示されている．測定時の地磁気日変化量は，油壺観測所を基準にとつて補正した．火山構造に従がい，最低 45165.3γ から最高 47851.3γ におよぶ全磁力の地域的変動が見出される．また，図から明らかなように，カルデラの中央部は，大きく数ケの異常地域に分けることができる．すなわち，神山周辺の大きな磁気異常によつて特徴附けられる部分，双子山の小さな全磁力によつて特徴附けられる部分，その間の駒ケ岳を中心とする部分，これら中央火口丘によつて区画された領域内に，不規則に分布する，きわめて大きな全磁力を示す斑点状の地域，が存在する．これらの異常は，この地域の地下構造物質の違いにもとずくものであることが，地質図より明瞭に読みとれる．中央火口丘によつて特徴附けられる異常地域は，それぞれの火口より流出した熔岩の帯磁の差によつて形成されたものであるし，斑点状に分布する地域の大きな磁気異常は，富士火山礫および火山灰の帯磁によるものと推定される．

700 m の水準面を基盤として，この地域の磁気異常をみると，神山の如きは，700 m の高さで 1500γ もの異常を示している．この異常は，神山と同じような安山岩質の火山である浅間山で得られた値の数倍にも達する．地形の影響を考慮しても，神山の帯磁の強さは異常に大きいと考えられる．

第 1 回目の測量結果は，概略以上の通りである．今回のような測量を繰り返すことによつて，箱根火山においても，活動の消長に伴う磁気変化が明らかになるものと期待される．

今回の測量に当つて，終始，適切な指導と支持を頂いた，力武博士に感謝するとともに，種々の便宜を計らい，折にふれて助言を与えられた，水上教授に深く謝意を表わす次第である．なお，現地での測量に際しては，神奈川県庁ならびに小田原土木出張所の諸氏の御好意，御尽力に負うところがきわめて多いことを附記して，関係各位に御礼を申し上げたい

BULLETIN OF THE EARTHQUAKE
RESEARCH INSTITUTE
Vol. 38 (1960), pp. 55-70

5. *On the Mud-flows of the 1926 Eruption of Volcano Tokachi-daké, Central Hokkaido, Japan.*

By Isamu MURAI,

Earthquake Research Institute.

(Read Dec. 22, 1959.—Received Dec. 28, 1959.)

Introduction

Tokachi-daké, situated in central Hokkaido, Japan, is noted for its characteristic eruption of 1926. Villages lying at the western foot of the volcano were severely damaged by the mud-flows resulted from the eruption. Volcano Tokachi-daké lies in the central part of the Tokachi Volcanic Chain which runs south-southwest from Asahi-daké (Volcano Daisetsu-zan). It is a composite conical volcano consisting of a small central cone, double somma and several parasitic cones, and mainly of basic andesites.

The volcano may have been in eruption sometimes in the past, but for about a score years previous to the 1926 eruption, it had been only in a state of fumarolic activity, displaying a number of fumaroles in and about the crater of the central cone. Since 1923, the activity of the central cone had gradually increased, and culminated in violent explosive eruption of May 24, 1926. The greater part of the southwest side of the central cone was destroyed by the eruption, and forcible mud-flows run down the northwestern slope of the volcano, devastating forests, farms, meadows, and villages in their course. As to the nature of the 1926 eruption of Tokachi-daké, various views have been put forward

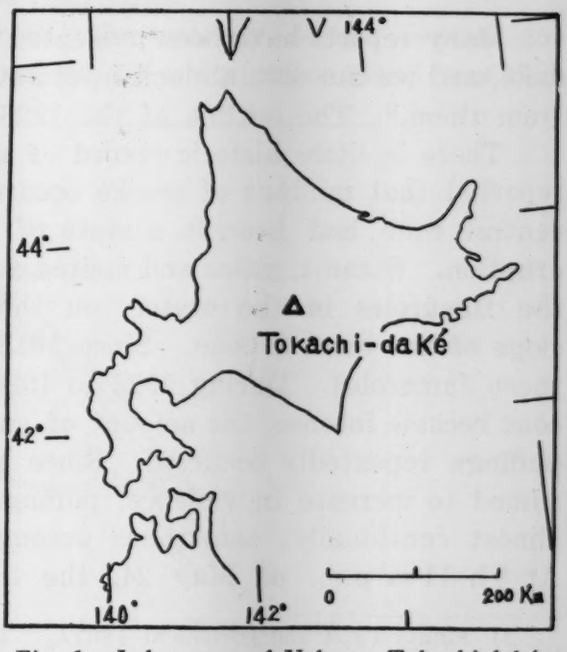

Fig. 1. Index map of Volcano Tokachi-daké.

by those who investigated the eruption, and particularly several questions about the origin and the mechanism of the mud-flows have been remained unsettled.

The writer had an opportunity to visit Tokachi-daké in 1959 and studied the deposits of the 1926 mud-flows on the spot. The field study and systematic sampling of the deposits have yielded information relating to the origin and mechanism of the mud-flows, which is presented in this report, with the results of the mechanical analyses of the deposits.

The writer wishes to express his sincere thanks to Prof. Hiromichi Tsuya of the Earthquake Research Institute, Tokyo University, for suggesting his investigation as well as for constant guidance in the course of the work. He is indebted to Mr. Matsuzo Nomura and Mr. Takeo Takeuchi of the Tokachi Sulfur Mine for giving facilities to his survey, and he is moreover indebted to Mr. Yoshichi Hosoya of the Komoro Branch of the Earthquake Research Institute, in Nagano Prefecture, for his aid in carrying out the mechanical analyses and as well as for preparation of figures in this paper.

Outline of the 1926 Eruption of Tokachi-daké

Many reports have been presented as to the 1926 eruption of Tokachi-daké, and we can obtain much information on the course of the eruption from them.[1] The outline of the 1926 eruption is as follows:

There is little historic record of violent eruption, though it has been reported that puffings of smoke occurred in 1854, 1887 and 1889. The central cone had been in a state of fumarolic activity before the 1926 eruption. Steams, gases and melted sulfur had emitted ceaselessly from the fumaroles in the crater, on the crater-rim and on the western slope of the central cone. Since 1918, sulfur had been mined out of these fumaroles. During 1923 to 1926, fumarolic activity of the central cone became intense, the amount of gases gradually increased and slight puffings repeatedly occurred. Since May 4, 1926, the activity had continued to increase in violence, puffings of smoke and rumbling occurred almost continually, sometimes accompanied by indistinct earthquakes. At 0 h 11 m p.m. of May 24, the first explosion occurred eventually.

1) Fumio TADA and Hiromichi TSUYA, "The Eruption of the Tokachi-dake Volcano, Hokkaidô, on May 24th, 1926", *Bull. Earthq. Res. Inst.*, **2** (1927), 49–84. (Japanese with English abstract.)

H. TANAKADATE, "The Eruption of Tokati-dake, Hokkaido, in the Year 1926," *Proc. 3rd Pan-Pac. Sci. Congr., Tokyo* (1926), 784–786.

The mud-flows swept away over the western slope of the volcano, damaged the Maruyama (Biei) hot spring and reached the Hatakeyama hot spring. It was inferred that the explosion occurred on the western slope of the central cone where many fumaroles had lain before. At about 2 h p.m. violent rumbling occurred, and at 4 h 18 m p.m. the second explosion occurred at the top of the central cone. Rumbling noises like the sound of distant thunder followed the explosion. The greater half of the northwest side of the central cone was destroyed with the explosion. The volume of the collapsed mass was estimated at about 2,000,000 m^3 or 4,000,000 m^3. The mud-flows rushed down with unexpected speed (estimated at about 50 m/sec on the average) over the western slope of the cone, poured into the valleys of the Biei-gawa and the Furano-gawa. The mud-flows finally flooded over the basin at the foot of the volcano, and about 25 minutes after the explosion they reached to the railway line running across the basin from north to south. Villages of Kami-Furano, Shimo-Furano and Biei, at about 25 km distant from the crater, were seriously devastated by the mud-flows, about 29 km^2 of land was washed away, 5080 houses were laid in ruin and 144 persons were drowned (Fig. 2). The ejection of bombs of about 3,000 m^3 followed after the tremendous mud-flows.

After the explosions of May 24, the activity of the central cone gradually diminished, but a large volume of white vapor cloud was rising

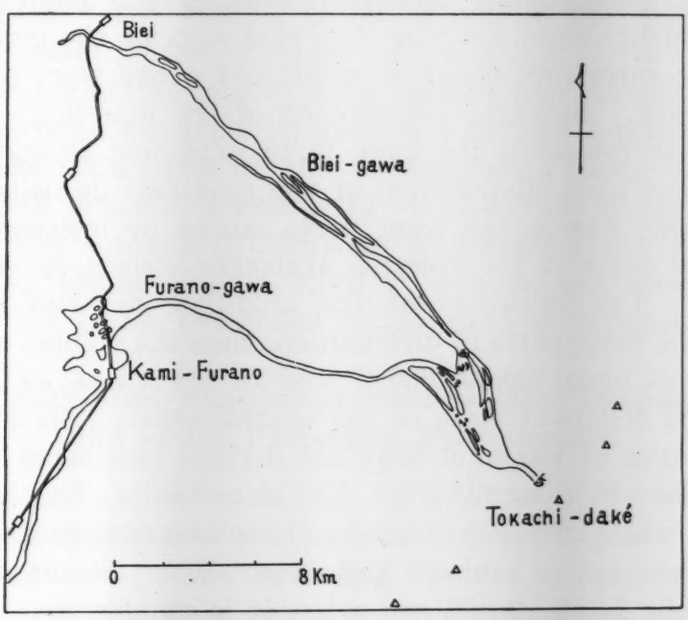

Fig. 2. Map showing the area covered with mud-flows.

continuously from the new explosion-crater. On Sep. 8, 1926, a heavy explosion occurred again, and after that the explosive activity continued for three years at intervals of about three months. Lately, the eruptive activity of the volcano has entirely ceased (Fig. 8). Steams and other gases are emitted from the fumaroles at the foot of the eastern crater-wall in the new explosion-crater of 1926. Sulphur is mined from these fumaroles (Fig. 8). Since 1942, other new fumaroles have grown at the spot of about 1 km north from the explosion-crater (Fig. 9).

Mud-flows

The greater half of the northwest side of the central cone collapsed at the second explosion of May 24, 1926. The mud-flows succeeded and poured down the mountain-side. Though the mud-flows also occurred at the first explosion, at 0 h 11 m p.m. on May 24, the second mud-flows were more tremendous and destructive. It was inferred that the huge mass of rock fragments thrown down from the west half of the central cone caused a hot volcanic avalanche on the western slope of the volcano, which suddenly melted the snow and brought about the mud-flows.

It is impossible to explain exhaustively the origin of the mud-flows by such inference, the writer considers. The front parts of the mud-flows which flooded over on the Kami-Furano Basin were explained as caused by such sudden melting of the snow on the mountain-side. It may be quite questionable, however, whether the main parts of the mud-flows which rushed down on the vast area of the gentle mountain-side with the surprising speed as mentioned above were also caused by melting of snow. Because, the deposits of the mud-flows occupy a vast area, and their volume is too huge to be explained by such mechanism. The area of the main distribution of the mud-flow deposits is computed at about 7 km^2, except the front parts caused by melting of snow and the uppermost parts of the volcanic avalanche caused by collapse of the central cone. The thickness of the mud-flow deposits is 3 m on the average in the main parts of distribution, then the volume of the deposits is calculated at about 20,000,000 m^3 and is ten times as great as the volume of the collapsed mass of the central cone. (See Figure 3.)

The deposits of the mud-flows are divided into three layers on their vertical section, in general (Figs. 13, 14 and 16). The lower layer is composed of white clay-rich deposits of rock fragments, the middle layer is of brown pumiceous ash and the upper layer is composed of black porous juvenile block, lapilli and ash. It is notable that a lot of charcoal is contained in the middle layer (Figs. 13 and 18). The lower layer

may represent the deposits of volcanic avalanche (volcanic mud-flow in strict sence) caused by collapse of the central cone, and it extends mainly on the upper slope immediately beneath the explosion-crater. The area of its main distribution is calculated at about 2.5 km², and its thickness is 2 m on the average. Then the volume of the white deposits (mud-flow) is estimated at about 5,000,000 m³. The writer tried to estimate the volume of the collapsed mass by using a small scale model (1 : 5,000) of clay, and obtained the same value. The mud-flows may have been caused by the collapse of crumbly rocks attacked by the fumarolic action. Both the first and the second explosion on May 24, 1926, raised such mud-flows. The mud-flows thus formed poured down the mountain-side, sweeping away the trees with which the mountain was thickly covered. They may have been fairly hot, but not been so hot to burn the trees.

At the second explosion, mud-flow, pumice-flow and scoria-flow succeeded consecutively, and the burning clouds of pumice and of scoria descended down the mountain-slope. The middle and the upper layer may represent the deposits of such pumice-flow and scoria-flow respectively. They have sometimes imperfectly welded parts. Trees buried in these pyroclastic flow deposits were altered to charcoal by their heat. The snow which had accumulated on the mountain-side melted at once by their heat, and consequently the melted water flooded in the valleys and on the basin. The burning clouds of pumice and scoria descended with volcanic gases, which withered up the plants on the mountain-side.

The thickness of the middle layer (pumice-flow deposits) and of the upper layer (scoria-flow deposits) are 2.5 m and 0.5 m respectively on the average, in the main parts of the distribution. Then, the volume of the pumice-flow deposits is calculated at 17,500,000 m³, and the volume of the scoria flow deposits is calculated at 3,500,000 m³. As the volume of the ejected bombs is only 3,000 m³, most of the juvenile materials effused from the crater descended in the state of pyroclastic flows.

Mechanical Analyses of the Mud-flow Deposits and of the Pyroclastic Flow Deposits

At the second explosion on May 24, 1926, of Volcano Tokachi-daké. The mud-flow deposits and the pyroclastic flow deposits lay in three layers as mentioned in the preceding chapter. The writer collected several specimens from these layers in various localities, and carried out the mechanical analyses of the specimens. Localities of the specimens

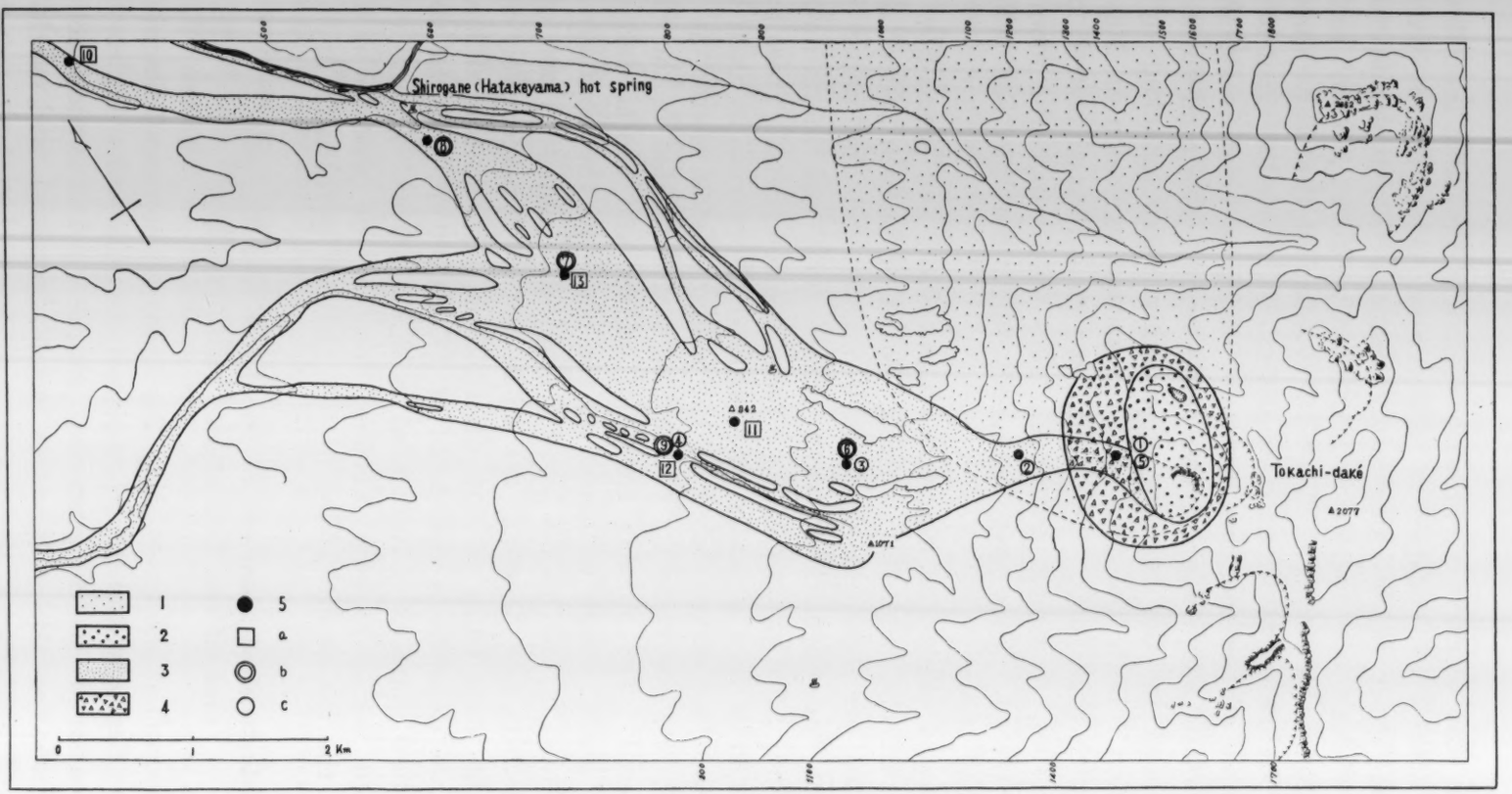

Fig. 3. The map of Volcano Tokachi-daké, showing the distribution of effusive materials. 1 : area covered with ash, 2 : area studded with new bombs, 3 : area covered with mud-flows and pyroclastic flows, 4 : area studded with ejected blocks, 5 : localities of specimens collected for the mechanical analyses, figures noted by them are the number of specimens, a : specimens of the mud-flow deposits, b : specimens of the pumice-flow deposits, c : specimens of the scoria-flow deposits.

collected are shown in Figure 3.

Each specimen, 0.5 to 1 kg weight, was divided into three parts: one, about 50 g weight, was put aside for preservation: another, about 30 to 50 g weight was prepared for the mechanical analyses of fine and medium fractions (mainly finer than 2 mm in diameters of particles), and the rest was used for analyses of coarse fractions (coarser than 2 mm in diameters of particles). The mechanical analyses of the second part were performed by means of sieving, decantation and pipette methods. The specimen was thrown into the 0.05 N solution of sodium hexametaphosphate for several days in order to accomplish perfect disaggregation of individual particles. Sometime specimens were disaggregated by mechanical manipulation. The second part of the specimen was divided into two parts by the decantation method, one coarser and the

Table 1. The results of the mechanical analyses. The result of the mechanical analysis of a given specimen is noted in the column beneath its specimen number with weight per cent of each fraction.

φ	1	2	3	4	5	6	7	8	9	10	11	12	13
−10∼−9	3.5	3.7						1.3					1.2
− 9∼−8	2.2	3.5			3.8	1.2	2.0	1.4		1.0	0.8		5.5
− 8∼−7	1.0	3.0	0.8		3.6	5.2	1.7	1.9		2.0	2.9	4.0	5.8
− 7∼−6	1.1	3.5	2.4		8.4	5.4	2.1	2.2		3.3	4.3	5.3	5.1
− 6∼−5	1.0	4.4	4.8	1.1	14.2	3.4	7.2	3.2		4.6	4.7	3.4	3.5
− 5∼−4	2.4	4.4	4.0	4.7	17.8	4.1	11.5	6.1		5.8	3.8	2.0	4.2
− 4∼−4	4.0	5.5	6.0	8.1	12.0	4.1	10.1	8.2		6.1	6.2	4.0	5.0
− 3∼−2	5.1	6.0	7.9	9.5	8.4	6.0	8.2	7.9	1.2	8.1	7.3	6.0	5.4
− 2∼−1	6.4	5.9	7.2	9.9	7.1	7.4	7.0	7.1	1.5	8.4	6.3	6.5	6.2
− 1∼ 0	12.5	8.3	7.1	13.3	7.6	10.5	9.2	10.2	3.5	10.0	10.6	8.8	9.1
0∼ 1	15.2	12.2	8.0	14.0	5.8	17.9	15.7	17.0	10.4	14.2	16.6	17.0	14.3
1∼ 2	15.2	10.0	7.9	9.6	3.2	16.8	12.0	14.8	15.3	12.3	15.0	15.7	12.7
2∼ 3	11.7	8.4	6.9	6.9	2.4	10.2	7.5	9.5	18.3	8.9	9.5	12.4	8.8
3∼ 4	7.0	5.8	6.2	5.3	1.9	4.2	2.8	4.5	18.9	6.0	6.1	7.2	5.9
4∼ 5	3.0	3.6	4.5	4.2	1.2	1.2	1.3	1.9	15.9	3.8	2.9	3.8	3.8
5∼ 6	1.7	2.9	3.9	3.4	0.6	0.7	0.5	0.7	5.4	1.9	1.3	1.2	1.6
6∼ 7	1.4	1.9	3.7	3.1	0.8	0.7	0.4	1.4	3.3	1.4	1.2	1.2	0.7
7∼ 8	2.1	1.5	4.1	2.2	0.7	0.5	0.5	0.4	2.4	0.8	0.3	0.6	0.8
8∼ 9	1.8	1.6	3.5	0.8	0.2	0.3	0.2	0.2	2.1	1.3	0.1	0.7	0.2
9∼	1.7	3.9	11.1	3.9	0.3	0.2	0.1	0.1	1.8	0.2	0.1	0.2	0.2

other finer than 1/32 mm in diameters of particles. The coarser part was dried up and sized by means of sieving with woven wire screens. The finer part was analysed by the pipette method. The remaining part

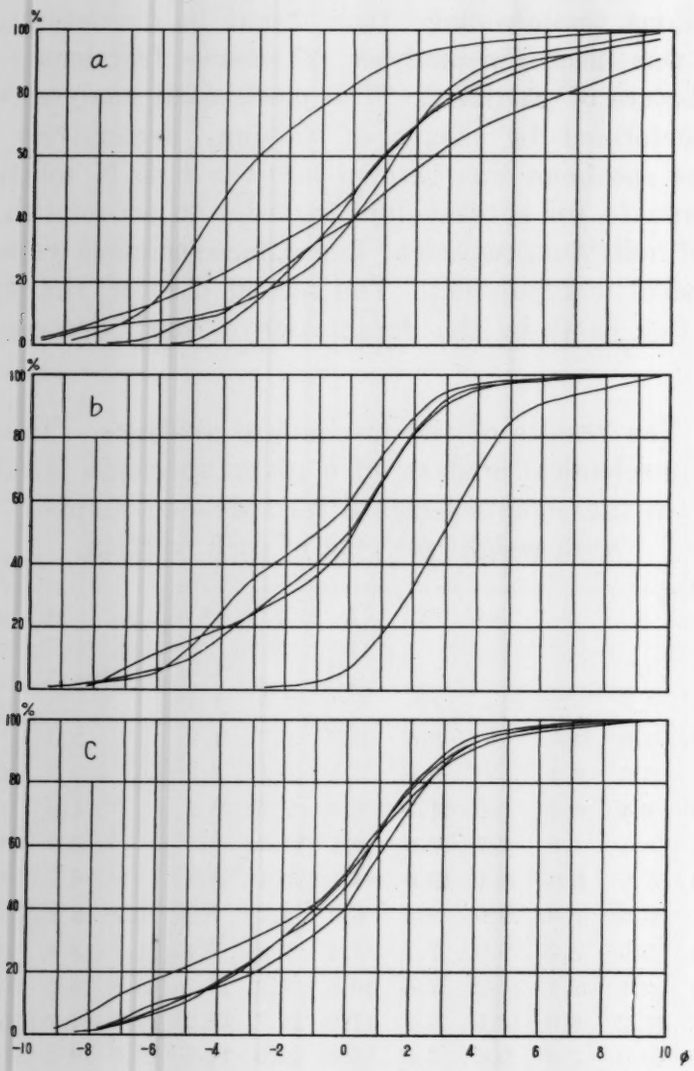

Fig. 4. Cumulative curves of particle size distribution.
a : mud-flow deposits (sp. nos. 1, 2, 3, 4, 5),
b : pumice-flow deposits (sp. nos. 6, 7, 8, 9),
c : scoria-flow deposits (sp. nos. 10, 11, 12, 13).

of the specimen was analysed by sieving the fractions coarser than 2 mm in diameter of the particles. Besides, the result obtained through such steps of mechanical analyses was corrected as to the fractions coarser than 16 mm in diameters of particles, referring to the photographs of

the outcrop from which the specimen was picked up. The final results of the mechanical analyses are shown in Table 1, each figure listed on the column represents the weight per cent of each fraction of the

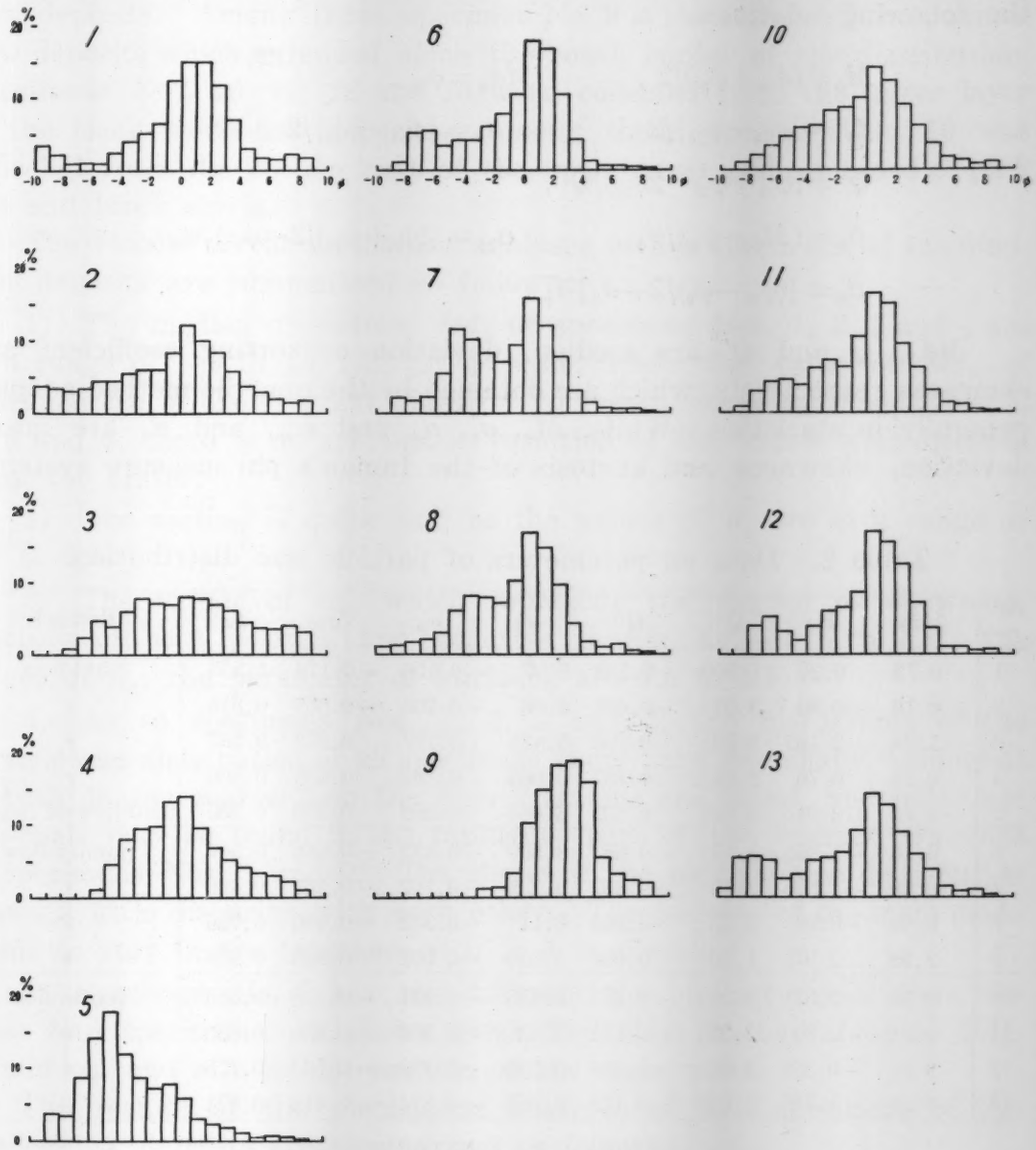

Fig. 5. Histograms of particle size distribution.
The number of specimen is noted on the left of each histogram.

specimen. Fig. 4 and Fig. 5 show the particle size distribution of the specimens by cumulative curves and histograms respectively. The diameters of particles in millimeters ξ are replaced here by ϕ as expressed $\phi = -\log_2 \xi$ for convenience.

The phi values of the percentiles, ϕ_5, ϕ_{16}, ϕ_{25}, ϕ_{50}, ϕ_{75}, ϕ_{84} and ϕ_{95} were read on the cumulative curves, and the approximate values of every sort of parameters of the particle size distribution were calculated from the following relations.

$$M_\phi=(\phi_{16}+\phi_{84})/2\ , \qquad Md_\phi=\phi_{50}\ ,$$
$$Q'=|\phi_{75}-\phi_{25}|/2\ , \qquad \sigma_\phi=|\phi_{84}-\phi_{16}|/2\ ,$$
$$Q''=(\phi_{75}+\phi_{25}-2\phi_{50})/Q'\ ,$$
$$\alpha_\phi=(M_\phi-\phi_{50})/\sigma_\phi\ , \qquad \alpha_{2\phi}=\{(\phi_5+\phi_{95})/2-\phi_{50}\}/\sigma_\phi\ ,$$
$$\beta_\phi=\{(\phi_{95}-\phi_5)/2-\sigma_\phi\}\sigma_\phi\ .$$

Md_ϕ, Q and Q' are median, deviation or sorting coefficient and skewness respectively, which are obtained by the quartile method adopted generally in statistics. While, M_ϕ, σ_ϕ, α_ϕ and $\alpha_{2\phi}$, and β_ϕ are mean, deviation, skewness and kurtosis of the Inman's phi measure system.[2)]

Table 2. Data on parameters of particle size distribution.

Sp. no.	Md_ϕ	M_ϕ	Q'	Q''	$\sigma\phi$	$\alpha\phi$	$\alpha_{2\phi}$	$\beta\phi$	Remark
1	0.73	0.25	1.805	−0.138	3.07	−0.156	−0.174	1.555	mud-flow
2	0.16	−0.80	3.01	−0.431	4.66	−0.206	−0.069	0.816	〃
3	1.23	2.195	3.72	0.198	5.425	0.177	0.272	0.537	〃
4	0.20	0.76	2.24	0.187	3.065	0.182	0.535	0.960	〃
5	−3.82	−2.915	2.125	0.625	3.065	0.309	0.539	0.786	mud-flow of Sept. 3
6	0.16	−1.355	2.13	−0.685	3.500	−0.432	−0.586	0.547	pumice-flow
7	−0.98	−1.505	2.48	−0.387	3.225	−0.162	−0.164	0.469	〃
8	0.04	−0.90	2.23	−0.663	3.11	−0.302	−0.490	0.725	〃
9	2.98	2.975	1.39	0.000	2.025	−0.002	0.323	0.933	〃
10	0.06	−0.575	2.305	−0.377	3.495	−0.181	−0.178	0.655	scoria-flow
11	0.21	−0.80	2.235	−0.612	3.33	−0.303	−0.430	0.635	〃
12	0.61	−0.335	2.06	−0.495	3.235	−0.292	−0.533	0.775	〃
13	−0.10	−1.735	2.895	−0.728	4.365	−0.374	−0.413	0.471	〃

The values of these parameters are listed in Table 2.

Specimens Nos. 1, 2, 3 and 4 were collected from the lower layer of the white mud-flow deposits. Specimen No. 5 is the sample of another brown mud-flow deposit which overlay the former on the western

2) D. L. INMAN, "Measures of Describing the Size Distribution of Sediments", *Jour. Sed. Petrol.*, **22** (1952), 125–145.

slope immediately beneath the explosion-crater (Fig. 11). Perhaps, these may have deposited at the explosion of Sep. 8, 1926. Specimens Nos. 6, 7, 8 and 9 were collected from the middle layer of the brown pumice-flow deposits. Among them, specimen No. 9 is the sample of the pumice-flow deposits which extended along the south border of the distribution. Specimens Nos. 10, 11, 12 and 13 were collected from the upper layer of the black scoria-flow deposits. Among them, specimen No. 10 was collected from the bottom part of the upper layer and composed of pink ash and black scoria.

The results of the mechanical analyses of five specimens of the mud-flow deposits are summarized as follows:

1) The median diameters, Md_ϕ of specimens Nos. 1, 2, 3 and 4 are in a range of -0.15 to 1.23 in ϕ scale, while the value of Md_ϕ of specimen No. 5 shows great disparity to them. As to specimens Nos. 1, 2, 3 and 4, there is no systematic variation of Md_ϕ values with distance from the crater.

2) The sorting is quite bad, as the values of σ_ϕ are in a range of 3.0 to 5.5.

3) The values of α_ϕ, which represent the degree of skewness, scatters in both positive and negative ranges, as -0.15 to 0.3. The values of β_ϕ, the parameter of kurtosis, are 0.5 to 1.5.

4) As to specimens Nos. 1, 2, 3 and 4, the histograms of the particle size distribution of all specimens show very flat shape, tailingout of both in the coarser and the finer fractions are found, and indistinct sub-mode may be found in the tailingout part of the coarser fractions of specimens Nos. 1 and 2. The shape of the particle size distribution shows a little disparity with each other. The position of the main mode seems to stay in the fractions of 0 to 2 in ϕ scale.

5) Specimen No. 5 has the different size characteristics from the other four specimens. It shows great disparities in the values of Md_ϕ, σ_ϕ and α_ϕ, and also in the position of the main mode.

The results of the mechanical analyses of four specimens of the pumice-flow deposits are summarized as follows:

1) The median diameters, Md_ϕ of specimens Nos. 6, 7 and 8 stay exclusively in a range between -1.0 to 0.2 in ϕ scale and the regular variation of Md_ϕ values with distance from the crater can not be found. The value of Md_ϕ of specimen No. 9 shows a large disparity to the other specimens.

2) The sorting is firly bad, as the values of σ_ϕ are in a range of

2.0 to 3.5, but may be not so bad as in the case of the mud-flow deposits.

3) The values of α_ϕ stay exclusively in a range of -0.4 to 0. The values of β_ϕ do not so widely scatter as in the case of the mud-flow deposits, and stay in a range of 0.4 to 0.9.

4) All specimens have quite similar size characteristics to each other, except that specimen No. 9 has smaller Md_ϕ value than the other specimens. As to specimens Nos. 6, 7 and 8, the shape of the particle size distribution shows well resemblance, each has a main mode on the fraction of 0 to 1 in ϕ scale, and has a sub-mode in the coarser fractions whose position varies in each specimen. Tailingout of both in the coarser and the finer fractions are found in every case. Specimen No. 9 seems to have no sub-mode.

The results of the mechanical analyses of four specimens of the scoria-flow deposits are summarized as follows:

1) The median diameters stay exclusively in a range of -0.1 to -0.6 in ϕ scale, and the regular variation of Md_ϕ values with the distance can not be found as in the case of the pumice-flow deposits.

2) The sorting is also fairly bad as in the case of the pumice-flow deposits, and the values of σ_ϕ are in a range of 3.2 to 4.4. It may be inferred that the degree of sorting of the scoria-flow deposits may lie in the intermediate range between the pumice-flow deposits and the mud-flow deposits.

3) The values of α_ϕ stay in a negative range of -3.7 to -1.8. The values of β_ϕ stay in the same range as in the case of the pumice-flow deposits.

4) The particle size distribution of four specimens shows well resemblance with each other, each has a main mode in the fraction of 0 to 1 in ϕ scale, and has a sub-mode in the coarser fractions whose position varies widely. Tailingout of both in the coarser and the finer fractions are also found in every specimen.

The pumice-flow deposits and the scoria-flow deposits of the 1926 eruption of Volcano Tokachi-daké have similar particle size distribution to each other, and show the typical features of size characteristics of the pyroclastics flow deposits. They show fairly bad sorting as the values of σ_ϕ is larger than 2, tailingout of both the coarser and the finer fractions, fluctuation of the values of skewness in negative ranges, lack of regular variation of coarseness with the distance to the source, constant main mode in the fraction of 0 to 1 in ϕ scale, sub-mode in the coarser fractions, Md_ϕ values staying in a narrow range, and the

other features (Fig. 6). Such features are the typical size characteristics of the pyroclastic flow deposits, being in striking contrast to the normal projected pyroclastic deposits. The cumulative curves of the pumice-flow deposits and the scoria-flow deposits of Tokachi-daké resemble closely those of the other pyroclastic flow deposits, for example, pumice-flow

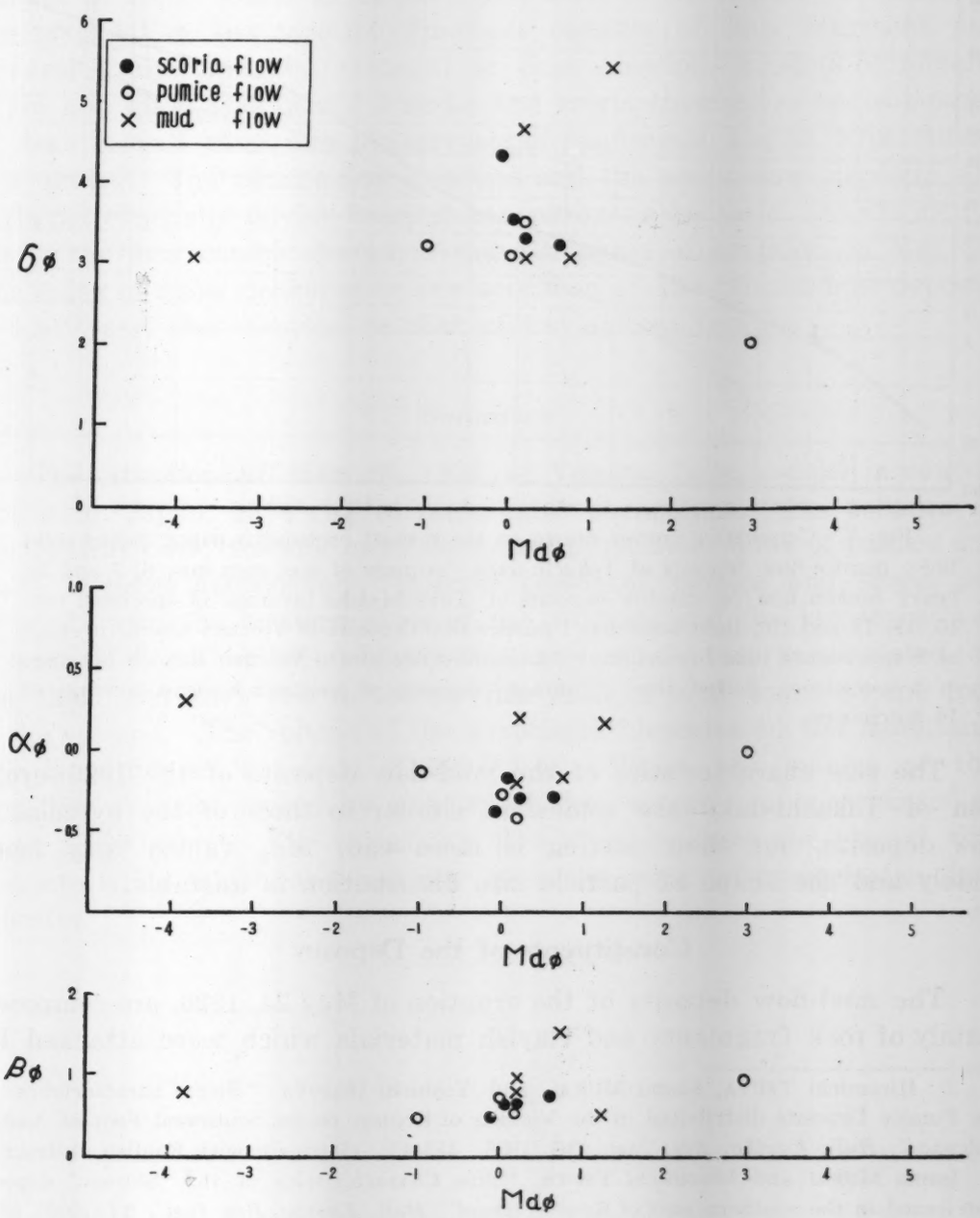

Fig. 6. The relation of the values of σ_ϕ, α_ϕ and β_ϕ to the values of Md_ϕ.

deposits of Volcano Asama and Volcano Hakone, and "Shirasu" deposits of southern Kyushu[3]. This may be recognized obviously in the diagram of cumulative curves plotted on the normal probability paper (Fig. 7).

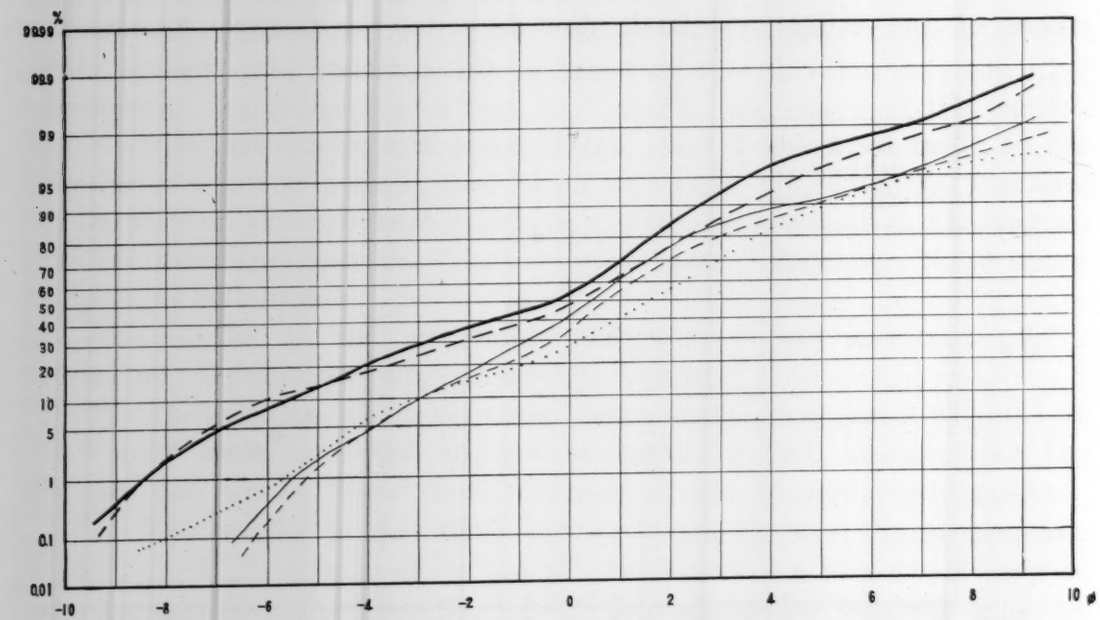

Fig. 7. Cumulative curves drawn on the normal probability paper. heavy solid line: pumice-flow deposits of Tokachi-daké (average of specimen nos. 6, 7 and 3), heavy broken line: scoria-flow deposits of Tokachi-daké (average of specimen nos. 10, 11, 12 and 13), light solid line: pumice-flow deposits of Volcano Asama (average of 9 specimens), light broken line: pumice-flow deposits of Volcano Hakone (average of 5 specimens), dotted line: "Shirasu" deposits of southern Kyushu (average of 10 specimens).

The size characteristics of the mud-flow deposits of the 1926 eruption of Tokachi-daké are somewhat similar to those of the pyroclastic flow deposits, but their sorting is more bad, Md_ϕ values vary more widely and the shape of particle size distribution is unstable.

Constituents of the Deposits

The mud-flow deposits of the eruption of May 24, 1926, are composed mainly of rock fragments and clayish materials which were attacked by

3) Hiromichi TSUYA, Isamu MURAI, and Yoshichi HOSOYA "Size Characteristics of the Pumice Deposits distributed in the Vicinity of Komoro on the Southwest Foot of Asama Volcano", *Bull. Earthq. Res. Inst.*, **36** (1958), 413–431. (Japanese with English abstract.)

Isamu MURAI and Hiromichi TSUYA, "Size Characteristics of the 'Shirasu' deposit distributed in the southern part of Kyushu Island", *Bull. Earthq. Res. Inst.*, **37** (1959), 637–647. (Japanese with English abstract.)

fumarolic action. Obviously, they are collapsed materials thrown down from the west half of the central cone at the explosion.

The pumice-flow deposits and the scoria-flow deposits consist of several different constituents, the material in the coarser fractions of mechanical composition consists dominantly of porous lava block and pumice or scoria which comes out in sub-mode of particle size distribution, the material in the medium fractions consists of lava fragment and mineral grain, and the material in finer fractions consists of mineral grain and glass fragment. Pumice and scoria themselves are composed of dark colored glass and phenocrysts of plagioclase, augite, hypersthene and olivine. The pumice-flow deposits and the scoria-flow deposits are both petrologically olivine-bearing two pyroxene andesite, and are identical to the new bombs ejected in the last phase of eruption on May 24. The index of glass measured on one specimen of the pumice-flow deposits is 1.519_5 and also identical to that of the ejected bombs.

Summary

The eruption of May 24, 1926, of Volcano Tokachi-daké in central Hokkaido, Japan, gave rise to remarkable phenomena. The collapse of the central cone, volcanic mud-flows and pyroclastic flows of pumice and scoria occurred successively. Burning clouds of pumice and scoria descended down the western slope of the volcano, and the hot deposits of pyroclastic flows melted suddenly the snow which had accumulated on the slope and gave rise to the terrible flood of mud water on the foot of the volcano. The volume of the pyroclastic deposits on the mountain-side is estimated at about 20,000,000 m^3. While, the volume of the mud-flow deposits caused by collapse of the central cone is estimated at about 5,000,000 m^3. The pyroclastic flow deposits show the typical size characteristics which are common in every case of pyroclastic flow deposits.

5. 北海道，十勝岳火山の泥流について

地震研究所　村　井　　勇

北海道の中央部に位置する十勝岳火山は，大正 15 年 (1926 年) 5 月 24 日に爆発を起し，その際発生した泥流によつて非常に大きな災害を惹き起した．十勝岳は不完全な形の三重火山で，中央火口丘は盛んに噴気をあげていたが，烈しい噴火活動の記録はほとんどなかつた．大正 13 年より 15 年にかけて噴気が烈しくなり，特に 15 年 5 月に入つてからは鳴動や地震を伴い，5 月 24 日遂に烈しい爆発が起つた．同日午後 0 時 11 分突然に最初の爆発が起り，泥流が発生して丸谷(美瑛)温泉を破壊し，更に流下して畠山温泉(現在の白金温泉の位置)に達した．爆発の起つた地点は中央火口丘の西方斜面上と推定された．更に午後 4 時 18 分第 2 回目の爆発が起つた．中央火口丘の西半分がこの爆発によつて破壊され，泥流が発生して非常な速度で西方斜面を流下していつた．その速度は平均 50m/sec 程度と計算された．山麓部の上富良野，美瑛および下富良野では，土砂や木材を混えた泥水が烈しい勢でおしよせ，土地および家屋に多くの被害を生じたばかりか，144 名の犠牲者を出した．中央火口丘の破壊された部分の体積は 2,000,000 m^3 あるいは 4,000,000 m^3 程度と計算された．また拋出された新火山弾は 3,000 m^3 と計算された．

上記のような大きな災害を惹き起した爆発の原因および泥流の成因については，多くの学者により様々な解釈が行なわれた．しかしそれらの間に意見の完全な一致は見られず，特に泥流発生の機構について多くの疑問が残された．その最も有力な解釈は，中央火口丘の破壊によつて生じた高温の崩壊物によつて積雪が急に融され，大規模な泥流が発生したとするものであつた．山麓部を襲つた泥水は，明らかに積雪の融解によるものと見られるが，山腹の広大な面積をおおつて流れた泥流の主流部は，そのような解釈によつては説明し尽すことはできないように考えられる(第 2 図参照)．筆者の調査によれば，泥流の主流部においては，堆積物は 3 層に分れており，下部の層は白色の粘土まじりの岩屑堆積物，中部の層は茶褐色の軽石をまじえた火山灰，上部の層は黒色の多孔質熔岩塊，岩滓および火山灰よりそれぞれ構成されている．中部層中には炭化木片が豊富に含まれており，また上部層，中部層とも部分的に不完全な熔結を示す場合が見られる．従つて中部層および上部層は堆積当時かなり高温であつたことは事実であり，その構成物質から見て，恐らく火山砕屑流の状態で流下し堆積したものと考えられる．中部層は軽石流，下部層は岩滓流の堆積物と呼んでよいであろう．一方，下部層の白色岩屑堆積物は，噴気作用を受けて変質した岩石破片および粘土よりなつており，明らかに爆発によつて中央火口丘が崩壊したために生じた岩屑の堆積したものであり，火山泥流と呼ぶべきものである．その主な分布の面積は約 2.5 km^2 であり，厚さを平均 2 m と見れば，体積は 5,000,000 m^3 となる．別に粘土で作つた 1/5,000 の模型から崩壊部の体積を計算したところ，同一の値が得られた．中部層および下部層の主な分布の面積は約 7 km^2 に達する．中部層の厚さは平均 2.5 m，上部層の厚さは平均 0.5 m と見られるから，それぞれの体積は 17,500,00 m^3 および 3,500,000 m^3 となる．下部層の泥流は余り高温であつたとは見られない．山麓部を襲つた泥水は，中部層および上部層の火砕流堆積物の熱によつて積雪が一時に融解したために生じたものと解釈される．5 月 24 日の第 2 回目の爆発と同時に泥流が発生し，それに引きつづいて，軽石流と岩滓流が山腹上を流下し，その熱によつて生じた融雪水の洪水が山麓の谷と平野の上を襲つたのである．

筆者は泥流，軽石流，岩滓流の堆積物の試料を数ケ所から採集して機械分析を行なつた．泥流堆積物は分級が非常に悪く，粒度分布の形は試料ごとに多少の変化が認められた．その中位粒径の値は火口からの距離に応じた規模的な変化をなんら示さないようであつた．軽石流堆積物および岩滓流堆積物は，火砕流堆積物に特徴的な粒度組成を示した．すなわち，分級は相当に悪く，粗粒部および細粒部に長く尾を引き，主モードの位置は変化がなく，粗粒部に副モードを持ち，採集地点の相異にかかわらず共通の粒度分布を示し，中位粒径の値も大きな変化を示さない，等の特徴を示した．

上記の軽石流堆積物および岩滓流堆積物はいずれも含橄欖石複輝石安山岩で，同時に拋出された火山弾と全く同一であつた．一つの試料についてガラス質破片の屈折率を測定したところ，1.519$_6$ の値を得たが，これも火山弾のガラス質部分の屈折率と全く同一であつた．

Fig. 8.

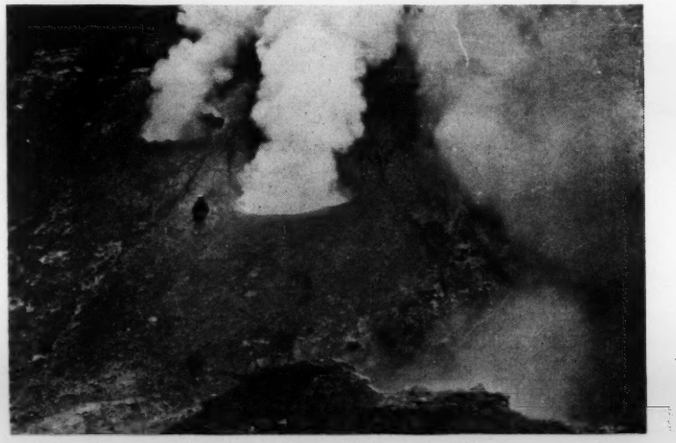

Fig. 9

Fig. 10.

Fig. 11.

Fig. 8. New explosion-crater of the 1926 eruption, looking from the south crater-rim.

Fig. 9. New fumalores which have grown since 1942.

Fig. 10. General view of Tokachi-daké, looking from the spot of 942 m height above the sea level on the west mountain-side. The right white cloud of vapor is that emitted from the new explosion-crater of 1926, and the left one is from the new fumalores.

Fig. 11. The surface of the 1926 mud-flow deposits, immediately beneath the explosion-crater.

（震研彙報 第三十八号 図版 村井）

（震研彙報 第三十八号 図版 村井）

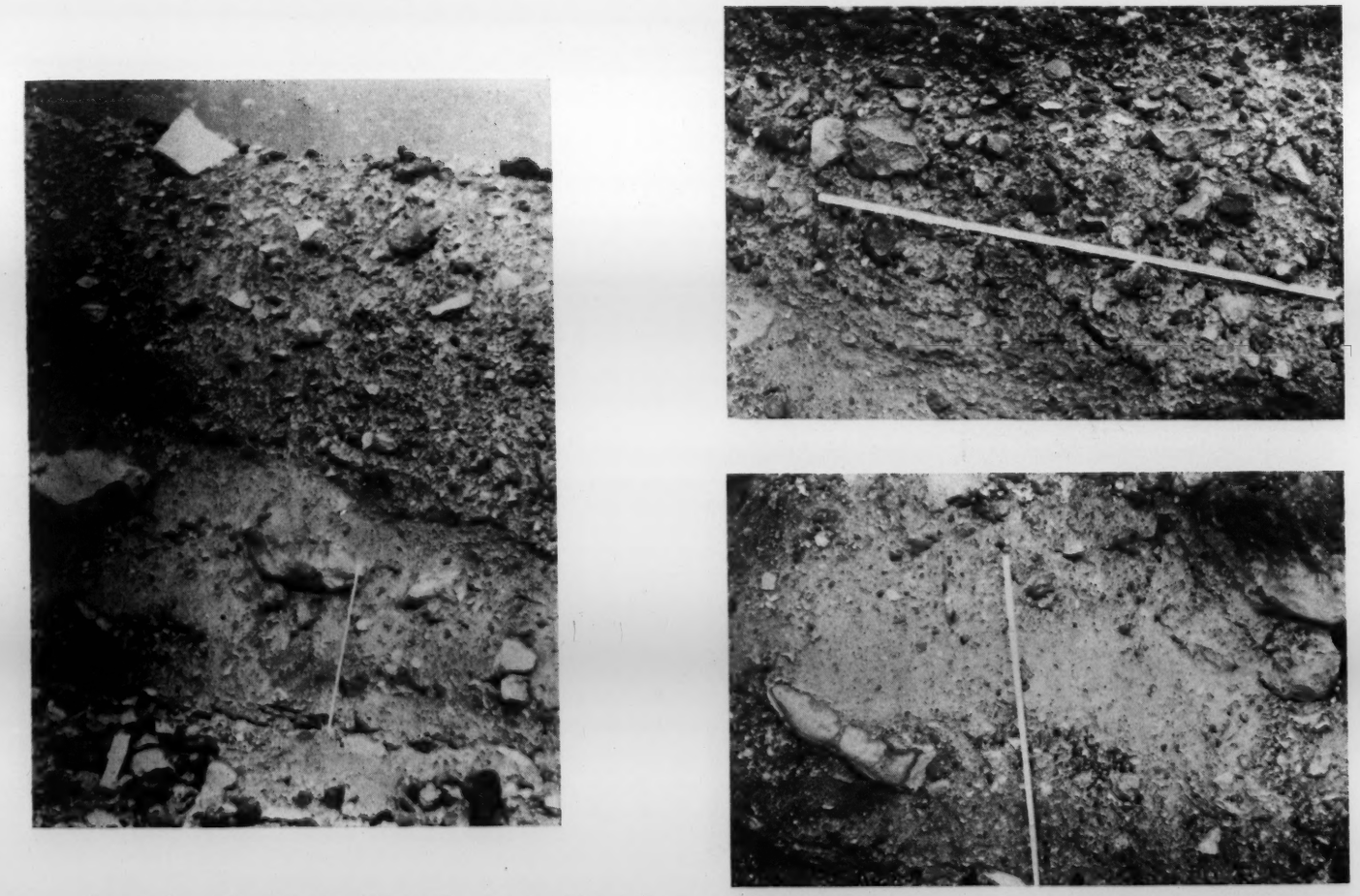

Fig. 12. The outcrop of mud-flow deposits from which specimen nos. 1 and 5 were collected, left is the whole section, upper right is the layer of brown mud-flow deposits (specimen no. 5) on Sept. 8, 1926, and lower right is the layer of white mud-flow deposits (specimen no. 1) on may 24, 1926.

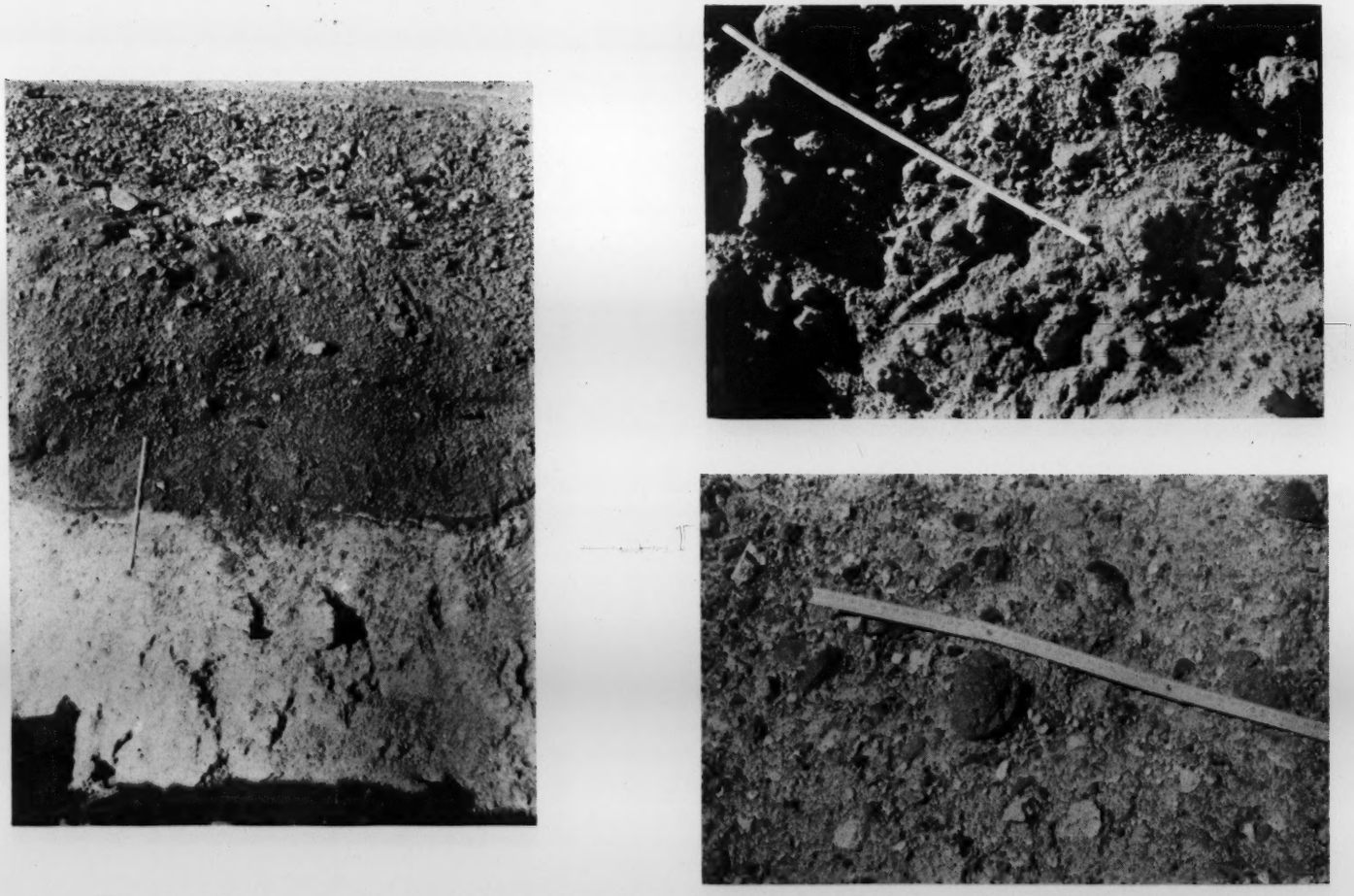

Fig. 13. The outcrop of mud-flow deposits and pumice-flow deposits from which specimen nos. 3 and 6 were collected, left is the whole section, upper right is the layer of pumice-flow deposits (specimen no. 6) containing small pieces of charcoal, and lower right is the layer of mud-flow deposits (specimen no. 3).

（震研彙報 第三十八号 図版 村井）

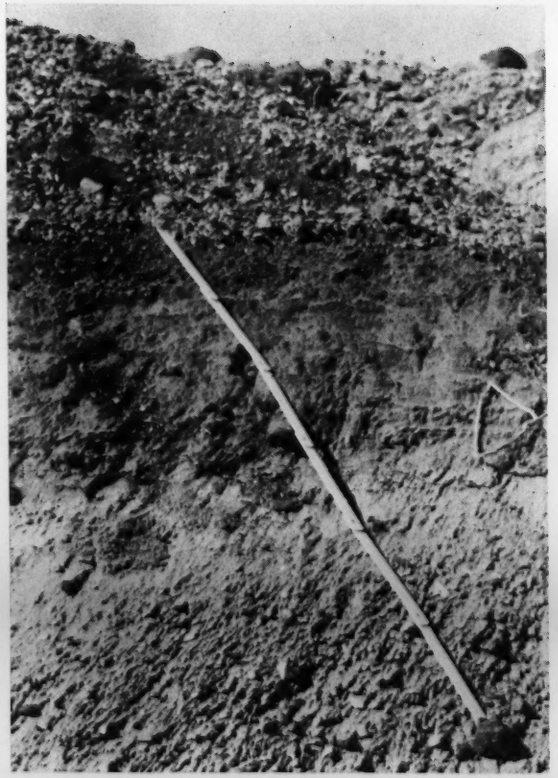

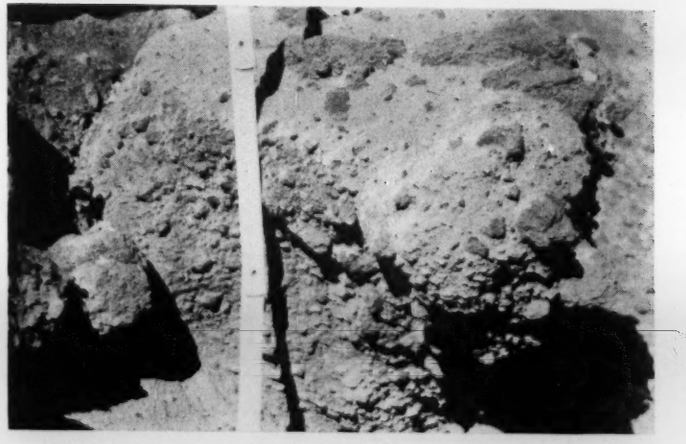

Fig. 14. The outcrop of scoria-flow deposits, fine pumice-flow deposits and mud-flow deposits, from which specimen nos. 4, 9 and 12 were collected, left is the whole section, upper right is the layer of scoria.flow deposits (specimen no. 12), and lower right is the layer of mud-flow deposits (specimen no. 4).

Fig. 15.

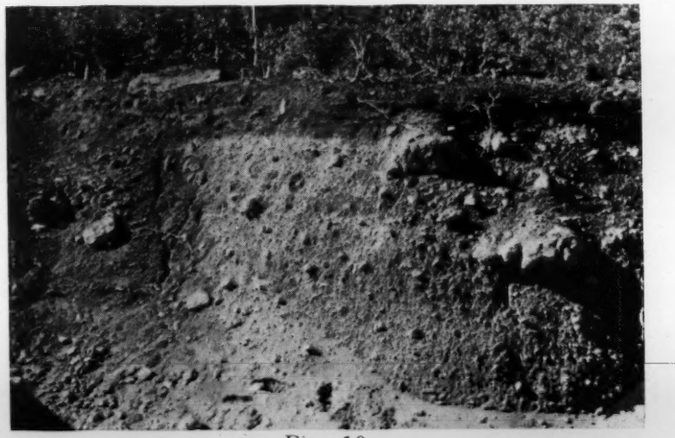

Fig. 16.

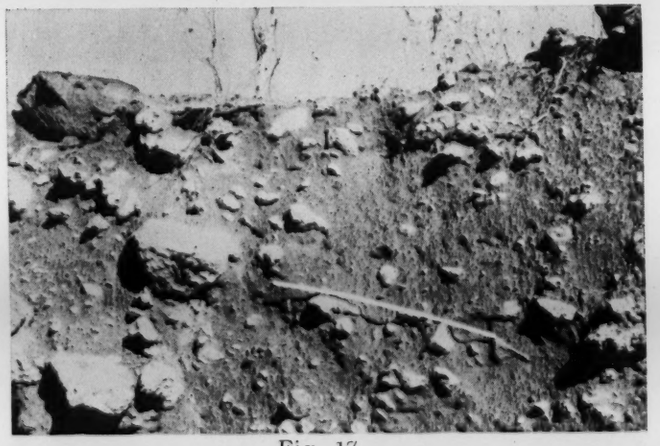

Fig. 17.

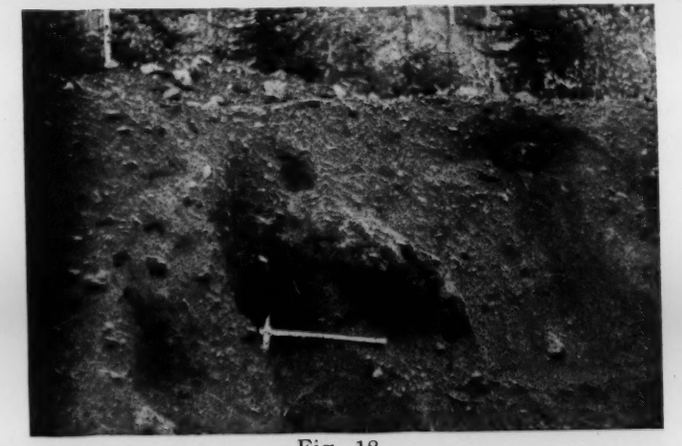

Fig. 18.

Fig. 15. Scoria-flow deposits and pumice-flow deposits in the valley of a tributary of the Biei-gawa, and the test plot of natural vegetation on the deposits, south of the Shirogane (Hatakeyama) hot spring.

Fig. 16. The outcrop of scoria-flow deposits and pumice-flow deposits, near the test plot of natural vegetation.

Fig. 17. The outcrop of scoria-flow deposits from which specimen no. 13 was collected, near the test plot of natural vegetation.

Fig. 18. The outcrop of pumice-flow deposits from which specimen no. 8 was collected, containing large pieces of charcoal, near the Shirogane (Hatokeyama) hot spring.

地震研究所彙報
第 38 号 (1960) 71-112 頁

6. 紀伊半島の局地地震 (第4報)

——臨時観測網による震源位置の決定——

地震研究所　宮村攝三

(昭和 34 年 3 月 24 日発表——昭和 34 年 12 月 28 日受理)

1952～1956 年 4 回にわたり実施した和歌山附近における臨時地震観測の験測結果を整理し，震源位置の決定をおこなつた．まず，もつとも多数の明確な p, s 着震時のえられた 1956 年の資料について，ことなれる型式の地震計をもつ観測点グループの資料を混用するときは，多数の資料の最小自乗法的処理によつても，p, s の着震時刻では合理的な結果がえられない．しかし，初期微動時間 $s-p$ ではおおむね適当な結果がえられる．そこで，つぎには資料の整一性をたもつため，主として石本式加速度計のみによる観測結果をもちい，すべての観測点のくみあわせについて $s-p$ 法で震源決定をおこなつた．そして，これらの結果の精度を検討し，個々の誤差を計算し，その誤差を考慮した平均値をもとめた．

えられた震源は北部の長瀞変成帯地域ではほぼ 10km 以浅に分布し，深度 2～3 km 程度の極浅発のものもあるが，南部の非変成秩父帯および四万十帯地域では震源はふかさ 10～30 km に分布し，北部にあるような極浅発のものはほとんどないらしいことが推定された．

1. 序　　言

すでにのべたように[1]，1952～1956 年 4 回にわたり和歌山附近に頻発する局地地震研究のために臨時的精密観測をおこなつた．大地震にともなう余震群の観測をはじめ，和歌山，伊東の群発地震など局地地震の震央地域における観測的研究は那須信治[2]の丹後地震余震 (1927) の観測以来しばしばおこなわれており，種々の興味ある事実が報告されている．これらの局地地震はその震源深度からかんがえて，地質学の対象となる地殻部分に生じているので，地質学からえられた知識との関連において考察するのにもつとも適当な地震活動であるとおもわれる．和歌山附近の地震群はかつて昭和初年の活動期に南海道地震との関連をかんがえて今村明恒[3]らにより研究されたが，筆者はさらにまた西南日本

1) S. MIYAMURA, "Local Earthquakes in Kii Peninsula, Central Japan, Part 3," *Bull. Earthq. Res. Inst.*, **37** (1959), 609–635.

2) N. NASU, "On the Aftershocks of the Tango Earthquake," *Bull. Earthq. Res. Inst.*, **6** (1929), 245–331; **7** (1929), 133–152; **13** (1935), 335–399.

3) A. IMAMURA, T. KODAIRA and H. IMAMURA, "The Earthquake Swarms of Nagusa and Vicinity," *Bull. Earthq. Res. Inst.*, **10** (1932), 636–648.

外帯に中央構造帯にそつて大井川上流，渥美湾附近，和歌山附近，剣山附近，大分県南部，熊本県，長崎県南部等点々と局地地震の活動が推定されることにも興味をもち，まづ紀伊半島の局地地震の地質学的意味を検討することに着手した．

局地地震の地質学的意義を検討するには，その震源位置を地質構造の単元と同程度の精度で決定することが必要である．そのために上述の臨時観測をおこなつたのであるが，もちろん震源位置の精密な決定には地震波速度についてのくわしい地下構造があらかじめしられていなければならない．地震観測網の設置された地域の人工地震による地下構造調査をおこなつて，それによりえられた構造にもとづく走時図を利用し，震源決定をおこなう方法は，もつとも理想的であるが，これはソ連において，トルクメンその他で若干実施されているだけである．われわれは自然地震の観測から地殻構造も同時にきめてゆかなくてはならない．現在，南アフリカ，タジックその他中央アジア各地および南カリフォルニアにおいては数百粁のひろがりに，非常に精密な常設観測網ができているが，わがくにの常設観測網は現在それらにくらべその感度と刻時の両面から不充分であり，紀伊半島における局地小地震の観測などにはあまり利用できない．われわれの和歌山附近における臨時観測では，前報告[1]でのべたように，同一標準時計による共通の分秒刻時を直接記象上に記入，記録紙速度も 4 mm/sec にして，常設観測網はもちろん，従来わがくにの余震観測等でこころみられたいかなる臨時的地震観測にくらべても，格段に精度のたかい観測をおこなつたので，南アフリカその他の一流の観測網に比肩しうる観測を，臨時的にではあるが，実現することができた．わがくにでは，従来，余震観測結果等の解析において，刻時の不備や，記録装置の故障，停電等により，各観測点で記録された地震の対応に，疑義をうむような事態に遭遇することがままあつた．特に計算または作図によつて適当な震央がもとめられなかつたり，震源深度が虚になつたりしたばあい，これが対応のまちがえによるとされることはしばしばあつた．事実，余震のような極浅発地震では，震央距離による波動勢力の減衰は非常にいちぢるしいものであり，そのような地震が観測網内の各地で頻発しているばあい，対応の疑義ということはきわめておこりうることなのである．もちろん適当な震源がもとめえられない理由は，けしてこれだけではなく，むしろおおくは位相同定のまちがえ，つまりちがつた種類の位相をとつてこれを同一の信号として計算したこと，あるいは解析の基礎となつた媒質の均一性の仮定の成立しないこと，等々によることがおおいものとかんがえられる．ただ，地震の対応ということも，しばしば解析にあたつて，困難な問題とされていたことも事実である．われわれの観測ではくりかえしのべたように同一標準時計による分秒刻時を地震と一緒に直接記録して各点の着震時をきめているので，このような疑義はまず生ずる心配がない．位相同定さえちがわなければ，±1/50 sec の精度が確保されていることもすでにのべたとおりである．一方，観測点の位置についての精度も，従来ほとんど考慮されていなかつた点をあらため，簡簡な測量をおこなつて ±10 m 程度にまで観測点の坐標を決定したことも，あたらしいことである．

本稿ではこのようなたかい観測精度のもとにえられた各点の地震記象を験測し，震源坐標と震源発震時刻,* 地震波速度をもとめ，それらの精度を検討し，震源分布，地震波速度等の地質構造との関連を考察した.

* 発震機巧に関連する諸量を動力学的震源要素とよぶのに対し，これらは運動学的震源要素とよぶことができる.

2. 着震時による震源位置の決定

2.1 観測点 S_i に地震波動の特定位相の到達した時刻（着震時 t_i）を利用して，震源 O の位置（x_0, y_0, z_0）と震源における発震時刻（震源時 t_0）とをもとめることは，験震業務として一般におこなわれている．既存の標準的走時表を利用するのが普通であるが，個々の地震について位相の伝播速度をも未知数としてもとめることもある．いずれにしても，一般の近地地震の解析では，かなりひろい範囲の観測点の資料をあつかうので，ほぼ ±0.1 sec の時刻精度で充分であるとされている．ところが非常に局地的な地震で，ごくせまい範囲でのみ観測がおこなわれる余震観測のようなばあい，着震時法ではこれよりはるかにたかい時刻精度が要求される．そのために従来わがくにではこのような局地地震の着震時刻による解析はほとんどおこなわれたことがなかつた．表俊一郎[4]は鳥取地震 (1943. IX. 10) の余震観測ではじめてラジオ放送の時報を地震記象に重畳する方式を導入して，着震時刻の観測をおこなつたが，4 点のみの観測であつて，着震時による震源決定をなすにいたらなかつた．ついで福井地震 (1948. VI. 28) の余震観測においても表俊一郎[5]はふたたびこの方法をもちい，はじめて，ただ1例であるが5点観測に成功して，その解析をこころみた.

その後今市地震 (1949. XII. 26) の余震観測でも絶対時刻の記入はわれわれの担当した舟生 1 点で実施されただけであつたので[6]，わがくにではなおこの方法の実際的検討はまつたくおこなわれていない状況であつた．和歌山地震群の臨時観測においては，この問題を，震源決定にあたりまず検討することにした.

2.2 もつとも簡単な仮定として半無限均一地殻内に震源があり，地表面で直達波の観測がおこなわれるばあいについてかんがえる.

観測点 S_i の坐標を x_i, y_i, z_i，観測点 S_i における直達波位相の着震時を t_i とし，震源 O の坐標を x_0, y_0, z_0，震源 O におけるその位相の発震時を t_0，伝播速度を v とする．基本式は

$$(x_i - x_0)^2+(y_i-y_0)^2+(z_i-z_0)^2=(t_i-t_0)^2v^2 , \qquad (1)$$

4) S. OMOTE, "The Preliminary Report on the Aftershocks of the Tottori Earthquake," *Bull. Earthq. Res. Inst.*, **22** (1944), 33–41.

5) S. OMOTE, "On the Aftershocks of the Fukui Earthquake, Part 2," *Bull. Earthq. Res. Inst.*, **28** (1951), 311–319.

6) S. MIYAMURA und T. AKIMA, "Uber die Beobachtung der Nachbeben des Imaichi-bebens am Dorfe Hunyu, Provinz Totigi," *Bull. Earthq. Res. Inst.*, **28** (1950), 421–433.

x_i, y_i, z_i, t_i は観測値で，x_0, y_0, z_0, t_0 および v が未知数である．

（1） 式を変形すると，

$$2x_ix_0+2y_iy_0+2z_iz_0+t_i^2v^2-2t_it_0v^2+(t_0^2v^2-x_0^2-y_0^2-z_0^2)=x_i^2+y_i^2+z_i^2\,, \qquad (2)$$

そこで，

$$X=2x_0,\ Y=2y_0,\ Z=2z_0,\ U=v^2,\ V=-2t_0v^2,\ W=t_0^2v^2-x_0^2-y_0^2-z_0^2\,, \qquad (3)$$

とおくと，(2) 式は

$$x_iX+y_iY+z_iZ+t_i^2U+t_iV+W=r_i^2 \qquad (4)$$

となる．ただし $r_i^2=x_i^2+y_i^2+z_i^2$.

x_0, y_0, z_0, t_0, v の 5 未知数に対してこれらの観測方程式は一次でない．したがつて $X\sim W$ の 6 個は独立でない．しかし，もし坐標の，xy 面を地表面に平行にとつておけば，観測点同志の標高差があまりないと，$z_i\approx 0$ とおくことができる．こうすると (4) 式から Z の項がきえて，

$$x_iX+y_iY+t_i^2U+t_iV+W=r_i^2\,, \qquad (5)$$

が観測方程式となる．これは X, Y, U, V, W の 5 未知数について一次であり，これは $i=5$ のばあいひとくみの解をあたえる．$i>5$ であれば最小自乗法的処理をくわえて，とくことができる．従来は x_0, y_0, z_0, t_0, v の近似値をもとめて，それによつて，(1) 式を一次化して，最小自乗法にかけるのが普通であつたようであるが，今回はこのように直接的に一次化した観測方程式 (5)をもちいた．

ただし，われわれのばあい，主として誤差をふくむとかんがえられる観測量は t_i であるが，(5) 式の左辺にある未知数 U, V の係数にこの誤差をふくむとかんがえられる量がはいつている．普通の最小自乗法では，観測方程式の未知数の係数は誤差をふくまぬ量で，観測量は右辺の常数項のみにはいつている．左辺の係数にも誤差をふくむ一般のばあいに対して適用すべき方法は W. E. Deming[7] によつて提出されている．しかし，もし誤差にもとづく係数のおもみがすべての観測方程式についてひとしいならば，結果は残差の平方の影響だけしかちがわないこともしれている[8]．われわれのばあいすべての観測点についての測定精度はもちろん実際には区々であるが，これを個々に推定することは，のちにものべるように，非常に繁雑であり，後節の誤差の議論では，これらに一応一定の誤差 $\delta t_i\equiv\delta t$ をかんがえているので，もしそうかんがえれば，(5) 式から普通の方法で正規方程式をつくつて，計算をすすめてよい．したがつて，ここでは，この式にしたがつて解析した．

2.3 われわれの和歌山附近における臨時観測は，しばしばのべたように刻時方式に特

7) W. E. Deming, *Statistical Adjustment of Data*, (John Wiley and Sons, Inc., New York, 1943).

8) *cf. loc. cit.* 7) chapter 10, Problem 8.

に重点をおいたので，±0.02 sec の精度が，すくなくとも刻時だけについては保証されている．したがつて着震時法による震源要素決定は相当多数の事例について，こころみうるはづである．しかし，実際には前報[9]でのべたように石本式加速度計をもつ基準観測点だけでは，着震時法による震源決定の最小必要観測数5点以上で観測された地震は約10% 程度にすぎず，しかも，感度の不足のために，そのうちには，鮮明な初動をすべての観測点でしめしているとはいえないものもある．そこで，初動の判定において疑問の生じえないように，高感度地震計の観測結果を採用するため，そのような観測点の多数が同時に運転された1956年4月の京都大学との共同観測時の資料について解析することにした．

この観測での観測点は，1) 石本式加速計によるもの (IA グループ)，2) 地震研究所の電子地震計（遠隔記録地震計 RTS, LTS をふくむ）によるもの (ES グループ)，3) 京都大学の電磁地震計によるもの (KU グループ)にわけられる．前2者の位置坐標は前報告[9]第3表に黒島($\varphi=34°01'N, \lambda=135°06'E$)を原点とし，水平面上，北方に $+x$，東方に $+y$，鉛直下方に $+z$ をとつた右手系直角坐標でしめした．後者の坐標は T. MIKUMO[10] により和歌浦 ($x=+20.91$ km, $y=+6.74$ km) を原点とし，南方に $+x$，東方に $+y$ とした坐標でしめされている．

これらの観測点の比較的多数点で初動乃至 S 相の着震時を記録しえた代表的10地震について，その preliminary readings を資料とし，**2.2** でのべた方式により，初動時刻について最小自乗法的処理をおこない，震源要素と伝播速度とをもとめた．（最小自乗法解析）その結果は Table 1 にしめすように，震央坐標は一応えられるが，速度，震源時刻，深度はすべて不合理なあたいとなつた．資料となつた初動の記象は Fig. 1 にしめしたように非常に明瞭なたちあがりであつて，よみとりの誤差はかんがえられない．S についての最小自乗法解析の結果も，Table 2 にしめすように，ほぼ同様に不合理な結果になつてしまつた．

そこで原記象について位相同定の再検討をこころみ，資料に若干の改訂をおこない，多少うたがわしいものはすて，あるいはふたつの時刻を保留的に採用した，その結果，preliminary readings にくらべ，資料数は減少した．そこで，計算に採用しうる観測数が必要最小数5にくらべあまり大でなくなつたことと，資料の誤差は確率的よみとり誤差よりも，位相同定の問題がおおきいことなどからみて，最小自乗法的処理も多少適当でないともかんがえられ，また宮山要太郎[11]も指摘してるように，不適当な資料の混入発見の

---

9) *loc. cit* 1).

10) T. MIKUMO, "On the Anomalous Time-Distance Curves Observed in Local Earthquakes," *Zisin*, [ii], **8** (1955) 158–160. T. MIKUMO, "Precise Seismometric Observations in the Epicentral Region of Local Shocks," *Memoir of the College of Science, Univ. of Kyoto*, Ser. A, **28** (1956), 161–207. T. MIKUMO, M. OTSUKA, and A. KAMITSUKI, "On the Nature of Local Earthquakes Orserved in Wakayama District," *Zisin*, [ii], (1956), 218–228.

11) Y. MIYAYAMA, "On the accuracy of determination of hypocentre," *Journ. Meteorol Soc., Japan*, [ii], **9** (1931), 23–32.

便宜のためということもあり，最小自乗法のかわりに，種々の 5 観測点のくみあわせについて，それぞれ 5 元連立方程式をといてゆく方法をとつた．(連立方程式法解析)．

その結果は Table 3, 4 にしめしたように，若干のくみあわせではもつともらしい解をうることができたが，やはり不合理な結果をあたえるばあいも相当あつた．

3. 初期微動時間法による震源決定

3.1 均質地殻内の震源決定についての **2.2** の議論において，採用する信号としての特定位相に仮想波 $s-p$ をとつたときには，その震源時は $t_0\equiv 0$ となる．したがつて観測方程式は，

$$x_iX+y_iY+t_i^2U+W=r_i^2\,, \tag{6}$$

$$X=2x_0,\ Y=2y_0,\ U=v_{s-p}^2\,,\quad W=-(x_0^2+y_0^2+z_0^2)\,, \tag{7}$$

ただし $r_i^2=x_i^2+y_i^2+z_i^2$ となる．

このばあいにも，左辺の未知数 U の係数が誤差をふくむ量であるが，そのおもみが i によらず一定であるとすれば，DEMING[12] により普通の方法で最小自乗法を適用できる．

しかし，このばあいには，左辺の誤差をふくむ係数をもつ項が 1 項だけであるから，

$$X'=2x_0/v_{s-p}^2,\quad Y'=2y_0/v_{s-p}^2,\quad U'=-1/v_{s-p}^2,\quad W'=-(x_0^2+y_0^2+z_0^2)/v_{s-p}^2 \tag{8}$$

とおいて，変数変換して，

$$x_iX'+y_iY'+r_i^2U'+W'=-t_i^2 \tag{9}$$

を観測方程式としておけば，この問題をさけることはできる．

3.2 着震時法をこころみた 1956 年の 10 地震について，同一の資料で $s-p$ 法により震源要素の決定をこころみてみると，preliminary readings を最小自乗法で処理したばあいも，資料再検討後にいろいろのくみあわせで 5 元連立方程式法でといたばあいも，いづれも Table 5 にしめすように，仮想波速度 v_{s-p} としてかならずしも一定値はあたえないが，大体合理的な解をうることができた．

s 位相の同定は C. F. RICHTER[12] ものべているように，いろいろ問題がおおいし，特にわれわれのばあい，1 成分観測もおおいので，s による着震時法のうまくゆかないことはうなづけるが，p については，Fig. 1 にしめした記象例でもわかるように，相当はつきりしたものがおおい．しかもその着震時法はすべて失敗している．そして同一の資料で $s-p$ 法では比較的合理的な解がえられたということは，きわめて不思議におもえる．

同様の結果は三雲健[14]によりすでに報告されており，これについて三雲は震源の問題に

---

12) *loc. cit.* 7, 8).

13) C. R. RICHTER, *Elementary Seismology*, (W. H. Freeman and Co. San Fransisco, 1958), pp. 292–294.

14) T. MIKUMO, *loc. cit.* 10).

関係づけて興味ある見解を発展させた．筆者はしかし，なおこれについて，震源決定法に関して若干詳細の検討をおこなつてみたいとかんがえた．そこでまず $s-p$ 法による震源決定を同一型式の地震計による観測資料でいろいろの面から検討することにした．

3.2 震源決定が初期微動時間法でもうまくゆかないばあいのあることは，位相の混用がひとつの原因となつてるとおもわれたので，これをできるだけさけるため，観測計器の整一性をたもつように石本式加速度計の観測だけをあつかつてみた．これは3成分観測であるから S の同定には有利であるが，感度の点で初動がちいさくなる．そのために4点以上で明確な資料をあたえる地震は 1952～1954 年の 3 回の観測で約 50 にすぎなかつた．1956 年にも前述の 10 地震以外に若干の資料があつたが，今回は解析しなかつた．資料となつた石本式加速度計の記象例を Fig. 2～4 にしめした．

これら 1952～1954 年の主として石本式加速度計による観測結果について，初期微動時間法による震源決定をこころみた．4 点以上の観測のあるものは，観測点数を n とするとき $N=\binom{n}{4}$ のすべてのくみあわせについて，震源決定をおこなつた．Table 6 の E_i がこれである．n が 4 にくらべあまり大でないばあい，前節でも言及したように最小自乗法を利用するよりも，この方法の方が適切とかんがえた．震源決定法には高橋竜太郎[15]の作図法をもちいた．

また **4** でのべる方法で，初期微動観測値が正規分布誤差 δt_i をもつばあいに期待される，震源坐標 x_0, y_0, z_0 と $s-p$ 仮想波速度 v_{s-p} の誤差を個々のばあいすべてについて計算した．そして，一地震に対してのこれらのいくくみかの数値を上記の誤差に応じて荷重平均したものを，その地震の震源要素の平均値としてさだめた．これが Table 6 の E_0 である．

こうしてえられた各地震についての v_{s-p} の x_0, y_0, z_0 との関係をしらべると，**5** でのべるごとく $x_0>9$ km の地域においては，ほぼ v_{s-p} を一定とかんがえられるので，その平均値をつくつた．ただしここでも δt に対する δv_{s-p} に応じた荷重平均をとると結局その平均値として，$\bar{v}_{s-p}=6.80\pm0.11$ km/s がえられる．

そこで $x_0>9$ km の北部地帯のものは $\bar{v}_{s-p}=6.80\pm0.11$ km/s をもちいて，ふたたび $\binom{n}{3}$ のくみあわせの震源 E_i をきめなおした．そしてそれぞれの誤差に応じたおもみによる荷重平均を E_0 とした．（第6表 E_i, E_0）．3 点のみ観測資料のある地震で $x_0>9$ km と推定されるものも，この平均仮想波速度 6.80 km/s をもちいて震源をもとめた．このようにしてもとめた震源位置の分布については後節で論ずる．

4. 初期微動時間法震源決定の精度

4.1 半無限均一地殻内の震源からの直達波を地表で観測するばあいの基本関係式は **2.2** の (1) にしめした．直達波として $s-p$ 仮想波をとり，観測点の標高があまりたか

15) R. TAKAHASHI, "A Graphical Determination of the Position of the Hypocenter of an Earthquake and the Velocity of the Propagation of the Seismic Waves," *Bull. Earthq. Res. Inst.*, **6** (1929), 232-244.

くなく，ほぼ $z_i=0$ ととることができれば，これは

$$(x_i-x_0)^2+(y_i-y_0)^2+z_0^2=t_i^2v^2\ ,\quad (i=1,2,\cdots n)\ , \tag{10}$$

となる．高橋竜太郎の作図法も当然この式の $n=4$ とした 4 元連立方程式にもとづくわけで，解析的にあらわせば，それをといて，

$$\left.\begin{aligned} x_0&=x_0(x_i\,y_i,\,t_i)\ ,\\ y_0&=y_0(x_i,\,y_i,\,t_i)\ ,\\ z_0&=z_0(x_i,\,y_i,\,t_i)\ ,\\ v_{s-p}&=v_{s-p}(x_i,\,y_i,\,t_i)\ ,\quad i=1,2,3,4\ , \end{aligned}\right\} \tag{11}$$

をもとめているのである．

すでにのべたように，われわれの観測では観測点位置 x_i, y_i の精度は，初期微動時間 t_i の精度にくらべはるかにたかいとかんがえられるから，誤差は主として t_i の観測値のみからはいつてくるとみなしうる．

この独立変数 t_i に 0 のまわりに標準偏差 δt_i をもつて正規分布する確率的誤差があるとき，従属変数 x_0, y_0, z_0, v_{s-p} に期待される確率的誤差はそれぞれのあたいのまわりに，つぎのような標準偏差をもつて正規分布をするはづである．すなわち，

$$\left.\begin{aligned} \delta x_0&=\pm\sqrt{\sum_{i=1}^{4}\left(\frac{\partial x_0}{\partial t_i}\right)^2(\delta t_i)^2}\ ,\quad \delta y_0=\pm\sqrt{\sum_{i=1}^{4}\left(\frac{\partial y_0}{\partial t_i}\right)(\delta t_i)^2}\ ,\\ \delta z_0&=\pm\sqrt{\sum_{i=1}^{4}\left(\frac{\partial z_0}{\partial t_i}\right)^2(\delta t_i)^2}\ ,\ \delta v_{s-p}=\pm\sqrt{\sum_{i=1}^{4}\left(\frac{\partial v_{s-p}}{\partial t_i}\right)^2(\delta t_i)^2}\ , \end{aligned}\right\} \tag{12}$$

である．δt_i は実際には地震ごとに，観測点ごとに，すべてことなつているわけであるが，それを推定することは，不可能ではないにしても，かなり繁雑になる．それで一応すべての観測に対して一定値 δt をとるものとする．これは t_p, t_s の位相のよみの誤差 δt_p, δt_s から，$\delta t=\sqrt{(\delta t_p)^2+(\delta t_s)^2}$ で計算する．$\delta t_p, \delta t_s$ は ±0.05 sec 程度であるから $\delta t=\pm0.07$ sec になる．ここでは位相同定のまちがえは無視しているわけであるが，若干そのようなことも考慮して，以下では一応 $\delta t=\pm0.1$ sec に対して誤差計算をすることにする．

$\partial x_0/\partial t_i, \partial y_0/\partial t_i, \partial z_0/\partial t_i, \partial v/\partial t_i$ $(i=1,2,3,4)$ のあたいは (10) 式を t_i に関して偏微分した式からつぎのようにしてもとめられる．すなわち (10) 式より

$$\left.\begin{aligned} (x_i-x_0)\frac{\partial x_0}{\partial t_j}+(y_i-y_0)\frac{\partial y_0}{\partial t_j}-z_0\frac{\partial z_0}{\partial t_j}+vt_i^2\frac{\partial v}{\partial t_j}+\delta_{ij}v^2t_i=0\ ,\\ \delta_{ij}=\begin{cases}1 & i=j\\ 0 & i\neq j\end{cases},\quad i,j=1,2,3,4\ . \end{aligned}\right\} \tag{13}$$

この 16 個の 1次方程式を $\partial x_0/\partial t_i$, $\partial y_0/\partial t_i$, $\partial z_0/\partial t_i$, $\partial v/\partial t_i$, $(i=1,2,3,4)$ についての 4 くみの 4 元連立方程式としてといて $\partial x_0/\partial t_i$ $\partial y_0/\partial t_i$ $\partial z_0/\partial t_i$, $\partial v/\partial t_i$ をもとめる．このばあ

い，係数にはいつている x_0, y_0, z_0, v には作図法でえられた数値をもちいればよい．

こうして $\delta t=\pm 0.1$ sec に対して計算された x_0, y_0, z_0, v の誤差が Table 6 の E_0 に附記されている第 1 種の誤差である．

4.2 一地震について $n>4$ の t_{s-p} の観測がえられたときには，前節でふれたように $N=\binom{n}{4}$ の観測点のくみあわせについて作図法で震源要素 $x_{0i}, y_{0i}, z_{0i}, v_i\ (i=1, 2, \cdots, N)$ の決定をおこない，それぞれについての上述の誤差を計算した．そしてその誤差の 2 乗に逆比例したおもみをつけて荷重平均値 $\bar{x}_0, \bar{y}_0, \bar{z}_0, \bar{v}$ をつくつた．すなわちこの平均値の精度には，おのおのの震源要素の第 1 種誤差から誤差伝播によつてえられる誤差，つまり観測値に ± 0.1 sec の誤差があつたとしたときに期待される誤差（第 1 種誤差）とともに，これら N ケの数値に対するその平均値の分散として推定される誤差がある．後者については，小数例の母平均信頼限界[16] として，5% の危険率におけるあたいをとつて，第 2 種の誤差として，Table 6 の E_0 に斜字体で附記した．これはいろいろの観測点のくみあせわでえられた作図結果の一致する程度をしめすものであつて，4 点以上の資料を最小自乗法で処理したときに計算される誤差にちかい性質をもつものであり，各点の t_{s-p} 観測値に一定の誤差(たとえば $\delta t_{s-p}=\pm 0.1$ sec) があつたとき，観測点位置 (x_i, y_i) や，震源位置等 (x_0, y_0, z_0, v) の関係で先験的にきまる第 1 種の誤差とは，その意味がちがつている．Fig. 5 に震央位置だけについて，その関係をあらわす若干の実例をしめした．破線にて個々のくみあわせの震央位置 E_i とその第 1 種誤差をしめし，実線にてその荷重平均値 E_0 と第 1 種誤差をしめした．そしてその第 2 種誤差としての 5%危険率平均値信頼限界をふとい線であらわした．

4.3 v_{s-p} を一定既知値としたばあいには，(11) 式は

$$\begin{aligned} x_0&=x_0(x_i, y_i, t_i, v)\,,\\ y_0&=y_0(x_i, y_i, t_i, v)\,,\\ z_0&=z_0(x_i, y_i, t_i, v)\,,\quad (i=1, 2, 3)\,, \end{aligned} \tag{14}$$

となり，(12) 式は

$$\begin{aligned} \delta x_0&=\pm\sqrt{\sum_{i=1}^{3}\left(\frac{\partial x_0}{\partial t_i}\right)^2(\delta t_i)^2+\left(\frac{\partial x_0}{\partial v}\right)^2(\delta v)^2}\,,\\ \delta y_0&=\pm\sqrt{\sum_{i=1}^{3}\left(\frac{\partial y_0}{\partial t_i}\right)^2(\delta t_i)^2+\left(\frac{\partial y_0}{\partial v}\right)^2(\delta v)^2}\,,\\ \delta z_0&=\pm\sqrt{\sum_{i=1}^{3}\left(\frac{\partial z_0}{\partial t_i}\right)^2(\delta t_i)^2+\left(\frac{\partial z_0}{\partial v}\right)^2(\delta v)^2}\,, \end{aligned} \tag{15}$$

となる，$\delta t_i\equiv\delta t=\pm 0.1$ sec, $\delta v=\pm 0.11$ km/sec として，(13) 式に対応した，9 個の一次式，

16) M. MASUYAMA, *Syōsū Rei Matomekata to Zikken-Keikaku*, (Kawa-ide Syobō, Tokyo, 1944).

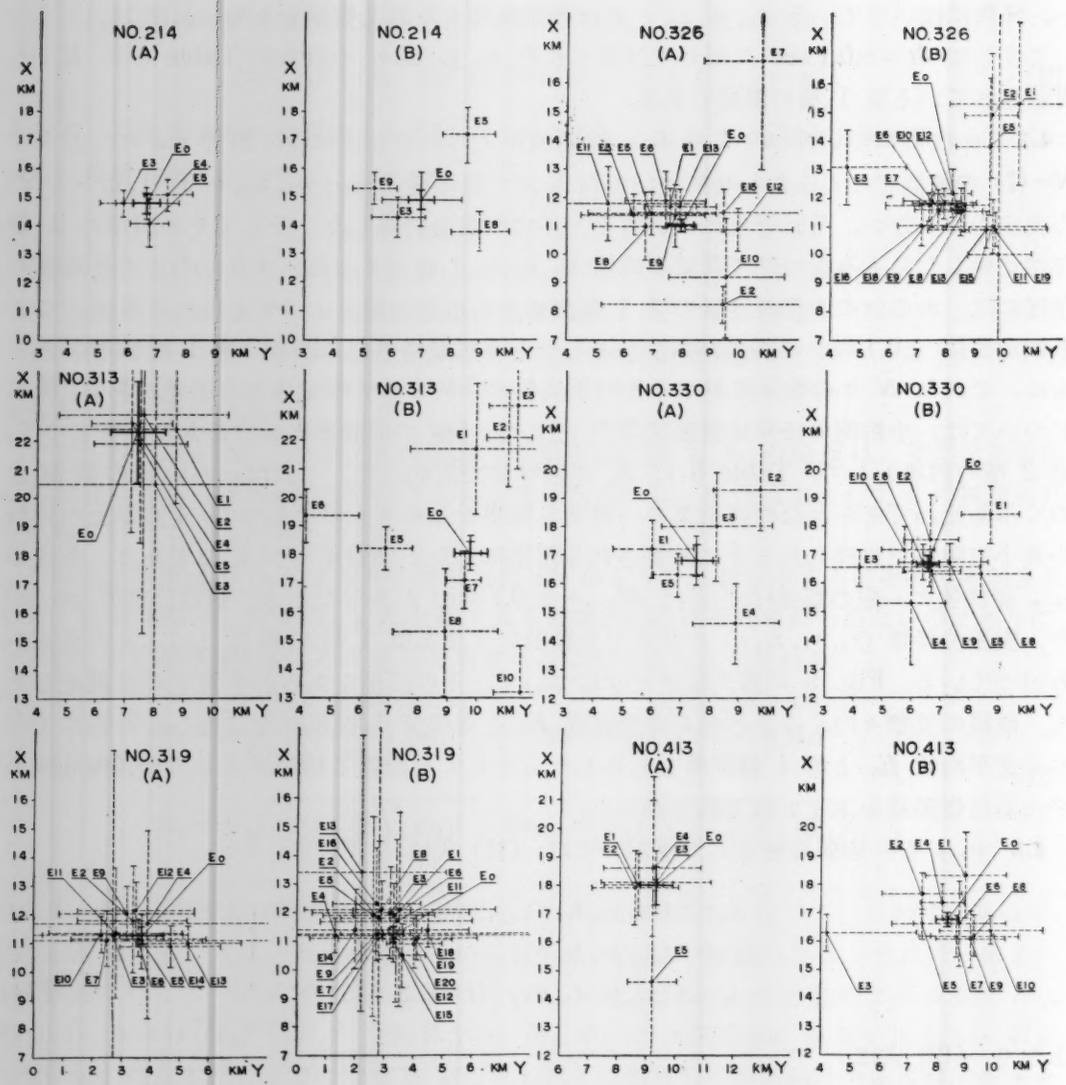

Fig. 5. Errors of epicenter coordinates, δx and δy, expected by observational errors $\delta t=\pm 0.1$ sec in $s-p$ intervals at four (A) or three (B) staions adopted in the locations. (1st kind errors) E_i is an epicenter by a combination of stations and E_0 is their weighted mean value. Thick lines indicate the limit of confidence at 5% risk attributed to E_o. (2nd kind errors.) Number of earthquake should be referred to Table 6.

$$\left.\begin{aligned}&(x_i-x_0)\frac{\partial x_0}{\partial t_i}+(y_i-y_0)\frac{\partial y_0}{\partial t_i}-z_0\frac{\partial z_0}{\partial t_i}+\delta_{ij}v^2t_j=0\\&\delta_{ij}=\begin{cases}1, & i=j\\0, & i\neq j\end{cases},\quad i,j=1,2,3\end{aligned}\right\}\tag{16}$$

がえられ，この3くみの3元連立方程式から $\partial x_0/\partial t_i$, $\partial y_0/\partial t_i$, $\partial z_0/\partial t_i$ $(i=1,2,3)$ をもと

め，連立方程式

$$(x_i-x_0)\frac{\partial x_0}{\partial v}+(y_i-y_0)\frac{\partial y_0}{\partial v}-z_0\frac{\partial z_0}{\partial v}+\delta_{ij}t_i^2v=0 \tag{17}$$

から $\partial x_0/\partial v, \partial y_0/\partial v, \partial z_0/\partial v$ をもとめると，これで (15) によつて $\delta x_0, \delta y_0, \delta z_0$ がもとまる．こうして計算したものが Table 6 にしめした 3 点観測のばあいの第 1 種誤差である．荷重平均およびその第 1 種，第 2 種誤差は 4 点観測のばあいと同様のかんがえで計算できる．

4.4 前節で論じた正規分布誤差 $\delta x_0, \delta y_0, \delta z_0, \delta v$ は実はたがいに相関関係にある．たとえば，δt_i に対してかりに +0.1 sec, 0.0 sec, −0.1 sec, といつたあたいをとり，これが 4 観測点 S_i の $t_{s-p,i}$ それぞれに独立に生ずるくみあわせは $3^4=81$ あり，それぞれのばあいに δx_0, etc. を

$$\delta x_0=\sum_i^4\frac{\partial x_0}{\partial t_i}\delta t_i\,,$$

etc. から計算できる．こうしてえた 81 の空間の点はひとつの誤差空間をしめる．Fig. 6 に x_0, y_0 面のきりくちを 1 例としてしめす．あきらかにほぼ原点を中心とした楕円的分布をなしている．このような誤差空間において，一般に原点を中心とする 4 次元の楕円体をかんがえ，誤差点の分布確率がその内外でひとしいとしたとき，これを誤差楕円体とよぶ．その主軸のながさと方向とは，$\delta x_0, \delta y_0, \delta z_0, \delta v$ およびおのおのあいだの偏相関係数とから計算できる．これらを個々に計算することはのちの機会にゆずり，ここではただ震源決定の誤差表示としてはここまでおこなうべきものであることを注意するにとどめておく．

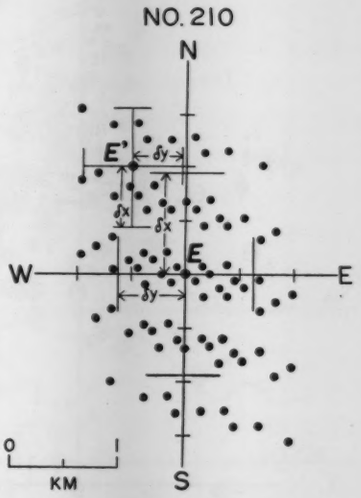

Fig. 6. An example of the distribution of error ellipsoid points of an epicenter, E, obtained by 4 station $s-p$ intervals with +0.1, 0.0, −0.1 sec observational errors in $3^4=81$ combinations. E' is the mean position of epicenter obtained by 3 station $s-p$ intervals, with $v_{s-p}=6.80$ km/s.

5. $s-p$ 仮想波速度と震源の空間分布

5.1 上述の計算によりえられた個々の地震についての v_{s-p} のあたいの，x_0, y_0, z_0 との関係を Fig. 7 に図示した．v_{s-p} と y_0 はなんら相関もないが，x_0 については $x_0>9$ km のものが，ややちいさいあたいをしめすことがわかる．しかし $x_0<9$ km では観測網からはずれるものもあり，誤差がおおきいし，事例もすくないので，あまり確定的なことはいえないが，南部の非変成古生層乃至中生層の部分が，北部の変成岩帯にくらべ v_{s-p} が小であることは，多少の意味をもつものかもしれない．今後の事例の増加をまつて再

検討をくわえたい．z_0 との関係は従来丹後地震余震[17]，和歌山地震群[18]などで明示されているのであるが，ここでは $z_0<3$ km 程度の極浅発のものは，観測網の密度と地震の規模との関係で4点観測のできたものがすくなく，わづかに2例にすぎず，一方 $z_0>10$ km のものはすべて後節でのべるように場所的に偏在しており（$x_0<9$ km），またいづれも精度がわるい，$10>z_0>3$ km の範囲内での v_{s-p} と z_0 との関係には z_0 にともなう v の増

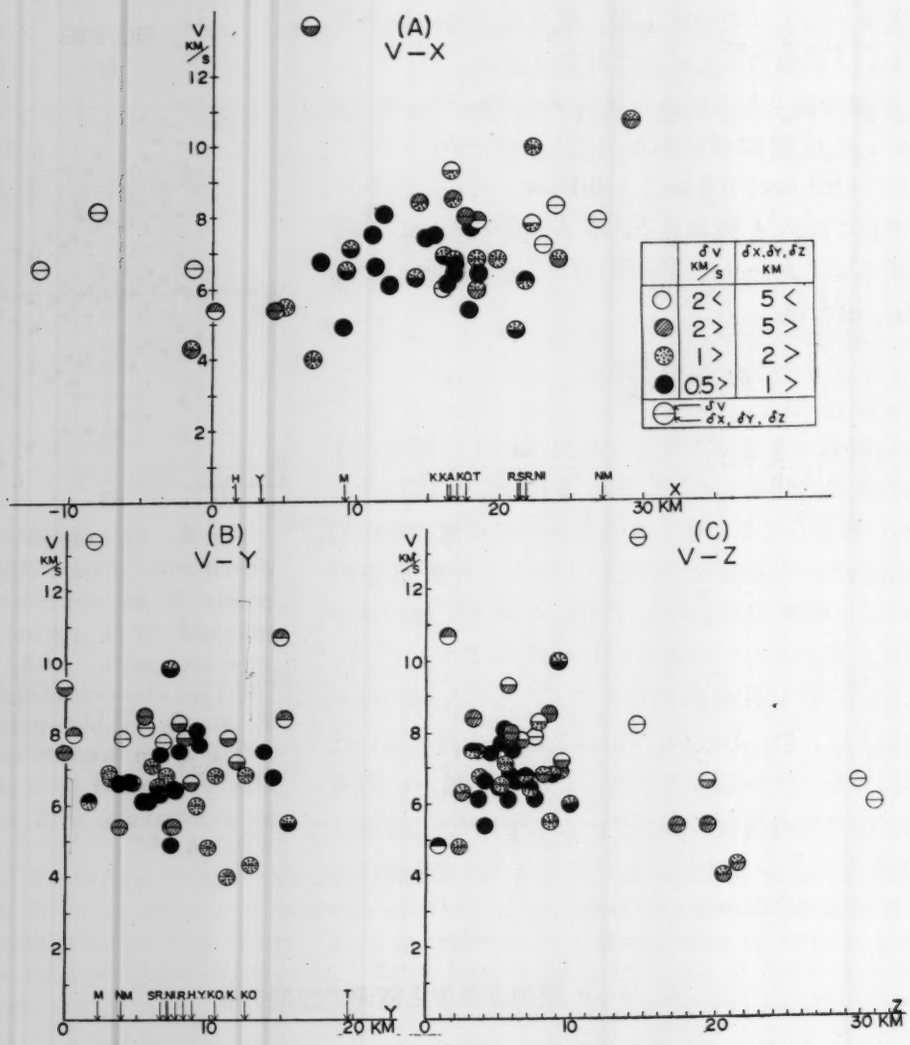

Fig. 7. Velocity of $s-p$ wave, v_{s-p} and the coordinates of origins x_0, y_0, z_0, simultaneously obtained as the result of weighted means for the earthquakes observed at more than 4 stations. *H*, *Y*, etc., mean abbreviations of station names, which should be referred to the previous paper *loc. cit* 1.)

17) *loc. cit.* 15).
18) *loc. cit.* 3), 10).

加がうかがえるが，全体としてはつきりしたものとはいえない．これも今後事例の増加をみたのちに再検討したい．

5.2 和歌山附近の v_{s-p} の地下分布は今村明恒[19]のしめしたところによると，ごくうすい 50 m ほどの堆積表層（v_{s-p}＝1 km/sec）のしたに，v_{s-p}＝3.8 km/sec の基盤が 10 km あたりまで存在することになつている．今村明恒の結果を前節の議論にしたがつて誤差評価すると，Table 7 のようになり，深度のふかい 3 例（$z_0 \geq 4$ km）はやや誤差が大であるから，v_{s-p}=3.8 km/sec 層の 3～4 km 以深の存在は疑問としてよい．

一方，三雲健[20]は 1954,1956 年のわれわれとの共同観測の解析で，表面に4km程度のあつさの層をおき，v_p=4.3km/sec, v_s=2.5km/sec（したがつて v_{s-p}=3.4 km/sec）とし，そのしたのふかさ 10 km までを v_p=5.4～5.6 km/sec, v_s=3.2 km/sec（したがつて v_{s-p}=7.7 km/sec）の層とする地殻構造を推定している．

われわれの結果ではこれらのいづれがただしいかを決定するだけの極浅発地震の事例もすくなく，4 km 以深の地震の結果だけから，三雲健の構造を独立に推定することも，やや困難にみえるので，一応第一近似として，z_0 による変化はなく v_{s-p} 一定とし，成層構造の決定は今後の問題にのこした．

v_{s-p} を一定として，$10 > z_0 > 4$ km の事例のみについて，第1

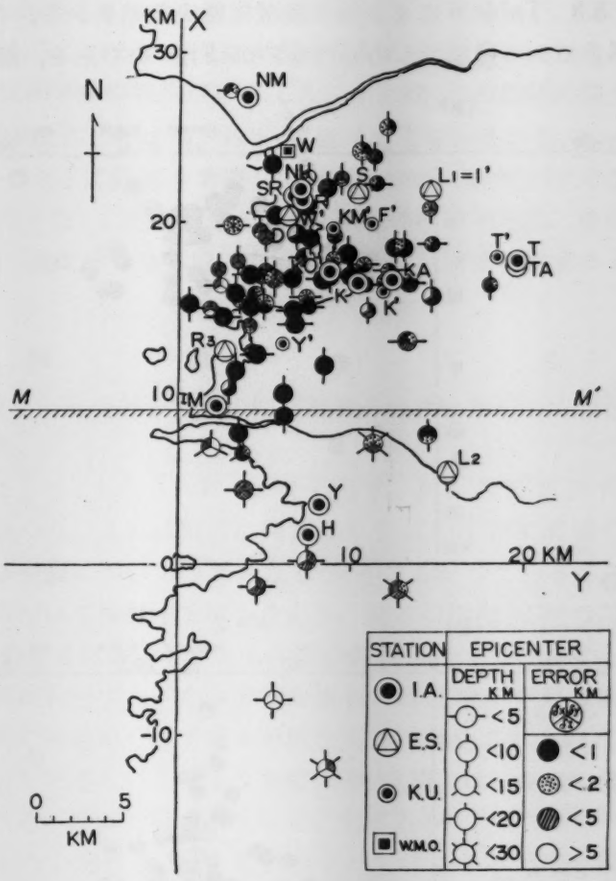

Fig. 8. Epicenters determined by $s-p$ method using the data of I.A. stations in the 3 expeditions in 1952–1954. I.A.: Ishimoto accelerograph station. E.S.: Electronic seismograph station of E.R.I.K.U.: Kyoto university station with electromagnetic seismograph. W.M.O.: Wakayama Meteorological Observatory. Errors shown are the 1st kind errors. Epicenters indicated by small circles are those determined only by 3 stations, taking v_{s-p}=6.80 km/sec. *H*, *Y*, etc., mean abbreviations of the station names, which should be referred to the previous paper. (*loc. cit.* 1).

19) *loc. cit.* 3).
20) *loc. cit.* 10).

種誤差の自乗に逆比例するおもみをつけて，荷重平均をつくると

$$\bar{v}_{s-p}=6.80\pm0.11\ \mathrm{km/sec}$$

となつた．

5.3 Table 6 にまとめた震源位置決定結果から，この地方の震央分布を深度と第1種誤差による種別でしめしたものが Fig. 8 である．深度 10 km 以深のものは北部長瀞変

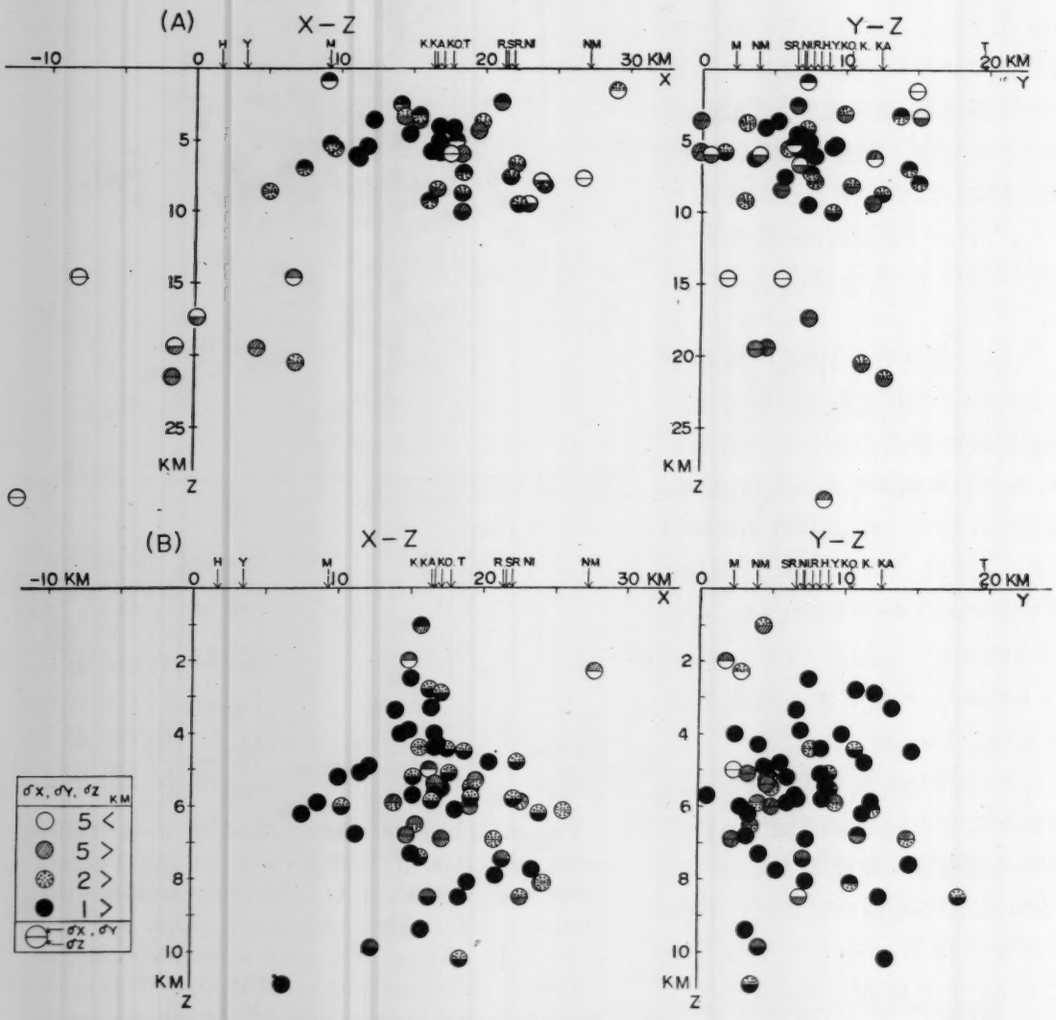

Fig. 9. Hypocenters projected to the vertical planes. 1st kind errors are shown for the respective coordinates. *H*, *Y*, etc. mean abbreviations of the station names, which should be referred to the previous paper, (*loc. cit.* 1.) (A): 4 station result. (B): 3 station result.

成帯地域にはなく，MM' でしめした $x=9$ km の線をさかいとして，南部非変成古生層，中生層地域には深度 10～30 km の地震が分布していることが明示されている．MM' はいわゆる御鉾構造線とよばれているものにほぼ一致する．

深度分布をさらによくみるために，東西および南北の垂直断面に震源を射影して図示したものが Fig. 9 である．

$x_0<9$ km のものは v_{s-p} の平均値をつくるにいたらなかつたので．震源決定に4点観測を要し，事例がすくなく，誤差もおおきいのでなお断定的結論はくだせないが，極浅発のものがすくないことはたしかである．このことは初期微動時間の頻度分布からも推定できる[21)]．$x_0>9$ km において $z_0>10$ km の地震が存在しないことは，この期間に関するかぎり，まづまちがいない．$x_0<9$ km について南方ほど深度がましていること，$z_0=10\sim15$ km にほとんど地震のないことなどは誤差を考慮してもめだつが，事例がすくないので，これもまだはつきり結論はできない．北部地域の $z_0<4$ km の極浅発地震，特にその分布上限，南部地域の震源分布，速度分布などは，なお今後観測，研究をすすめるべき課題としておきたい．

6. 結　　語

和歌山附近に1952～1956年に頻発した局地的小地震の臨時観測の結果を解析してつぎの諸点をあきらかにすることができた．

1) 相当精度のたかい観測をおこなうことができたにもかかわらず，p,s の着震時による震源要素の決定はうまくゆかなかつた．これは解析に採用した各点の位相に異種のものが混入してることと，伝播および発震についての単純な仮定がまちがつていることが，おもな原因とおもわれる．後者について検討するにさきだち，前者の位相同定の問題をふくめて，なお観測の精密化がのぞまれる．もつとも多数の観測点をもうけることができた1956年の京大との共同観測においても，なお詳細の検討には点数が不足であり，かつ異種の地震計の混用は，波動の性質について種々困難な問題が想定されるので，さけなければならない．波動減衰のいちぢるしいこのような極浅発地震では，各点に周波数特性が一定で，相当感度範囲のひろい観測計器をもちいる必要がある．

2) p,s 着震時で適当な解のえられない地震も $s-p$ 時間をとつて解析すると，比較的適切な解がえられる．これは p において異種の位相をとつたばあいにも，それに対応する s をとれば，それらの伝播速度において大差なければ $s-p$ 波としては同種の信号とかんがえうることによるのではないかとおもわれる．

3) したがつて，今回の観測結果から震源分布の概況をえるために，同一地震計の観測資料で，$s-p$ 法による解析をくわしくおこなつた．すなわち1952～1954年の石本式加速度計の資料から多数の震源を作図法にもとづいてもとめた．その結果の精度は $s-p$ の観測に ±0.1 sec の誤差があつたときの誤差（第1種誤差）として，個々に計算してみた．これは観測点と震源との位置関係から，いろいろのあたいになるが，良好なばあいは震源位置で数百メートル以下の誤差となるが，観測網からはづれた震源では数 km をこえてしまうこともある．

4) ひとつの地震についていくくみかの観測点の別々のくみあわせで震源決定をして

21) S. MIYAMURA, *loc. cit.* 1).

みると，それぞれ，適当な誤差で，もつともらしい解がえられるが，それらはもちろん完全には一致しない．ばあいによると相当ちがつた位置がえられる．不適当な資料が混入してるときは，その観測点をふくむくみあわせがすべて不合理な結果をあたえるはずであるが，作図可能で合理的結果がえられて，それらがちがつているばあい，そのいづれがただしい解であるかはわからない．4 点の観測だけでひとつの解をえたとき，そのただしさを保証するものはない．ただ一応それを震源とする以外に方法がないから，それをとるというにすぎない．いくくみかの結果がえられたときは，それらの第 1 種誤差の自乗に逆比例したおもみをつけて，平均値をつくる．この平均値には，第 1 種誤差とは別に，平均値の分散度から推定される信頼限界をそのただしさを保証するめやすとしてあたえることができる．これを第 2 種の誤差とした．第 1 種の誤差よりも第 2 種の誤差の方がちいさいばあいもあれば，逆のばあいもある．第 1 種の誤差は観測誤差をきめれば観測点と震源の位置関係から先験的にきまつてくるものであるが，第 2 種の誤差は，観測の実際の誤差から事後的にきまるものである．後者は必要最小数の観測しかないときには当然もとめえないものであつて，今回の計算結果からみると，必要最小数による震源決定についてはかなりの誤差を期待しなくてはならないようにおもわれる．5%危険率の F 分布による信頼限界が事例数に応じて急激に増大し $N=2\sim3$ ではかなり大となるのが普通である．一方第 1 種誤差が大でも，事例がおおければ，第 2 種誤差はかなり小となりうるようである．

5) このような誤差を考慮して，えられた $s-p$ 仮想波速度を対応する震源位置との関係において考察すると，水平的には北部 $x_0>9$ km の地域においては，$z_0<10$ km であり，v_{s-p} は第 1 近似として，ほぼ一定値をもつとかんがえ，$\bar{v}_{s-p}=6.80\pm0.11$ km/sec (第 1 種誤差) とした．南部 $x_0<9$ km では，事例がすくないが，$z_0>10$ km であるにもかかわらず，v_{s-p} はややちいさいあたいをもつようである．地質的にみると北部には変成岩層，南部は非変成堆積層が分布しているので，興味をひくが，なお事例がましてから詳論したい．今村明恒は表層に 50 m の $v_{s-p}=1$ km/s 層をおき，そのしたに $v_{s-p}=3.8$ km/sec の層をかんがえた．また三雲健は $z<4$ km に堆積層が存在する成層地殻構造をこの地方に推定した．われわれの資料だけではこの点なお充分明瞭でないので，一応北部では v_{s-p} については均質の地殻構造をもつものとかんがえ，くわしい地殻構造については今後の研究にのこした．

6) 北部で $\bar{v}_{s-p}=6.80$ km/sec として 3 点の観測の資料も利用し，合計 82 の震源をきめた．その深度分布は北部 $x_0>9$ km の長瀞変成岩帯においては $z_0<10$ km にかぎられる．$z_0=2\sim3$ km のものもあるが，これら極浅発のものはその規模と，観測網の密度と感度とのため，おおくの事例を決定できなかつた．

7) 南部 $x_0<9$ km の秩父帯，四万十帯では $z_0=10\sim30$ km のややふかい地震があり，南方ほどふかくなつており，$z_0=2\sim3$ km の極浅発のものはないらしい．しかし事例がすくないので，今後の観測と研究とを必要とする．

7. 謝　　辞

本研究の基礎になつた 1952～1956 年の臨時観測については前報告[22]の謝辞であげたような多数のかたがたの御支援をうけた．あらためて謝意をのべる．本稿の準備にあたつて特別の協力をえた同僚堀実教官にこころから感謝の意を表したい．計算の一部は富士電算機計算所(有隣電機精機株式会社)の近末卓三氏その他のおせわでおこなうことができた．付記してその御厚意に感謝する．また，三雲健，大塚道男両氏はじめ京都大学地球物理学教室のかたがたには共同観測中はもちろん，機会あるごとに議論をしていただき，うるところがあつた．同教室佐々憲三，西村英一両教授の御配慮を感謝する．

6. *Local Earthquakes in Kii Peninsula, Central Japan. Part 4. —— Location of Earthquakes by the Temporary Network of Stations near Wakayama ——*

By Setumi MIYAMURA,
Earthquake Research Institute.

1. As reported in the previous paper,[1] 4 expeditions were made in 1952–1956, for the purpose of locating the origins of local shocks then occurring in swarms in Wakayama district, in order to deduce any seismo-geological implication of the seismicity. Observation accuracy of the operations was said to be the highest ever realized for such local earthquake programmes, including many aftershock observations worked out in our country, since the classical work of N. Nasu[2] after the Tango Earthquake, 1927. For the wider areas precise networks were of late realized in Southern California and Central Asia but the method is classical and the accurcy is limited (presumably of the order of ± 0.1 sec). A more modern network was operated in South Africa which seemed to be the highest model of local shock observations and only it can be superior to our operations in time accuracy. As the emphasis was laid exclusively on the time service we got an accuracy of ± 0.05 sec, with the recording paper speed of about 4 mm/sec. Of course, many complicated problems are encountered in phase identifications which may result in much greater time difference, leading even serious misinterpretation in the location of origin. But, excepting this identification problem it seemed to us enongh to solve the fundamental but ever unsolved problem of earthquake origin location.

2. At first we analyse the data obtained in the last expedition in 1956, operated in collaboration with T. MIKUMO and others[10] of Kyoto University. For, at that time many electronic and electromagnetic seismographs of high sensitivity were used, enabling the fixing of accurate on-sets of the first arrivals of the earthquake motions. Preliminary readings of P and S were obtained at several to ten odd stations for ten selected shocks, and we analysed them by the least squares method (L.S.M.), using the observation equations (5), directly linearized, instead of making use of lst approximation

22) *loc. cit.* 1).

values as usual, from the fundametual relation (1) for the direct waves p and s, in the uniform homogeneous medium.

As shown in Table 1 and 2 we could not obtain by this L.S.M. analysis any reasonable solutions for the kinematic elements of the shocks, i.e. for the coordinates of epicenters, depths, origin times and the propagation velocity of the wave used.

After re-examination of the original seismograms, we omitted some dubious readings and thus the number of data available for the location of a shock by arrival times was somewhat reduced, which circumstance makes the least squares method rather inadequate. Moreover, as the nature of data dispersion seems not due to ordinary observation errors but mainly due to mixing of different phases, the least squares procedure may not be adequate.[11] Thus we solved the simultaneous equations for selected combinations of 4 stations. (Simultaneous Equations Method, S.E.M.) Nevertheless, reasonble solutions were obtained only for several combinations of stations shown in gothic numerals in Table 3 and 4.

3. On the contrary, when we analyse the same data by the $s-p$ intervals method, using the observational equations (6), we found reasonable solutions both by L.S.M. and by S.E.M. as shown in Table 5. Failure of the arrival times method and success of the $s-p$ method in location of earthquake origin thus far mentioned were reported also by T. MIKUMO.[10]

Though the identification of S may involve many complicated problems as C. F. Richter wrote in his book[13] there seems to be no ambiguity in p on-sets in our data, as indicated in examples of seismograms given in Fig. 1. S.E.M. for combination of data suggests that the mixed use of different types of seismographs may be responsible in part. But it cannot be the sole reason of the difference between the arrival times method and the $s-p$ method in earthquake location. T. MIKUMO[10] developed an interesting discussion on this problem relating it to a mechanism of origins. The present writer, however, tried to check the accuracy of locations in some detail before advancing into such elaborate discussion with T. MIKUMO.

Thus, considering the results of preliminary analysis given above for 1956 data, we decided to adopt the $s-p$ method for the lst approximation analysis, and selected the data from Ishimoto accelerograph stations in the lst three expeditions, 1952–1954. In these years seismicity was rather high and a considerable number of shocks was recorded at more than 4 stations, the least necessary number of stations for the $s-p$ method analysis, although it even seemed to be too small compared to the total mumber of shocks recorded at all stations. Above all, as at these stations all 3-component, two horizontal and one vertical, identical instruments were used, it was very suitable for the identification of both p and s phases. Examples of seismograms are shown in Fig. 2~4.

Among many existing methods of analysis we adopted the graphical method by R. TAKAHASHI.[15] When there were $n>4$ $s-p$ data, we search for $N=\binom{n}{4}$ solutions corresponding to all N combinations of 4 stations out of n. Among them are included irrational solutions that could not give real epicenter or depth. Excepting such irrational solutions, we calculated the weighted means of each solutions, weights of which are taken as proportional to the inverse squares of errors, that might be expected when $s-p$ intervals at 4 stations have equal Gaussian errors $\delta t_i=\delta t\mp\pm 0.1$ sec. The results are listed in Table 6 together with the data used.

4. Formulae for the calculation of the above mentioned errors of the kinematic elements of earthquake origins in homogeneous medium determined by the $s-p$ method

are given by eqs. (12) and (13).

On the other hand the weighted mean values of the solutions by combinations of 4 stations out of n for an earthquake have their own limits of confidence, based on the small sample theory of statistics for example to 5% risk (cf. M. MASUYAMA'S book[16]). The latter are given for each case in italic numerals in Table 6.

For the constant v_{s-p} with δv_{s-p} errors, the errors derived by the formulae (15) and (16) and the results are also shown in Table 6. Limits of confidence to 5% risk are given in italic numerals in this case, too.

5. The velocity of fictitious s–p wave, v_{s-p}, obtained not only for a shock for each combination of 4 stations, but also for the earthquakes with similar hypocentral positions must be common, but the calculated values given in Table 6 differ in considerable range. Plotting the v_{s-p} values versus coordinates of corresponding origins x_0, y_0 and z_0, we get Fig. 7, in which we also indicate the errors of lst kind of the velocity and coordinate values in the upper and lower parts of circles respectively. While v_{s-p}～y_0 diagram shows only a mere scattering of points, we can notice the following features in v_{s-p}～x_0 and v_{s-p}～z_0 diagrams. Values of v_{s-p} at $x_0<9$ km seem to be small compared to the values at $x_0>9$ km. It may probably reflect the situation, that the geological formations are divided by the so-called Mikabu Tectonic Line approxiately coincident with the parallel of MM′ at $x_0=9$ km into the northern metamorphic Nagatoro and southern non-metamorphic Titibu and Simanto terrains.

Relation between v_{s-p} and z_0 was investigated by many authors in various regions, among which we can refer to the results by R. TAKAHASHI in Tango[15] district and by A. IMAMURA[3] in Wakayama district.

Our diagram of v_{s-p}～z_0 in Fig. 7 illustrates that v_{s-p} at $z_0>15$ km have very small values contrary to the general expectation. They all belong to the epicenters in the southern area at $x_0<9$ km as stated above and some geological implication may be surmised. At $z_0<10$ km slight increase of v_{s-p} with z_0 are seen, but, as there are very small number of events at $z_0<4$ km, we dare not decide whether the crust be a medium of linearly increasing v_{s-p} with z_0 or of constant v_{s-p} underlain by another surface layer of smaller v_{s-p}. The latter structure was proposed by T. MIKUMO[10] as a 2nd approximation, but, for the time being, we decided to restrict ourselves only in lst approximation discussion.

For $x_0>9$ km i.e. $z_0<10$ km, we assume v_{s-p}=constant and obtained the weighted mean $\bar{v}_{s-p}$ using the weight proportional to inverse squares of the lst kind error calculated for each v_{s-p}. Thus we get $\bar{v}_{s-p}=6.80\pm0.11$ km/sec. This value was used for the redetermination of the elements for all combinations out of formerly treated data at more than 4 stations. Data obtained only at 3 stations were also analysed, making use of this $\bar{v}_{s-p}$, value, if the epicenters were supposed to lie in the northern area, $x_0>9$ km.

They are also listed in Table 6 after the results of more than 4 station shocks for respective years.

6. Geographical distributions of the epicenters located by s–p method for 1952–1954 expeditions are illustrated in Fig 8, discriminating their depths and hypocentral errors, attributable to *a priori* observational errors of ±0.1 sec in s–p intervals. (lst kind errors) Epicenters determined only by 3 station data are shown by small circles with the same signs of depths and errors as the epicenters by more than 4 station data. Of course, 3 station data epicenters are restricted in the northern area, $x_0>9$ km.

The plots of these epicenters are distributed uniformly over the network of stations, but outside the network they are found only in its southern neighbourhood. To the

north of Wakayama City, to the west in Kii Strait and to the east of Todoroki (T), there might have been found as many epicenters as to the south of Yuasa (Y), considering the relation in distance from the stations, but we can hardly find them in those northern, western and eastern vicinities.

Distribution of the earthquake origins in solid or the depths of the hypocenters indicated in Fig. 8 will be made clearer in Fig. 9, taking the vertical projection of the hypocenters in xz and yz planes.

It is very clear that no earthquake originates at a depth greater than 10 km in the northern three-quarters of the area covered by the network, i.e. in the area at $x>9$ km. Further south from the parallel MM′ at $x=9$ km the origin becomes deeper as it goes southward. Owing to the small number of origins determined in the southern area, it seems premature to conclude the latter as a fact, but the errors of their locations may support the conclusion. Between the depth 10～14 km, we could locate no earthquake by our network, and it seems to mean something, if we think of the existence of a crustal asthenosphere of plastic nature. In the northern area there are many extremly shallow oirgins but in the southern area no such earthquake, at least one strong enough to be detected by our network, was found. It will be a future problem to locate such extremely shallow shocks both in the northern and southern areas.

Table 1. Data and results of p-arrival time analysis by least squares method for the 1956 temporary observation in Wakayama district. (unit in km and sec.)

No.	Date and Time (J.S.T.)	Data of p Arrival Times at I.A. station (in sec)		E.S. station (in sec)		K.U. station (in sec)		Results of Analysis (in km and sec)	
1	IV 14	*NI*	39.70	R_3	39.84	F'	40.04	x_0:	14.69
	13h 38m	*KO*	39.86	L_1	41.83	N'	41.02	y_0:	7.97
				L_2	40.65	K'	40.18	z_0:	
				K^E	40.06	Y'	39.00	t_0:	
				KO^E	39.83			v_p:	$\sqrt{-7.5}$
2	IV 15	*NI*	31.89	R_3	31.56	W'	31.90	x_0:	10.91
	16h 03m	*KO*	31.38	L_1	32.01	F'	31.92	y_0:	8.77
		KA	31.79	L_2	32.52	K'	31.63	z_0:	
		TA	32.71	K^E	31.50	Y'	30.90	t_0:	
		M	30.38	KO^E	31.7			v_p:	$\sqrt{-29.6}$
		Y	31.20	TA^E	32.62				
3	IV 16			L_2	50.00	W'	49.59	x_0:	17.01
	13h 28m			KO^E	49.26	N'	50.18	y_0:	10.18
						K'	49.41	z_0:	
						Y'	49.79	t_0:	
								v_p:	$\sqrt{-3.2}$
4	IV 19	*NI*	03.92	L_1	06.38	W'	04.04	x_0:	17.59
	09h 25m	*KO*	04.28	L_2	04.63	F'	04.32	y_0:	11.37
		KA	04.66	KO^E	04.23	N'	05.33	z_0:	$\sqrt{-16}$
		TA	05.39			K'	04.84	t_0:	04.09
		Y	07.08			Y'	04.80	v_p:	4.85
5	IV 19	*KA*	57.22	L_1	57.89	W'	55.66	x_0:	12.65
	14h 47m	*TA*	56.42	L_2	55.13	F'	55.37	y_0	13.33
				KO^E	56.09	N'	55.76	z_0:	
						K'	55.82	t_0:	59.6
						Y'	56.40	v_p:	1.44

(to be continued)

(continued)

No.	Date and Time (J.S.T.)	Data of p Arrival Times at I.A. station (in sec)		E.S. station (in sec)		K.U. station (in sec)		Results of Analysis (in km and sec)	
6	IV 21	*KO*	25.72	R_2	26.89	W'	26.20	x_0:	11.98
	16h 33m	*KA*	26.15	L_1	26.03	F'	26.35	y_0:	10.66
		TA	27.06	L_2	27.01	N'	26.73	z_0:	$\sqrt{-849}$
				K^E	26.10			t_0:	
				KO^E	25.69			v_p:	1.45
7	IV 22	*M*	54.99	R_3	55.41	W'	56.75	x_0:	7.01
	12h 44m			L_1	53.19	F'	56.49	y_0:	9.04
				L_2	56.89	N'	56.28	z_0:	$\sqrt{-18}$
				KO^E	55.99	K'	55.70	t_0:	54.5
								v_p:	6.21
8	IV 22	*KO*	20.90	R_2	22.34	W'	21.40	x_0:	18.46
	17h 03m	*KA*	21.53	L_2	22.03	F'	21.46	y_0:	11.21
				K^E	21.63	N'	22.29	z_0:	$\sqrt{-29}$
				KO^E	20.89	K'	21.45	t_0:	21.
								v_p:	5.2
9	IV 22	*KO*	53.23	R_2	55.08	W'	53.75	x_0:	17.06
	17h 11m			L_2	54.43	F'	53.74	y_0:	11.51
				K^E	54.08	N'	54.50	z_0:	
				KO^E	53.21	Y'	54.50	t_0:	
								v_p:	$\sqrt{-7.4}$
10	IV 22			R_2	06.97	W'	07.50	x_0:	9.78
	17h 35m			R_3	06.35	N'	07.32	y_0:	11.71
				L_1	05.22	K'	06.74	z_0:	$\sqrt{-32.7}$
				L_2	07.95	Y'	06.5	t_0:	05.19
				K^E	06.49			v_p:	4.24
				KO^E	06.52				

Table 2. Data and results of *s*-arrival time analysis by least squares method for the 1956 temporary observation in Wakayama district. (unit in km and sec.)

No.	Date and Time (J.S.T.)	Data of *s* Arrival Times at I.A. station (in sec)		E.S. station (in sec)		K.U. station (in sec)		Results of Analysis (in km and sec)	
1	IV 14	*NI*	40.90	R_3	41.09	*K'*	41.54	x_0:	13.77
	13h 38m	*KO*	41.04	L_1	43.95			y_0:	−0.01
				L_2	42.28			z_0:	
				K^E	41.38			t_0:	
				KO^E	40.88			v_s:	$\sqrt{-84}$
2	IV 15	*NI*	34.28					x_0:	**10.19**
	16h 03m	*KO*	33.38					y_0:	**4.25**
		KA	33.85					z_0:	**4.69**
		TA	35.63					t_0:	**30.47**
		M	31.83					v_s:	**3.40**
		Y	33.23						
3	IV 16	*KO*	50.02	L_2	50.84	*W'*	50.43	x_0:	17.36
	13h 28m			K^E	50.20	*F'*	51.52	y_0:	9.83
				KO^E	49.94	*Y'*	50.76	z_0:	
								t_0:	
								v_s:	0.6
4	IV 19	*NI*	04.98	L_1	08.25	*F'*	05.36	x_0:	18.29
	09h 25m	*KO*	05.36	L_2	05.89	*N'*	07.01	y_0:	10.20
		KA	05.82	KO^E	05.21	*K'*	06.02	z_0:	$\sqrt{-165}$
		TA	07.13			*Y'*	06.12	t_0:	04.49
		Y	08.96					v_s:	3.47
5	IV 19	*TA*	57.42	L_2	55.95	*W'*	56.76	x_0:	20.01
	14h 47m			KO^E	57.29	*F'*	56.29	y_0:	12.80
						N'	56.94	z_0:	
						K'	57.14	t_0:	47.6
						Y'	58.10	v_0:	1.62

(to be continued)

(continued)

No.	Date and Time (J.S.T.)	Data of s Arrival Times at I.A. station (in sec)		E.S. station (in sec)		K.U. station (in sec)		Results of Analysis (in km and sec)	
6	IV 21	KO	27.32	L_2	29.18	F'	27.82	x_0:	14.06
	16h 33m	KA	27.44	K^E	27.72	N'	28.39	y_0:	10.77
		TA	29.43	KO^E	27.30	K'	27.45	z_0:	
						Y'	27.29	t_0:	
								v_s:	$\sqrt{-1.4}$
7	IV 22	KO	59.69	R_3	58.35	N'	60.08	x_0:	10.35
	12h 44m	KA	59.70	L_1	55.99	K'	59.39	y_0:	9.52
		M	58.31	L_2	61.44	Y'	58.51	z_0:	$\sqrt{-108}$
		Y	56.47	KO^E	59.79			t_0:	58.2
								v_s:	4.17
8	IV 22	KO	21.54	R_2	23.91	F'	22.23	x_0:	18.33
	17h 03m	KA	21.16	L_2	22.98	N'	32.90	y_0:	10.99
						K'	22.24	z_0:	$\sqrt{-22}$
								t_0:	21.7
								v_s:	3.71
9	IV 22	KO	53.83	R_2	56.55	F'	54.54	x_0:	16.20
	17h 11m			L_2	55.39	N'	55.97	y_0:	13.56
				KO^E	53.95			z_0:	
								t_0:	
								v_s:	$\sqrt{-0.3}$
10	IV 22			R_2	10.09	W'	10.03	x_0:	10.10
	17h 35m			R_3	08.35	N'	09.87	y_0:	10.90
				L_1	06.52	K'	09.11	z_0:	$\sqrt{-21}$
				L_2	10.77	Y	08.70	t_0:	07.37
				K^E	09.27			v_s:	3.40
				KO^E	09.27				

Table 3. Data and results of p-arrival time analysis by simultaneous equations method for the 1956 temporary observation in Wakayama district. (unit in km and sec.)

1) IV14 13h 38m								2) IV15 16h 03m			
L_1	41.82	L_1	41.82	L_1	41.82	L_1	41.82	R_3	30.56	R_3	30.56
K^E	40.07	K^E	40.07	K^E	40.07	K^E	40.07	L_1	32.01	L_1	32.01
KO^E	39.83	KO^E	39.83	KO^E	39.83	KO^E	39.83	L_2	32.52	L_2	32.52
L_2	40.65	L_2	40.65	L_2	40.50	L_2	40.50	KO^E	31.37	KO^E	31.37
R_3	39.80	K'	40.18	R_3	39.80	K'	40.18	K'	31.50	TA^E	32.62
x_0:	**19.59**	x_0:	18.17	x_0:	**21.63**	x_0:	**18.75**	x_0:	**9.04**	x_0:	11.01
y_0:	**1.73**	y_0:	11.44	y_0:	**0.07**	y_0:	**11.43**	y_0:	**−1.63**	y_0:	7.87
z_0:	**9.52**	z_0:	$\sqrt{-7}$	z_0:	**9.65**	z_0:	**2.45**	z_0:	**16.12**	z_0:	$\sqrt{-24}$
t_0:	**37.40**	t_0:	40.07	t_0:	**36.72**	t_0:	**40.04**	t_0:	**26.94**	t_0:	30.85
v_p:	**4.98**	v_p	7.62	v_p:	**4.99**	v_p:	**7.74**	v_p:	**4.70**	v_p:	7.06

4) IV19 09h 25m				5) IV19 14h 47m		6) IV21 16h 33m					
W'	04.04	W'	04.04	L_1	57.64	R_2	26.91	R_2	26.91	W'	26.20
F'	04.32	F'	04.32	L_2	55.13	L_1	26.03	L_1	26.03	L_1	26.03
R_3	06.37	N'	05.33	W'	55.66	KO^E	25.71	KO^E	25.71	KO^E	25.71
L_2	04.63	K'	04.84	F'	55.37	L_2	27.47	L_2	27.03	N'	26.80
KO^E	04.26	Y'	04.80	N'	55.76	K^E	26.11	K^E	26.11	Y'	26.02
x_0:	22.46	x_0:	−91	x_0:	**25.31**	x_0:	12.19	x_0:	10.30	x_0:	15.56
y_0:	2.61	y_0:	70	y_0:	**13.62**	y_0:	15.56	y_0:	11.76	y_0:	15.86
z_0:		z_0:		z_0:	**7.14**	z_0:	$\sqrt{-26}$	z_0:	$\sqrt{-38}$	z_0:	
t_0:		t_0:		t_0:	**53.57**	t_0:	26.47	t_0:	26.08	t_0:	
v_p:	$\sqrt{-14}$	v_p:	35	v_p:	**5.24**	v_p:	7.62	v_p:	10.76	v_p:	$\sqrt{-264}$

7) IV22 12h 44m				8) IV22 17h 03m				9) IV22 17h 11m	
M	55.06	W'	56.75	R_2	22.52	K'	21.45	L_2	54.58
R_3	55.41	F'	56.49	KO^E	21.13	KO^E	21.13	KO^E	53.37
L_1	53.19	N'	56.28	W'	21.40	W'	21.40	W'	53.75
L_2	56.89	K'	55.70	F'	21.46	F'	21.46	F'	53.74
KO^E	55.99	KO^E	55.99	N'	22.29	N'	22.29	N'	54.50
x_0:	−8.07	x_0:	5.07	x_0:	13.77	x_0:	**17.16**	x_0:	9.45
y_0:	11.91	y_0:	6.52	y_0:	6.62	y_0:	**7.81**	y_0:	6.62
z_0:	$\sqrt{-386}$	z_0:	$\sqrt{-3.5}$	z_0:		z_0:	**2.95**	z_0:	
t_0:	54.22	t_0:	54.36	t_0:		t_0:	**20.78**	t_0:	
v_p:	8.28	v_p:	7.25	v_p:	$\sqrt{-6.2}$	v_p:	**7.27**	v_p:	$\sqrt{-61}$

Table 4. Data and results of *s*-arrival time analysis by simultaneous equations method for the 1956 temporary observation in Wakayama district. (unit in km and sec.)

1) IV14 13h 38m				2) IV15 16h 03m		4) IV19 09h 25m				5) IV19 14h 47m	
KO	41.04	*KO*	41.04	*KO*	33.31	*NI*	05.04	L_2	05.89	*TA*	57.07
R_3	41.05	R_3	41.05	*KA*	33.85	*KO*	05.37	*F'*	05.36	L_2	55.95
L_2	42.32	L_2	42.32	*TA*	35.70	*KA*	05.96	*N'*	07.01	*W'*	56.76
K'	41.54	*K'*	41.54	*M*	31.79	*K'*	06.02	*K'*	06.02	*F'*	56.29
K^E	41.54	K^E	41.39	*Y*	33.21	*Y'*	06.12	*Y'*	06.12	*N'*	56.94
x_0:	9.81	x_0:	12.40	x_0:	10.19	x_0:	25.95	x_0:	**24.53**	x_0:	20.99
y_0:	9.44	y_0:	7.51	y_0:	5.66	y_0:	2.7	y_0:	**4.36**	y_0:	12.18
z_0:		z_0:	$\sqrt{-18}$	z_0:	$\sqrt{-7}$	z_0:		z_0:	**8.39**	z_0:	2.64
t_0:	41.36	t_0:	41.20	t_0:	31.41	t_0:		t_0:	**02.09**	t_0:	36.19
v_s:	11.91	v_s:	9.73	v_s:	3.58	v_s:	$\sqrt{-147}$	v_s:	**3.60**	v_s:	9.27

6) IV21 16h 33m				8) IV22 17h 03m	
L_2	29.18	L_2	29.18	R_2	24.13
K^E	27.76	K^E	27.76	L_2	23.22
KO^E	27.41	KO^E	27.41	*F'*	22.23
K'	27.45	*K'*	27.45	*N'*	23.90
Y'	27.82	*Y'*	27.29	*K'*	22.24
x_0:	18.10	x_0:	13.94	x_0:	12.37
y_0:	11.01	y_0:	9.59	y_0:	−21.18
z_0:	$\sqrt{-1.4}$	z_0:	$\sqrt{-7.3}$	z_0:	$\sqrt{-802}$
t_0:	27.99	t_0:	27.73	t_0:	19.57
v_s:	3.67	v_s:	6.21	v_s:	6.56

Table 5. Data and results of $s-p$ interval analysis by the least squares method (L.S.M) and the simultaneous equations method (S.E.M) for the 1956 temporary observation in Wakayama district. (unit in km and sec.)

Earthq.	1) IV14 13h 38m								2) IV15 16h 03m			
Method	L.S.M.				S.E.M.		S.E.M.		S.E.M.		L.S.M.	
Data ($s-p$)	NI 1.20	KO 1.12			KO 1.20		KO 1.20		KO 1.20		NI 2.20	M 1.45
	R_3 1.25	L_1 2.12			R_3 1.25		R_3 1.25		R_3 1.25		KO 2.00	Y 2.03
	L_2 1.63	K^E 1.30			L_2 1.67		L_2 1.67		L_2 1.67		KA 2.06	
	KO^E 1.05	K' 1.36			K^E 1.47		K^E 1.32		K' 1.36		TA 2.92	
Results	x_0: **17.59**				x_0: **18.67**		x_0: 26.27		x_0: **16.48**		x_0: **11.31**	
	y_0: **5.83**				y_0: **3.49**		y_0: -2.37		y_0: **5.17**		y_0: **3.80**	
	z_0: **8.94**				z_0: **8.89**		z_0: $\sqrt{-104}$		z_0: **9.87**		z_0: **9.92**	
	v_{s-p} **8.45**				v_{s-p} **8.75**		v_{s-p} 8.57		v_{s-p} **8.79**		v_{s-p} **6.70**	

Earthq.	2)						3) IV16 13h 28m					
Method	S.E.M.		S.E.M.		S.E.M.		L.S.M.				S.E.M.	S.E.M.
Data ($s-p$)	KO 1.94		KO 1.94		KO 1.94		KO 0.75	W' 0.84			W' 0.84	W' 0.84
	TA 3.00		TA 3.00		KA 2.05		L_2 0.84	N' 1.34			N' 1.34	N' 1.34
	KA 2.05		M 1.42		M 1.42		KO^E 0.68	K' 0.79			K' 0.79	K' 0.79
	Y 2.02		Y 2.02		Y 2.02			Y' 0.97			Y' 0.97	KO^E 0.68
Results	x_0: **10.56**		x_0: **11.35**		x_0: 10.09		x_0: **18.15**				x_0: **17.81**	x_0: 27.51
	y_0: **8.22**		y_0: $-$**0.46**		y_0: 10.14		y_0: **9.83**				y_0: **8.55**	y_0: 18.47
	z_0: **7.37**		z_0: **10.58**		z_0:		z_0: **4.46**				z_0: **6.61**	z_0:
	v_{s-p}: **5.08**		v_{s-p}: **7.83**		v_{s-p}: $\sqrt{-7}$		v_{s-p}: **7.35**				v_{s-p}: **8.93**	v_{s-p}: $\sqrt{-82}$

Earthq.	4) IV19 09h 25m								5) IV19 14h 47m			
Method	L.S.M.						S.E.M.	S.E.M.			L.S.M.	
Data ($s-p$)	NI 1.06	Y 1.88	KO^E 0.98				NI 1.07	F' 1.04	TA 1.0		F' 0.92	
	KO 1.05	L_1 1.87	F' 1.04				KO 1.11	N' 1.68	L_3 0.82		N' 1.18	
	KA 1.16	L_2 1.26	N' 1.68				KA 1.17	K' 1.18	KO^E 1.20		K' 1.32	
	TA 1.74	L^E 1.25	K' 1.18				L_2 1.22	Y' 1.32	W' 1.10		Y' 1.70	
			Y' 1.32									
Results	x_0: **17.28**						x_0:	x_0: **19.65**			x_0: **21.41**	
	y_0: **7.98**						y_0:	y_0: **7.92**			y_0: **13.94**	
	z_0: 8.81						z_0:	z_0: **7.35**			z_0: **5.78**	
	v_{s-p}: 8.58						v_{s-p}: $\sqrt{-80}$	v_{s-p}: **7.73**			v_{s-p} **7.62**	

(to be continued)

(continued)

Earthq.	5)	6) IV21 16h 33m								
Method	S.E.M.	L.S.M.						S.E.M.	S.E.M.	S.E.M.
Data ($s-p$)	F' 0.92	KO 1.60	K^E 1.12	K' 1.55				L_2 2.15	L_2 2.15	L_2 2.15
	L_2 0.82	KA 1.29	KO^E 1.61	Y' 1.27				KO^E 1.70	KO^E 1.70	KO^E 1.70
	N' 1.18	TA 2.37	F' 1.47					K' 1.55	K^E 1.65	K^E 1.65
	W' 1.10	L_2 2.12	N' 1.66					Y' 1.27	Y' 1.27	K' 1.55
Results	x_0: **24.17**		x_0: **15.40**					x_0: −17.50	x_0: −34.52	x_0: 22.14
	y_0: **13.20**		y_0: **12.39**					y_0: 13.25	y_0: 4.61	y_0: 11.40
	z_0: **6.87**		z_0: **1.29**					z_0:	z_0:	z_0:
	v_{s-p}: **9.09**		v_{s-p} **3.28**					v_{s-p}: $\sqrt{195}$	v_{s-p}: 18.5	v_{s-p}: $\sqrt{-12.5}$

Earthq.	7) IV22 12h 44m						8) IV22 17h 03m					
Method	L.S.M.				S.E.M.	S.E.M.	L.S.M.				S.E.M.	
Data ($s-p$)	KO 3.60	R_3 2.94			RO 3.63	KO 3.63	KO 0.64	F' 0.77			L_2 1.19	
	KA 3.38	L_1 2.89			L_1 2.80	L_1 2.80	KA 0.43	N' 1.61			F' 0.77	
	M 3.25	L_2 4.55			L_2 4.55	L_2 4.55	R_2 1.62	K' 0.79			N' 1.61	
	Y 2.50	KO^E 3.80			K' 3.69	Y' 3.51	L_2 1.19				Y' 0.79	
		N' 3.80										
		K' 3.69										
		Y' 3.51										
Results	x_0: **8.50**				x_0: −16.42	x_0: **9.78**	x_0: 18.88				x_0: **18.18**	
	y_0: **11.36**				y_0: −6.74	y_0: **13.78**	y_0: 0.46				y_0: **12.69**	
	z_0: **5.93**				z_0: $\sqrt{-390}$	z_0: **7.58**	z_0:				z_0: **1.88**	
	v_{s-p} **3.26**				v_{s-p}: 8.59	v_{s-p}: **3.20**	v_{s-p}: $\sqrt{-4.2}$				v_{s-p}: **3.79**	

Earthq.	8)	9) IV22 17h 11m			10) IV22 17h 35m				
Method	S.E.M.	L.S.M.		S.E.M.	L.S.M.				S.E.M.
Data ($s-p$)	L_2 1.19	KO 0.60		L_2 1.11	R_2 3.12	K^E 2.78			R_2 3.12
	F' 0.77	R_2 1.47		KO^E 0.74	R_3 2.00	KO^E 2.75			K^E 2.76
	N' 1.61	L_2 0.96		F' 0.80	L_1 1.30	W' 2.53			N' 2.55
	R_2 1.61	KO^E 0.74		N' 1.47	L_2 2.82	N' 2.55			K' 2.37
		F' 0.80				K' 2.37			
		N' 1.47				Y' 2.20			
Results	x_0: 17.24	x_0: 15.95		x_0: **19.53**	x_0: 14.86				x_0: **19.05**
	y_0: 18.95	y_0: 15.23		y_0: **7.39**	y_0: 12.82				y_0: **14.35**
	z_0: $\sqrt{-87}$	z_0:		z_0: **5.67**	z_0:				z_0: **1.86**
	v_{s-p}: $\sqrt{-33}$	v_{s-p}: $\sqrt{-12}$		v_{s-p} **8.56**	v_{s-p}: $\sqrt{-6.8}$				v_{s-p}: **1.85**

Table 6. Data and results of $s-p$ interval analysis by R. TAKAHASHI's graphical method for the 1952–1954 expeditions near Wakayama.

No. Date Time (J.S.T.)	Epicenter x_0	Epicenter y_0	Depth z_0	Velocity of $s-p$ wave v_{s-p}	Remarks: stations and $s-p$ intervals used
1952	km	km	km	km/s	
1–203* X28 12h 16m	7.0 ±1.2	11.2 ±1.2	20.5 ±4.7	3.97±0.76	E_0: $K_{5.70}$, $T_{6.20}$, $M_{5.68}$, $H_{5.40}$
2–204 XI5 11h 47m	18.50±0.64	7.60±0.78	7.2 ±1.2	6.40±0.33	E_0: $NM_{1.85}$, $K_{1.24}$, $T_{2.20}$, $H_{2.85}$
	17.6 ±1.3	6.8 ±1.1	7.60±0.96		E_1: $NM_{1.85}$, $K_{1.24}$, $T_{2.20}$
	20.0 ±1.1	6.5 ±1.4	6.7 ±1.8		E_2: $K_{1.24}$, $T_{2.20}$, $H_{2.85}$
	18.95±0.64	7.64±0.87	8.70±0.71		E_3: $NM_{1.85}$, $T_{2.20}$, $H_{2,85}$
	19.20±0.73	9.5 ±1.9	7.90±0.69		E_4: $NM_{1.85}$, $K_{1.24}$, $H_{2.85}$
	18.96±0.41	7.39±0.59	8.07±0.43		E_0: *Weighted mean of* E_1, E_2, E_3, E_4
	±0.49	*±0.76*	*±0.51*		
3–208* XI22 21h 32m	−1.5±4.9	12.8 ±1.2	21.5 ±4.7	4.30±0.97	E_0: $K_{6.60}$, $T_{6.90}$, $M_{6.10}$, $H_{5.20}$
4–210 XI24 18h 35m	15.40±0.93	13.80±0.63	3.2 ±1.1	7.50±0.39	E_0: $NM_{2.10}$, $K_{0.62}$, $T_{0.94}$, $M_{1.80}$
	17.30±0.96	13.84±0.52	2.4 ±1.0		E_1: $NM_{2.10}$, $K_{0.62}$, $T_{0.94}$
	15.98±0.71	11.70±0.93	4.00±0.89		E_4: $NM_{2.10}$, $K_{0.62}$, $M_{1.80}$
	16.45±0.57	13.33±0.45	3.29±0.66		E_0: *Weighted mean of* E_1, E_4
	±5.7	*±8.2*	*±7.1*		
5–211 XI25 13h 32m	9.30±0.93	6.4 ±1.0	5.2 ±1.9	6.52±0.55	E_0: $NM_{2.90}$, $T_{2.54}$, $M_{1.00}$, $H_{1.40}$
	8.40±0.82	6.25±0.82	5.5 ±1.0		E_1: $NM_{2.90}$, $T_{2.54}$, $M_{1.00}$
	9.05±0.79	5.96±0.72	5.75±0.65		E_2: $T_{2.54}$, $M_{1.00}$, $H_{1.40}$
	8.50±0.69	5.2 ±1.8	6.10±0.69		E_3: $NM_{2.90}$, $M_{1.00}$, $H_{1.40}$
	8.70±0.53	6.4 ±1.0	6.30±0.97		E_4: $NM_{2.90}$, $T_{2.54}$, $H_{1.40}$
	8.67±0.34	6.10±0.46	5.91±0.39		E_0: *Weighted mean of* E_1, E_2, E_3, E_4
	±0.19	*±0.28*	*±0.25*		
6–214 XII10 18h 04m	15.0	7.3	*imaginary*	6.8	E_1: $NM_{1.80}$, $T_{1.80}$, $M_{1.00}$, $H_{1.90}$
	16.4	5.6	0.0	7.8	E_2: $K_{0.78}$, $T_{1.80}$, $M_{1.00}$, $H_{1.90}$
	14.80±0.47	5.83±0.84	2.9 ±1.7	7.17±0.41	E_3: $NM_{1.80}$, $K_{0.78}$, $M_{1.00}$, $H_{1,90}$
	15.10±0.58	7.35±0.88	5.0 ±1.3	7.52±0.36	E_4: $NM_{1.80}$, $K_{0.78}$, $T_{1.80}$, $H_{1.90}$
	14.10±0.86	6.73±0.71	4.4 ±1.3	7.88±0.53	E_5: $NM_{1.80}$, $K_{0.78}$, $T_{1.80}$, $M_{1.00}$
	14.78±0.35	6.60±0.46	4.52±0.81	7.43±0.25	E_0: *Weighted mean of* E_1〜E_5
	±0.57	*±1.1*	*±1.4*	*±0.53*	
	14.30±0.70	6.20±0.93	2.4 ±1.4		E_3: $K_{0.78}$, $M_{1.00}$, $H_{1.90}$
	17.2 ±1.0	8.55±0.90	4.90±0.83		E_5: $NM_{1.80}$, $K_{0.78}$, $T_{1.80}$
	13.78±0.72	9.0 ±1.0	4.45±0.86		E_8: $K_{0.78}$, $T_{1.80}$, $H_{1.90}$
	15.30±0.55	5.38±0.75	1.2 ±2.5		E_9: $NM_{1.80}$, $K_{0.78}$, $M_{1.00}$
	14.92±0.35	6.99±0.44	3.90±0.54		E_0: *Weighted mean of* E_1, E_5, E_8, E_9. *Other 6 combinations of stations do not give definite epicnters*
	±0.94	*±1.4*	*±1.0*		
7–215 XII14 09h 08m	17.6 ±4.2	0.6 ±5.4	5.9 ±4.6	8.0±1.8	E_0: $K_{1.45}$, $T_{2.50}$, $M_{1.30}$, $H_{2.30}$
	12.8 ±2.9	5.4 ±1.8	7.55±0.71		E_1: $K_{1.45}$, $T_{2.50}$, $M_{1.30}$
	14.87±0.99	5.1 ±1.5	8.1 ±1.5		E_2: $K_{1.45}$, $T_{2.50}$, $H_{2.30}$
	15.13±0.95	3.3 ±1.3	6.7 ±1.2		E_3: $K_{1.45}$, $M_{1.30}$, $H_{2.30}$
	15.6 ±1.2	4.00±0.89	6.1 ±1.7		E_4: $T_{2.50}$, $M_{1.30}$, $H_{2.30}$
	15.06±0.58	4.16±0.62	7.28±0.53		E_0: *Weighted mean of* E_1〜E_4
	±0.50	*±0.64*	*±0.54*		

* $x_0 < 9$ km

(to be continued)

(continued)

No. Date Time (J.S.T.)	Epicenter x_0	Epicenter y_0	Depth z_0	Velocity of $s-p$ wave v_{s-p}	Remarks: stations and $s-p$ intervals used
1952	km	km	km	km/s	
8–216 XI 5 18h 19m	17.1 ±1.8	12.10±0.83	2.90±0.83		E_0: $K_{0.49}$, $T_{1.20}$, $M_{1.90}$
9–217 XI 8 20h 09m	15.00±0.67	7.47±0.86	2.5 ±1.0		E_0: $M_{1.20}$, $K_{0.60}$, $W_{1.60}$
10–218 XI12 03h 58m	16.5 ±1.1	11.90±0.78	5.87±0.62		E_0: $T_{1.45}$, $K_{0.89}$, $W_{1.70}$
11–219 XI14 10h 41m	23.9 ±1.2	11.3 ±1.0	6.2 ±1.0		E_0: $T_{1.79}$, $K_{1.44}$, $NM_{1.50}$
12–220 (207) XI18 20h 55m	22.3 ±1.1	11.40±0.86	4.80±0.98		E_0: $NM_{1.50}$, $K_{1.12}$, $T_{1.56}$
13–221 XII 1 22h 36m	22.6 ±1.1	7. ±13.	8.5 ±5.0		E_0: $NM_{1.50}$, $K_{2.66}$, $M_{5.95}$
14–222 XII 2 02h 21m	16.3 ±2.8	18.0 ±1.6	8.5 ±1.0		E_0: $K_{1.30}$, $T_{2.14}$, $M_{1.83}$
15–223 XII12 02h 08m	10.3 ±1.1	2.90±0.71	6.00±0.80		E_0: $T_{2.85}$, $M_{0.89}$, $H_{1.70}$
16–224 XI13 09h 48m	16.3 ±1.6	10.80±0.67	2.80±0.62		E_0: $K_{0.40}$, $T_{0.95}$, $M_{1.66}$
17–225 XII 1 22h 36m	22.55	7.00	8.50		E_0: $NM_{1.50}$, $K_{1.63}$, $M_{2.44}$
1953					
1–301 X27 16h 23m	29.1 ±1.8	14.9 ±6.1	1.5 ±18.5	10.7 ±1.4	E_0: $KO_{1.27}$, $KA_{1.18}$, $M_{2.19}$, $T_{1.15}$
	17.2 ±2.5	12.1 ±1.9	8.00±0.58		E_1: $KO_{1.27}$, $KA_{1.18}$, $M_{2.19}$
	14.8 ±1.9	15.04±0.81	5.6 ±1.0		E_3: $KO_{1.27}$, $T_{1.5}$, $M_{2.19}$
	15.7 ±1.5	14.60±0.75	7.40±0.51		E_0: *Weighted mean of E_1, E_3. Other 2 combinations of stations cannot give real epicenters*
	±11.	*±9.4*	*±9.2*		
2–302 X28 06h 18m	15.4 ±2.4	−0.1±4.7	3.6 ±5.0	7.5 ±1.5	E_0: $KO_{1.30}$, $T_{2.70}$, $M_{1.00}$, $Y_{2.00}$
	14.40±0.83	1.6 ±1.2	4.5 ±1.6		E_1: $KO_{1.30}$, $M_{1.00}$, $Y_{2.00}$
	13.6 ±1.8	2.6 ±1.4	5.3 ±1.3		E_2: $KO_{1.30}$, $T_{2.70}$, $M_{1.00}$
	14.8 ±1.2	2.00±0.83	3.90±0.24		E_3: $T_{2.70}$, $M_{1.00}$, $Y_{2.00}$
	14.37±0.82	2.6 ±1.3	5.7 ±2.0		E_4: $KO_{1.30}$, $T_{2.70}$, $Y_{2.00}$
	14.39±0.50	2.52±0.55	3.98±0.24		E_0: *Weighted mean of E_1~E_4*
	±0.27	*±0.51*	*±0.30*		

(to be continued)

(continued)

No. Date Time (J.S.T.)	Epicenter x_0	Epicenter y_0	Depth z_0	Velocity of $s-p$ wave v_{s-p}	Remarks: stations and $s-p$ intervals used
1953	km	km	km	km/s	
3–306*	5.8 ±2.0	15.1 ±1.2	7.9 ±2.7	5.10±0.91	E_1: $KO_{2.98}$, $T_{2.94}$, $M_{3.04}$, $Y_{2.10}$
X31	0.2 ±5.3	18.3 ±3.3	9.2 ±8.7	6.9 ±1.7	E_2: $KA_{2.91}$, $T_{2.94}$, $M_{3.04}$, $Y_{2.10}$
20h 37m	8. ±11.	16.0 ±5.6	31. ±37.	11. ±11.	E_3: $KO_{2.98}$, $KA_{2.91}$, $T_{2.94}$, $M_{3.04}$
	5.1 ±1.9	15.51±0.90	8.6 ±1.9	5.52±0.79	E_0: *Weighted mean of E_1, E_2, E_3. Other 2 combinations of stations cannot give real epicenters*
	±3.3	±1.8	*±3.6*	*±1.3*	
4–307*	4.3 ±4.7	3.8 ±3.5	19.5 ±4.4	5.4 ±1.4	E_0: $R_{4.85}$, $KA_{4.60}$, $T_{5.25}$, $M_{3.74}$
XI 1					
17h 53m					
5–312	23.9 ±5.4	7.9 ±2.1	7.8 ±1.3	8.3 ±2.5	E_0: $R_{1.00}$, $KO_{1.25}$, $KA_{1.40}$, $M_{2.10}$
XI 7	22.7 ±2.5	9.0 ±2.7	6.4 ±1.6		E_1: $R_{1.00}$, $KO_{1.25}$, $KA_{1.40}$
19h 42m	21.2 ±1.1	5.8 ±2.2	6.68±0.96		E_2: $R_{1.00}$, $KO_{1.25}$, $M_{2.10}$
	20.70±0.88	7.3 ±1.1	6.76±0.63		E_3: $R_{1.00}$, $KA_{1.40}$, $M_{2.10}$
	19.1 ±2.5	8.5 ±2.1	8.2 ±1.3		E_4: $KO_{1.25}$, $KA_{1.40}$, $M_{2.10}$
	20.90±0.64	7.44±0.84	6.90±0.47		E_0: *Weighted mean of E_1~E_4*
	±0.63	*±0.85*	*±0.49*		
6–313	22.4 ±2.6	8.7 ±6.4	8.3 ±6.5	8.9 ±5.3	E_1: $R_{0.95}$, $KO_{1.10}$, $KA_{1.21}$, $T_{1.63}$
XI 7	22.9 ±7.6	7.6 ±2.9	9.8 ±3.3	10.4 ±4.8	E_2: $R_{0.95}$, $KO_{1.10}$, $KA_{1.21}$, $M_{1.70}$
21h 48m	20.5 ±9.9	8.0 ±4.3	9.6 ±2.1	9.4 ±2.9	E_3: $KO_{1.10}$, $KA_{1.21}$, $T_{1.63}$, $M_{1.70}$
	22.6 ±3.8	7.2 ±1.4	9.5 ±1.7	10.10±0.86	E_4: $R_{0.95}$, $KO_{1.10}$, $T_{1.63}$, $M_{1.70}$
	21.9 ±3.5	7.5 ±1.6	9.3 ±1.7	9.7 ±1.8	E_5: $R_{0.95}$, $KA_{1.21}$, $T_{1.63}$, $M_{1.70}$
	22.3 ±1.8	7.41±0.97	9.45±0.97	9.98±0.76	E_0: *Weighted mean of E_1~E_5*
	±0.26	*±0.18*	*±0.15*	*±0.13*	
	21.7 ±2.3	9.9 ±2.3	5.8 ±1.5		E_1: $R_{0.95}$, $KO_{1.10}$, $KA_{1.21}$
	22.1 ±1.7	10.98±0.79	5.2 ±1.2		E_2: $R_{0.95}$, $KO_{1.10}$, $T_{1.63}$
	23.2 ±2.2	11.3 ±1.0	4.6 ±2.1		E_3: $R_{0.95}$, $KA_{1.21}$, $T_{1.63}$
	18.20±0.77	6.83±0.96	5.68±0.60		E_5: $R_{0.95}$, $KA_{1.21}$, $M_{1.70}$
	19.33±0.99	4.1 ±1.9	5.4 ±1.3		E_6: $R_{0.95}$, $KO_{1.10}$, $M_{1.70}$
	17.10±0.77	9.55±0.61	4.30±0.84		E_7: $R_{0.95}$, $T_{1.63}$, $M_{1.70}$
	15.3 ±2.2	8.9 ±1.8	7.30±0.47		E_8: $KO_{1.10}$, $KA_{1.21}$, $M_{1.70}$
	8.4	13.8	0.0		E_9: $KA_{1.21}$, $T_{1.63}$, $M_{1.70}$
	13.2 ±1.6	11.50±0.91	5.8 ±1.1		E_{10}: $KO_{1.10}$, $T_{1.63}$, $M_{1.70}$
	18.06±0.42	9.75±0.35	6.10±0.30		E_0: *Weighted mean of E_1~E_{10} except E_4, E_9*
	±0.64	*±0.57*	*±0.33*		
7–314	24.1 ±2.1	10.4 ±1.5	8.1 ±2.6	6.80±0.98	E_0: $R_{1.35}$, $KO_{1.60}$, $KA_{1.66}$, $T_{2.05}$
XI 7	24.1 ±3.3	10.3 ±3.3	8.2 ±2.6		E_1: $R_{1.35}$, $KO_{1.60}$, $KA_{1.66}$
22h 58m	24.1 ±2.5	10.5 ±1.0	8.1 ±1.6		E_2: $R_{1.35}$, $KO_{1.60}$, $T_{2.05}$
	24.2 ±2.9	10.5 ±1.3	8.1 ±1.9		E_3: $R_{1.35}$, $KA_{1.66}$, $T_{2.05}$
	25. ±13.	10.4 ±1.4	7. ±15.		E_4: $KO_{1.60}$, $KA_{1.66}$, $T_{2.05}$
	24.2 ± 1.6	10.47±0.67	8.10±1.1		E_0: *Weighted mean of E_1~E_4*
	±0.10	*±0.05*	*±0.08*		
8–315	18.4 ±4.6	4. ±10.	5.9 ±2.9	7.9 ±4.2	E_0: $R_{0.90}$, $KO_{0.95}$, $KA_{1.30}$, $T_{2.10}$
XI10	18.8 ±2.0	5.9 ±2.3	5.5 ±1.3		E_1: $R_{0.90}$, $KO_{0.95}$, $KA_{1.30}$
02h 20m	19.2 ±1.6	6.77±0.94	5.70±0.62		E_2: $R_{0.90}$, $KO_{0.95}$, $T_{2.10}$
	20.1 ±2.4	7.1 ±1.3	6.00±0.72		E_3: $R_{0.90}$, $KA_{0.95}$, $T_{2.10}$
	19.23±1.1	6.77±0.72	5.79±0.44		E_0: *Weighted mean of E_1~E_3 (KO, KA, T) cannot give real epicenter*
	±0.92	*±0.58*	*±0.30*		

(to be continued)

(continued)

No. Date Time (J.S.T.)	Epicenter x_0	Epicenter y_0	Depth z_0	Velocity of $s-p$ wave v_{s-p}	Remarks: stations and $s-p$ intervals used
1953	km	km	km	km/s	
9–316*	−12.1	15.0	*imaginary*	10.6	E_1: $KO_{1.90}$, $KA_{1.75}$, $T_{1.95}$, $R_{2.50}$
XI13	9.8 ±2.8	12.4 ±1.2	8.0 ±7.6	6.0 ±2.2	E_2: $KO_{1.90}$, $KA_{1.75}$, $M_{2.16}$, $R_{2.50}$
22h 58m	10.3 ±2.2	12.2 ±3.1	8.1 ±1.9	5.8 ±1.4	E_2': $KO_{1.90}$, $KA_{1.75}$, $M_{2.20}$, $R_{2.50}$
	7.5	12.5	*imaginary*	4.3	E_3: $KO_{1.90}$, $KA_{1.75}$, $Y_{1.40}$, $R_{2.50}$
	8.2 ±4.9	14.3 ±1.9	11.6 ±8.9	8.1 ±2.4	E_4: $KO_{1.90}$, $KA_{1.75}$, $M_{2.16}$, $T_{1.95}$
	5.8 ±3.3	14.2 ±1.9	10.0 ±7.0	8.5 ±3.5	E_5: $KO_{1.90}$, $KA_{1.75}$, $Y_{1.40}$, $T_{1.95}$
	6.9 ±2.2	17.2 ±4.3	3.0 ±7.1	7.1 ±1.6	E_6: $R_{2.50}$, $KO_{1.90}$, $M_{2.16}$, $Y_{1.40}$
	2.7 ±10.	21. ±16.	1. ±123.	9.4 ±5.4	E_7: $R_{2.50}$, $KA_{1.75}$, $M_{2.16}$, $Y_{1.40}$
	0.5	26.	6.	10.	E_7': $R_{2.50}$, $KA_{1.75}$, $M_{2.20}$, $Y_{1.40}$
	—	—	—	—	E_8: $R_{2.50}$, $T_{1.95}$, $M_{2.20}$, $Y_{1.40}$
	8.6 ±1.5	14.4 ±1.1	7.0 ±3.1	6.50±0.96	E_9: $R_{2.50}$, $KO_{1.90}$, $T_{1.95}$, $M_{2.16}$
	7.2 ±1.7	14.4 ±1.2	6.0 ±3.1	6.8 ±1.2	E_{10}: $R_{2.50}$, $KO_{1.90}$, $T_{1.95}$, $Y_{1.40}$
	6.1 ±1.9	15.1 ±1.6	7.6 ±2.2	7.5 ±1.1	E_{11}: $R_{2.50}$, $KA_{1.75}$, $T_{1.95}$, $Y_{1.40}$
	7.7 ±2.1	15.1 ±1.5	8.6 ±2.6	7.2 ±1.0	E_{12}: $R_{2.25}$, $KA_{1.75}$, $T_{1.95}$, $M_{2.16}$
	8.0 ±1.1	14.50±0.86	2.3 ±5.7	5.80±0.92	E_{13}: $KO_{1.90}$, $T_{1.95}$, $M_{2.16}$, $Y_{1.40}$
	6.5 ±1.5	15.5 ±1.3	5.2 ±2.7	6.70±0.98	E_{14}: $KA_{1.75}$, $T_{1.96}$, $M_{2.16}$, $Y_{1.40}$
	9.8	10.1	*imaginary*	2.5	E_{15}: $KO_{1.90}$, $KA_{1.75}$, $M_{2.16}$, $Y_{1.40}$
	7.49±0.57	14.40±0.43	6.92±1.2	6.76±0.39	E_0: *Weighted mean of* $E_1 \sim E_{15}$
	±0.21	*±0.19*	*±0.37*	±0.15	*except* E_1, E_2', E_3, E_7 E_8, E_{15}
10–319	—	—	—	—	E_1: $R_{1.80}$, $KO_{1.50}$, $KA_{1.83}$, $T_{2.80}$
XI16	11.8 ±1.9	3.4 ±1.9	6.9 ±2.9	6.8 ±1.9	E_2: $R_{1.80}$, $KO_{1.50}$, $KA_{1.82}$, $M_{1.08}$
04h 59m	11.3 ±6.5	2.7 ±2.4	6.4 ±4.4	7.1 ±1.5	E_3: $R_{1.80}$, $KO_{1.50}$, $KA_{1.82}$, $Y_{1.63}$
	11.7 ±3.3	3.9 ±4.8	6.4 ±1.8	6.5 ±1.4	E_4: $KO_{1.50}$, $KA_{1.82}$, $T_{2.80}$, $M_{1.08}$
	11.10±0.99	3.7 ±5.6	5.8 ±1.4	6.5 ±1.7	E_5: $KO_{1.50}$, $KA_{1.82}$, $T_{2.80}$, $Y_{1.63}$
	11.15±0.66	3.6 ±2.3	7.3 ±2.0	7.2 ±1.3	E_6: $R_{1.80}$, $KO_{1.50}$, $M_{1.08}$, $Y_{1.63}$
	11.10±0.94	2.5 ±3.3	8.0 ±2.6	7.7 ±1.8	E_7: $R_{1.80}$, $KA_{1.82}$, $M_{1.08}$, $Y_{1.63}$
	—	—	—	—	E_8: $R_{1.80}$, $T_{2.80}$, $M_{1.08}$, $Y_{1.63}$
	12.05±0.96	3.2 ±2.2	6.5 ±1.3	6.69±0.83	E_9: $R_{1.80}$, $KO_{1.50}$, $T_{2.80}$, $M_{1.08}$
	11.30±0.63	2.3 ±3.0	5.5 ±1.8	6.91±0.98	E_{10}: $R_{1.80}$, $KO_{1.50}$, $T_{2.80}$, $Y_{1.63}$
	11.35±0.62	2.8 ±2.3	5.4 ±2.1	6.74±0.87	E_{11}: $R_{1.80}$, $KA_{1.82}$, $T_{2.80}$, $Y_{1.63}$
	12.15±0.95	3.5 ±2.0	6.3 ±1.4	6.52±0.89	E_{12}: $R_{1.80}$, $KA_{1.82}$, $T_{2.80}$, $M_{1.08}$
	11.00±0.59	5.3 ±1.8	5.5 ±1.7	5.95±0.82	E_{13}: $KO_{1.50}$, $T_{2.80}$, $M_{1.08}$, $Y_{1.63}$
	10.90±0.74	4.7 ±1.8	6.2 ±1.6	6.30±0.83	E_{14}: $KA_{1.82}$, $T_{2.80}$, $M_{1.08}$, $Y_{1.63}$
	10.6	7.2	*imaginary*	4.2	E_{15}: $KO_{1.50}$, $KA_{1.82}$, $M_{1.08}$, $Y_{1.63}$
	11.28±0.24	3.67±0.68	6.22±0.52	6.60±0.11	E_0: *Weighted mean of* $E_1 \sim E_{15}$
	±0.27	*±0.55*	*±0.37*	*±0.23*	*except* E_1, E_8, E_{15}
	12.1 ±3.4	3.5 ±3.3	7.2 ±5.4		E_1: $R_{1.80}$, $KO_{1.50}$, $KA_{1.82}$
	11.8 ±2.7	2.8 ±1.3	6.4 ±3.8		E_2: $R_{1.80}$, $KO_{1.50}$, $T_{2.80}$
	12.0 ±1.6	3.2 ±2.7	6.85±0.67		E_3: $R_{1.80}$, $KO_{1.50}$, $M_{1.08}$
	11.20±0.61	1.3 ±6.8	4. ±13.		E_4: $R_{1.80}$, $KO_{1.50}$, $Y_{1.63}$
	11.9 ±3.5	2.6 ±1.7	5.0 ±7.4		E_5: $R_{1.80}$, $KA_{1.82}$, $T_{2.80}$
	11.9 ±1.1	3.3 ±1.4	6.80±0.63		E_6: $R_{1.80}$, $KA_{1.82}$, $M_{1.08}$
	11.3 ±8.9	2.8 ±7.4	5.5 ±2.1		E_7: $R_{1.80}$, $KA_{1.82}$, $Y_{1.63}$
	12.1 ±1.0	2.9 ±1.0	6.80±0.66		E_8: $R_{1.80}$, $T_{2.80}$, $M_{1.08}$
	11.28±0.61	2.67±1.2	5.5 ±1.8		E_9: $R_{1.80}$, $T_{2.80}$, $Y_{1.63}$
	8.7	3.0	0.0		E_{10}: $KO_{1.50}$, $KA_{1.82}$, $T_{2.80}$
	11.7 ±2.9	3.4 ±2.6	6.88±0.79		E_{11}: $KO_{1.50}$, $KA_{1.82}$, $M_{1.08}$
	11.10±0.81	3.3 ±2.9	6.3 ±3.0		E_{12}: $KO_{1.50}$, $KA_{1.82}$, $Y_{1.63}$
	13.4 ±4.9	2.2 ±2.9	6.1 ±3.3		E_{13}: $KA_{1.82}$, $T_{2.80}$, $M_{1.08}$
	11.4 ±1.4	2.0 ±2.3	5.2 ±4.6		E_{14}: $KA_{1.82}$, $T_{2.80}$, $Y_{1.63}$
	10.5 ±1.1	3.60±0.80	7.15±0.70		E_{15}: $T_{2.80}$, $M_{1.08}$, $Y_{1.63}$
	12.3 ±2.0	2.7 ±1.5	6.70±0.87		E_{16}: $T_{2.80}$, $M_{1.08}$, $KO_{1.50}$
	11.10±0.77	2.8 ±1.4	5.5 ±1.9		E_{17}: $KO_{1.50}$, $T_{2.80}$, $Y_{1.63}$
	11.40±0.62	4.5 ±1.4	6.70±0.57		E_{18}: $R_{1.80}$, $M_{1.08}$, $Y_{1.63}$

(to be continued)

(continued)

No. Date Time (J.S.T.)	Epicenter x_0	Epicenter y_0	Depth z_0	Velocity of $s-p$ wave v_{s-p}	Remarks: stations and $s-p$ intervals used
1953	km	km	km	km/s	
	11.05±0.76	4.1 ±1.2	6.85±0.58		E_{19}: $KO_{1.50}$, $M_{1.08}$, $Y_{1.63}$
	10.90±0.91	4.00±0.96	6.95±0.65		E_{20}: $KA_{1.82}$, $M_{1.08}$, $Y_{1.63}$
	11.29±0.23	3.30±0.34	6.78±0.21		E_0: *Weighted mean of* $E_1 \sim E_{20}$
	±0.041	*±0.068*	*±0.035*		*except* E_{10}
11–320* XI16 21h 10m	6.8 ±5.0	1.9 ±9.7	14.6 ±6.1	13.4 ±6.6	E_0: $KA_{1.53}$, $T_{1.90}$, $M_{1.10}$, $Y_{1.21}$
12–321* XI17 03h 13m	−12. ±24	8.7 ±4.4	29.9 ±7.6	6.6 ±3.4	E_0: $KA_{6.30}$, $T_{6.60}$, $M_{5.64}$, $Y_{5.10}$
13–322 XI19 07h 57m	22.5 ±3.8	5.7 ±1.3	7.7 ±1.6	6.7 ±1.7	E_1: $R_{1.20}$, $KO_{1.48}$, $KA_{1.78}$, $M_{2.34}$
	22.5 ±2.7	5.7 ±1.0	7.1 ±8.7	5.8 ±1.0	E_2: $R_{1.20}$, $KA_{1.78}$, $M_{2.34}$, $Y_{3.20}$
	25.1 ±7.9	5.5 ±1.9	8.2 ±1.4	7.8 ±2.6	E_2': $R_{1.20}$, $KA_{1.78}$, $M_{2.34}$, $Y_{3.00}$
	14.0 ±7.7	8.2 ±2.5	5 ±11.	3.9 ±3.4	E_3: $KO_{1.48}$, $KA_{1.78}$, $M_{2.34}$, $Y_{3.20}$
	21.6 ±2.2	5.0 ±1.7	7. ±10.	6.19±0.79	E_4: $R_{1.20}$, $KO_{1.48}$, $M_{2.34}$, $Y_{3.20}$
	21.9 ±3.0	6.2 ±1.8	7.4 ±1.1	6.25±0.96	E_5: $R_{1.20}$, $KO_{1.48}$, $KA_{1.78}$, $Y_{3.20}$
	21.8 ±1.4	5.83±0.64	7.47±0.90	6.11±0.49	E_0: *Weighted mean of* $E_1 \sim E_6$
	±0.91	*±0.44*	*±0.16*	*±0.26*	*except* E_2'
	22.1 ±3.0	5.3 ±3.3	7.90±0.96		E_1: $R_{1.20}$, $KO_{1.48}$, $KA_{1.78}$
	22.4 ±1.0	6.1 ±1.8	7.97±0.73		E_2: $R_{1.20}$, $KO_{1.48}$, $M_{2.34}$
	23.9 ±1.0	9.7 ±6.2	7.3 ±2.1		E_3: $R_{1.20}$, $KO_{1.48}$, $Y_{3.20}$
	23.45±0.80	3.6 ±2.6	7.0 ±1.7		E_4: $R_{1.20}$, $M_{2.34}$, $Y_{3.20}$
	22.6 ±1.0	5.7 ±1.4	7.95±0.93		E_5: $R_{1.20}$, $KA_{1.78}$, $M_{2.34}$
	23.65±0.92	6.7 ±2.0	7.80±0.87		E_6: $R_{1.20}$, $KA_{1.78}$, $Y_{3.20}$
	23.0 ±3.0	5.4 ±2.6	7.3 ±4.3		E_7: $KO_{1.48}$, $KA_{1.78}$, $M_{2.34}$
	24.0 ±1.2	5.6 ±2.9	6.7 ±3.0		E_8: $KO_{1.48}$, $KA_{1.78}$, $Y_{3.20}$
	24.4 ±1.6	4.5 ±1.8	4.5 ±5.8		E_9: $KA_{1.78}$, $M_{2.34}$, $Y_{3.20}$
	24.1 ±1.2	4.2 ±2.3	5.4 ±3.4		E_{10}: $KO_{1.48}$, $M_{2.34}$, $Y_{3.20}$
	23.41±0.36	5.40±0.69	7.76±0.40		E_0: *Weighted mean of* $E_1 \sim E_{10}$
	±0.15	*±0.23*	*±0.11*		
14–323 XI21 01h 52m	19.0 ±2.5	6.2 ±4.8	6.8 ±1.2	4.9 ±1.5	E_1: $R_{1.48}$, $KO_{1.53}$, $KA_{1.94}$, $T_{3.08}$
	16.5 ±1.8	−1.4±5.5	6.0 ±3.1	7.8 ±3.0	E_2: $R_{1.48}$, $KO_{1.53}$, $KA_{1.94}$, $M_{1.28}$
	16.4 ±1.4	−0.8±3.1	3.5 ±3.4	6.77±0.87	E_3: $R_{1.48}$, $KO_{1.53}$, $T_{3.08}$, $M_{1.28}$
	15.80±0.95	1.5 ±2.1	4.4 ±1.3	6.12±0.75	E_4: $R_{1.48}$, $KA_{1.94}$, $T_{3.08}$, $M_{1.28}$
	13.1 ±8.4	4.1 ±3.8	5.9 ±1.1	5.6 ±1.0	E_5: $KO_{1.53}$, $KA_{1.94}$, $T_{3.08}$, $M_{1.28}$
	15.9 ±1.1	1.2 ±2.4	4.4 ±1.3	6.27±0.77	E_6: $R_{1.48}$, $K_{1.67}$, $T_{3.08}$, $M_{1.28}$
	16.25±0.70	1.6 ±1.4	5.70±0.66	6.11±0.48	E_0: *Weighted mean of* $E_1 \sim E_5$
	±0.66	*±1.4*	*±0.62*	*±0.40*	
	16.14±0.59	1.49±0.84	5.44±0.59	6.14±0.41	E_0': *Weighted mean of* $E_1 \sim E_6$
	±0.44	*±0.93*	*±0.51*	*±0.28*	
	17.5 ±3.3	1.8 ±3.5	7.6 ±3.8		E_1: $R_{1.48}$, $KO_{1.53}$, $KA_{1.94}$
	17.1 ±2.6	0.8 ±1.6	6.5 ±2.6		E_2: $R_{1.48}$, $KO_{1.53}$, $T_{3.08}$
	16.5 ±1.4	−0.8±2.6	3.7 ±3.9		E_3: $R_{1.48}$, $KO_{1.53}$, $M_{1.28}$
	16.0 ±3.6	0.5 ±1.9	5.3 ±5.6		E_4: $R_{1.48}$, $KA_{1.94}$, $T_{3.08}$
	15.9 ±1.0	0.4 ±1.4	5.2 ±1.8		E_5: $R_{1.48}$, $KA_{1.94}$, $M_{1.28}$
	15.90±0.93	0.5 ±1.1	5.2 ±1.5		E_6: $R_{1.48}$, $T_{3.08}$, $M_{1.28}$

(to be continued)

(continued)

No. Date Time (J.S.T.)	Epicenter x_0	Epicenter y_0	Depth z_0	Velocity of $s-p$ wave v_{s-p}	Remarks: stations and $s-p$ intervals used
1953	km	km	km	km/s	
	12. ±16.	1.1 ±1.6	5. ±15.		E_7: $KO_{1.53}$, $KA_{1.94}$, $T_{3.08}$
	14.6 ±3.0	1.4 ±2.8	6.8 ±2.7		E_8: $KO_{1.53}$, $KA_{1.94}$, $M_{1.28}$
	15.9 ±5.3	0.4 ±3.2	5.2 ±7.8		E_9: $KA_{1.94}$, $T_{3.08}$, $M_{1.28}$
	15.0 ±2.1	0.9 ±1.6	6.4 ±2.1		E_{10}: $KO_{1.53}$, $T_{3.08}$, $M_{1.28}$
	15.22±0.54	0.62±0.56	5.70±0.83		E_0: *Weighted mean of* $E_1 \sim E_{10}$
	±0.22	*±0.11*	*±0.20*		
15–324	12.2 ±6.5	0. ±12.	7.2 ±3.4	9.2 ±3.6	E_1: $KO_{1.37}$, $KA_{1.67}$, $M_{0.90}$, $T_{2.40}$
XI21	16.8	−16.	*imaginary*	14.3	E_1' $KO_{1.37}$, $KA_{1.67}$, $M_{0.90}$, $T_{2.24}$
23h 15m	9.0	−1.8	*imaginary*	9.3	E_2: $KO_{1.37}$, $KA_{1.67}$, $Y_{1.18}$, $T_{2.40}$
	7.7	−20.	*imaginary*	15.1	E_2': $KO_{1.37}$, $KA_{1.67}$, $Y_{1.18}$ $T_{2.24}$
	10.1	8.6	*imaginary*	2.9	E_3: $KO_{1.37}$, $KA_{1.67}$, $M_{0.90}$, $Y_{1.18}$
	9.5 ±1.1	5.8 ±3.0	5.4 ±2.6	7.1 ±1.8	E_4: $KO_{1.37}$, $M_{0.90}$, $Y_{1.18}$, $T_{2.40}$
	9.3 ±1.1	4.9 ±3.0	6.8 ±2.5	8.1 ±1.8	E_4': $KO_{1.37}$, $M_{0.90}$, $Y_{1.18}$, $T_{2.24}$
	8.6 ±1.4	4.5 ±2.7	6.8 ±2.1	7.9 ±1.6	E_5: $KA_{1.67}$, $M_{0.90}$, $Y_{1.18}$, $T_{2.40}$
	7.4 ±2.9	1.0 ±6.5	9.0 ±1.8	10.3 ±3.3	E_5': $KA_{1.67}$, $M_{0.90}$, $Y_{1.18}$ $T_{2.24}$
	9.85±0.82	6.7 ±1.7	3.8 ±2.0	6.5 ±1.1	E_6: $K_{1.30}$, $M_{0.90}$, $Y_{1.18}$, $T_{2.40}$
	9.80±0.81	5.7 ±1.7	5.6 ±1.9	7.6 ±1.1	E_6': $K_{1.30}$, $M_{0.90}$, $Y_{1.18}$, $T_{2.24}$
	9.55±0.58	6.0 ±1.3	5.5 ±1.2	7.09±0.78	E_0: *Weighted mean of* $E_1 \sim E_6$
	±0.47	*±1.0*	*±1.3*	*±0.69*	
	9.51±0.63	5.3 ±1.5	7.3 ±1.2	7.92±0.89	E_0': *Weighied mean of* $E_1' \sim E_6'$
	±0.94	*±1.8*	*±2.7*	*±1.22*	
	22.8 ±1.3	5.7 ±1.3	8.4 ±9.7		E_1: $KO_{1.37}$, $KA_{1.67}$, $T_{2.40}$
	11.3 ±2.6	4.1 ±2.4	5.55±0.62		E_2: $KO_{1.37}$, $KA_{1.67}$, $M_{0.90}$
	9.65±0.67	3.9 ±2.7	2.7 ±5.4		E_3: $KO_{1.37}$, $KA_{1.67}$, $Y_{1.18}$
	9.3 ±1.7	6.5 ±1.3	4.5 ±1.1		E_4: $KO_{1.37}$, $M_{0.90}$, $T_{2.40}$
	9.50±0.64	6.5 ±1.2	4.9 ±1.1		E_5: $KO_{1.37}$, $Y_{1.18}$, $T_{2.40}$
	9.52±0.61	6.15±0.94	4.80±0.63		E_6: $KO_{1.37}$, $M_{0.90}$, $Y_{1.18}$
	8.9 ±1.2	8.0 ±2.1	6.4 ±1.1		E_8: $KA_{1.67}$, $Y_{1.18}$, $T_{2.40}$
	9.68±0.82	6.28±0.66	4.60±0.75		E_9: $T_{2.40}$, $M_{0.90}$, $Y_{1.18}$
	9.04±0.72	5.65±0.79	5.10±0.60		E_{10}: $KA_{1.67}$, $M_{0.90}$, $Y_{1.18}$
	10.06±0.28	6.07±0.37	5.19±0.29		E_0: *Weighted mean of* $E_1 \sim E_{10}$
	±0.76	*±0.17*	*±0.12*		*except* E_7 *(by KA, T, M) which could'nt be obtained*
16–326	11.70±0.59	7.55±0.90	5.0 ±2.7	7.2 ±1.2	E_1: $R_{1.50}$, $KA_{1.17}$, $M_{1.06}$, $Y_{1.34}$
XI22	8.25±0.66	9.4 ±4.2	8.6 ±4.2	10.5 ±5.3	E_2: $R_{1.50}$, $KO_{1.17}$, $KA_{1.17}$, $M_{1.06}$
11h 09m	11.40±0.70	6.3 ±1.8	7.4 ±2.6	8.3 ±1.5	E_3: $R_{1.50}$, $KO_{1.17}$, $M_{1.06}$, $Y_{1.34}$
	12.6	11.4	*imaginary*	7.0	E_4: $R_{1.50}$, $T_{1.93}$, $M_{1.06}$, $Y_{1.34}$
	11.45±0.77	6.9 ±2.2	8.1 ±2.4	8.5 ±1.4	E_5: $R_{1.50}$, $KO_{1.17}$, $T_{1.93}$, $Y_{1.34}$
	11.9 ±1.0	7.4 ±1.4	5.7 ±2.2	7.6 ±1.1	E_6: $KA_{1.17}$, $T_{1.93}$, $M_{1.06}$, $Y_{1.34}$
	16.8 ±3.8	10.7 ±2.0	6.5 ±2.1	5.8 ±1.7	E_7: $R_{1.50}$, $KO_{1.17}$, $KA_{1.17}$, $T_{1.93}$
	11.0 ±1.2	6.7 ±1.8	7.1 ±2.6	8.3 ±1.3	E_8: $R_{1.50}$, $KO_{1.17}$, $T_{1.93}$, $M_{1.06}$
	11.4 ±1.1	7.75±0.96	5.3 ±2.1	7.50±0.87	E_9: $R_{1.50}$, $KA_{1.17}$, $T_{1.93}$, $M_{1.06}$
	9.2 ±2.1	9.5 ±2.0	1. ±26.	6.9 ±1.2	E_{10}: $KO_{1.17}$, $KA_{1.17}$, $T_{1.93}$, $M_{1.06}$
	11.8 ±1.3	5.4 ±3.4	8.7 ±3.1	9.2 ±2.2	E_{11}: $KO_{1.17}$, $T_{1.93}$, $M_{1.06}$, $Y_{1.34}$
	10.90±0.73	9.9 ±1.9	4.7 ±3.0	6.7 ±1.2	E_{12}: $KO_{1.17}$, $KA_{1.7}$, $T_{1.93}$, $Y_{1.34}$
	11.70±0.61	7.9 ±1.2	5.7 ±2.0	7.49±0.84	E_{13}: $R_{1.50}$, $KA_{1.17}$, $T_{1.93}$, $Y_{1.34}$
	—	—	—	—	E_{14}: $KO_{1.7}$, $KA_{1.17}$, $M_{1.06}$, $Y_{1.34}$
	11.50±0.86	9.9 ±3.7	8.9 ±3.9	9.0 ±2.4	E_{15}: $R_{1.50}$, $KO_{1.17}$, $KA_{1.17}$, $Y_{1.34}$
	11.08±0.23	7.86±0.44	6.01±0.71	7.54±0.35	E_0: *Weighted mean of* $E_1 \sim E_{15}$
	±0.21	*±0.19*	*±0.23*	*±0.13*	*except* E_4, E_{14}, *which could'nt be obtained*

(to be continued)

(continued)

No. Date Time (J.S.T.)	Epicenter x_0	Epicenter y_0	Depth z_0	Velocity of $s-p$ wave v_{s-p}	Remarks: stations and $s-p$ intervals used
1953	km	km	km	km/s	
	15.3 ±2.7	10.5 ±2.4	7.62±0.88		E_1: $R_{1.50}$, $KO_{1.17}$, $KA_{1.17}$
	14.9 ±2.2	9.48±0.91	7.6 ±1.2		E_2: $R_{1.50}$, $KO_{1.17}$, $T_{1.93}$
	13.1 ±1.3	4.8 ±2.1	5.64±0.60		E_3: $R_{1.50}$, $KO_{1.17}$, $M_{1.06}$
	13.8 ±2.4	9.5 ±1.2	6.7 ±2.0		E_6: $R_{1.50}$, $KA_{1.17}$, $T_{1.93}$
	11.92±0.92	7.50±0.99	4.2 ±1.0		E_6: $R_{1.50}$, $KA_{1.17}$, $M_{1.06}$
	11.75±0.50	7.4 ±1.5	3.7 ±1.4		E_7: $R_{1.50}$, $KA_{1.17}$, $Y_{1.34}$
	11.55±0.85	8.50±0.74	2.80±1.73		E_8: $R_{1.50}$, $T_{1.93}$, $M_{1.06}$
	11.80±0.51	8.60±0.86	3.6 ±1.2		E_9: $R_{1.50}$, $T_{1.93}$, $Y_{1.34}$
	11.78±0.51	7.9 ±1.2	3.7 ±1.3		E_{10}: $R_{1.50}$, $M_{1.06}$, $Y_{1.34}$
	10. ±10.	9.8 ±1.1	3. ±21.		E_{11}: $KO_{1.17}$, $KA_{1.17}$, $T_{1.93}$
	10.88±0.65	9.9 ±2.1	5.00±0.71		E_{13}: $KO_{1.17}$, $KA_{1.17}$, $Y_{1.43}$
	11.00±0.95	9.6 ±1.6	5.0 ±1.0		E_{15}: $KA_{11.7}$, $T_{1.93}$, $Y_{1.34}$
	11.03±0.70	7.15±0.83	5.05±0.63		E_{16}: $KO_{1.17}$, $M_{1.06}$, $Y_{1.34}$
	12.15±0.87	8.22±0.67	2.8 ±1.6		E_{17}: $T_{1.93}$, $M_{1.06}$, $Y_{1.34}$
	11.60±0.72	7.70±0.82	4.20±0.77		E_{18}: $KA_{1.17}M_{1.06}$, $Y_{1.34}$
	10.90±0.62	9.70±0.98	5.05±0.76		E_{19}: $KO_{1.17}$, $T_{1.93}$, $Y_{1.34}$
	11.61±0.19	8.41±0.25	5.07±0.24		E_0: *Weighted mean of* $E_1 \sim E_{20}$
	±0.089	*±0.12*	*±0.16*		*except* E_4, E_{12}, E_{14}, E_{20} *which covld not be obtained*
17–327	9.10±0.46	7.32±0.80	0.86±6.1	4.86±0.45	E_0: $KO_{1.67}$, $T_{3.10}$, $M_{1.06}$, $Y_{1.20}$
XI23	12.7 ±2.1	0.2 ±1.6	6.0 ±1.8		E_1: $KO_{1.67}$, $T_{3.10}$, $M_{1.06}$
17h 16m	8.05±0.69	5.8 ±1.1	6.25±0.54		E_3: $KO_{1.67}$, $M_{1.06}$, $Y_{1.20}$
	5.80±0.93	3.05±0.78	6.20±0.70		E_4: $T_{3.10}$, $M_{1.06}$, $Y_{1.20}$
	7.56±0.53	3.46±0.60	6.22±0.40		E_0: *Weighted mean of* E_1, E_3,
	±3.0	*±3.1*	*±0.11*		E_4. *KO, T, Y cannot give a real epicenter* E_2
18–329	12.65±0.69	5.2 ±1.0	3.0 ±1.9	6.05±0.59	E_1: $R_{1.54}$, $KA_{1.45}$, $T_{2.56}$, $M_{0.91}$
XI25	12.85±0.71	5.4 ±1.0	3.9 ±1.6	6.10±0.58	E_1': $R_{1.54}$, $KA_{1.45}$, $T_{2.56}$, $M_{1.00}$
05h 07m	12.30±0.46	5.1 ±1.3	2.6 ±2.9	6.17±0.60	E_2: $R_{1.54}$, $KA_{1.45}$, $T_{2.56}$, $Y_{1.58}$
	12.35±0.50	5.1 ±1.3	4.0 ±2.4	6.48±0.98	E_3: $R_{1.54}$, $KA_{1.45}$, $Y_{1.58}$, $M_{0.91}$
	12.6	11.4	*imaginary*	6.0	E_4: $R_{1.54}$, $T_{2.56}$, $Y_{1.58}$, $M_{0.9191}$
	12.05±0.73	5.7 ±1.2	3.7 ±1.7	6.00±0.65	E_5: $KA_{1.45}$, $T_{2.56}$, $Y_{1.58}$, M_0.
	12.32±0.28	5.27±0.59	3.55±0.88	6.12±0.33	E_0: *Weighted mean of* $E_1 \sim E_5$
	±0.25	*±0.37*	±0.68	*±0.21*	*except* E_4
18–329	12.16±0.95	5.0 ±1.1	4.84±0.68		E_2: $R_{1.54}$, $KA_{1.45}$, $M_{0.91}$
XI25	12.15±0.55	5.0 ±1.7	5.2 ±1.7		E_5: $R_{1.54}$, $KA_{1.45}$, $Y_{1.58}$
05h 07m	12.20±0.55	4.7 ±1.2	4.90±0.69		E_6: $R_{1.54}$, $M_{0.91}$, $Y_{1.58}$
	12.25±0.56	3.7 ±1.1	4.2 ±1.9		E_7: $R_{1.54}$, $T_{2.56}$, $Y_{1.58}$
	12.45±0.84	4.80±0.84	4.65±0.90		E_9: $KA_{1.45}$, $M_{0.91}$, $Y_{1.58}$
	11.9 ±1.0	4.20±0.73	5.30±0.93		E_{10}: $T_{2.56}$, $M_{0.91}$, $Y_{1.58}$
	12.20±0.27	4.50±0.40	4.89±0.37		E_0: *Weighted mean of* E_2, E_5,
	±0.058	*±0.20*	*±0.12*		E_6, E_7, E_9, E_{10}. *Other 4 combinations cannot give real epicenters*
19–330	17.2 ±1.0	6.0 ±1.4	5.3 ±1.1	7.02±0.66	E_1: R_{100}, $KO_{0.90}$, $T_{2.10}$, $Y_{2.10}$
XI25	19.3 ±1.5	9.7 ±1.6	3.9 ±1.8	5.1 ±1.0	E_2: $R_{1.00}$, $KO_{0.90}$, $KA_{1.07}$, $T_{2.10}$
06h 08m	18.0 ±1.9	8.2 ±1.9	6.9 ±1.6	7.7 ±1.1	E_3: $R_{1.00}$, $KO_{0.90}$, $KA_{1.07}$, $Y_{2.10}$
	14.6 ±1.4	8.9 ±1.5	4.6 ±1.3	5.79±0.75	E_4: $KO_{0.90}$, $KA_{1.07}$, $T_{2.10}$, $Y_{2.10}$
	16.30±0.77	6.90±0.83	4.0 ±1.5	6.43±0.51	E_5: $R_{1.00}$, $KA_{1.07}$, $T_{2.10}$, $Y_{2.10}$
	16.78±0.50	7.53±0.57	4.99±0.62	6.44±0.32	E_0: *Weighted mean of* $E_1 \sim E_5$
	±0.78	*±0.76*	*±0.60*	*±0.42*	

(to be continued)

(continued)

No. Date Time (J.S.T.)	Epicenter x_0	Epicenter y_0	Depth z_0	Velocity of $s-p$ wave v_{s-p}	Remarks: stations and $s-p$ intervals used
1953	km	km	km	km/s	
	18.4 ±2.0	8.7 ±2.0	6.00±0.47		E_1: $R_{1.00}$, $KO_{0.90}$, $KA_{1.07}$
	17.5 ±1.6	6.65±0.94	5.72±0.83		E_2: $R_{1.00}$, $KO_{0.90}$, $T_{2.10}$
	16.55±0.67	4.2 ±4.2	4.0 ±4.3		E_3: $R_{1.00}$, $KO_{0.90}$, $Y_{2.10}$
	15.3 ±2.2	6.0 ±1.2	4.9 ±2.8		E_4: $R_{1.00}$, $KA_{1.07}$, $T_{2.10}$
	16.68±0.62	7.3 ±1.3	5.10±0.86		E_5: $R_{1.00}$, $KA_{1.07}$, $Y_{2.10}$
	16.67±0.60	6.40±0.86	5.03±0.93		E_6: $R_{1.00}$, $T_{2.10}$, $Y_{2.10}$
	16.30±0.79	8.4 ±1.7	6.05±0.72		E_8: $KO_{0.90}$, $KA_{1.07}$, $Y_{2.10}$
	16.40±0.78	6.70±0.99	5.80±0.89		E_9: $KO_{0.90}$, $T_{2.10}$, $Y_{2.10}$
	17.15±0.80	5.76±0.79	5.3 ±1.0		E_{10}: $KA_{1.07}$, $T_{2.10}$, $Y_{2.10}$
	16.67±0.28	6.55±0.38	5.69±0.28		E_0: *Weighted mean of* $E_1 \sim E_{10}$
	±0.11	*±0.21*	*±0.11*		*except* E_7 *which was not real*
20–333 XI29 00h 14m	16. ±45.	−48. ±1714.	31. ±1323	6. ±81.	E_0: $R_{1.05}$, $KO_{10.75}$, $M_{9.6}$, $Y_{10.6}$
21–336 XII 2 17h 54m	22.2 ±2.0	6.8 ±7.8	6.6 ±3.3	7.8 ±4.2	E_0: $R_{0.85}$, $KO_{1.10}$, $KA_{1.33}$, $T_{1.95}$
	21.7 ±2.2	7.8 ±2.4	6.10±0.81		E_1: $R_{0.85}$, $KO_{1.10}$, $KA_{1.33}$
	22.0 ±1.6	8.52±0.87	5.60±0.88		E_2: $R_{0.85}$, $KO_{1.10}$, $T_{1.95}$
	22.8 ±2.4	8.8 ±1.2	5.4 ±1.3		E_3: $R_{0.85}$, $KA_{1.33}$, $T_{1.95}$
	22.13±1.1	8.54±0.69	5.79±0.54		E_0: *Weighted mean of* E_1, E_2,
	±0.69	*±0.44*	*±0.53*		E_3. E_4 *(by KO, KA, T) is not real*
22–337 XII 2 17h 57m	26.8 ±6.4	11.3 ±4.3	7.6 ±8.5	7.9 ±5.6	E_0: $R_{1.30}$, $KO_{1.60}$, $KA_{1.63}$, $T_{1.85}$
	25.1 ±3.2	11.2 ±3.3	6.8 ±3.9		E_1: $R_{1.30}$, $KO_{1.60}$, $KA_{1.63}$
	25.5 ±2.4	11.95±0.96	6.2 ±2.7		E_2: $R_{1.30}$, $KO_{1.60}$, $T_{1.85}$
	26.3 ±2.8	12.2 ±1.2	5.4 ±3.9		E_3: $R_{1.30}$, $KA_{1.63}$, $T_{1.85}$
	25.60±1.6	12.01±0.75	6.14±1.9		E_0: *Weighted mean of* E_1, E_2,
	±0.83	*±0.38*	*±0.86*		E_3. E_4 *(by KO, KA, T) is not real*
23–339 XII 4 11h 35m	21.13±0.83	9.9 ±1.6	2.3 ±3.1	4.78±0.92	E_0: $R_{0.75}$, $KO_{1.00}$, $KA_{1.20}$, $T_{2.24}$
	21.7 ±1.7	8.5 ±2.2	4.85±0.84		E_1: $R_{0.75}$, $KO_{1.00}$, $KA_{1.20}$
	20.6 ±1.5	5.6 ±1.0	4.85±0.77		E_2: $R_{0.75}$, $KO_{1.00}$, $T_{2.24}$
	17.4 ±2.3	4.7 ±1.3	2.4 ±4.9		E_3: $R_{0.75}$, $KA_{1.20}$, $T_{2.24}$
	20.41±0.99	5.64±0.75	4.82±0.56		E_0: *Weighted mean of* E_1, E_2,
	±2.7	*±2.0*	*±0.48*		E_3. E_4 *(by KO, KA, T) is not real*
24–341 XII 6 07h 14m	23. ±12.	11.9 ±2.3	9.4 ±2.8	7.2 ±2.6	E_0: $KO_{1.60}$, $K_{1.60}$, $T_{1.77}$, $M_{2.56}$
	24. ±12.	12.7 ±1.4	7. ±11.		E_1: $KO_{1.60}$, $K_{1.60}$, $T_{1.77}$
	18.6 ±2.4	13.0 ±1.1	10.00±0.72		E_2: $KO_{1.60}$, $T_{1.77}$, $M_{2.56}$
	20.2 ±4.6	11.1 ±4.5	10.2 ±1.2		E_3: $KO_{1.60}$, $K_{1.60}$, $M_{2.56}$
	17.2 ±3.3	13.7 ±1.6	10.40±0.59		E_4: $K_{1.60}$, $T_{1.77}$, $M_{2.56}$
	18.50±1.8	12.98±0.75	10.22±0.43		E_0: *Weighted mean of* $E_1 \sim E_4$
	±0.37	*±0.45*	*±0.20*		
25–343 XII10 13h 19m	14.4 ±2.0	15.2 ±7.9	3.3 ±3.4	8.4 ±1.4	E_0: $KO_{0.90}$, $KA_{0.57}$, $T_{0.78}$, $Y_{1.60}$
	12.98±0.64	13.2 ±1.3	1.6 ±2.7		E_2: $K_{0.90}$, $KA_{0.57}$, $Y_{1.60}$ *Other 3 combinations could not give real epicenters*
26–346 XII11 05h 50m	14.15±0.67	6.60±0.79	2.5 ±2.1	6.32±0.80	E_0: $R_{1.20}$, $KO_{0.70}$, $KA_{1.07}$, $M_{1.10}$
	13.1	5.9	0.0		E_1: $R_{1.20}$, $KO_{0.70}$, $KA_{1.07}$
	13.7 ±1.0	7.4 ±1.5	3.2 ±1.2		E_2: $R_{1.20}$, $KO_{0.70}$, $M_{1.10}$
	13.95±0.77	6.69±0.87	3.60±0.87		E_3: $R_{1.20}$, $KA_{1.07}$, $M_{1.10}$
	14.7 ±1.6	6.1 ±1.4	3.1 ±1.1		E_4: $KO_{0.70}$, $KA_{1.07}$, $M_{1.10}$
	13.96±0.58	6.69±0.68	3.35±0.60		E_0: *Weighted mean of* E_2, E_3,
	±0.45	*±0.58*	*±0.32*		E_4

(to be continued)

(continued)

No. Date Time (J.S.T.)	Epicenter x_0	Epicenter y_0	Depth z_0	Velocity of $s-p$ wave v_{s-p}	Remarks: stations and $s-p$ intervals used
1953	km	km	km	km/s	
27–347	16.0 ±5.3	2.9 ±9.1	2. ±19.	7.2 ±3.1	E_1: $R_{1.00}$, $KO_{0.90}$, $KA_{1.38}$, $T_{2.38}$
XII 11	16.75±0.89	4.30±0.94	3.8 ±2.2	6.5 ±1.0	E_2: $R_{1.00}$, $KO_{0.90}$, $KA_{1.38}$, $M_{1.33}$
05h 59m	16.75±0.90	4.7 ±1.1	3.95±0.86	6.60±0.48	E_3: $R_{1.00}$, $KO_{0.90}$, $T_{2.38}$, $M_{1.33}$
	17.0 ±1.0	4.2 ±1.4	4.4 ±1.4	6.78±0.76	E_4: $R_{1.00}$, $KA_{1.38}$, $T_{2.38}$, $M_{1.33}$
	17.3 ±4.5	4.0 ±3.8	3.9 ±3.9	6.8 ±1.3	E_5: $KO_{0.90}$, $KA_{1.38}$, $T_{2.38}$, $M_{1.33}$
	16.80±0.63	4.38±0.63	4.05±0.68	6.65±0.36	E_0: *Weighted mean of* $E_1 \sim E_5$
	±0.08	*±0.13*	*±0.13*	*±0.07*	
	16.3 ±2.1	3.6 ±2.3	3.2 ±5.1		E_1: $R_{1.00}$, $KO_{0.90}$, $KA_{1.38}$
	16.5 ±1.6	4.1 ±1.1	3.9 ±2.1		E_2: $R_{1.00}$, $KO_{0.90}$, $T_{2.38}$
	16.70±0.93	4.6 ±1.7	4.5 ±1.0		E_3: $R_{1.00}$, $KO_{0.90}$, $M_{1.33}$
	17.0 ±2.6	4.2 ±1.4	4.4 ±3.4		E_4: $R_{1.00}$, $KA_{1.38}$, $T_{2.38}$
	16.97±0.75	4.0 ±1.0	4.3 ±1.1		E_5: $R_{1.00}$, $KA_{1.38}$, $M_{1.33}$
	16.90±0.74	4.20±0.83	4.40±0.93		E_6: $R_{1.00}$, $T_{2.38}$, $M_{1.33}$
	19. ±11.	3.9 ±1.1	3.4 ±6.1		E_7: $KO_{0.90}$, $KA_{1.38}$, $T_{2.38}$
	17.2 ±1.5	4.0 ±1.2	3.9 ±2.2		E_8: $KO_{0.90}$, $T_{2.38}$, $M_{1.33}$
	17.0 ±4.0	4.2 ±2.4	4.4 ±5.8		E_9: $KA_{1.38}$, $T_{2.28}$, $M_{1.33}$
	17.4 ±2.0	3.8 ±1.9	3.5 ±3.6		E_{10}: $KO_{0.90}$, $KA_{1.38}$, $M_{1.33}$
	16.88±0.40	4.08±0.39	4.29±0.51		E_0: *Weighted mean of* $E_1 \sim E_{10}$
	±0.055	*±0.45*	*±0.060*		
28–348	19.2 ±2.4	10.5 ±2.1	4.5 ±2.9	7.4 ±2.1	E_1: $R_{0.80}$, $KO_{0.70}$, $KA_{0.75}$, $T_{1.41}$
XII 14	18.3 ±2.1	9.9 ±2.3	6.4 ±1.9	9.4 ±2.3	E_2: $R_{0.80}$, $KO_{0.70}$, $KA_{0.75}$, $M_{1.44}$
22h 12m	18.8 ±1.9	10.2 ±1.9	5.19±0.89	8.2 ±1.1	E_3: $R_{0.80}$, $KO_{0.70}$, $KA_{0.75}$, $Y_{2.00}$
	16.1 ±3.4	9.9 ±1.5	5.4 ±1.5	8.0 ±1.2	E_4: $KO_{0.70}$, $KA_{0.75}$, $T_{1.41}$, $M_{1.44}$
	19.5 ±3.1	10.4 ±1.8	5.2 ±1.0	8.5 ±1.3	E_5: $KO_{0.70}$, $KA_{0.75}$, $T_{1.41}$, $Y_{2.00}$
	17.8 ±1.2	7.0 ±1.6	5.2 ±1.2	7.64±0.87	E_6: $R_{0.80}$, $KO_{0.70}$, $M_{1.44}$, $Y_{2.00}$
	16.50±0.97	7.90±0.76	1.4 ±5.0	6.50±0.92	E_7: $R_{0.80}$, $KA_{0.75}$, $M_{1.44}$, $Y_{2.00}$
	—	—	—	—	E_8: $R_{0.80}$, $T_{1.41}$, $M_{1.44}$, $Y_{2.00}$
	18.2 ±1.5	8.8 ±1.0	5.9 ±1.3	8.74±0.95	E_9: $R_{0.80}$, $KO_{0.70}$, $T_{1.41}$, $M_{1.44}$
	18.7 ±1.3	9.60±0.99	5.5 ±1.1	8.12±0.79	E_{10}: $R_{0.80}$, $KO_{0.70}$, $T_{1.41}$, $Y_{2.00}$
	19.3 ±1.3	10.60±0.91	5.3 ±1.1	8.43±0.72	E_{11}: $R_{0.80}$, $KA_{0.75}$, $T_{1.41}$, $Y_{2.00}$
	17.4 ±1.1	8.90±0.70	5.4 ±1.3	8.45±0.83	E_{12}: $R_{0.80}$, $KA_{0.75}$, $T_{1.41}$, $M_{1.44}$
	21.9	7.1	*imaginary*	9.1	E_{13}: $KA_{0.75}$, $T_{1.41}$, $M_{1.44}$, $Y_{2.00}$
	27.8	4.5	*imaginary*	11.5	E_{14}: $KO_{0.70}$, $KA_{0.75}$, $M_{1.44}$, $Y_{2.00}$
	11.89±0.44	9.13±0.34	5.36±0.39	8.06±0.30	E_0: *Weighted mean of* $E_1 \sim E_{15}$
	±0.21	*±0.22*	*±0.095*	*±0.14*	*except* E_8, E_{13}, E_{14}, E_{15}. *which were not real*
	19.3 ±1.6	10.5 ±1.5	4.80±0.77		E_1: $R_{0.80}$, $KO_{0.70}$, $KA_{0.75}$
	19.5 ±1.2	10.98±0.64	3.50±0·79		E_2: $R_{0.80}$, $KO_{0.70}$, $T_{1.41}$
	17.50±0.76	6.0 ±1.4	3.80±0.78		E_3: $R_{0.80}$, $KO_{0.70}$, $M_{1.44}$
	16.66±0.51	8.0 ±1.6	2.9 ±1.5		E_5: $R_{0.80}$, $M_{1.44}$, $Y_{2.00}$
	16.60±0.62	8.14±0.68	2.70±0.92		E_6: $R_{0.80}$, $KA_{0.75}$, $M_{1.44}$
	16.70±0.58	8.2 ±1.0	2.7 ±1.1		E_7: $R_{0.80}$, $KA_{0.75}$, $Y_{2.00}$
	16.80±0.56	10.25±0.60	1.2 ±2.8		E_9: $R_{0.80}$, $T_{1.41}$, $Y_{2.00}$
	20.0 ±1.5	11.12±0.84	3.55±0.87		E_{10}: $R_{0.80}$, $KA_{0.75}$, $T_{1.41}$
	14.2 ±1.5	9.8 ±1.1	3.65±0.98		E_{12}: $KO_{0.70}$, $KA_{0.75}$, $M_{1.44}$
	16.10±0.73	10.1 ±1.3	4.45±0.52		E_{13}: $KO_{0.70}$, $KA_{0.75}$, $Y_{2.00}$
	15.55±0.92	11.9 ±1.1	4.95±0.69		E_{15}: $KA_{0.75}$, $T_{1.41}$, $Y_{2.00}$
	16.04±0.73	11.20±0.68	4.03±0.69		E_{18}: $KO_{0.70}$, $T_{1.41}$, $Y_{2.00}$
	16.15±0.75	7.5 ±1.4	4.50±0.69		E_{19}: $KO_{0.70}$, $M_{1.44}$, $Y_{2.00}$
	16.72±0.98	8.1 ±1.1	2.5 ±2.2		E_{20}: $KA_{0.75}$, $M_{1.44}$, $Y_{2.00}$
	16.68±0.20	9.88±0.24	4.01±0.22		E_0: *Weighted mean of* $E_1 \sim E_{20}$
	±0.14	*±0.23*	*±0.11*		*except* E_4, E_8, E_{11}, E_{14}, E_{16}, E_{17}, *which were not real*
29–350 XII 16 13h 50m	40.7	9.9	*imaginary*	9.7	E_0: $KO_{1.50}$, $KA_{1.60}$, $T_{1.72}$, $M_{2.74}$

(to be continued)

(continued)

No. Date Time (J.S.T.)	Epicenter x_0	Epicenter y_0	Depth z_0	Velocity of $s-p$ wave v_{s-p}	Remarks: stations and $s-p$ intervals used
1953	km	km	km	km/s	
30–351 XII17 23h 57m	17.0 ±5.1	8.7 ±2.6	10.4 ±2.0	6.2 ±1.3	E_1: $KO_{1.70}$, $KA_{1.80}$, $T_{2.44}$, $M_{2.32}$
	19.4 ±4.1	9.4 ±2.4	9.9 ±1.1	5.8 ±1.2	E_2: $KO_{1.70}$, $KA_{1.80}$, $T_{2.44}$, $Y_{3.20}$
	—	—	—	—	E_3: $KO_{1.70}$, $KA_{1.80}$, $M_{2.32}$, $Y_{3.20}$
	—	—	—	—	E_4: $KO_{1.70}$, $T_{2.44}$, $M_{2.32}$, $Y_{3.20}$
	29.3	2.5	*imaginary*	7.8	E_5: $KA_{1.80}$, $T_{2.44}$, M_{232}, $Y_{3.20}$
	19.4 ±3.2	9.1 ±1.8	10.02±0.96	5.97±0.88	E_0: *Weighted mean of* E_1, E_2
	±11.	*±3.1*	*±1.9*	*±1.8*	
	14. ±15.	8.0 ±1.5	11.1 ±3.9		E_1: $KO_{1.70}$, $KA_{1.80}$, $T_{2.44}$
	17.9 ±3.3	8.6 ±2.7	11.50±0.92		E_2: $KO_{1.70}$, $KA_{1.80}$, $M_{2.32}$
	22.8 ±1.3	9.3 ±3.1	10.0 ±1.2		E_3: $KO_{1.70}$, $KA_{1.80}$, $Y_{3.20}$
	18.6 ±2.4	7.7 ±1.4	11.4 ±1.0		E_4: $KO_{1.70}$, $T_{2.44}$, $M_{2.32}$
	22.9 ±1.3	7.5 ±1.3	9.9 ±1.4		E_5: $KO_{1.70}$, $T_{2.44}$, $Y_{3.20}$
	23.1 ±1.3	2.4 ±2.3	7.5 ±2.8		E_6: $KO_{1.70}$, $M_{2.32}$, $Y_{3.20}$
	20.0 ±4.9	7.0 ±2.7	10.4 ±3.6		E_7: $KA_{1.80}$, $T_{2.44}$, $M_{2.32}$
	23.7 ±2.2	6.5 ±2.2	8.0 ±4.3		E_8: $KA_{1.80}$, $T_{2.44}$, $Y_{3.20}$
	24.5 ±1.6	3.8 ±1.8	1.7 ±1.6		E_9: $KA_{1.80}$, $M_{2.32}$, $Y_{3.20}$
	24.17±1.63	10.47±0.67	8.10±1.1		E_0: *Weighted mean of* $E_1 \sim E_9$
	±0.10	*±0.05*	*±0.08*		E_{10} *(by T, M, Y) is not real*
31–352 X 31 19h 18m	15.66±0.72	4.4 ±1.1	1.0 ±4.7		E_0: $KO_{0.70}$, $M_{1.00}$, $Y_{1.90}$
32–353 XI 3 01h 47m	17.5 ±1.7	10.7 ±1.4	4.43±0.51		E_0: $KO_{0.70}$, $R_{1.00}$, $KA_{0.71}$
33–354 XI 4 19h 47m	14.8 ±9.1	10.95±0.99	6.8 ±2.9		E_0: $KO_{1.10}$, $KA_{1.06}$, $T_{1.69}$
34–355 XI26 09h 13m	15.4 ±2.5	3.5 ±2.3	6.5 ±1.7		E_0: $KO_{1.25}$, $KA_{1.63}$, $M_{1.32}$
35–356 XI27 03h 54m	19.1 ±2.1	5.0 ±2.3	6.0 ±2.5		E_0: $R_{1.00}$, $KO_{0.95}$, $KA_{1.36}$
36–357 (334) XI30 23h 51m	17.2 ±2.8	2.3 ±2.6	6.9 ±3.1		E_0: $KO_{1.40}$, $KA_{1.81}$, $M_{1.55}$
37–358 (335) XII 1 12h 23m	12.4 ±3.2	4.2 ±2.8	9.85±0.62		E_0: $KO_{1.75}$, $KA_{2.00}$, $M_{1.49}$
38–359 XI 1 10h 45m	22.6 ±2.6	9.4 ±2.6	5.9 ±1.9		E_0: $R_{0.95}$, $KO_{1.30}$, $KA_{1.32}$
39–360 XI13 01h 27m	16.7 ±2.2	4.7 ±2.4	5.4 ±2.6		E_0: $R_{1.10}$, $KO_{1.00}$, $KA_{1.39}$

(to be continued)

(continued)

No. Date Time (J.S.T.)	Epicenter x_0	Epicenter y_0	Depth z_0	Velocity of $s-p$ wave v_{s-p}	Remarks: stations and $s-p$ intervals used
1953	km	km	km	km/s	
40–361 XII 1 02h 04m	27.7 ±3.8	2.9 ±1.8	2.3 ±9.2		E_0: $R_{1.20}$, $KA_{2.20}$, $T_{2.90}$
41–362 XII 1 23h 17m	14.9 ±2.3	1.8 ±2.2	2.0 ±7.0		E_0: $KO_{1.10}$, $KA_{1.60}$, $M_{0.88}$
42–363 XII 3 04h 06m	19.5 ±2.2	4.7 ±2.5	5.3 ±1.8		E_0: $R_{0.90}$, $KO_{10.5}$, $KA_{1.45}$
43–364 XI30 20h 52m	13.9 ±2.4	4.1 ±2.2	5.9 ±1.2		E_0: $KO_{1.20}$, $KA_{1.54}$, $M_{1.12}$
1954					
1–401* XI10 06h 12m	−1.3±8.0	4.6 ±4.9	19.4 ±4.2	6.6 ±2.1	E_0: $KA_{4.20}$, $T_{4.72}$, $M_{3.38}$, $Y_{3.09}$
2–402 XI12 22h 16m	16.7 ±1.6	5.5 ±2.1	8.4 ±2.1	8.5 ±1.4	E_0: $KO_{1.05}$, $SR_{1.14}$, $M_{1.38}$, $Y_{1.88}$
3–403* XI12 23h 28m	−8. ±18.	5.6 ±5.8	14.6 ±5.5	8.2 ±3.5	E_0: $KO_{3.57}$, $T_{4.00}$, $M_{2.80}$, $Y_{2.30}$
4–405 XI16 16h 42m	19.8 ±1.4	3.1 ±1.5	3.7 ±1.9	6.75±0.75	E_0: $SR_{0.79}$, $KO_{1.07}$, $M_{1.66}$, $Y_{2.60}$
5–408 XI20 11h 21m	18.5 ±2.2	12.7 ±3.5	8.7 ±1.5	6.9 ±1.7	E_1: $SR_{1.59}$, $KA_{1.28}$, $KO_{1.40}$, $M_{2.38}$
	18.5 ±2.4	12.6 ±3.2	8.6 ±1.1	6.8 ±1.2	E_2: $SR_{1.59}$, $KA_{1.28}$, $KO_{1.40}$, $Y_{2.62}$
	18.4 ±1.9	12.3 ±2.8	8.7 ±1.6	6.8 ±1.0	E_3: $SR_{1.59}$, $KO_{1.40}$, $M_{2.38}$, $Y_{2.62}$
	18.2 ±2.1	12.3 ±2.6	8.4 ±1.7	6.7 ±1.3	E_4: $SR_{1.59}$, $KA_{1.28}$, $M_{2.38}$, $Y_{2.62}$
	21. ±61.	13 ±23.	8.9 ±1.0	8. ±22.	E_5: $KO_{1.40}$, $KA_{1.28}$, $M_{2.38}$, $Y_{2.62}$
	18.40±1.1	12.47±1.5	8.72±0.57	6.81±0.61	E_0: *Weighted mean of* E_1~E_5
	±0.08	*±0.11*	*±0.04*	*±0.07*	
	18.5 ±2.9	12.6 ±2.5	8.4 ±1.1		E_1: $SR_{1.59}$, $KO_{1.40}$, $KA_{1.28}$
	18.5 ±1.3	12.5 ±2.5	8.6 ±1.6		E_2: $SR_{1.59}$, $KO_{1.40}$, $M_{2.38}$
	18.35±0.92	12.2 ±5.8	8.7 ±3.1		E_3: $SR_{1.59}$, $KO_{1.40}$, $Y_{2.62}$
	18.5 ±1.1	12.5 ±1.1	8.50±0.68		E_4: $SR_{1.59}$, $KA_{1.28}$, $M_{2.38}$
	18.37±0.80	12.5 ±1.6	8.50±0.74		E_5: $SR_{1.59}$, $KA_{1.28}$, $Y_{2.62}$
	18.3 ±2.2	12.6 ±1.6	8.50±0.76		E_6: $KO_{1.40}$, $KA_{1.28}$, $M_{2.38}$
	18.4 ±1.0	12.5 ±2.2	8.48±0.73		E_7: $KO_{1.40}$, $KA_{1.28}$, $Y_{2.62}$
	18.3 ±1.0	12.6 ±2.2	8.5 ±1.4		E_8: $KO_{1.40}$, $M_{2.38}$, $Y_{2.62}$
	18.3 ±1.3	12.6 ±1.7	8.50±0.81		E_9: $KA_{1.28}$, $M_{2.38}$, $Y_{2.62}$
	18.36±0.72	12.6 ±2.6	8.4 ±2.1		E_{10}: $SR_{1.59}$, $M_{2.38}$, $Y_{2.62}$
	18.38±0.33	12.52±0.59	8.49±0.30		E_0: *Weighted mean of* E_1~E_{10}
	±0.014	*±0.012*	*±0.007*		

(to be continued)

(continued)

No. Date Time (J.S.T.)	Epicenter x_0	Epicenter y_0	Depth z_0	Velocity of $s-p$ wave v_{s-p}	Remarks: stations and $s-p$ intervals used
1954	km	km	km	km/s	
6–410	16.9 ±2.5	12.7 ±5.5	9.3 ±3.1	11.0 ±4.2	E_1: $SR_{1.10}$, $KO_{0.92}$, $KA_{0.85}$, $M_{1.45}$
XI24	18.7 ±1.9	11.6 ±2.2	5.92±0.84	7.5 ±1.0	E_2: $SR_{1.10}$, $KO_{0.92}$, $KA_{0.85}$, $Y_{2.24}$
05h 51m	16.58±0.81	5.3 ±1.2	4.9 ±1.3	6.2 ±0.60	E_3: $SR_{1.10}$, $KO_{0.92}$, $M_{1.45}$, $Y_{2.24}$
	15.3	7.5	*imaginary*	5.2	E_4: $SR_{1.10}$, $KA_{0.85}$, $M_{1.45}$, $Y_{2.24}$
	—	—	—	—	E_5: $KO_{0.92}$, $KA_{0.85}$, $M_{1.45}$, $Y_{2.24}$
	16.91±0.72	7.0 ±1.0	5.79±0.67	6.80±0.51	E_0: *Weighted mean of* $E_1 \sim E_4$
	±1.3	*±5.0*	*±1.6*	*±1.2*	
	19.0 ±2.0	11.4 ±1.7	5.2 ±1.0		E_1: $SR_{1.10}$, $KO_{0.92}$, $KA_{0.85}$
	16.50±0.90	5.8 ±1.7	5.50±0.58		E_2: $SR_{1.10}$, $KO_{0.92}$, $M_{1.45}$
	17.26±0.76	7.6 ±4.0	6.12±0.54		E_3: $SR_{1.10}$, $KO_{0.92}$, $Y_{2.24}$
	15.53±0.72	8.53±0.75	4.18±0.71		E_4: $SR_{1.10}$, $KA_{0.85}$, $M_{1.45}$
	17.48±0.66	10.2 ±1.1	5.30±0.56		E_5: $SR_{1.10}$, $KA_{0.85}$, $Y_{2.24}$
	12.3 ±1.7	10.9 ±1.3	3.1 ±2.5		E_6: $KO_{0.92}$, $KA_{0.85}$, $M_{1.45}$
	17.18±0.83	11.3 ±1.5	5.68±0.54		E_7: $KO_{0.92}$, $KA_{0.85}$, $Y_{2.24}$
	17.35±0.85	4.8 ±1.5	5.0 ±1.3		E_8: $KO_{0.92}$, $M_{1.45}$, $Y_{2.24}$
	17.00±0.56	4.2 ±1.8	5.70±0.83		E_{10}: $SR_{1.10}$, $M_{1.45}$, $Y_{2.24}$
	16.80±0.28	8.73±0.45	5.46±0.23		E_0: *Weighted mean of* $E_1 \sim E_{10}$
	±0.28	*±0.63*	*±0.16*		*except* E_9
7–412	16.6 ±1.1	−0.1±3.0	5.7 ±4.8	9.3 ±3.2	E_0: $SR_{1.09}$, $KO_{1.13}$, $KA_{1.48}$, $M_{1.02}$
XI24	18.6 ±2.3	5.3 ±2.4	6.7 ±1.4		E_1: $SR_{1.09}$, $KO_{1.13}$, $KA_{1.48}$
18h 16m	12.1 ±2.2	4.7 ±2.0	4.65±0.75		E_4: $KO_{1.13}$, $KA_{1.48}$, $M_{1.02}$
	15.2 ±1.6	4.9 ±1.5	5.16±0.69		E_0: *Weighted mean of* E_1, E_4.
	±29.	*±2.6*	*±8.1*		E_2, E_3 *are not real*
8–413	18.0 ±1.1	8.7 ±1.2	5.0 ±1.3	7.5 ±1.1	E_1: $SR_{0.86}$, $KO_{0.68}$, $KA_{0.86}$, $M_{1.60}$
XI29	17.9 ±1.3	8.6 ±1.5	5.2 ±1.1	7.78±0.94	E_2: $SR_{0.86}$, $KO_{0.68}$, $KA_{0.86}$, $Y_{2.00}$
03h 42m	18.1 ±1.1	9.3 ±1.9	5.15±0.99	7.82±0.53	E_3: $SR_{0.86}$, $KO_{0.68}$, $M_{1.60}$, $Y_{2.00}$
	18.6 ±2.4	9.2 ±1.7	5.9 ±2.1	8.2 ±1.7	E_4: $SR_{0.86}$, $KA_{0.86}$, $M_{1.60}$, $Y_{2.00}$
	14.6 ±7.2	9.19±0.85	3.2 ±9.9	5.8 ±4.6	E_5: $KO_{0.68}$, $KA_{0.86}$, $M_{1.60}$, $Y_{2.00}$
	17.99±0.64	9.31±0.56	5.17±0.60	7.74±0.40	E_0: *Weighted mean of* $E_1 \sim E_5$
	±0.22	*±0.26*	*±0.16*	*±0.14*	
	18.3 ±1.5	9.0 ±1.4	4.38±0.48		E_1: $SR_{0.86}$, $KO_{0.68}$, $KA_{0.86}$
	17.65±0.73	7.5 ±1.4	4.50±0.52		E_2: $SR_{0.86}$, $KO_{0.68}$, $M_{1.60}$
	16.28±0.67	4.2 ±3.1	1.7 ±7.2		E_3: $SR_{0.86}$, $KO_{0.68}$, $Y_{2.00}$
	17.37±0.66	8.20±0.73	4.02±0.66		E_4: $SR_{0.86}$, $KA_{0.86}$, $M_{1.60}$
	16.57±0.58	7.53±1.03	3.2 ±1.1		E_5: $SR_{0.86}$, $KA_{0.86}$, $Y_{2.00}$
	16.6 ±1.5	8.8 ±1.6	4.62±0.78		E_6: $KO_{0.68}$, $KA_{0.86}$, $M_{1.60}$
	16.15±0.73	8.7 ±1.3	4.55±0.63		E_7: $KO_{0.68}$, $KA_{0.86}$, $Y_{2.00}$
	16.16±0.74	9.3 ±1.5	4.53±0.76		E_8: $KO_{0.68}$, $M_{1.60}$, $Y_{2.00}$
	16.03±0.99	9.2 ±1.2	4.90±0.94		E_9: $KA_{0.86}$, $M_{1.60}$, $Y_{2.00}$
	16.87±0.49	9.9 ±1.8	1.9 ±4.1		E_{10}: $SR_{0.86}$, $M_{1.60}$, $Y_{2.00}$
	16.73±0.23	8.37±0.39	4.39±0.25		E_0: *Weighted mean of* $E_1 \sim E_{10}$
	±0.13	*±0.15*	*±0.096*		
9–421* XII10 01h 27m	0.2 ±5.7	7.5 ±2.4	17.4 ±3.3	5.4 ±1.3	E_0: $SR_{5.10}$, $KO_{4.48}$, $M_{3.75}$, $Y_{3.30}$
10–422	16.7 ±2.6	0.4 ±5.4	14.1 ±8.6	10.1 ±7.0	E_1: $SR_{1.62}$, $KO_{1.63}$, $KA_{1.85}$, $M_{1.61}$
XII14	18.0 ±3.3	4.1 ±2.7	12.4 ±4.5	8.1 ±2.2	E_2: $SR_{1.62}$, $KO_{1.63}$, $KA_{1.85}$, $Y_{2.40}$
16h 50m	16.7 ±1.5	0.8 ±3.0	9.4 ±1.9	7.5 ±1.3	E_3: $SR_{1.62}$, $KO_{1.63}$, $M_{1.61}$, $Y_{2.40}$

(to be continued)

(continued)

No. Date Time (J.S.T.)	Epicenter x_0	Epicenter y_0	Depth z_0	Velocity of $s-p$ wave v_{s-p}	Remarks: stations and $s-p$ intervals used
1954	km	km	km	km/s	
	15.5 ±1.0	4.0 ±1.6	7.6 ±2.2	6.2 ±1.1	E_4: $SR_{1.62}$, $KA_{1.85}$, $M_{1.61}$, $Y_{2.40}$
	—	—	—	—	E_5: $KO_{1.63}$, $KA_{1.85}$, $M_{1.61}$, $Y_{2.40}$
	16.10±0.79	3.0 ±1.2	9.2 ±1.4	6.89±0.79	E_0: *Weighted meam of* $E_1 \sim E_4$
	±0.79	*±1.5*	*±1.7*	*±0.88*	
	18.6 ±3.3	6.0 ±3.2	10.60±0.96		E_1: $SR_{1.62}$, $KO_{1.63}$, $KA_{1.85}$
	16.5 ±1.4	1.0 ±2.6	8.1 ±1.7		E_2: $SR_{1.62}$, $KO_{1.63}$, $M_{1.61}$
	15.65±0.88	−0.9±6.3	5.6 ±9.8		E_3: $SR_{1.62}$, $KO_{1.63}$, $Y_{2.40}$
	15.6 ±1.0	3.5 ±1.3	8.79±0.70		E_4: $SR_{1.62}$, $KA_{1.85}$, $M_{1.61}$
	16.06±0.75	3.9 ±2.0	9.2 ±1.2		E_5: $SR_{1.62}$, $KA_{1.85}$, $Y_{2.40}$
	12.7 ±3.0	5.5 ±2.7	9.78±0.51		E_6: $KO_{1.63}$, $KA_{1.85}$, $M_{1.61}$
	15.4 ±1.0	5.8 ±2.9	10.6 ±1.3		E_7: $KO_{1.63}$, $KA_{1.85}$, $Y_{2.40}$
	15.6 ±1.0	2.2 ±1.7	8.9 ±1.1		E_8: $KO_{1.63}$, $M_{1.61}$, $Y_{2.40}$
	16.4 ±1.2	3.0 ±1.3	8.3 ±1.5		E_9: $KA_{1.85}$, $M_{1.61}$, $Y_{2.40}$
	15.96±0.68	2.5 ±2.0	8.60±0.89		E_{10}: $SR_{1.62}$, $M_{1.61}$, $Y_{2.40}$
	15.83±0.33	3.25±0.63	9.37±0.30		E_0: *Weighted mean of* $E_1 \sim E_{10}$
	±0.13	*±0.30*	*±0.17*		
11–423 XII18 12h 59m	17.88±0.56	7.3 ±1.1	4.10±0.92	5.40±0.47	E_0: $S_{1.18}$, $SR_{1.01}$, $KO_{0.80}$, $M_{2.00}$
12–424 XI19 11h 29m	12.5	7.8	0.0		E_0: $KO_{0.65}$, $KA_{0.90}$, $M_{0.95}$
13–425 XI23 00h 24m	17.7 ±1.7	8.9 ±1.6	5.10±0.51		E_0: $KO_{0.77}$, $SR_{1.00}$, $KA_{0.94}$
	19.6	9.1	4.5		E_0': $KO_{0.77}$, $KA_{0.94}$, $W_{1.10}$
14–426 XI24 11h 56m	17.7 ±2.3	3.4 ±2.5	5.1 ±3.0		E_0: $KO_{1.09}$, $SR_{1.06}$, $KA_{1.55}$
15–427 XII 1 10h 14m	20.8 ±1.1	14.5 ±2.2	6.9 ±1.4		E_0: $KO_{1.25}$, $SR_{1.26}$, $M_{2.40}$
	21.9	10.2	6.6		E_0': $KO_{1.25}$, $M_{2.40}$, $W_{1.20}$
16–428 XII 3 08h 58m	21.4 ±2.6	7.2 ±2.6	7.45±0.70		E_0: $SR_{1.11}$, $KO_{1.31}$, $KA_{1.45}$
	20.2	7.1	7.3		E_0': $SR_{1.11}$, $KO_{1.21}$, $KA_{1.45}$
17–429 XII 9 05h 17m	16.3 ±2.6	2.4 ±8.4	5. ±11.		E_0: $SR_{1.21}$, $KO_{1.15}$, $W_{1.60}$
18–430 XII18 14h 51m	6.38±0.99	3.7 ±1.7	10.90±0.56		E_0: $KO_{2.35}$, $M_{1.67}$, $Y_{1.80}$
19–431 XI25 05h 05m	19.2 ±1.8	9.0 ±1.8	5.53±0.52		E_0: $SR_{0.94}$, $KO_{0.87}$, $KA_{1.03}$
20–432 XI29 21h 09m	18.7 ±1.8	14.66±0.70	4.50±0.76		E_0: $SR_{1.42}$, $KA_{0.81}$, $T_{1.00}$

(to be continued)

(continued)

No. Date Time (J.S.T.)	Epicenter x_0	Epicenter y_0	Depth z_0	Velocity of $s-p$ wave v_{s-p}	Remarks: stations and $s-p$ intervals used
1954	km	km	km	km/s	
21–433 XII 3 02h 53m	15.6 ±1.7	7.4 ±1.6	4.4 ±1.5		E_0: $SR_{1.09}$, $KO_{0.69}$, $KA_{1.00}$
22–434 XII 10 03h 45m	17.1 ±2.1	5.0 ±2.2	5.5 ±2.2		E_0: $SR_{1.06}$, $KO_{0.99}$, $KA_{1.37}$

Table 7. 1 st kind errors calculated by the present author for $k(=v_{s-p})$ and origins obtained by A. Imamura in Wakayama district.

No.	x_0	y_0	z_0	k
1	17.85± 0.29	7.55±0.35	1.57±1.99	3.10±0.84
2	15.68± 2.97	8.05±1.55	*5.93±5.99*	*3.90±3.30*
3	17.80± 0.41	7.50±0.40	0.60±4.47	3.00±0.47
4	18.00± 0.40	6.45±0.63	0.85±3.83	3.10±0.93
5	17.38± 0.22	7.50±0.36	1.00±3.52	3.26±1.02
6	18.40± 0.88	10.20±2.21	2.85±1.36	3.75±1.47
7	17.90± 0.50	9.50±1.72	2.90±2.04	3.75±1.55
8	17.25± 0.35	7.42±0.46	2.00±2.68	3.73±1.42
9	11.00±11.17	6.30±2.25	*6.90±2.67*	*5.76±5.16*
10	18.15± 0.60	8.20±0.77	2.64±2.24	3.90±1.44
11	14.75± 4.16	8.10±1.09	*4.00±3.31*	*4.30±3.17*

N.B. Hypocenters are shown in our coordinate system (*loc. cit.* 1) and No. of earthquakes are referred to the paper of A. Imamura (*loc. cit.* 3).

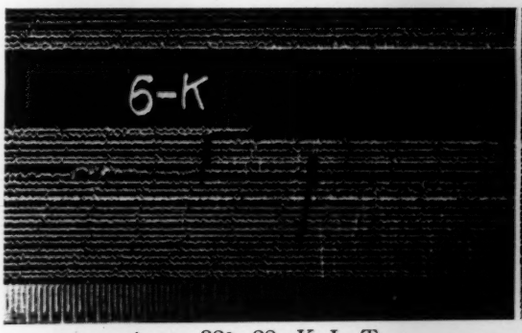

$t_p = -32^s$, 28, K. L. T
(30^s. 56, J. S. T.

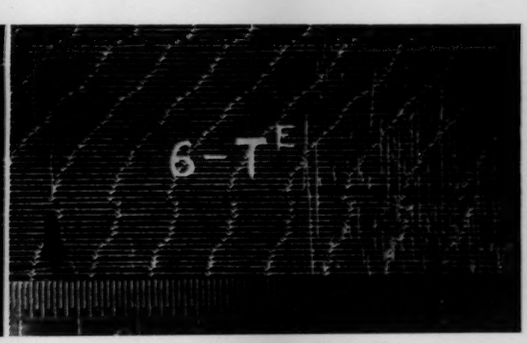

$t_p = -33^s$, 73, K. L. T.
(32^s. 01, J. S. T.)

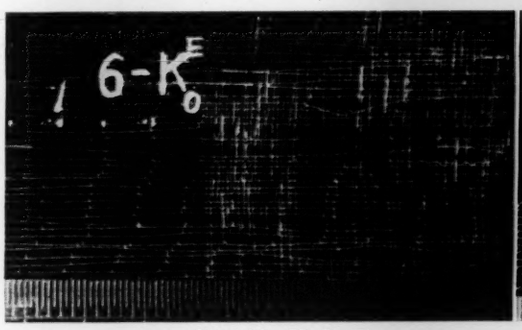

$t_p = -33^s$, 09, K. L. T.
(31^s, 37, J. S. T.)

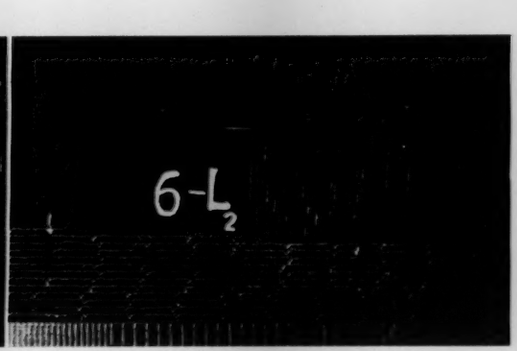

$t_p = -34^s$, 24, K. L. T.
(32^s, 52, J. S. T.)

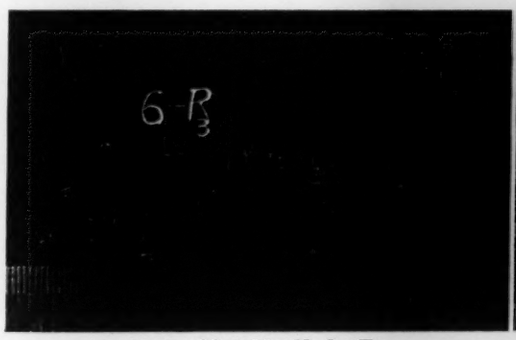

$t_p = -33^s$, 22, K. L. T.
(31^s, 50, J. S. T.)

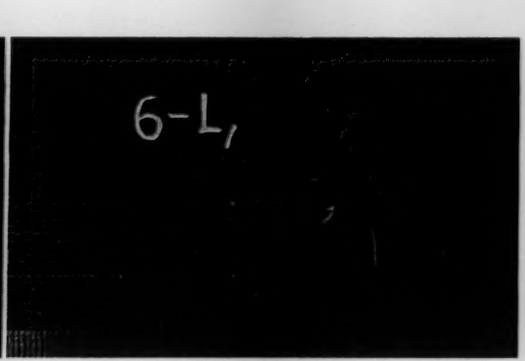

$t_p = -34^s$, 34, K. L. T.
(32^s, 62, J. S. T.)

Fig. 1. Seismograms of a shock obtained at the electronic stations of E. R. I. in the 1956 expedition in Wakayama district. J. S. T.: Japan Standard Time. K. L. T.: Kainan Local Time (by a chromometer at Kainan base station. cf. *loc. cit.* 1). R_3, L_1 etc.: Stations (cf. *loc. cit.* 1) Time marks are given at every second.

No. 326
1953 XII.22 11^h09^m

M
t_p : $07^s.04$

Y
t_p : $07^s.21$

KO
t_p : $07^s.22$

KA
t_p : $07^s.41$

T
t_p : $08^s.11$

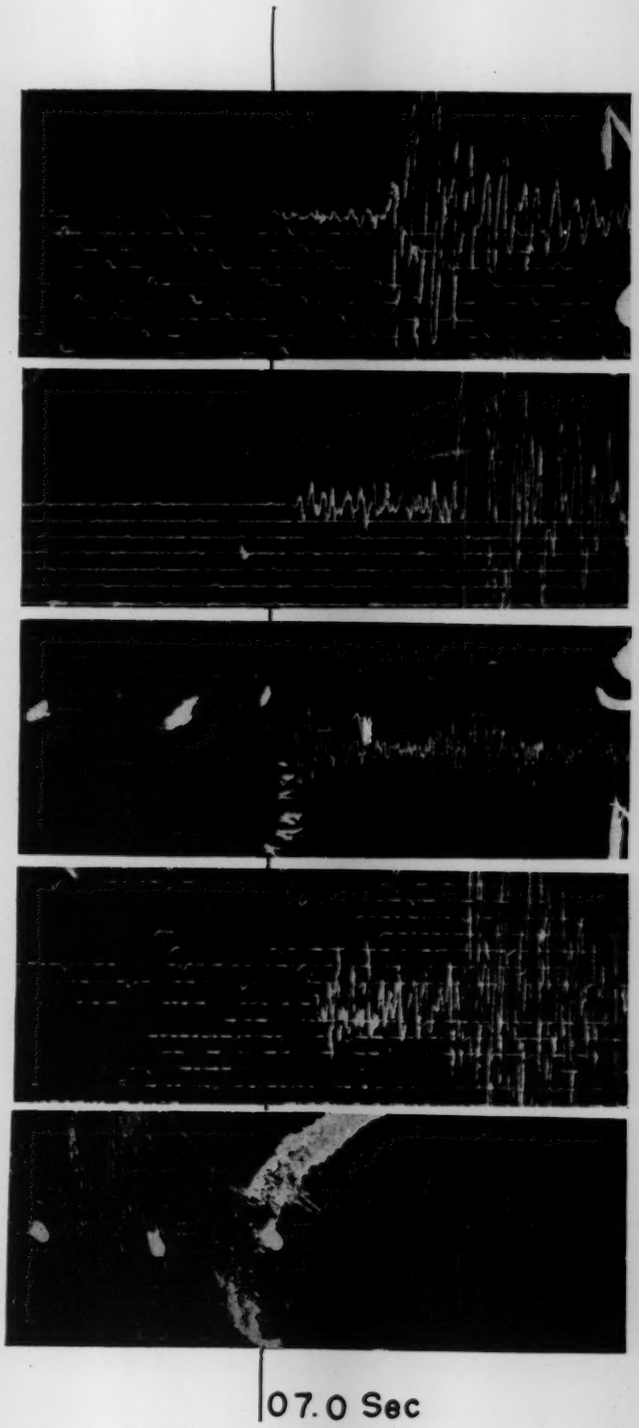

Fig. 2. Seismograms of an earthquake obtained at the Ishimoto accelerograph stations in the 1953 expedition in Wakayama district. (NS component.) *M*, *Y* etc.: Stations. (cf. *loc. cit.* 1.) Time marks are given at every second.

No. 326
1953 XII.22 11^h09^m

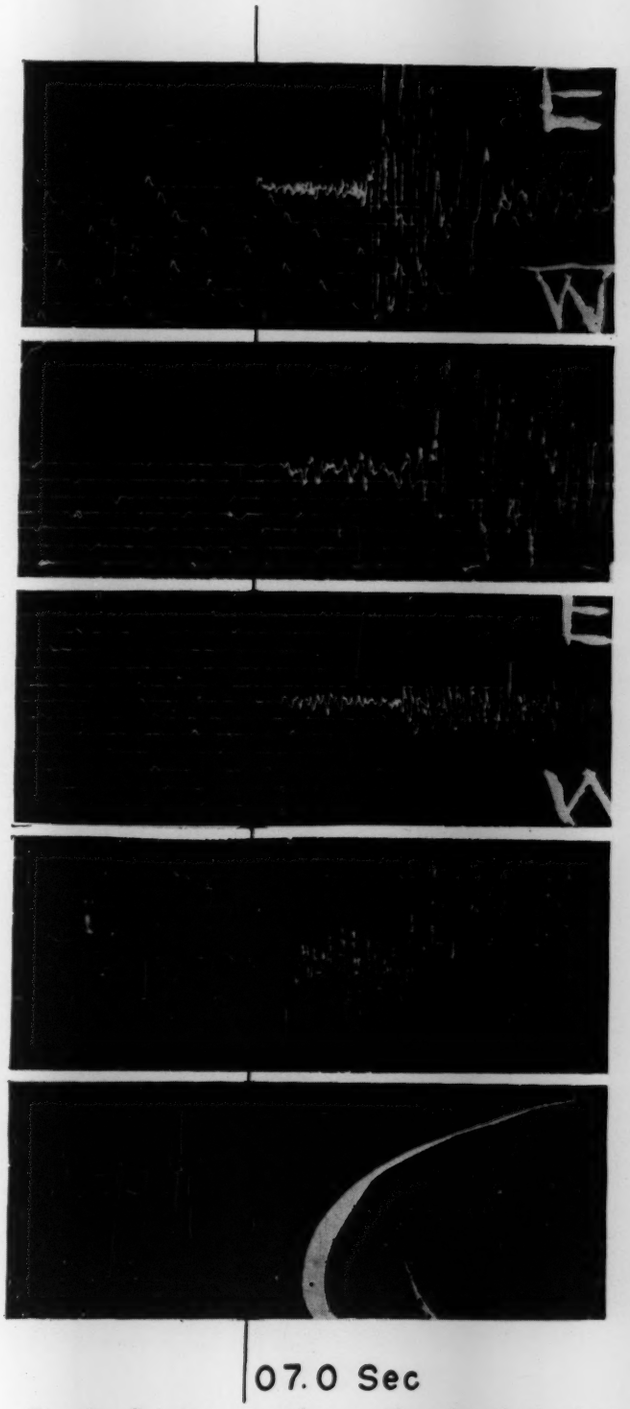

M
t_p : $07^s.00$

Y
t_p : $07^s.21$

KO
t_p : $07^s.21$

KA
t_p : $07^s.39$

T
t_p : $08^s.13$

Fig. 3. Seismograms of an earthquake obtained at Ishimoto accelerograph stations in the 1953 expedition in Wakayama district. (EW component) *M*, *Y*. etc. : Stations (cf. *loc. cit.* 1). Time marks are given at every second.

（震研彙報 第三十八号 図版 宮村）

No. 326
1953 XII22. 11^h09^m

M
t_p : $06^s.95$

K
t_p : $07^s.19$

KO
t_p : $07^s.21$

KA
t_p : $07^s.39$

T
t_p : $08^s.13$

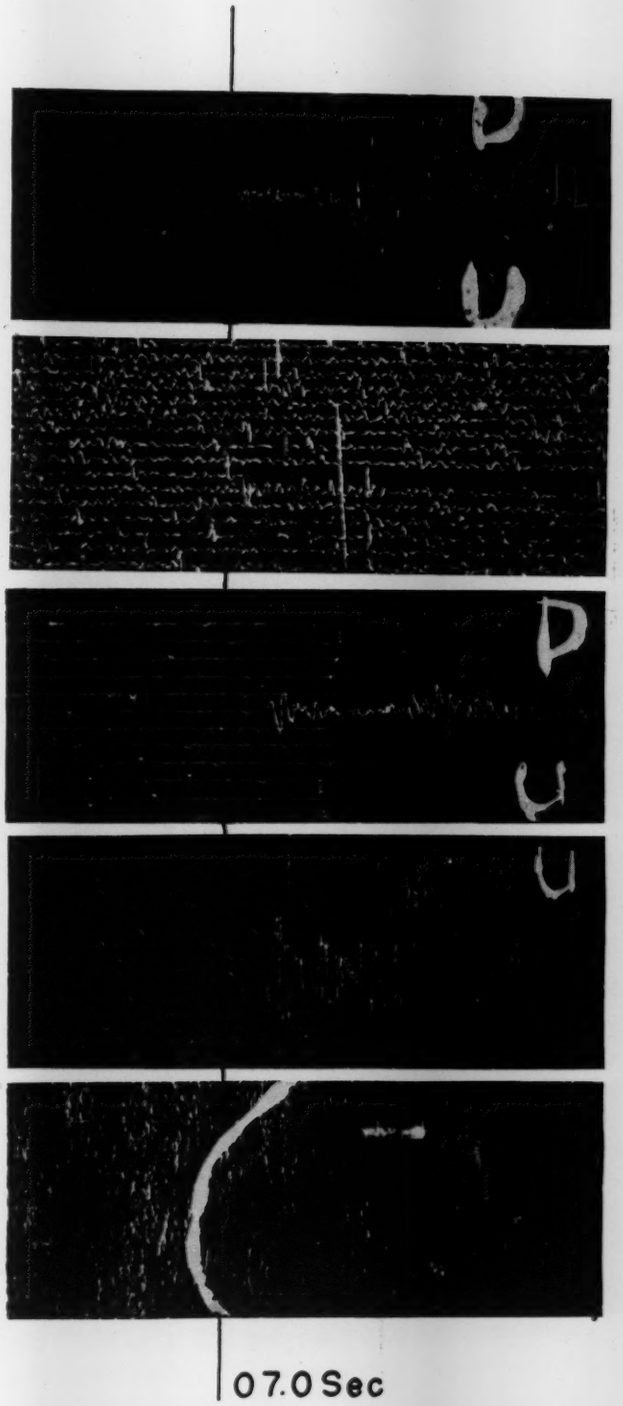

Fig. 4. Seismograms of an earthquake obtained at the Ishimoto accelerograph stations in the 1953 expedition in Wakayama district. (Z component) *Z* at *Y* was spoiled. At *K* was only vertical. *M*, *K* etc.: Stations (cf. *loc. cit.* 1). Time marks are given at every second.

地震研究所彙報
第38号(1960)113-124頁

7. 紀伊半島南端部附近の地殻変動について

地震研究所　岡田　惇

(昭和34年12月20日発表——昭和34年12月28日受理)

§1. Introduction

1946年12月21日に発生した南海道大地震の前後において，Fig. 1 に示すように紀伊半島，四国の全域にわたる広大な地域に，大きな地殻変動をもたらしたことは，多くの調査研究によつて明らかにされたところである[1),2),3),4)]. precise levelling の結果から垂直変動のいちぢるしく大きかつたのは紀伊半島南部と四国室戸岬および足摺岬の太平洋に突出する地方の 1 m に達する隆起であつた．また一方これらの突出部に続く内海の海岸線では 30～40 cm の沈降を示した[5),6)]．四国東南部の室戸岬の変動については地震発生直後から数年間測量を続けてその結果はすでに報告した[7),8)]. すなわち precise levelling の反復によつて隆起変動から次第に回復する傾斜変動を確認することができた．紀伊半島南端部串本附近においても同じような現象が起りつつあることは地理調査所で行なわれた1947年および1950年の levelling の結果からも明らかである[9)] (Fig. 3). 以来約 10 年の歳月が過ぎて，その間にどのような変動があつたかを調べる目的で紀伊半島南端部の串本から東北方約 20 km 浦神に至る levelling route について検測を行なつた．また半島周辺の海岸線に幾つかの験潮所があつて潮位の観測が気象庁や地理調査所によつて行なわれているが，幸にもこの levelling route の両端串本および浦神には気象庁の

1) Geographical Survey Institute, *Review*, No. 6, Jan. (1949) 4–6.

2) T. NAGATA, "Summary of the Geophysical Investigations on the Great Earthquake in Southwestern Japan on December 21, 1946", *Trans. Amer. Geophys. Union* **31** (1950) 1–6.

3) T. OKUDA, "On the Mode of the Vertical Land-Deformation Accompanying the Great Nankaidô Earthquake 1946", *Bull. Geogr. Surv. Inst.* **2** (1950) 37–60.

4) 永田武 "昭和 21 年 12 月南海大地震の調査研究から" 科学 **17** (1947) 163–171.

5) N. MIYABE, "Vertical Earth Movement in Nankai District", *Bull. Geogr. Surv. Inst.*, **4** (1955) 1-14.

6) N. MIYABE, "Vertical Earth Movements in Japan as Deduced from the Results of Rerunning the Precise Levels", *Bull. Earthq. Res. Inst.*, **30** (1952) 127–162.

7) T. NAGATA, A. OKADA, "Land Deformation of Muroto Point before and after the Nankaidô Great Earthquake on Dec. 21, 1946", *Bull. Earthq. Res. Inst.*, **25** (1948) 85–89.

8) A. OKADA, T. NAGATA, "Land Deformation of the Neigbourhood of Muroto Point after the Nankaidô Great Earthquake in 1946", *Bull. Earthq. Res. Inst.*, **31** (1953) 169–177.

9) 地理調査所　昭和 6 年度一等水準点検測成果蒐録
地理調査所　一等水準点検測成果集録　第 1 巻　昭和 30 年 3 月

驗潮所があるのでこれらの附属 bench mark に取付観測を行いこの約10年間の潮位の変化から得られる ground level の変動の様子と levelling survey から見た傾斜変動を比較考察した結果の報告である.

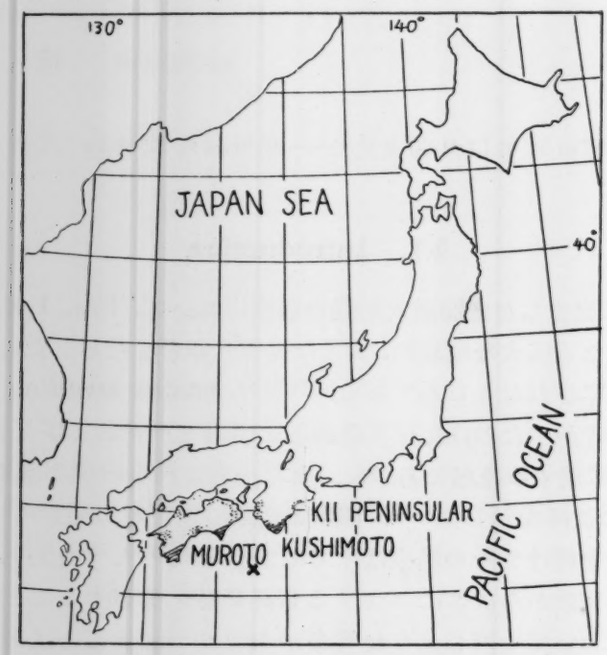

Fig 1. Location map of Nankaido Earthquake: Dec. 21, 1946, magnitude 8.1, depth 30 km.
Real line : uplifted area
Dotted line: subsided area
× : epicenter, latitude 33°N, longitude 135.6°E

§ 2. Levelling Survey

Instrument は Fig. 2 に示すような Zeiss-Opton Automatic Level Ni 2 (with plane plate micrometer) を使用し, field work において従来の Zeiss および Wild precise level とその性能について比較観測を行なつた結果 plane plate micrometer および invar precise staff を使用するならば first order precise levlling として優秀な器械であることが分つた. 本器に関する論文は幾つかある[10),11)12),13)]. 日本で plane plate micrometer 使用についてその測量成果の報告は未だ発表されていないようである.

10) M. DRODOFSKY, "Neue Nivellierinstrumente", *Zeitschrift für Vermessungswesen*, **5** (1951), 225–231.

11) K. HERRMAN, "Messungen mit dem Zeiss-Opton Nivellier Ni 2", *Vermessungstechn. Rundschau*, Nrs. **6**, **7** (1951).

12) E. WEGENER, "The Level Ni 2 Zeiss-Opton experiences and results as well as a comparison with the Zeiss Level B with plane-plate micrometer", *Zeitschrift für Vermessungswesen*, **5** (1951), 137–146.

13) 地理調査所 "Ni 2 による吉野地方水準測量成果について" 地理調査所時報 **16** (1953), 20–21.

Automatic levelling up という能率的なこと，一回の観測時間の短縮は標尺台の沈下移動等による不定誤差の導入を防ぐこととなつて精度も向上すると思われる．しかし，本器附属として輸入された invar staff は常数が決定されていないので，現在は補正常数の分つている古い Zeiss の invar staff を使用している．何となれば比較観測の結果から標高差が小さいときは誤差の範囲で一致しているが大きくなると当然 staff constant が効いてくるからである．これらのことはまた別の機会に報告する．

Fig. 2 The Zeiss-Opton precise level Ni 2 with automatic levelling up.

Survey にあたつては Fig. 3 に示すような区間すなわち串本町袋 JMA mareograph 附属 BM より浦神にある同附属 BM までその間 GSI BM 11 点について検測を行なつた．器械は上述のように Zeiss-Opton Ni 2 を用い，invar precise staff を使用した．

1959 年 9 月 26 日に当地方を襲つた伊勢湾台風直後のため levelling route である紀伊半島海岸線国道にも多くの土砂崩れや波浪による道床流出が散見されたが，この区間の bench mark には損傷はなかつた．しかし浦神湾内の JMA 験潮所は台風当時湾内に避難船が錯綜し，そのために験潮儀収容建物が破壊され 11 月上旬現在観測設備は未だ復旧されていない状態であつた．Fig. 3 の下には levelling route に沿う海岸線附近の geology を示した．主に Tertiary からなりほぼ東西に走る Neogene の成層構造が見られその間と南端部には潮岬の突出部および大島等 intrusive rock が露出しかついくつかの断層線に区切られるやや複雑な地質構造と考えられる．しかしこの地方の立地条件が四国南部室戸岬，足摺岬等と全く類似していることは吾人の眼で観察できるところである．また個々の bench mark および験潮所の位置と地質構造との対応は Fig. 3 で分るように No. 4980, 4981, 浦神験潮所は Kumano acidic rock (Ka) の上に，No. 4982, 4983 と，No. 4984 以南串本までは，それぞれ Neogene の Oguchi formation (Tl, Tu) の上にあつて代表していると考えられる．ただ実際には海岸線に沿う国道の路傍あるいは山際の標高 2～10 m 附近の極く浅い deposits の上に設置されてあつて地質構造を代表する露頭に直接構築されてある場合は少ない．

3. Result of Observation and Tilting Motion

南海道大地震後の紀伊半島における海岸線に沿う田辺——新宮間についての水準点の垂直変動は Fig. 4 に示すような結果で田辺市 BM 9184 号を不動とした時の様子である[14]. 1928 年 1931 年の観測に対し地震直後の 1947 年と 1950 年の比較結果から見ると串本を頂点として半島東西両部がほぼ対称的に変動していることが分る. かつ 1947 年から 1950 年の変動は串本附近でわずかながら明瞭なくぼみがあり, 両側にかすかなふくらみが見られる.

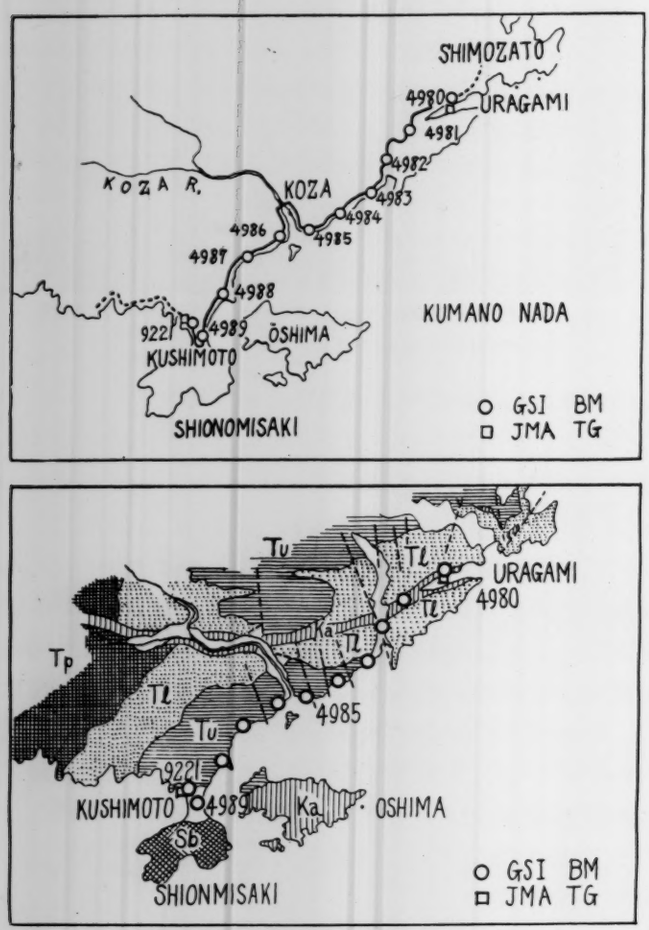

Fig. 3 The maps of the levelling route and geology neighbourhood of the southern part of the Kii Peninsula.
Tu: Oguchi formation (upper)
Tl: Oguchi formation (lower) } Tertiary.
Tp: Muro beds (older Tertiary)
Ka: Kumano acidic rscks } intrusive rocks.
Sb: Shionomisaki basic rocks
(after Wakayama Pref.)

Fig. 4 図中点線でかこんだ部分が今回検測調査した区間でその結果は Table 1 に表わしてある. Table 2 はこの区間, すなわち浦神 (BM. No. 4980)——串本 (BM. No. 9221) 間の 1899 年以来の変動量を浦神を不動と仮定したときの値である.

先きに述べたような四国室戸岬では最大傾斜の方向が South 2°～10° West を示したのであるが, この地域では地形的に最大傾斜軸の方向を決定するには困難であるので, Fig. 4 に見られるように半島南端を頂点とする全く東西対称な変動と仮定して South-North 軸上の傾斜変動を考えるならば, これに投影して Table 2 の結果を一まとめに plot すると Fig. 5 に示すようになる. Fig. 5 から浦神を不動としたときの 1899 年以来約 60 年間の傾斜変動が良く分り, これは全く室戸岬の変動と類似している.

14) *loc. cit.*, 9)

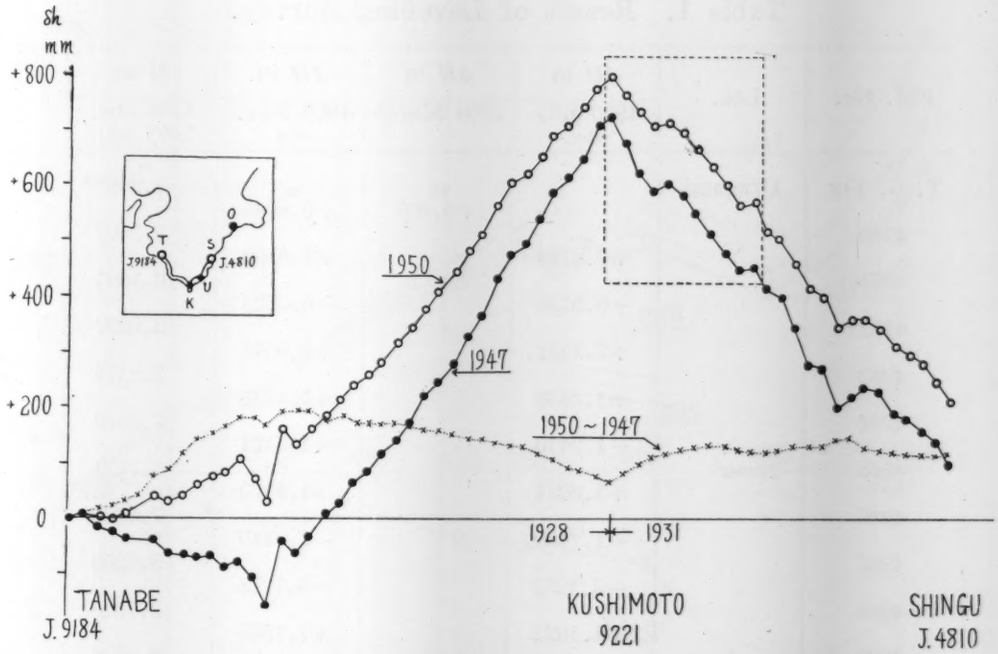

Fig. 4 Change in the heights of bench marks on the route from Tanabe (No. J. 9184) to Singu (No. J. 4810) along the coast line (after G. S. I).

大地震ではね上つた傾斜が漸次再び下り始めるという傾斜変動の推移は，いわゆる回復運動(rebound theory による)と見るべきであろう．そしてこれが1931～1899年の South 方向へのゆるやかな傾動に相当するものであるかどうかは今後の問題であるが，この傾斜変動の特性は四国室戸岬の場合と一致している．以上の関係をさらに定量的に考察したのが S–N 方向の傾斜角の変遷であつて Fig. 6 に示したような結果である．上には比較のために室戸岬の結果を示したもので地震直後の反復測量によつて傾斜量の変化が exponential に減少して行く様子が良く分る．

室戸岬に対して下には紀伊半島南部を示したもので観測回数が少ないけれど，特性は全く同じであると考えて差支えないようである．これから全く同一の傾動を辿りつつあることは証明されよう．換言すれば南海道地震の震央に対して両者がほぼ等距離にあること，海洋底を含めて地質構造および地形学的形成の相似等すべての条件に極めて高い相関にあることを意味しているのであろう．

§4. Relations Between Mean Sea Level and Ground Level

海岸地帯における局部的な地盤沈下を含めて地殻変動が進行する時，つねに問題になるのは mean sea level と ground level との関係である．四国地方全域についてはすでに南海道地震後詳しい報告があり，[15] また日本列島周辺の平均潮位の差と地殻変動の関

15) 河角 広・表俊一郎・越川善明 "験潮記録より知らるる四国地方の地盤変動" 四国地方地盤変動調査専門委員会 第三輯·第六輯.

Table 1. Result of Levelling Survey.

BM. No.	Loc.	ΔH in 1950 July obs.	ΔH in 1959 March	ΔH in 1959 Nov. obs.	H in 1950 obs. 1953 adj.
					m
T. G. Fix	Uragami	—	+0.405	+0.4045	1.956**
4980		m +7.8189		+7.8158	2.3607
4981		−6.5156		−6.3521	10.1801
4982*		+2.1521		+1.9861	3.8297
4983		+1.4839		+1.4838	5.8178
4984		−1.5410		−1.5421	7.3024
4985	Koza	+1.8074		+1.8073	5.7621
4986		−1.7439		−1.7449	7.5702
4987		−3.1252		−3.1278	5.8269
4988		+1.1625		+1.1565	2.7023
4989		−1.0281		−1.0335	3.8655
9221		+0.2747		+0.2743	2.8379
F. 41		—	−0.928	−0.9284	3.1126
T. G. Fix	Kushimoto				2.185**
		[GSI]	[JMA]	[ERI]	[GSI]

*: 1959 Jan. reestablished, new-old = −0.1645 m.
**: 1959 JMA obs.

Table 2. Change in the Heights of Bench Marks
(Assum. BM. No. 4980 fixed)

BM No.	1931-1899	1947-1899	1950-1899	1959-1899
	mm	mm	mm	mm
4980	0.0	0.0	0.0	0.0
81	− 10.3	+ 18.9	+ 26.7	+ 23.6
82	− 25.6	+ 40.4	+ 46.3	+ 42.2
83	− 19.0	+ 83.5	+ 79.4	+ 74.0
84	− 31.6	+101.2	+ 96.6	+ 91.0
85	− 34.8	+118.8	+111.0	+104.3
86	− 36.8	+105.6	+101.8	+ 95.0
87	− 43.2	+127.4	+114.5	+106.7
88	−103.8	+118.7	+ 92.6	+ 82.2
89	− 68 3	+206.7	+162.6	+146.2
9221	− 70.6	+187.0	+144.8	+123.0

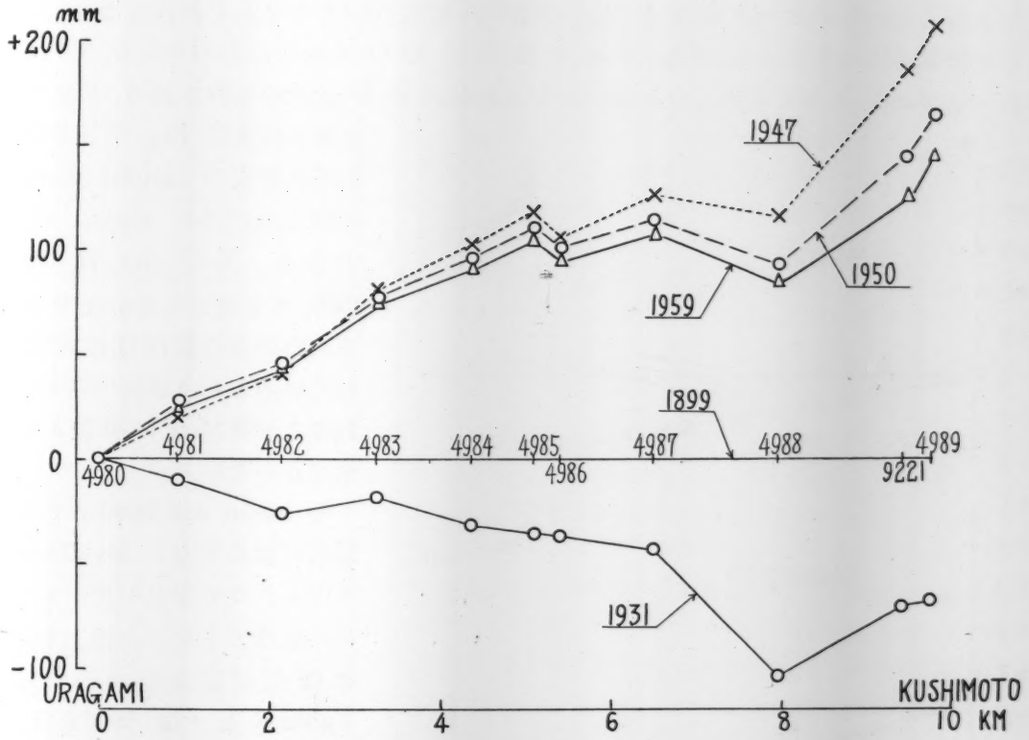

Fig. 5 Change in the heights of bench marks on the route from Uragami to Kushimoto. (projected on a vertical plane in N–S component)

係についての究研がある.[16]この調査では狭い地域とはいえ前述のように両端に JMA の mareograph が設置されてあるので驗潮記録と比較検討するのにはなはだ好都合であつた. 西南日本の驗潮記録から得られる mean sea level より, 串本, 浦神両驗潮所の潮位について 1950–1952, 1956 以後にやや乱れがあることはすでに指摘されている[17]がいまここでは両驗潮所間の levelling survey から見た変動とあわせて mean sea level の変化の関係を考察して見よう.

Fig. 7 には串本, 浦神および紀伊半島東部の尾鷲の三驗潮所の monthly mean sea level の結果を気象要覧よりそれぞれ plot したものである. 点線と白丸は annual mean sea level の変化を示したもので straight line はそれぞれの期間の mean value である. Fig. 7 からつぎのことに気がつくであろう.

(1) 串本で 1951～1952 および 1955 年に異常がある.

(2) 浦神では 1952 年にやや異常がある.

(3) 以上をそれぞれ異常と考へるならば串本ではこの期間内に secular variaton が見えないが, 浦神, 尾鷲では 1955 年を境として変化の様子が異る.

16) 津村建四郎 "平均潮位の差から求めた地殻変動の研究" 地震 [ii], **10** (1957), 67–78.

17) H. YOSHIZAWA, "On the variation of the monthly mean sea level in the western parts of Japan", *Umi to Sora*, **33** (1957), 34–38.

以上のことから串本—浦神(K–U)および浦神—尾鷲(U–O)のそれぞれ差を取つて見るとその関係がはつきり分る. Fig. 8 には K–U と U–O を示したものである. U–O はほぼ constant と見ても差し支えないようであるが K–U はやや事情が異る. Fig. 8 の点線と白丸は Fig. 7 と同様それぞれ変化の annual mean と直線は全期間の mean value である. K–U からは 1954, 1955 年を境としてかなり乱れているがその傾向はほぼ相反していることは事実である. これは大変興味深い現象と考えねばならない.

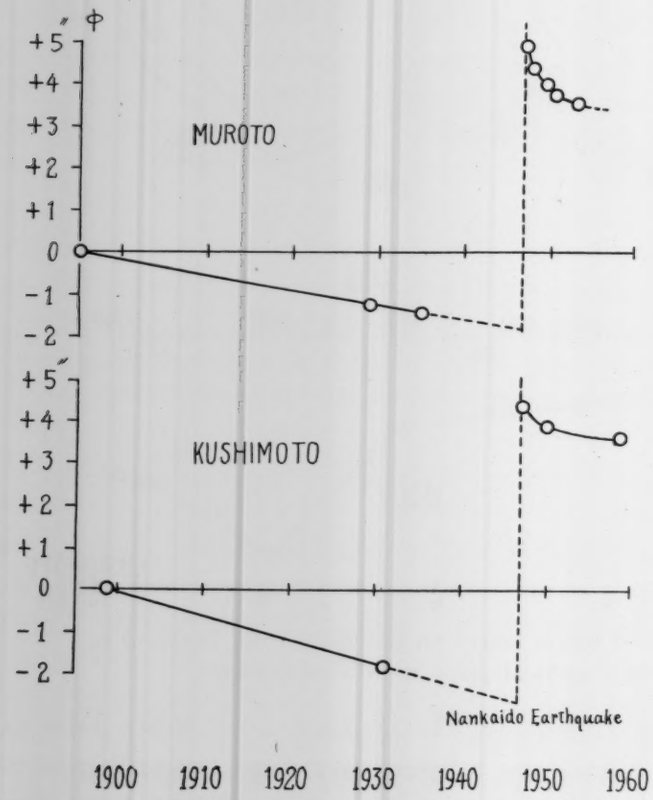

Fig. 6 Amount of tilt during 60 years.
Upper: Muroto Point, Shikoku Isl. into the southerly dip.
Lower: Southern Part of the Kii Peninsula into the southerly dip.

今 mean sea level から見た地殻の傾斜変動と levelling から得られた変動量を比べるために両験潮所を結ぶ直線上で両者の傾斜変動量を求めたのが Table 3 と Fig. 9 である.

1950～1958 年間の両験潮所の mean sea level を constant と考えた場合 ground level の変化は Fig. 9 の実線(黒丸)のような傾向になり, 一方 levelling から測定された傾動は破線(白丸)のような関係になる. これを見ても分るように 1951 年の異常を除いて両者を比べるならば tide の方に seasonal な変動はあつても mean sea level より推定される傾斜変動の傾向は一致していると考えられる. ただ傾斜量が問題で levelling から得られた量の数倍の振巾をもつて変動している. この振巾は何を意味しているのであろうか.

海水の温度, 気温, 気圧等の関係も大きな factor であろう[18),19),20)]. しかしさらにもつと大きな要素がこの接近した 15 km 足らずの潮候に影響しているのではなかろうか.

18) S. YAMAGUTI, "Abnormal Change of Mean Sea-Water Temperature, during the period of 52 years (1900–1951)" *Science Reports of the Gumma University*, **3** (1954), 1–10.
19) S. YAMAGUTI, "On the Changes in the Heights of Mean Sea-Levels, before and after the Great Earthquakes", *Bull. Earthq. Res. Inst.*, **33** (1955), 27–31.
20) S. YAMAGUTI, "On the Change in the Height of Bench Mark referred to Mean Sea-Level", *Bull. Japan Geodetic Society*, **3** (1957), 69–71.

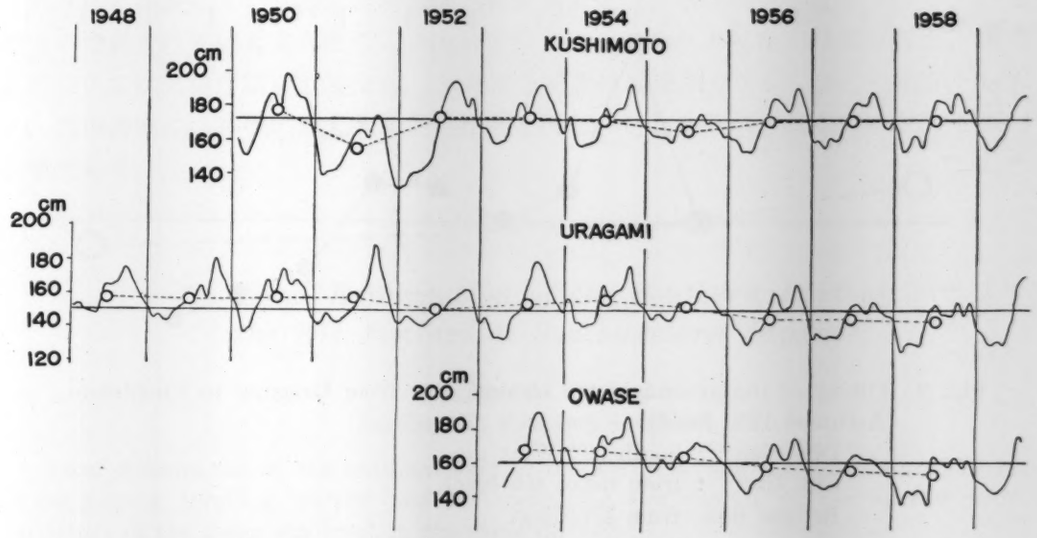

Fig. 7 Variations of monthly mean sea levels at three stations

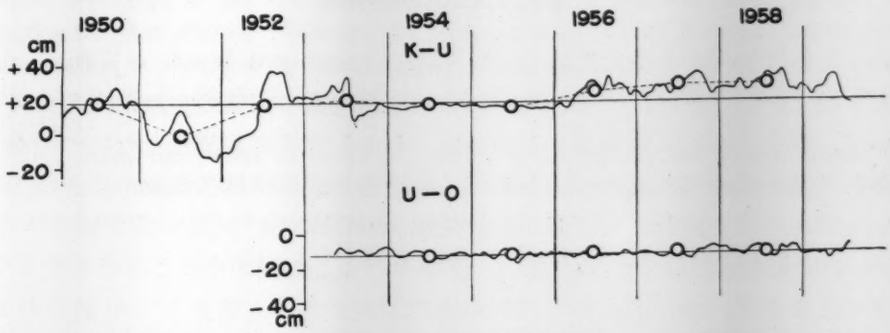

Fig. 8 Differences of monthly mean sea levels between each two stations.
K: Kushimoto U: Uragami O: Owase

levelling の結果から判定する傾斜量がある期間の平均的なものであるに対し mean sea level が示すのはより短週期であるにしても，しかしここでは同じ傾向を示して mean sea level の永年変化の説明にいささか寄与していることである.

Table 3. Tilting Angle of the Ground

From levelling		From mean sea level	
	"		"
1947	0.00	1950	0.00 (Assumed)
1950	−0.60	1951	+2.78
1959	−1.04	1952	+0.47
		1953	0.00
		1954	+0.45
		1955	+0.54
		1956	−0.77
		1957	−1.10
		1958	−1.51

Direction: S 52°W dip.
Distance : 14.5 km.

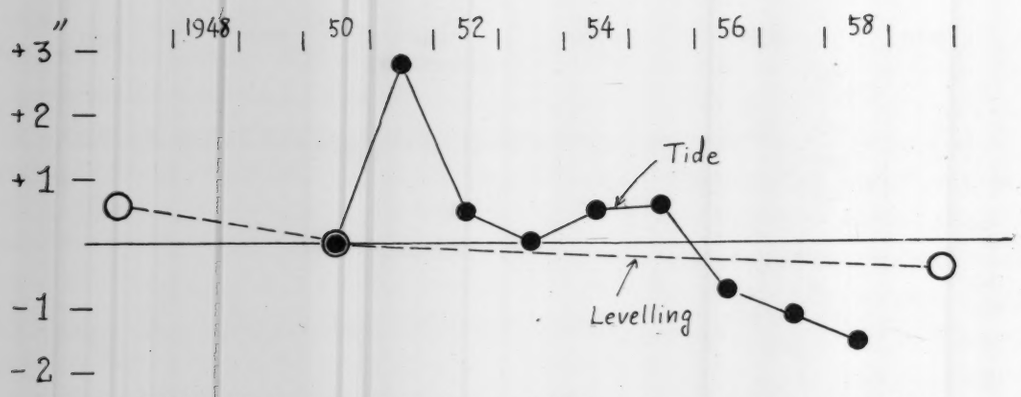

Fig. 9 Tilting of the ground in the straight line from Uragami to Kushimoto. (Assumed 1950 fixed)
Direction : South 52° West dip.
Full line : from mean sea level.
Broken line: from levelling.

§ 5. Conclusion

一般に 10 年間以内のような比較的短い期間の mean sea level の変動が，ただちに地殻変動を示すかどうかは，特別の場合たとえば大地震の前後の急激な隆起あるいは沈降を除いて，判定するのに困難なことが多い．しかし非常に相接近した二つの驗潮結果から得られる差を求めて，これに表われてくる変動の説明は地殻変動が大きな役割を果たしているであろうと思われた．しかし結果は consistent には一致を見ないで mean sea level の変化の方がはるかに大きい．陸地の方がこの期間中にこんなに大きく動いていると考えるよりは，海洋潮夕の方に何か他の原因があると考える方が順当のように思われる．たとえば台風接近による気圧低下から起る潮位上昇は 950 mb 以下の超A級台風で monthly mean sea level におよぼす影響は約 4 cm である．また海況の変化殊に冷水域の発達移動あるいは上昇から起る海水の温度変化による unbalance が，いわゆる isostatic compensation のため潮位変化を起すであろう．この量はあるいは数十糎に達することもあり得る．他にももつといろいろな factor が重なり合つているであろうが，この浦神，串本のような至近距離にあつて同時に影響を受ける可能性はきわめて強く，差を検出することは困難である．ただ後者は 1950～1952 年頃熊野灘に発達した冷水域の影響が何れかを支配したかも分らない．いづれにしても津村氏の述べる本邦太平洋岸の月平均潮位の変化は紀伊半島南端附近で著しい不連続を示すことに関係があるようである．

Levelling の検測と mean sea level から見た地殻変動の関係の一例を示したのであるが，もつと永い眼で見るならば，海洋潮汐の諸問題の解明と相俟つて説明ができると思われる．また前に述べたように構造地質の立場から見た場合もそれぞれの構造間には顕著な変化は見出すことができなかつた．

終りに本調査にあたつては宮村摂三助教授が現地調査の機会を与えて下さつた．また潮汐の問題では高橋竜太郎教授山口生知教授よりそれぞれ有益な御指導を得た．験潮記録については気象庁田口竜造技官，水準測量成果は地理調査所から多くの教示をいただき，現地作業には和歌山県土木部の御援助を得た．ここにそれぞれの方に謝意を表する次第である．

---

7. *Land Deformation of the Southern Part of the Kii Peninsula, Southwestern Japan.*

By Atsushi OKADA,
Earthquake Research Institute.

Land deformation of the southern part of the Kii Peninsula was investigated by means of the precise levelling survey and by comparing the results of the survey with the variations of the mean sea level in the same district.

(1) Levelling resurvey:

Precise levellings of the Kii Peninsula, Wakayama prefecture, were carried out four times during the past seventy years by the Geographical Survey Institute, and a remarkable land deformation represented by the uplifting of about 72 cm of the southern point of the peninsula has been ascertained as occurring on the occasion of the Nankaido Earthquake. (Dec. 21, 1946)

In Nov., 1959, the writer repeated a precise levelling of the route, about 20 km in distance from Uragami to Kushimoto in the southern part of the peninsula. The tiltings of the ground of the area as revealed by the survey are as follows.

Year	Mean value
	″
1899	0.00(Assumed)
1931	−1.74
1947	+4.28
1950	+4.12
1959	+3.80

N–S component of tilting
+: southerly dip

These values are consistent with the tiltings of the Muroto Point, Shikoku Isl. and show a slight recovery after the large uplifting by the great earthquake of 1946. (Fig. 6)

(2) Mean sea level:

Fig. 7 shows the monthly mean sea levels observed at three stations on the peninsula during ten years after the great earthquake of 1946, and Fig. 8 their differences. The annual mean sea level is shown by the dotted line. The difference of the sea level at Uragami and Owase is constant, while that at Kushimoto and Uragami is irregular.

As already pointed out by some investigators, these differences may be considered as due to the hydrographic condition of the sea and also to some long period tides, but it is noticeable that the tiltings of the ground calculated from the differences of the sea level

show a tendency corresponding to those obtained by means of the levelling resurvey in the past ten years.

Thus the tilting of the ground in a straight line from Uragami to Kushimoto is shown Fig. 9, and the tilting angles are as follows.

From levelling		From mean sea level	
	″		″
1947	0.00 (Assumed)	1950	0.00 (Assumed)
1950	−0.60	1951	+2.78
1959	−1.04	1952	+0.47
		1953	0.00
		1954	+0.45
		1955	+0.54
		1956	−0.77
		1957	−1.10
		1958	−1.51

Direction: S 52° W dip
Distance : 14.5 km

Excepting for the amplitudes of long period tidal oscillations (3–4 years), the curve (full line) in Fig. 9 seems to show a southwesterly tilting of the ground, in the same manner as revealed by the levelling survey (broken line). The tilting may be regarded as representing a continuous subsidence of the southern part of the Kii Peninsula in recent years.

地震研究所彙報
第 38 号 (1960) 125-143 頁

8. プロトン磁力計の試作研究 (続報)

文部省科学試験研究費研究班
(代表者 力 武 常 次)

(昭和 34 年 11 月 24 日発表 — 昭和 34 年 11 月 30 日受理)

1. 緒 言

前報[1]においては,「プロトン磁力計の試作研究」に関する文部省科学試験研究費研究班の活動状況および昭和 32 年度文部省科学試験研究費補助金により試作した固定観測所用プロトン磁力計について報告した.

この研究組織はその後も活動を継続し, 昭和 33 年度文部省科学試験研究費補助金によりトランジスター型プロトン磁力計を製作するとともに, 第 2, 3 および 4 次南極地域観測用として海上用プロトン磁力計ならびに周波数直読型プロトン磁力計の設計製作に協力した. 本報においてはこれら磁力計の概略を述べるとともに, 地震研究所伊豆大島観測所に設置した固定観測所用プロトン磁力計の使用状況について報告する.

2. 研 究 組 織

「プロトン磁力計の試作研究」に関する研究班の組織はつぎの通りである.

分担事項	所 属	氏 名	分担事項	所 属	氏 名
記録方式の研究	東京教育大学	小島昌治	比較測定および南極観測	東京大学理学部	永田 武
	お茶の水女子大学	小川静子		東京大学地震研究所	力武常次*
	東京学芸大学	鳥塚一男			
標準周波計および増幅器の製作	日本電子光学研究所	関 利正	比較測定およびロケット観測	東京大学理学部	福島 直
	同	草鹿履一郎			
比較測定	建設省地理調査所	坪川家恒	海上観測	工業技術院地質調査所	佐藤光之助
	同	瀬戸孝夫		同	長谷川 博
	同	田島 稔			
	東京大学理学部	秋本俊一	テレメータリング	東京大学地震研究所	辻浦 賢
	東京大学地震研究所	上田誠也			

* 代表者

3. 伊豆大島観測所に設置した固定観測所用プロトン磁力計の概況

前報[1]においてその性能を報告した固定観測所用プロトン磁力計は, 1959 年 4 月以来地震研究所伊豆大島観測所に設置されている. 磁力計の増幅器, 標準周波発振器, 記録

1) 文部省科学試験研究費研究班 (代表者力武常次) 地震研究所彙報 **36** (1958), 433.

Fig. 1. The detector coil hung above the GSI magnetometer in the absolute measurement room of Oshima Geophysical Observatory.

計などは，観測所本館内の観測室に設置され，検出コイルは約 20 m 離れた地磁気絶対測定室内の地理調査所型磁気儀の直上に置かれている．その状況はそれぞれ第 1 および 2 図に示してある．

同観測所においては，地磁気 3 成分変化計による連続観測を実施しているが，変化計の基線値は，地理調査所型磁気儀による偏角および伏角観測とプロトン磁力計による全磁力観測とを組合せて決定される．

火山活動と地磁気全磁力変動との関連を調べるためには，長期間の観測を必要とすることはいうまでもないが，現在の試験的段階においては，つぎに述べるような観測方法を採用している．このプロトン磁力計は自動記録方式ではないので，観測員の労力をも考慮して，原則として午前 10 時，10 時 20 分，10 時 40 分および 11 時に観測を行なうこととし，その平均 F_0 をつくる．一方，柿岡地磁気観測所の報告から 10～11 時の平均 F_k を求め，$F_0 - F_k$ をつくることによつて，磁気嵐などの一般的地磁気変化を除去し，伊豆大島に固有の変化を求めようというわけである．

この方法の精度を調べるために，1959 年 6 月の観測結果について，つぎのような吟味

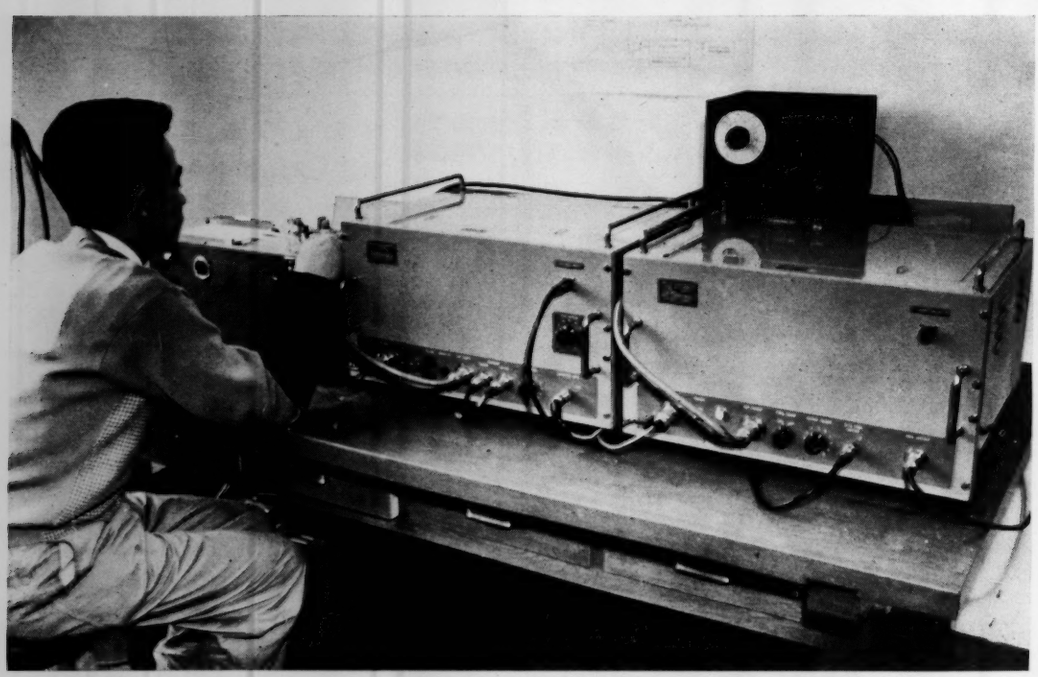

Fig. 2. The proton magnetometer in the observation room of Oshima Geophysical Observatory.

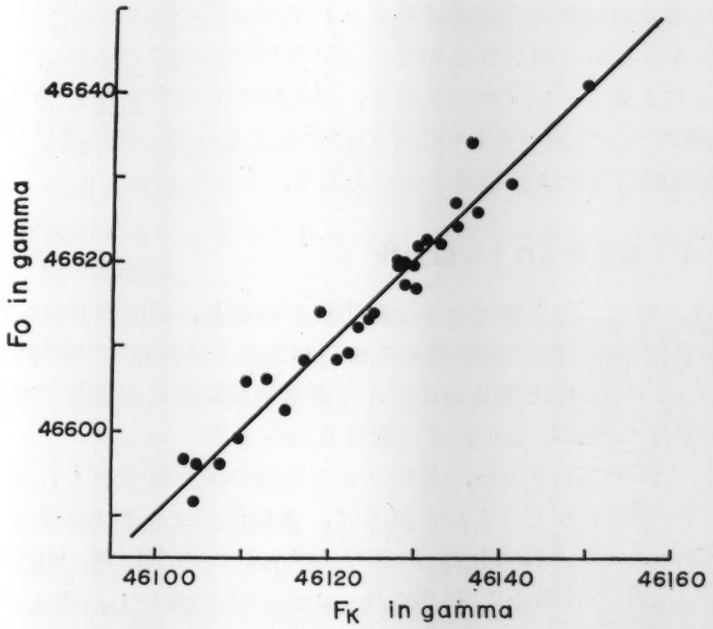

Fig. 3. The relation between the geomagnetic total intensities as observed at Oshima (F_0) and Kakioka (F_k) for the 30 days in June, 1959.

を行なつた．F_0, F_k および F_0-F_k は第1表の通りである．

F_0 と F_k との関係を図に示すと，第 3 図のようになり，地磁気変動の大部分が伊豆大島および柿岡に共通であることがわかるが，なお若干のばらつきが存在する．このばらつきが全く偶然であるとすれば

F_0-F_k の平均値
$=490.3\pm0.4\gamma$

となり，表中の値の probable error は $\pm1.9\gamma$ ということになる．

Table 1. The geomagnetic total intensities as observed at Oshima (F_0) and Kakioka (F_k) in June, 1959.

Date	F_0	F_k	F_0-F_k	Date	F_0	F_k	F_0-F_k
June, 1959				June, 1959			
1	46609.0γ	46122.1γ	486.9γ	16	20.1γ	27.8	92.3
2	29.2	41.2	88.0	17	08.1	17.1	91.0
3	01.9	14.9	87.0	18	19.9	28.5	91.4
4	08.1	21.0	87.1	19	40.7	49.9	90.8
5	13.7	25.1	88.6	20	22.5	31.1	91.4
6	16.6	30.1	86.5	21	19.5	28.0	91.5
7	26.9	34.5	92.4	22	21.9	30.2	91.7
8	24.2	34.8	89.4	23	14.0	18.8	95.2
9	34.0	36.4	97.6	24	06.0	10.5	95.5
10	06.1	12.7	93.4	25	46596.6	03.1	93.5
11	17.2	28.7	88.5	26	46621.3	32.8	88.5
12	12.2	23.4	88.8	27	46596.1	04.6	91.5
13	13.1	24.6	88.5	28	99.0	09.5	89.5
14	25.7	37.2	88.5	29	95.8	07.5	88.3
15	19.5	29.8	89.7	30	91.4	04.4	87.0

しかしながら，従来実施中の偏角連続観測の結果からも，1 週間程度の短期間中にも伊豆大島観測所特有の変化があることが予想されるので，上記の誤差の計算はこのような系統的変化をも含んだものといえよう．いずれにしても，長期間の地磁気変動を論じる場合には，例えば 15 日平均値について調べるという手つづきをとるので，現在採用している方法によつても，1～2γ程度の変化は信用できるであろう．

4. 海上用プロトン磁力計

1957 年の第 2 次南極地域観測の際に，海上用プロトン磁力計を製作し，観測船「宗谷」に積込んで，東支那海，印度洋，南極海域等の磁気測量に使用したことは前報[1]に報告した通りである．この海上用プロトン磁力計は第 3 および 4 次南極地域観測にも若干の改良を施して，引きつづき使用されている．ここではその概略を報告する．

プロトン磁力計は動揺に対して鈍感であるから，検出コイルを船の後方に曳行し，船体磁気の影響をさけて，全磁力の測定を行なうという試みは，外国に於ても行なわれている．Cambridge 大学 Department of Geodesy and Geophysics の M. N. Hill[2] は検出コイルおよび前置増幅器を納めた "fish" を 700 *ft* のケーブルで曳行し，大西洋の磁気測量を行なつた．また New Zealand の D. Christoffel[3] は海上用プロトン磁力計を製作して，New Zealand—McMurdo Sound および Ross 海の磁気測量を実施したとのことである．

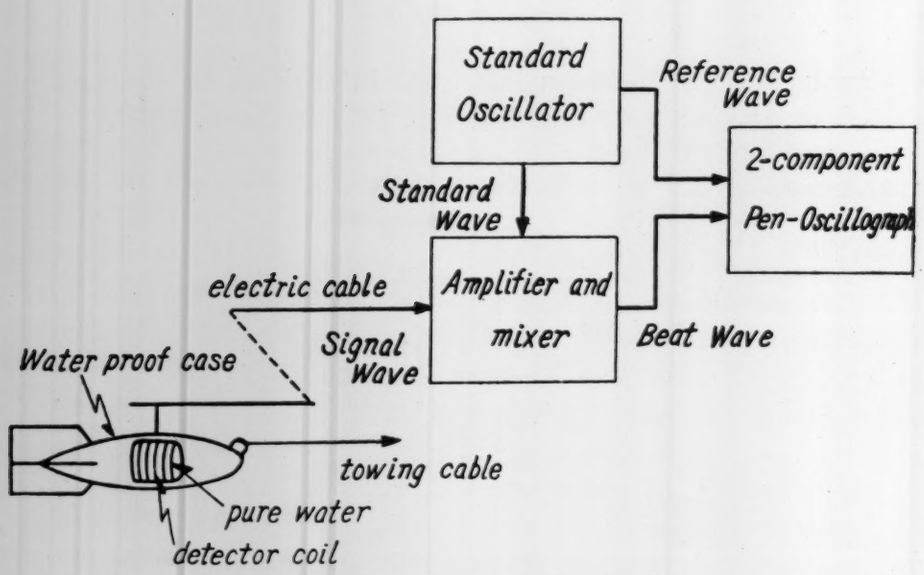

Fig. 4. Block diagram of the sea-borne proton magnetometer.

2) M. N. HILL, *Deep-Sea Research*, **5** (1959), 309.
3) GEOPHYSICS LABORATORY, UNIV. OF BRITISH COLUMBIA, *Annual Report*, (1958-1959).

本研究組織の設計製作した海上用プロトン磁力計も上記外国文献に見られるものと，本質的差違はない．

1) 構成

第4図は海上用プロトン磁力計のブロックダイヤグラムを示したもので，前報に報告した固定観測所用プロトン磁力計と原理的には同じである．第3次南極観測以後は，観測員が不在でも観測できるよう，スイッチ操作を自動的に行なう時限装置をつけ加えた．

2) 検出部

第5図に見られる長さ約 1 *m* の水密流線形容器に偏極および検出コイルを納める．容器はポリエステル樹脂およびガラスファイバーでつくられ，曳行された場合に水面下数 *m* に位置する．容器の形は水槽実験により安定性を大きくするよう設計されているが，実際には曳行速度も一定でなく，航跡の渦の影響もあり，果してどのような運動をしているか明らかでない．

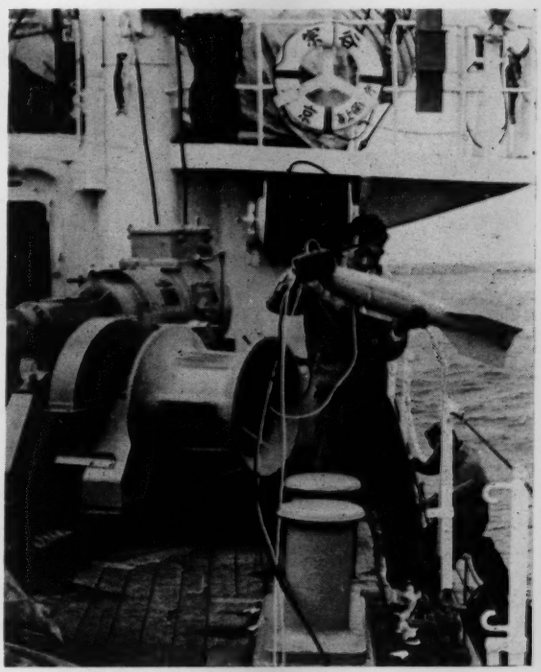

Fig. 5. The stream-lined case for the detector coil.

偏極および検出コイルは，内径 67 *mm*，内長 70 *mm* の円筒型硬質塩化ビニール製容器に蒸溜水約 200 *cc* をいれ，その外側に径 1 *mm* のエナメル銅線を 540 回巻いてある．

コイルは長さ 200 *m* のテフロン被覆同軸ケーブル（径 14 *mm*）に接続されて船上に導かれる．この電線は径 8 *mm* のナイロンロープにとめられ，電線に張力がかからないように留意されている．南極観測船「宗谷」で使用する場合には，通常船の後方 130 *m* に検出部を曳行した．

3) 励磁電源

励磁電源は交直両用とし，増幅器と同一シャシーに納められている．直流用のときには，24 *V* 蓄電池をパネルの所定端子に接続する．

約5アンペアの電流で励磁し，スイッチを増幅器側に切換えることにより，励磁コイルは検出コイルとして兼用される．緩和時間を考慮して，プロトンを飽和値にまで配向するためには，数秒の励磁時間が必要である．

4) 増幅器

検出コイルに誘起した信号電圧は，同軸ケーブルを経て，増幅器の結合変圧器に導かれる．

増幅器の構造は，前報[1]の固定観測所用プロトン磁力計の場合と類似している（前報結

線図参照). ただし，東京一昭和基地間では全磁力が広範囲にわたつて変化しているので，狭帯域増幅器としては，1.3～2.0 *kc/s* の間を 0.1 *kc/s* ごとに 8 組を準備し，適当に切換えて使用する．この増幅器の電圧利得は約 140 *db* である．

増幅器の出力は，混合回路に導かれ，標準周波発振器より供給される標準周波電圧との唸信号が出力として記録計に導かれる．

5) 標準周波発振器

標準周波発振器としては，2.6, 2.8, 3.0, 3.2, 3.4, 3.6 および 3.8 *kc/s* の水晶発振器からマルティバイブレーター方式により逓降した 1.3, 1.4, 1.5, 1.6, 1.7, 1.8 および 1.9*kc/s* と 100 *kc/s* の水晶発振器から，ブロッキング発振方式 2 段により逓降した 2 *kc/s* を使用している．水晶発振器の精度から考えて，精度 1γ の測定には恒温装置を必要としない．また 2 *kc/s* よりさらにマルティバイブレーター方式により逓降して 40 *c/s* をつくり，記録紙上のタイムマークを供給している．

第 6 図は標準周波発振器のブロックダイヤグラムを示したもので，標準周波出力は必要に応じて切換えて混合回路に供給する．この発振器を使用した上で気がついた点は，時たまブロッキング発振の分周が不安定になることである．

この点を防ぐためには，精度の若干の低下を考慮しても，4 *kc/s* の水晶発振器からマルティバイブレーター方式により 2 *kc/s* および 40 *c/s* をつくつたほうが有利であろう．

6) 記録計

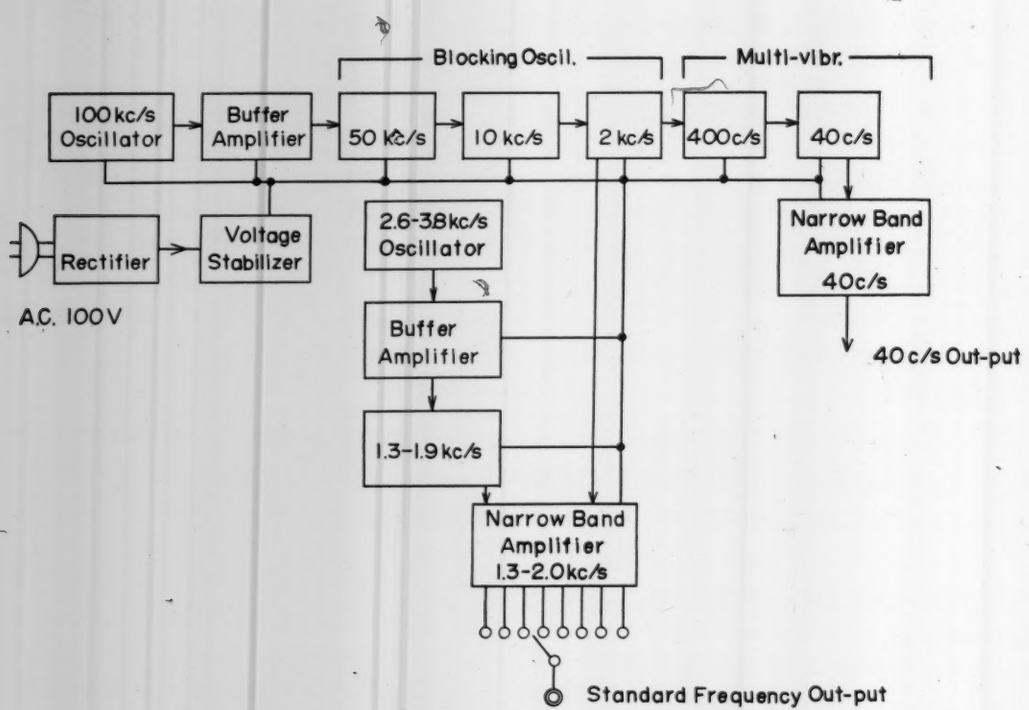

Fig. 6. Schematic diagram of the standard frequency oscillator of the sea-borne magnetometer.

記録計としては，2成分ペン・オッシログラフを使用し，感度は 0.5 *mm/mA* で 60 *c/s* ぐらいまではほぼ平坦な周波数特性を有する．記録紙の送りは通常 12.5 *cm/sec* である．

7) Hermanus 観測所における比較観測

第3次南極地域観測隊の小口，柿沼両隊員は観測船「宗谷」が南アフリカ Cape Town に寄港したさい，プロトン磁力計を Hermanus 地磁気観測所 (34°26′*S*, 19°14′*W*) に運び，1958年12月22および23日にわたつて比較観測を実施した．その詳細は省略するが，第7図のような結果が得られ，同観測所基準値は 10.34γ 過大であることがわかつた．

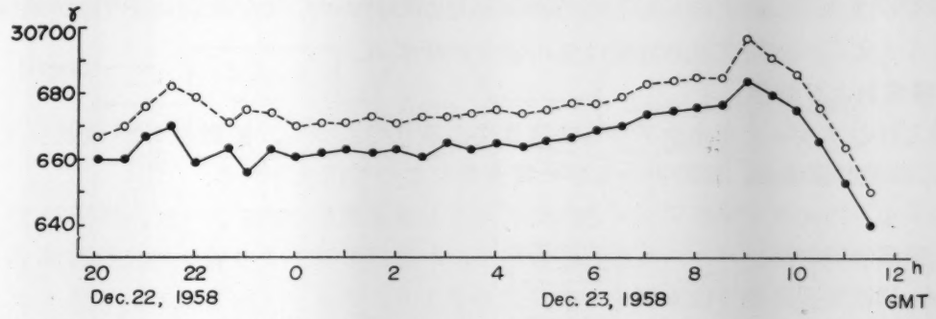

Fig. 7. Comparison of the results observed by the sea-borne proton magnetometer (black circle) with those observed by the magnetograph (hollow circle). From Dec. 22 to 23, 1958 at Hermanus Magnetic Observatory, near Cape Town, South Africa. (After T. Oguti and S. Kakinuma of the Japanese Antarctic Research Expedition).

この値の平均誤差は ±1.92γ である．この結果から見て，プロトン磁力計を各地磁気観測所に運んで基準値の比較観測を行なうことは有意義である．

8) 東京一昭和基地間海上磁気測量

第2, 3および4次南極地域観測の往復途上において，本磁力計による磁気測量が行な

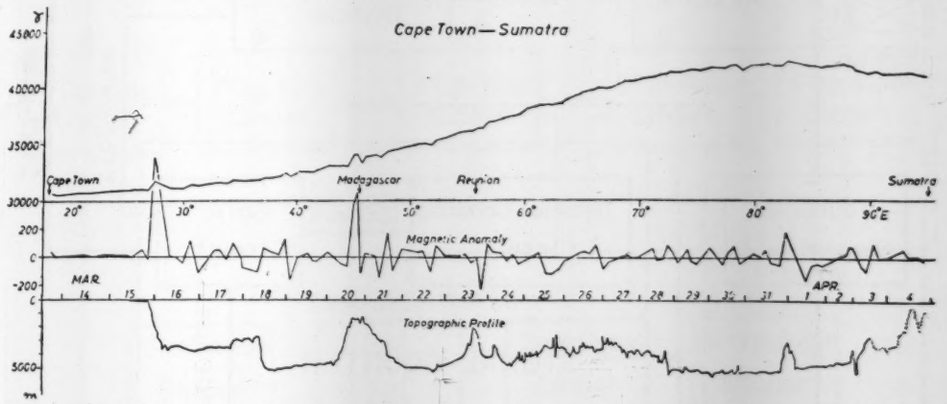

Fig. 8. Total geomagnetic force, magnetic anomaly and topographic profile measured during the voyage of s.s. Soya of the Japanese Antarctic Research Expedition. (After T. Oguti and S. Kakinuma).

4) T. NAGATA, T. OGUTI and S. KAKINUMA, *Proc. Japan Acad.*, **34** (1958), 427.
5) T. OGUTI and M. KODAMA, *Nature*, **183** (1959), 103.
6) T. OGUTI and S. KAKINUMA, *Antarctic Record*, **7** (1959), 389.

われ，多くの有用な結果を得たが，それらはすでに発表[4),5),6)]されていることであるし，ここでは 1957 年 3～4 月の Cape Town—Sumatra 間の結果を海底地形とともに図示するにとどめよう．(第 8 図)

5. 周波数直読型プロトン磁力計

本プロトン磁力計は，広範囲の測定の簡易化および読取りの労力を節約する目的をもつて試作したもので，1959 年 2 月以来南極昭和基地に設置してある．期日の関係で日本においてじゆうぶんのテストを行なう時間がなかつたので，ここには本磁力計の概略を述べることとし，使用状況の詳細は他の機会にゆずる．

1) 構成および動作

本磁力計のブロックダイヤグラムは第 9 図の通りであつて，励磁および検出コイル，増幅器，周波数逓降器，測時計ならびに電源部によつて構成される．

検出コイルによりピックアップされたプロトン歳差運動のシグナルは，増幅器で増幅され，振幅制限回路，パルス整形回路を経て，2 進計数回路より成る周波数逓降器に送られる．周波数逓降器ではシグナルの任意の点より，スタートおよびストップシグナルを取り出して，測時計の 100 *kc/s* の標準周波数をゲートし，両シグナル間に含まれる標準周波数の数 n を計数する．

n とプロトン歳差運動周波数 f との間には

$$f=\frac{f_0 N}{n}$$

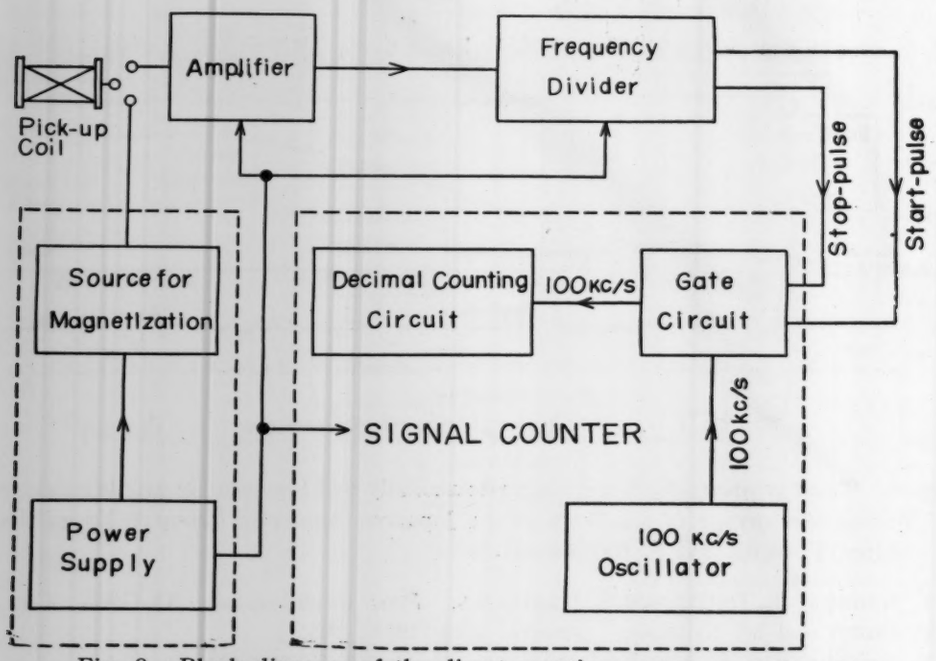

Fig. 9. Block diagram of the direct-counting proton magnetometer

という関係がある．ただし N はあらかじめ選定されているスタートおよびストップパルス間のパルス数，f_0 は標準周波数 100 *kc/s* である．したがつて，f を *c/s* で測つた場合，$F=23.4865f\gamma$ によつて全磁力が与えられる．この比例常数は前報においては 23.4861 を採用したが，その後 23.4865 を採用することが，本研究班の会合で暫定的に決定されている．

2) 増幅器

固定観測所用および海上用プロトン磁力計の増幅器と大差ないが，全磁力の値に応じ

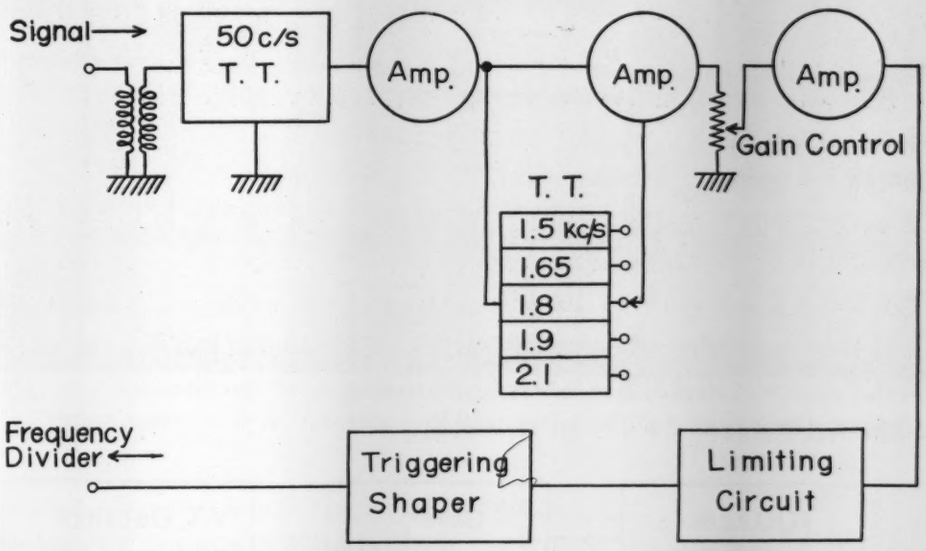

Fig. 10. Block diagram of the amplifier of the direct-counting proton magnetometer.

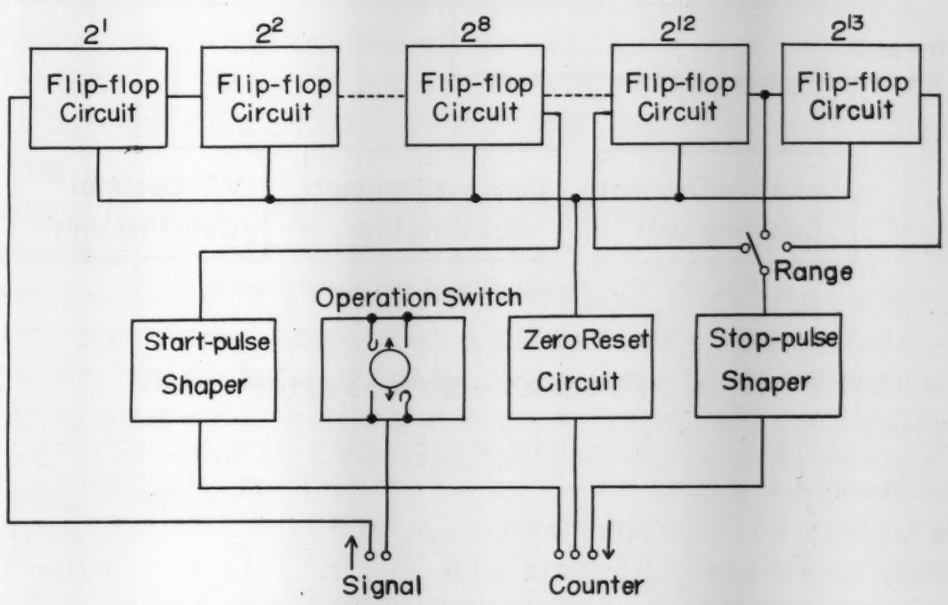

Fig. 11. The constitution of the frequency divider

て T.T. 回路を切換えて使用する．振幅制限回路およびトリガー回路を通じて，整形されたパルスを周波数逓降器に送る．第10図は増幅器の概念図である．

3) 周波数逓降器

この部分は第11図のような構成になつている．真空管13個を使用して，フリップフロップ回路により，2^{13} の計数回路を構成しているが，励磁によるリレー切換のショックをさけるために，入力信号のはじめの部分を捨てるように，2^6～2^9 の間の適当な値を計数して後，測時計のゲートが開くようにする．このためのスタートパルスはトリガー回路を通して整形される．ストップパルスもまた同様である．また零リセット回路から負のパルスを出し，フリップフロップ回路，ゲート回路，10 進計数回路のリセットを行なう．操作スイッチを備えているので，単一操作により，励磁，計数およびリセットを行なうことができる．

4) 測時計

この部分は標準周波数発振器，ゲート回路，真空管10進計数回路およびデカトロン10進計数回路より成り，第12図のようになつている．

標準周波数は水晶発振器よりの 100 *kc/s* を使用し，ゲートの開いている間の 100 *kc/s* の波数を計数する．100 *kc/s*～1 *kc/s* までの逓降は真空管10進計数回路，1*kc/s*～1 *c/s* までの逓降はデカトロン10進計数回路で行なつている．

第13図に周波数直読型プロトン磁力計の概観を示す．

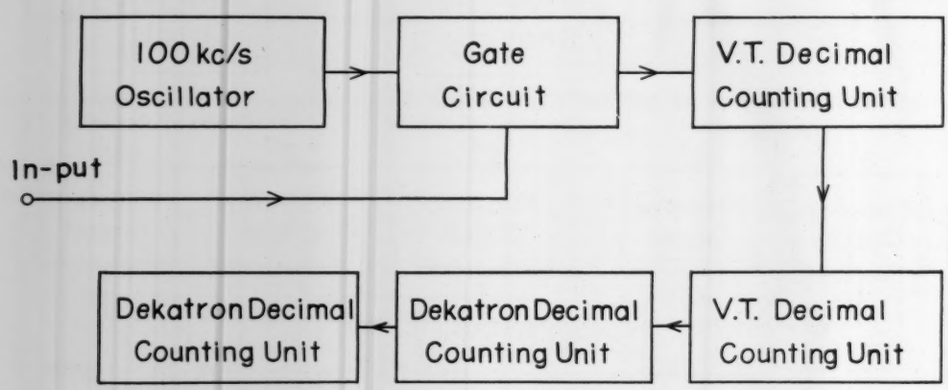

Fig. 12. The constitution of the signal counter.

6. トランジスター型プロトン磁力計

プロトン磁力計をトランジスター化する試みは，各国において行なわれている．米国 Varian Associates 社は超小型のトランジスター型プロトン磁力計を製作販売し，日本にも輸入されている．これは振動片の共鳴により，信号周波数と標準周波数との唸周波数を測定する方式のもので，測定精度は ±10γ といわれる．また G. S. Waters[7] 等も

7) G. S. WATERS and P. D. FRANCIS, *Journ. Sci. Instr.*, **35** (1958), 88.

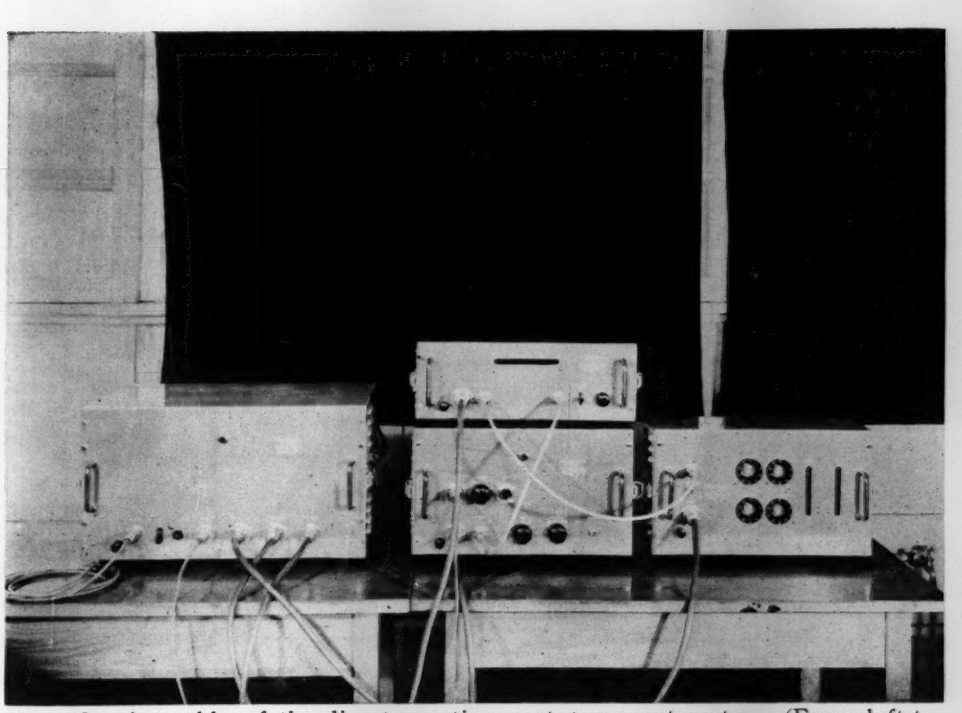

Fig. 13. Assembly of the direct-counting proton magnetometer. (From left to right: power source, frequency divider and amplifier and signal counter).

周波数直読式トランジスター型プロトン磁力計を製作した．

日本においても，建設省地理調査所の坪川，瀬戸[8]らは，トランジスター型ペン書きプロトン磁力計を試作し，小型軽量化に優秀な成績をあげた．本研究班においても，昭和33年度に交付された文部省科学試験研究費補助金により，トランジスター型プロトン磁力計1台を試作する方針をたて，経費の不足のため充分の小型軽量化には成功しなかつたとはいえ，一応野外用として使用できる器械を製作したので，その概略を報告する．

1) 構成

本磁力計は火山地域等において，迅速に絶対磁気測量を行なうことを目的とし，$1\sim2\gamma$ の精度を目標とする．また記録を残すためにペン書き方式とした．本邦において使用するために，水晶発振器よりの1.9および2 *kc/s* の標準周波数との唸周波数を記録する．したがつて，本磁力計の構成は前報[1]に報告した固定観測所用プロトン磁力計の構成と全く同等であつて，増幅器，標準周波発振器，リレーをとりまとめて一つの筐体に納め，他に励磁および検出コイル，記録計，電源が附属する．筐体の寸法は 350 *mm*×290 *mm* ×230 *mm*，重量約 10 *kg* である．第14図は本磁力計のブロックダイヤグラムである．

2) 励磁および検出コイル

固定観測所用プロトン磁力計のものと同一である．

8) 坪川家恒・瀬戸孝夫　昭和34年10月日本地球電気磁気学会講演．

3) 主増幅器

トランジスター (ST-302) 7 箇を使用した電圧増幅部と標準周波数との唸周波数をつくる混合部よりなり，9 V の乾電池を電源とする．第 15 図は主増幅器の結線図である．

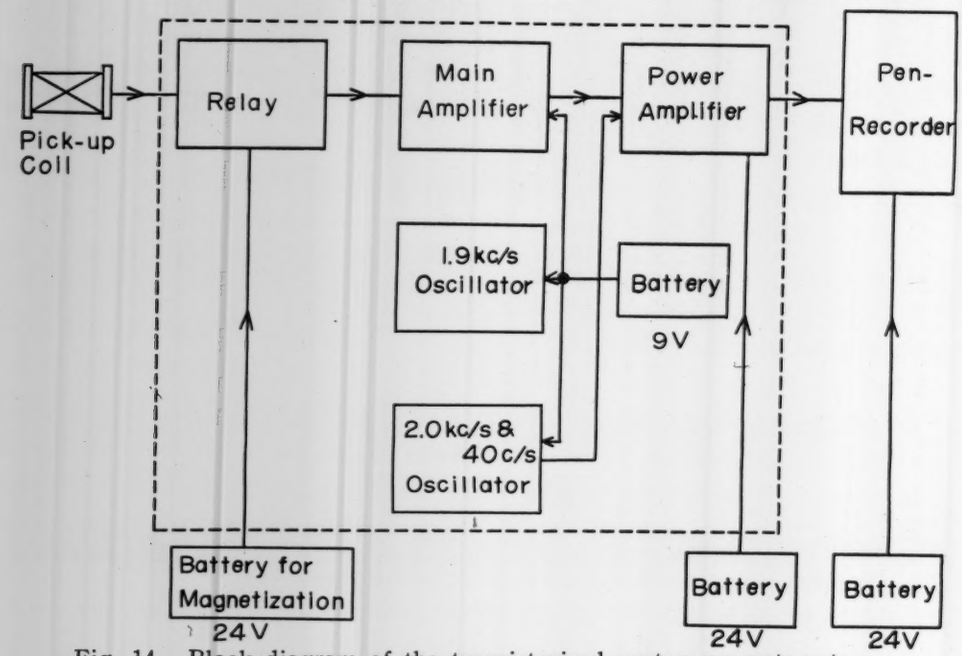

Fig. 14. Block diagram of the transistorized proton magnetometer.

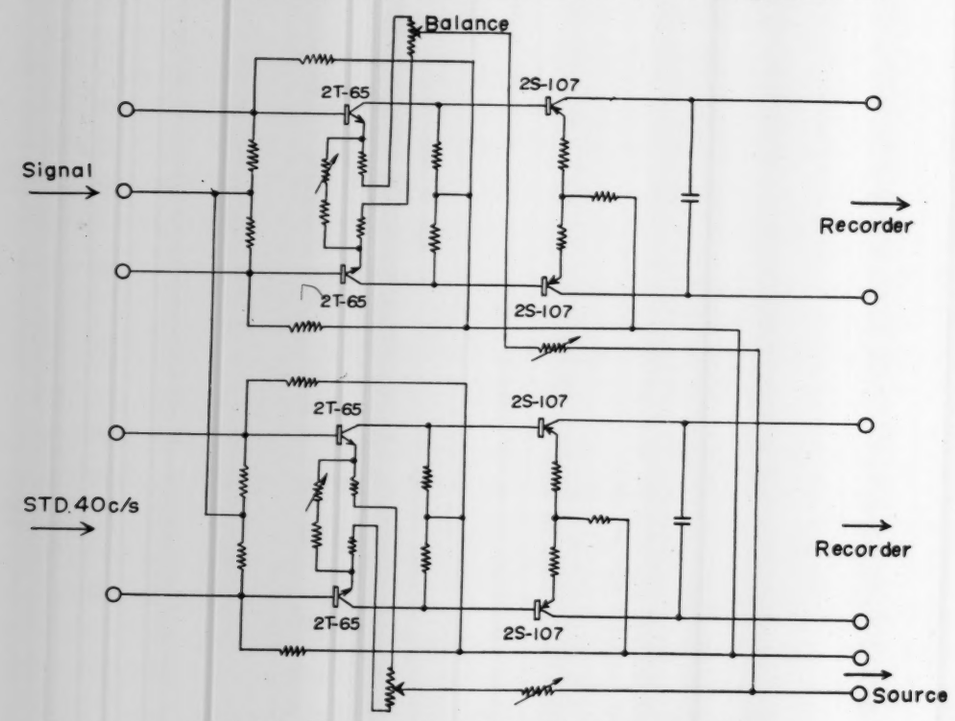

Fig. 16. Electric circuit for the power amplifier.

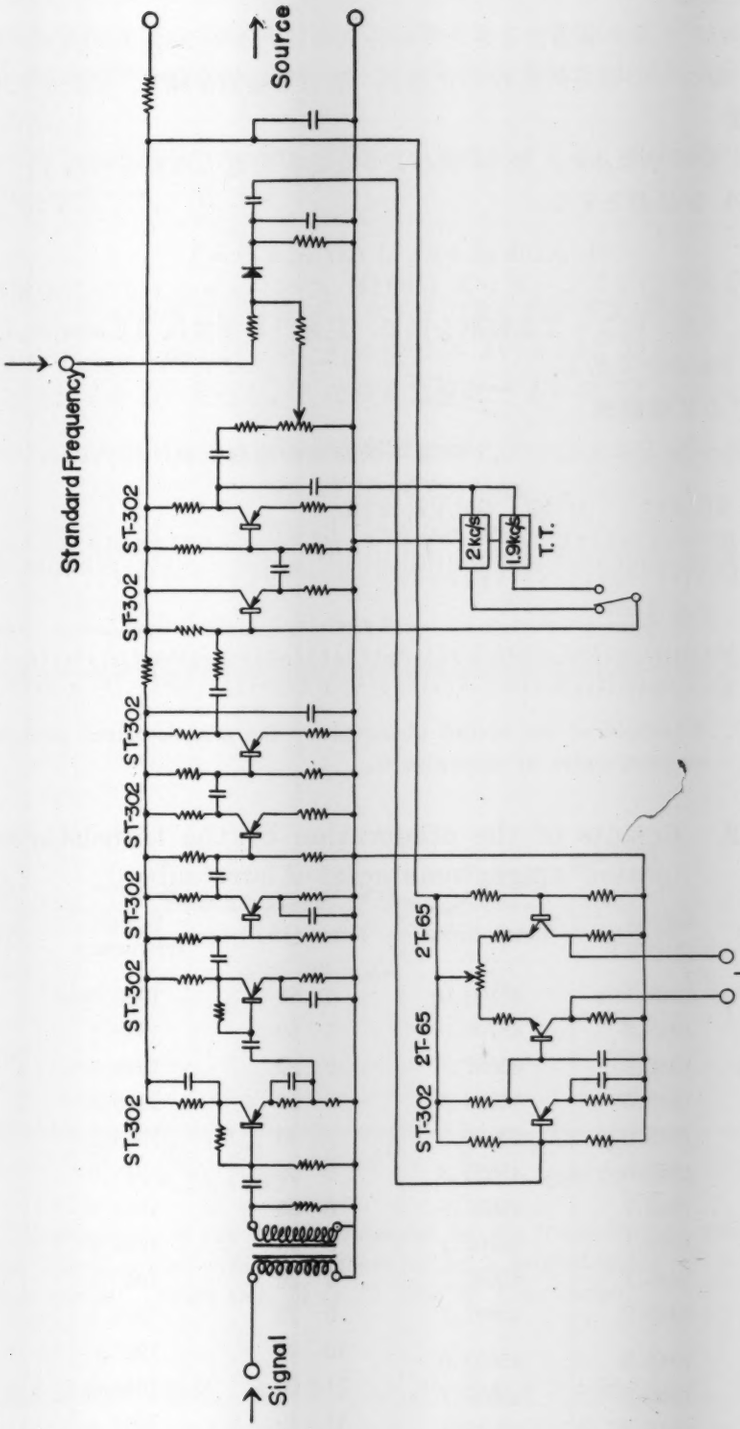

Fig. 15. Electric circuit for the main amplifier.

4) 標準周波発振器

4 および 3.8 *kc/s* 水晶発振器を2分の1に分周して，2 および 1.9 *kc/s* の標準周波数をつくる．また 40 *c/s* の標準周波数を分周し，電力増幅器を経て，記録計に供給する．

5) 電力増幅器

記録計のペンを動かすために，第16図のような結線で電力増幅を行なう．電源としては 24 *V*, 400 *mA* を必要とする．

6) 記録計

記録計としては低入力インピーダンス (150 Ω) のペンオッシログラフを使用し，直流 24 *V* (励磁電源と共用) によって記録紙を送る．記録計の感度は 0.2 *mm/mA*，記録紙の送りは通常 12.5 *cm/sec* である．

7) 油壺における比較観測

1959年10月21～22日にわたつて，神奈川県油壺の臨海実験所構内において本磁力計

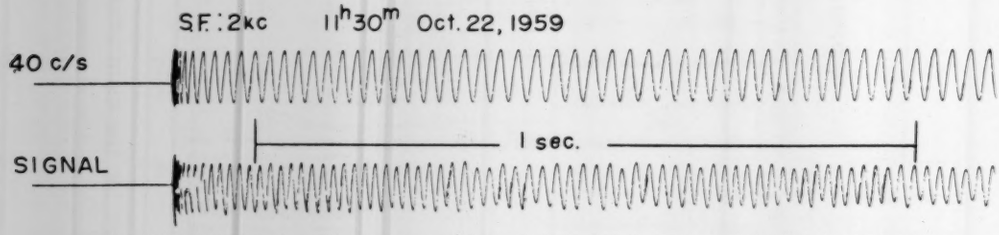

Fig. 17. Example of the record obtained by the transistorized proton magnetometer at Aburatsubo.

Table 2. Results of the observation by the transistorized proton magnetometer at Aburatsubo.

Time (JST)	Signal frequency	Total force	Time (JST)	Signal frequency	Total force
Oct. 21, 1959			Oct. 22, 1959		
15*h* 59*m*	1945.8*c/s*	45700.0γ	4 59	1946.0*c/s*	45704.7γ
17 00	1945.8	45700.0	5 59	1946.1	45707.1
18 00	1945.7	45697.7	6 29	1946.3	45711.8
18 59	1945.6	45695.3	6 58	1946.2	45709.4
19 59	1945.6	45695.3	7 30	1945.3	45688.3
21 01	1945.6	45695.3	8 05	1945.0	45681.2
21 59	1945.7	45697.6	8 30	1944.8	45676.5
22 59	1946.1	45707.1	9 00	1944.5	45669.5
23 17	1945.7	45697.7	9 30	1943.8	45653.1
23 59	1945.7	45697.7	9 59	1944.4	45667.2
Oct. 22, 1959			10 29	1943.9	45655.4
1 30	1945.5	45693.0	11 00	1944.0	45657.2
1 59	1945.7	45697.7	11 30	1944.4	45667.2
2 59	1945.9	45702.4	12 00	1945.2	45685.9
3 59	1946.0	45704.7			

の試験を行ない，地磁気変化計と比較した．今回の比較観測では，磁力計は地磁気変化計の設置してある観測壕より約 400 m の距離にセットされ，約 20 時間にわたつて，30 分から 1 時間間隔で測定を行なつた．第 17 図は 2 kc/s を標準周波数とした場合の記録の例である．

測定結果は第2表の通りであつた．測定結果を図示すると，第18図の黒点のようになる．前報[1]にならつて，

$$F=F_0+S_H\cos I_0\cdot\Delta h+S_Z\sin I_0\cdot\Delta z \qquad (1)$$

の関係から，変化計の全磁力基線値 F_0，水平分力変化計の感度 S_H および鉛直分力変化計の感度 S_Z をプロトン磁力計と変化計の読取値 Δh および Δz より最小自乗法によつて決定することができる．ただし，I_0 は伏角基線値で $I_0=48°22'$ を仮定する．その結果

$$F_0=45593.0\pm0.4\gamma$$
$$S_H=1.46\pm0.02\gamma/mm$$
$$S_Z=3.17\pm0.03\gamma/mm$$

を得た．

第18図の白点はこのようにして定められたパラメーターの値を使用し，(1) 式によりプロトン磁力計による測定時刻に対応する時刻の全磁力を変化計の記録から求めたものである．

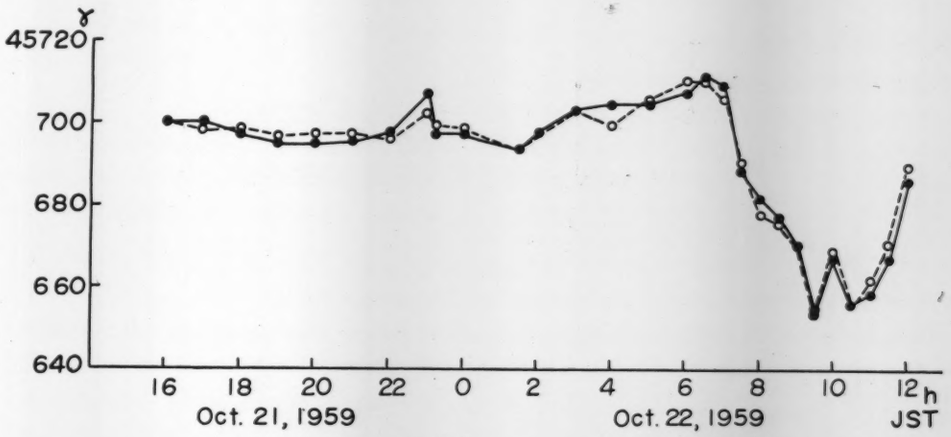

Fig. 18. Comparison of the results observed by the transistorized proton magnetometer (black circle) with those observed by a magnetograph of ordinary type (hollow circle). From Oct. 21 to 22, 1959 at Aburatsubo.

このような比較観測の結果，本トランジスター型プロトン磁力計は，前報の固定観測所用プロトン磁力計とほぼ同等の精度を有し，野外磁気測量用としてほぼ充分な性能を有すると考えられる．第19図は本磁力計の外観を示したものである．

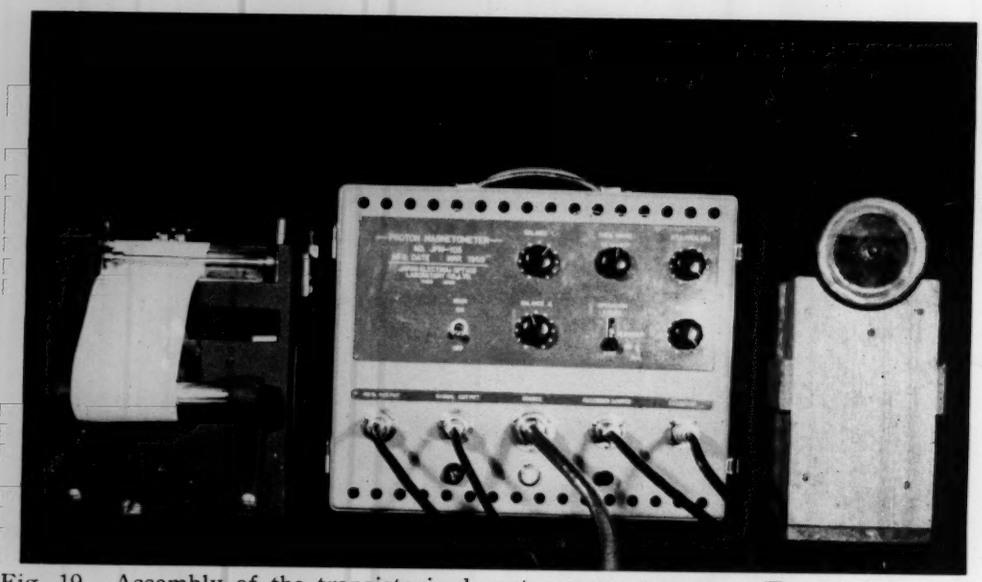

Fig. 19. Assembly of the transistorized proton magnetometer. (From left to right: recorder, amplifier and standard frequency oscillator, and detecting coil)

7. 結　　語

本報においては，「プロトン磁力計の試作研究」に関する文部省科学試験研究費研究班が設計製作した海上用，周波数直読式ならびにトランジスター型プロトン磁力計の構造および使用状況の概略について述べ，また先に試作した固定観測所用プロトン磁力計の伊豆大島観測所における実用状況についても報告した．

これらの各磁力計はそれぞれの特徴を有し，目的に応じて適当なプロトン磁力計を選べば，地磁気観測の精度を高め，測定時間を短縮できることがはつきりした．

残された問題としては

1) テレメータリング
2) ロケット搭載
3) 測定値のパンチング
4) 小型化

などがあるが，1) および 2) については，ロケット計器研究グループのほうで，研究が進行している．また 3) および 4) の点については，困難は主として経費の点で，例えば 4) の小型化のためには，小型軽量の記録計および電池をいかにするかという点に問題がしぼられる．

このような点を除けば，プロトン磁力計の実用化試験は一応成功したものといえよう．

この試作研究においては，南極地域観測隊の小口，柿沼および村石隊員が南極観測船「宗谷」および昭和基地における測定を担当し，南極観測用機械の準備には東京大学理学部地球物理学教室の前川氏の御協力を得た．また地震研究所の行武，棚岡両氏は各種磁力

計の比較観測に従事し，日本電子光学研究所の伊藤，只野，伴の諸氏は設計製作に努力された．これらの諸氏に深く感謝する．終りに財政的援助を賜つた文部省当局に感謝する．

---

8. *Proton Magnetometers.*

By Research Group for Proton Magnetometer.

The Research Group for Proton Magnetometer designed and constructed a nuclear precession magnetometer for station-use as has been already reported in this bulletin. Since April, 1959, the magnetometer has been installed at Oshima Geophysical Observatory in the hope of detecting changes in the earth's magnetic field related to volcanic activities. It is approximately proved that averages of the observations made there four times every 20 *minutes* may represent the hourly smoothed value. By comparing them with those at Kakioka Magnetic Observatory, influences of magnetic storms, daily variations, general secular variations and such like may be eliminated.

The activity of the Research Group is still continuing. A sea-borne magnetometer that has been mainly used by the Japanese Antarctic Research Expedition, a proton magnetometer with a counter and a transistorized proton magnetometer were constructed by the Research Group and will be here briefly described.

1. *Sea-borne proton magnetometer*

The detector coil is wound around a bottle containing 200 *cc.* of pure water. The coil is put in a stream-lined water-proof case, made of synthetic resin and glass fibre (Fig. 5), which is towed behind the ship on which the amplifier, standard frequency oscillator and recorder are set. The case is towed by a nylon rope of 8 *mm* in diameter about 130 *m* behind the ship from her centre. A teflon covered coaxial cable, 14 *mm* in diameter and 200 *m* in length, is used for electric connection. The cable is taped to the rope in a suitable way so as to avoid the tension of towing. The speed of towing usually ranges from 9 to 11 *knots*. Although the stability of the case has been tested in laboratory, we do not know what is really happening in the course of towing.

The block-diagram of the magnetometer is shown in Fig. 4. Protons in water are magnetized by the magnetic field produced by the electric currents, 5 *A* in intensity, flowing through the coil which is also used for the detection. When the electric currents in the coil are abruptly switched off, presession of protons around the earth's magnetic flux is excited. The voltage induced in the coil is introduced to the amplifier with narrow-band filters centred respectively at 1.3, 1.4, 1.5, 1.6, 1.7, 1.8, 1.9 and 2.0 *kc/s*. Since the magnetometer is used on s. s. Soya of the Japanese Antarctic Research Expedition, it is necessary to cover such a wide range of frequencies for measuring all the geomagnetic total forces from Japan to Prince Harald Coast in the Antarctic. The right band should be selected according to the intensity of total force.

The signal is mixed with the standard frequency which is supplied from the standard oscillator containing a quartz oscillator. The standard frequencies are provided at an interval of 0.1 *kc/s* over a range from 1.3 to 2.0 *kc/s*. The beat thus produced is given to one of the galvanometers of the oscillograph through the power amplifier. A 40 *c/s* standard

frequency that is also supplied from the standard oscillator is given to another galvanometer of the oscillograph serving as the reference of time. The paper-speed of the oscillograph is usually 12.5 *cm/sec*. The beat frequency is readily counted with an accuracy of 0.05 *c/s*.

Comparison of the magnetometer was carried out at Hermanus Magnetic Observatory, near Cape Town, South Africa, on Dec. 22–23, 1958. As can be seen in Fig. 7, a systematic difference was found between the values observed by both the instruments, though the daily variation curves seemed to agree very well. It was concluded that the base-line value for the total intensity of Hermanus is larger than that determined by the proton magnetometer by $10.34 \pm 1.92\gamma$. Judging from this comparison, it may be said that a proton magnetometer is useful for comparing the base-line value of one observatory to that of another.

The accuracy of the proton magnetometer itself is estimated at $1–2\gamma$. The practical accuracy, however, depends on rotational disturbances of the detector coil in wake and also on the magnetization of the ship amounting to 7×10^8 *e.m.u.* in this case. The practical accuracy then becomes about $\pm 15\gamma$. The results of the magnetic survey between Japan and the Antarctic have been already published elsewhere. Only the results between Cape Town and Sumatra are illustrated together with the topography of sea-bottom in Fig. 8 as an example.

2. Direct-reading proton magnetometer

If we measure geomagnetic forces covering a wide range, it seems to be more convenient to count directly the frequency of precession than reading the number of beat frequencies recorded. By making use of a digital signal counter, the labour of counting wave numbers as has been necessary in the cases of the proton magnetometers reported in the above, would decrease, though we can have no record in such a case.

In order to be used by the wintering party at Syowa Station, where we have very few observers with a lot of observations to perform, the Research Group constructed a direct-reading proton magnetometer with a signal counter. The magnetometer is now installed at Syowa Station and we hear rather little about the actual observation by it, so that only the design and construction of the magnetometer are described here. The results of the observation will be reported by the Japanese Antarctic Research Expedition in the future.

As can be seen in the block-diagram in Fig. 9, the magnetometer consists of pick-up and magnetization coil, amplifier, frequency divider, signal counter and power supply. The coil is the same as those for the proton magnetometers already reported. The amplifier, that is not greatly different from the previous ones, amplifies the precession signals. The gain of the amplifier exceeds 120 *db*. In Fig. 10 can be seen a limiting circuit of amplitude and a triggering shaper through which pulses of precession frequency are sent to the frequency divider.

The divider is composed of 13 steps of flip-flop circuit which work as a binary counter. In order to avoid the electric shock due to the switching off the magnetizing electric currents, the start-pulse of the signal counter of the next stage should be taken up after counting a suitable number of pulses ranging $2^6–2^9$. A stop-pulse is also sent to the gate circuit after a suitable number of pulses. The general idea of the divider is given in Fig. 11. An operation-switch and a zero reset circuit are also provided.

Fig. 12 shows the construction of the signal counter which consists of a gate circuit, vacuum tube and dekatron decimal counting circuits and a standard frequency oscillator of 100 *kc/s*. During the time-interval between start- and stop-pulses, the gate is opened, while the number of signal waves during this interval is known. If the number of 100 *kc/s* frequency waves corresponding to the interval can be counted, we can easily obtain the

frequency of the signal wave. By providing two vacuum tube counters and four dekatron counters, we can count the frequency up to the necessary accuracy of about $\pm 1\gamma$. The general arrangement of the apparatus is shown in Fig. 13.

3. Transistorized proton magnetometer

In order to construct a portable proton magnetometer, the Research Group tried to design and construct an all-transistorized proton magnetometer. The construction is the same in principle as that of the proton magnetometer reported in the previous paper. The block-diagram of the magnetometer is shown in Fig. 14.

The main amplifier (Fig. 15), that is driven by a 9 *V* battery, contains the part for the amplification of the signal wave and the one for mixing it with the standard frequency wave. The standard frequencies, 2 and 1.9 *kc/s*, are provided from the two quartz oscillators, 4 and 3.8 *kc/s* respectively. For a magnetic survey in Japan, those two frequencies are sufficient in order to have beat frequencies which can be recorded by a pen-recording oscillograph. The beat waves and 40 *c/s*, which is demultiplied from the 2 *kc/s* and is used as the time-reference, are introduced to a power amplifier (Fig. 16). The power amplifier is driven by a 24 *V* battery with an electric current of approximately 400 *mA*. The two amplifiers and standard oscillator are set in a case (350 *mm* × 290 *mm* × 230 *mm*) which weighs about 10 *kg*. The pen-recording oscillograph is of usual type. The galvanometers are of low-impedance having an in-put impedance of 150 *ohm*.

Since we could afford no special batteries and oscillographs, the whole assembly of the magnetometer is not so small or light as that which was intended in the beginning of research work. If we can improve these points, the magnetometer would become much convenient for field-use.

According to the results of the observation at Aburatsubo (Figs. 17 and 18), it is proved that the magnetometer has almost the same accuracy as that of the proton magnetometer for station-use. A magnetic survey over Hakone Volcano was successfully made with the transistorized magnetometer.

BULLETIN OF THE EARTHQUAKE
RESEARCH INSTITUTE
Vol. 38 (1960), pp. 145-175

9. *On the Changes in the Heights of Mean Sea-levels, before and after the Great Earthquakes.*

By Seiti YAMAGUTI,

Earthquake Research Institute.

(Read June 23, 1959.—Received Dec. 28, 1959.)

Introduction

Investigations on the changes in the heights of the mean sea-levels have been made, and the results have already been reported in my recent papers.[1)]

To arrange the results finally and also to make the probable error of the monthly mean sea-level smaller than the preceding one when corrected, the next procedure was taken.

First, I will explain here once more in detail the value of the change in the height of monthly mean sea-level.

We have calculated the secular mean values of sea-level, L_m, barometric pressure, b_m, sea-water temperature at the depth of one meter from the surface, T_m, for 40 years, at Aburatubo, Hosoima, Wazima and Osyoro, and obtained the next Table 1. Those for Kôti, Kainan, Asamusi, Nezugaseki, and Kasiwazaki, during the period of 5～9 years, are also shown in Table 1.

Table 1. Secular mean Sea-level, Barometric Pressure and Sea-water Temperature.

	Aburatubo	Hososima	Wazima	Osyoro	Koti	Kainan	Asamusi	Nezuga-seki	Kasiwa-zaki
L_m, in mm	3336	2594	1916	1593	2877	2626	2908	2094	2534
b_m, in mmHg	760.6	761.5	761.3	759.3	762.5	760.8	761.2	761.8	761.9
T_m, in °C	16.8	19.0	15.6	11.3	20.1	18.6	12.6	15.4	16.8

Monthly deviations of sea-levels from 40 years' mean for each month are calculated with the corrections shown in Table 2, a, b, and denoted by $\Delta L'$.

1) S. YAMAGUTI, *Bull. Earthq. Res. Inst.*, **19** (1941), **21** (1943), **33** (1955), and *Bull. Geog. Surv. Inst.*, **1** (1948), **2** (1950).

Table 2, a, b. Corrections, deduced from 40 years' annual mean of Sea-level, Sea-water Temperature, and Barometric Pressure.

(a)

	Corrections to ΔL, ΔT, and Δb											
	Aburatubo			Hososima			Wazima			Osyoro		
Month	ΔL	ΔT	Δb	ΔL	ΔT	Δb	ΔL	ΔT	Δb	ΔL	ΔT	Δb
January	38	5.0	−1.6	124	5.1	−4.6	54	4.8	−3.3	29	6.6	−0.8
February	54	6.0	−1.4	128	5.7	−3.4	117	6.2	−3.1	69	7.5	−1.2
March	79	5.3	−1.3	118	5.1	−2.1	142	6.4	−2.4	75	7.2	−1.1
April	73	3.1	−0.7	80	2.9	−0.2	133	4.9	−0.5	59	5.1	0.1
May	23	0.4	1.3	20	0.1	2.0	58	2.1	1.5	− 2	2.0	1.0
June	−25	−2.1	3.4	− 53	−2.4	4.4	− 34	−1.4	3.9	− 54	−1.6	2.3
July	−56	−5.2	3.0	− 81	−4.6	4.4	−103	−4.5	4.2	−105	−5.7	2.8
August	−78	−6.9	2.8	−145	−6.8	4.4	−172	−7.8	3.7	−139	−9.4	1.9
September	−97	−6.7	0.7	−137	−6.1	2.5	−125	−7.4	1.7	−107	−8.5	−0.1
October	−82	−3.6	−2.1	−106	−3.1	−1.3	− 68	−3.8	−2.1	− 54	−4.8	−2.7
November	−43	−0.5	−3.1	− 9	0.1	−3.5	− 51	−0.7	−3.7	− 41	−0.2	−3.0
December	− 5	2.7	−3.2	78	3.1	−4.2	− 7	2.7	−3.1	− 15	4.0	−1.5

(b)

	Corrections to ΔL, ΔT, and Δb														
	Koti			Kainan			Asamusi			Nezugaseki			Kasiwazaki		
Month	ΔL	ΔT	Δb	ΔL	ΔT	Δb	ΔL	ΔT	Δb	ΔL	ΔT	Δb	ΔL	ΔT	Δb
January	118	5.8	−2.6	96	7.9	−3.5	29	4.4	0.5	19	6.7	−1.3	62	5.9	−2.1
February	135	6.2	−1.8	136	8.6	−2.9	59	6.0	0.7	126	8.0	−1.1	110	7.4	−2.2
March	110	5.0	−1.5	143	6.9	−2.2	101	6.2	−0.5	136	7.7	−2.0	137	7.8	−1.5
April	88	2.8	−0.3	108	3.0	−0.7	107	5.0	−0.3	159	5.4	−1.1	131	5.4	−0.7
May	7	0.2	1.5	19	−0.3	1.5	32	2.4	1.9	68	1.0	1.3	64	1.7	1.6
June	− 91	−2.8	4.0	−107	−4.0	4.3	− 5	−0.3	2.2	− 9	−3.2	2.7	− 26	−2.4	3.1
July	− 81	−5.5	3.4	−108	−7.7	5.1	− 58	−3.0	2.3	−106	−7.3	2.9	−117	−6.3	4.5
August	−109	−7.9	3.2	−123	−9.0	4.4	−100	−6.1	2.2	−132	−10.6	2.9	−149	−8.3	3.2
September	−138	−5.7	2.3	−124	−6.8	2.5	− 71	−7.6	0.0	− 81	−8.7	0.4	− 83	−7.6	0.9
October	−105	−2.6	−1.0	− 92	−3.1	−1.2	− 43	−5.7	−2.3	− 42	−4.5	−2.0	− 42	−4.3	−1.6
November	− 3	0.6	−3.7	− 5	0.7	−3.8	− 21	−2.6	−3.9	− 53	0.2	−3.2	− 44	0.2	−3.2
December	72	3.9	−4.2	67	4.7	−4.4	− 26	1.3	−0.8	− 48	4.3	−1.7	− 20	3.7	−2.5

ΔL is measured in millimetre, ΔT in degree centigrade and Δb in mmHg.

Similarly, monthly deviations of barometric pressure, and those of sea-water temperature from 40 years' mean for each month are calculated and denoted by $\Delta b'$ and $\Delta T'$, respectively. Residual values of $\Delta L'$, corrected with $\Delta b'$ and $\Delta T'$, represented by the equation

$$\Delta L''=\Delta L'-p\Delta b'-q\Delta T' \text{ , were calculated.}$$

In this equation, as the value of p, theoretical value, 13.2 was taken for all stations commonly, and as the values of q, 13.3, 19.7, 16.5, 11.2, 17.1, 15.6, 14.0, 12.6 and 15.5 were taken for Aburatubo, Hososima, Wazima, Osyoro, Kôti, Kainan, Asamusi, Nezugaseki and Kasiwazaki, respectively, by the method of least squares, $\Delta L'$ being measured in millimetres, $\Delta b'$ in mmHg, and $\Delta T'$ in degrees centigrade.

Next, we have smoothed the value of $\Delta L''$, by taking $\Delta L''_m=\frac{1}{4}(\Delta L''_{n-1}+2\Delta L''_n+\Delta L''_{n+1})$ instead of $\Delta L''_n$, where n is the order of the months, the probable error of $\Delta L''_m$, $\pm$15mm being obtained from preceding results.

The magnitudes of the great earthquakes, M in Gutenberg's or Pasadena scale, used here, were calculated mostly by Prof. H. Kawasumi, Prof. Ch. Tsuboi in Tokyo University, and partly by members of the Earthquake Section of the Meteorological Agency, and printed by Meteorological Agency.

The values of the observed monthly mean sea-level, L, barometric pressure, b, and sea-water temperature, T, and those deviations from annual mean for 40 years, $\Delta L'$, $\Delta b'$ and $\Delta T'$, and also the values of the corrected, $\Delta L''$ and the smoothed, $\Delta L''_m$ of the monthly mean sealevels, are calculated and L, $\Delta L''$, $\Delta b'$, $\Delta T'$ are shown in Table 3.

Method of Investigation, and Results

After taking the monthly mean sea-levels, corrected and smoothed, $\Delta L''_m$ for Aburatubo, Hososima, Wazima, during the period of about 60 years, for Osyoro during the period of about 54 years, and for Kôti, Kainan, Asamusi, Nezugaseki, Kasiwazaki, during the period of about 5～9 years, diagrams were plotted with these values as ordinates against the months taken as abscissa as shown in Fig. 1.

On these diagrams, we have marked the months of great earthquakes with magnitudes M, equal to or greater than 7, whose epicentral distances from the mareographic stations, d, being less than 200 kilometers, 300km,

400km, and 500km, corresponding to the magnitudes, $M=7.0\sim7.3$, $M=7.4\sim7.6$, $M=7.7\sim7.9$, and $M\geqq8.0$, respectively.

The values of $\Delta L''_m$ for the months of equal phase measured from the month of earthquake, were averaged for different earthquakes and plotted as ordinate against the months as shown in Fig. 2. a, b.

In this case, in order to avoid the accidental distribution of the curve, or of the appearance of a false period of half an year, we have taken the means of $\Delta L''_m$, till 18 months preceding the month of earthquake.

In the case of taking the average of $\Delta L''_m$ for different earthquakes with magnitude M, greater than 7, which occurred in wide regions, within epicentral distances, d, equal and less than 500km, not considering the variation of M and d, the feature of the curve shows rather random or irregular distribution of the curve. This fact may be considered to show that, according to the magnitude of earthquakes, only such mareographic stations as are situated in proper distances, within 500km, namely, $d\leqq200$km, 300km, 400km, and 500km, are affected by earthquakes with corresponding sufficiently great magnitude.

From Fig. 2, we may be able to say that, in the time over 12 months preceding the earthquake, the monthly mean sea-level does not fluctuate so violently, but from about half an year before the earthquake, it begins to fluctuate with large amplitude and the value of its curve reaches maximum at about 4 months before and becomes minimum at about 1 or 2 months before the earthquake. Rather conspicuous maximum and minimum of the curve, i. e. rather conspicuous subsidence and upheaval of the earth's crust may be observed in the months, about 4 and 1 or 2 preceding an earthquake respectively.

The mean errors ε, of the mean of $\Delta L''_m$ for many earthquakes, were also calculated and tabulated as shown in Table 4. These values of ε are satisfactorily small when compared with the values of the mean $\Delta L''_m$ in the curve, shown in Fig. 2.

It is interesting to note that the mean sea-levels, $\Delta L''_m$ for many earthquakes are negative in the month of earthquake in both cases for Aburatubo ($N_1=53$), and for taking other 4 stations, Hososima, Wazima, Osyro, Kôti, together with Aburatubo ($N_2=99$). In former case, mean of $\Delta L''_m=(-6.6\pm3.2)$mm, and in the latter, mean of $\Delta L''_m=(-4.8\pm2.3)$mm, the secular mean of sea-level for 40 years (1900~1939), being taken as zero.

Incidentally, we want to note that the values of $\Delta L''_m$, in the curve,

Table 4. Mean errors of the mean sea-level, $\Delta L''_m$ for each month before and after the great earthquakes.

month	for Aburatubo only $N_1=53$	for Aburatubo, Hososima, Wazima, Osyoro, Koti $N_2=99$	month	for Aburatubo only $N_1=53$	for Aburatubo, Hososima, Wazima, Osyoro, Koti $N_2=99$
−18	±2.4	±1.4	−2	±2.0	±1.2
−17	±2.9	±1.7	−1	±1.8	±1.3
−16	±3.5	±1.9	0		
−15	±3.4	±1.8	1	±1.5	±1.1
−14	±3.3	±1.6	2	±1.7	±1.2
−13	±3.3	±1.7	3	±2.3	±1.4
−12	±3.2	±1.6	4	±2.2	±1.5
−11	±3.2	±1.6	5	±2.3	±1.4
−10	±3.3	±1.6	6	±2.7	±1.7
− 9	±3.0	±1.6			
− 8	±2.8	±1.6			
− 7	±2.9	±1.8			
− 6	±2.7	±1.4			
− 5	±2.7	±1.4			
− 4	±2.7	±1.3			
− 3	±2.4	±1.3			

N_1 and N_2 are number of earthquakes. 0-month denotes the month, in which earthquake occurred.

shown in Fig. 1, as well as in Table 3, may have the same reliability as those data obtained by Levelling Survey. The comparison of these two values are already made and reported in my recent paper.[2)]

Finally, yearly mean sea-levels were calculated from the values of monthly mean sea-levels, corrected and smoothed, $\Delta L''_m$, and plotted against the year, as shown in Fig. 3.

Many oceanographers in the world say that the total mass of ocean water has been increasing lately, but the result of my investigation on the change in the height of mean sea-level during the period of about 60 years at four stations, Aburatubo in Kanagawa Prefecture, Hososima in Miyazaki Prefecture, Wazima in Isikawa Prefecture, Osyoro in Hokkaido, in Japan, as shown in Fig. 1, and 3, shows no increasing tendency in the height of mean sea-level, except the slight fluctuation of sea-level with long period of about 18 years around the secular mean of 40 years. So called rise of mean sea-level, may be the apparent phenomena caused by the oceanic and meteorological tides which govern the change in the height of mean sea-level. So that, if proper corrections due to oceanic and meteorological tides may be added to the observed value of mean

2) S. YAMAGUTI, *Bull. Earthq. Res. Inst.*, **37** (1959).

sea-level as in the case of my investigation, apparent increase in the height of mean sea-level would vanish, and actual small subsidence of earth's crust relative to the mean sea-level would be observed, along various coasts of the world.

I hope many oceanographers in the world will try, first, the correction due to annual change of mean sea-levels, obtained from secular years, as long as possible, second, correction due to residual changes of barometric height and sea-water temperature, similarly to the method of my investigation here explained.

In conclusion, I wish to express my hearty thanks to the Geographical Survey Institute, as well as to the Meteorological Agency in Japan for the kindness of putting abundant valuable data at my disposal throughout the whole investigation. The writer also wishes to express hearty thanks to Miss K. Ogata in his laboratory, who has rendered laborious assistance in aranging Tables and Diagrams in the paper.

---

9. 大地震前後の平均海水面変化について

地震研究所　山　口　生　知

1: 平均海水面変化についてはこれまで度々報告しているように，永年の値より求めた年周変化の値を先づ取り去つた後，更に海水温度や気圧の変化による残差修正を施して，その値を $\Delta L''$ としておつたが，この度は $\Delta L''$ 曲線の細かい変化をなくして滑かにするため $\Delta L''_m=\frac{1}{4}\{\Delta L''_{n-1}+2\Delta L''_n+\Delta L''_{n+1}\}$ を計算して $\Delta L''_m$ 曲線を示した．ここに n は月の順番を示したものである．

2. この曲線の上に magnitude M が 7 以上の地震を盛り込んで見たのであるが，験潮場から震源までの距離 d はmagnitude の大さに応じて適当に採つた．すなわち

M=7.0～7.3 は d=200 km まで
M=7.4～7.6 は d=300 〃 〃
M=7.7～7.9 は d=400 〃 〃
$M\geqq 8$ は $d\leqq 500$ 〃 〃

とした

3. 地震のあつた月の 18ケ月前から 6ケ月後までの各月毎の $\Delta L''_m$ の平均をとつてみると，$\Delta L''_m$ の値は地震の 1ケ年以前にはそれ程大きな変動がないが約半年前頃より大きく変動を始めて約 4カ月前にその値は最大に達し，1ケ月か 2ケ月前に最小になる傾向を示している．この $\Delta L''_m$ の変動は相対的な地盤の変動とみることができる．

Table 3. Monthly mean values of Sea-level, Sea-water Temperature and Barometer.

(a) Aburatubo

Date	L	$\Delta L''$	$\Delta T'$	$\Delta b'$	Date	L	$\Delta L''$	$\Delta T'$	$\Delta b'$	Date	L	$\Delta L''$	$\Delta T'$	$\Delta b'$
1900	mm				1904	mm				1908	mm			
1	3404	− 20	0.8	1.5	1	3409	− 11	−0.8	1.0	1	3393	− 6	0.8	1.8
2	3479	− 84	0.6	1.0	2	3490	− 71	0.0	2.2	2	3340	33	1.6	0.3
3	3485	− 80	0.7	−0.1	3	3457	− 29	−0.1	0.9	3	3464	− 42	0.1	0.6
4	3473	− 49	0.4	1.5	4	3511	− 78	0.4	2.2	4	3469	− 47	0.3	1.3
5	3408	− 85	0.9	−1.8	5	3411	− 53	0.1	0.0	5	3381	− 25	0.2	0.0
6	3460	−140	1.4	2.1	6	3359	− 49	0.4	0.3	6	3334	− 37	0.4	−0.7
7	3423	−159	−0.7	−1.9	7	3273	− 12	1.1	−0.3	7	3186	100	−1.0	−0.5
8	3400	−131	−0.1	1.1	8	3250	− 1	1.3	0.6	8	3409	−141	0.4	1.1
9	3397	−158	0.3	0.3	9	3228	− 17	0.5	−1.6	9	3272	− 8	−1.0	0.9
10	3401	−143	1.2	1.5	10	3291	− 56	0.6	−0.8	10	3297	− 44	0.0	−0.1
11	3372	−106	2.1	0.1	11	3337	− 69	−0.1	−2.0	11	3234	26	−0.2	−3.0
12	3455	−139	0.6	−0.5	12	3336	− 29	0.6	−1.2	12	3336	− 15	0.2	−0.5
1901					1905					1909				
1	3463	− 81	1.3	1.9	1	3385	− 33	1.0	−0.7	1	3339	48	0.4	1.4
2	3471	−146	1.2	−3.7	2	3428	− 64	0.6	−1.4	2	3403	− 38	0.7	−1.2
3	3517	−112	1.7	1.0	3	3518	− 51	−0.5	3.4	3	3416	23	−0.2	1.6
4	3525	−106	0.9	1.7	4	3421	− 2	−0.4	0.4	4	3386	17	0.2	−0.2
5	3458	−135	2.4	−0.3	5	3392	− 10	−0.5	1.2	5	3366	− 19	0.7	−0.2
6	3404	−115	0.7	−1.0	6	3352	− 55	0.8	−0.2	6	3372	− 72	0.6	−0.2
7	3341	− 64	−0.9	−1.1	7	3350	− 75	0.6	0.2	7	3339	− 28	−0.2	2.1
8	3310	− 40	0.1	1.0	8	3320	− 57	−0.6	−0.2	8	3241	− 6	1.1	−0.6
9	3271	− 62	0.9	−1.4	9	3274	− 1	−0.8	1.7	9	3190	28	1.2	−0.4
10	3243	− 4	0.9	−0.2	10	3281	− 23	0.4	0.7	10	3197	49	0.3	−0.3
11	3395	−117	0.0	−1.1	11	3286	15	0.7	1.3	11	3336	− 45	−0.4	−0.5
12	3398	− 83	−0.3	−1.5	12	3369	− 68	1.7	−0.5	12	3367	− 38	−0.2	−0.4
1902					1906					1910				
1	3442	− 63	−0.7	−0.3	1	3421	− 47	0.6	0.6	1	3340	18	0.8	−0.4
2	3571	−138	−0.6	2.7	2	3435	− 51	−0.8	−1.3	2	3383	− 26	0.1	−2.4
3	3502	− 87	0.3	0.3	3	3416	− 10	−0.2	−0.9	3	3419	− 16	−0.1	−1.0
4	3468	− 77	0.6	−0.8	4	3397	− 11	0.5	−1.2	4	3456	− 27	−0.3	1.2
5	3383	− 28	0.4	0.1	5	3380	− 14	0.3	0.8	5	3339	23	0.4	0.6
6	3400	−103	0.2	−0.8	6	3348	− 27	−0·1	0.7	6	3358	− 71	0.9	−0.9
7	3396	−119	−1.3	−1.5	7	3295	− 45	−0.3	−2.6	7	—			−0.7
8	3345	− 58	−1.5	0.7	8	3251	− 19	0.8	−1.1	8	—			−1.7
9	3295	− 72	−0.3	−1.5	9	3211	39	−0.3	0.5	9	3305	− 63		0.2
10	3323	− 56	0.4	1.4	10	3253	8	0.0	0.5	10	3209	79	−2.0	0.6
11	3407	−102	0.9	1.8	11	3330	− 24	0.4	1.4	11	3306	− 21	0.1	−0.5
12	3314	− 20	0.3	−2.5	12	3388	−102	0.0	−3.4	12	3367	− 48	−0.6	−1.5
1903					1907					1911				
1	3423	− 49	0.6	0.6	1	3340	45	0.3	1.1	1	3406	4	−0.9	1.8
2	3464	− 83	1.8	1.1	2	3427	− 37	−0.1	−0.1	2	3483	− 53	0.0	3.0
3	3522	− 84	0.4	2.1	3	3492	− 74	0.3	0.5	3	3348	64	0.5	0.3
4	3506	− 83	0.8	1.9	4	3465	− 36	−0.2	1.3	4	3361	17	0.5	−1.8
5	3417	− 46	0.0	0.9	5	3416	− 94	0.6	−2.2	5	3406	− 11	−0.3	2.4
6	3328	− 14	−1.5	−1.3	6	3371	− 63	0.0	−0.2	6	3260	44	0.5	0.0
7	3340	− 24	−3.3	−0.6	7	3258	30	−0.6	0.0	7	3162	113	−0.3	−0.1
8	3318	− 12	−2.3	1.3	8	3303	− 74	0.7	−1.5	8	3269	− 8	0.3	0.5
9	3341	− 62	−2.2	0.8	9	3213	26	0.3	0.3	9	3219	36	0.3	1.5
10	3301	− 23	−1.7	0.1	10	3217	35	0.4	0.2	10	3254	− 32	0.5	−1.9
11	3330	− 1	−2.8	−0.1	11	3293	4	0.6	0.9	11	3269	23	0.6	0.5
12	3409	− 54	−3.6	−1.8	12	3318	− 10	0.1	−1.7	12	3297	38	0.2	0.5

(to be continued)

(continued)

Date	L	$\Delta L''$	$\Delta T'$	$\Delta b'$	Date	L	$\Delta L''$	$\Delta T'$	$\Delta b'$	Date	L	$\Delta L''$	$\Delta T'$	$\Delta b'$
1912	mm				1916	mm				1920	mm			
1	3356	27	−0.1	0.6	1	3402	− 29	1.4	1.4	1	3340	11	−0.1	−1.8
2	3363	18	0.6	−0.1	2	3378	− 21	1.0	−1.5	2	3406	29	−0.9	2.5
3	3381	42	−1.4	−0.8	3	3425	− 26	−0.3	−1.5	3	3479	− 4	−0.9	3.6
4	3381	20	0.4	−0.2	4	3402	17	0.5	1.3	4	3445	− 31	0.6	1.0
5	3332	13	0.5	−0.5	5	3356	− 17	1.9	0.4	5	3264	36	0.7	−3.8
6	3275	5	0.5	−1.8	6	3347	− 46	1.4	0.7	6	3280	10	1.2	−0.4
7	3290	− 33	0.2	−1.5	7	3320	− 56	0.2	−1.0	7	3223	47	1.9	1.1
8	3183	72	0.8	0.6	8	3182	43	0.8	−1.7	8	3214	18	1.6	−1.1
9	3244	− 11	−0.4	−0.8	9	3270	− 43	1.5	0.6	9	3165	84	0.1	0.8
10	3364	− 90	−0.6	0.9	10	3288	− 19	0.4	1.5	10	3214	26	0.2	−0.8
11	3257	40	−0.6	−0.3	11	3311	25	−0.5	2.7	11	3229	52	0.8	−0.1
12	3237	122	−0.2	1.9	12	3296	23	0.2	−0.7	12	3271	52	0.7	0.1
1913					1917					1921				
1	3381	17	−0.6	1.2	1	3330	23	−0.3	−1.9	1	3373	13	−0.3	0.6
2	3333	47	0.2	−0.5	2	3394	− 36	−0.9	−3.3	2	3354	27	−0.6	−1.3
3	3431	− 17	−0.8	−0.9	3	3473	− 41	−0.7	0.6	3	3352	43	−0.4	−1.9
4	3403	18	0.1	1.0	4	3438	− 62	0.5	−2.0	4	3412	16	0.2	1.7
5	3315	21	0.2	−1.5	5	3372	− 59	1.6	−1.9	5	3333	6	0.3	−1.2
6	3288	− 3	0.2	−1.7	6	3297	20	−0.5	−0.1	6	3321	− 2	−0.5	0.1
7	3235	33	−0.3	−1.2	7	3287	− 3	0.8	1.1	7	3289	5	0.5	1.6
8	3105	111	0.4	−2.8	8	3196	46	1.1	−0.1	8	3243	− 4	0.8	−0.6
9	3137	110	−0.6	0.0	9	3240	11	0.4	1.3	9	3242	17	−0.8	0.7
10	3228	6	0.3	−1.2	10	3242	− 9	0.7	−0.9	10	3198	52	−0.5	−0.8
11	3346	− 12	−0.9	2.2	11	3276	8	−0.5	−1.2	11	3386	−100	−1.3	−1.8
12	3373	− 45	−1.1	1.4	12	3294	− 22	−0.9	−5.4	12	3392	− 42	−1.5	−0.1
1914					1918					1922				
1	3428	− 43	−0.5	0.3	1	3390	− 29	−1.2	−2.2	1	3396	10	−1.8	0.6
2	3383	36	−0.5	1.7	2	3404	30	−0.5	2.8	2	3417	− 4	−0.5	1.2
3	3342	76	0.6	0.8	3	3454	− 23	−0.3	0.9	3	3436	− 17	−0.4	−0.1
4	3377	4	0.0	−2.1	4	3422	9	−0.4	1.3	4	3415	6	−0.3	0.6
5	3315	57	0.5	1.5	5	3371	− 11	−0.1	0.0	5	3378	− 12	0.5	0.9
6	3295	− 1	1.0	−0.3	6	3356	− 46	0.0	−0.1	6	3302	− 26	1.4	−1.2
7	3239	6	1.1	−1.6	7	3318	− 65	0.9	−1.1	7	3329	− 51	1.3	1.1
8	3219	7	1.6	−0.8	8	3193	53	2.0	1.1	8	3243	− 22	1.9	−0.9
9	3190	48	1.4	1.4	9	3196	9	1.2	−1.4	9	3225	14	1.5	1.5
10	3272	− 21	0.6	0.4	10	3224	42	0.2	1.1	10	3263	− 25	0.8	−0.4
11	3337	− 48	0.9	0.6	11	3209	92	0.2	0.8	11	3252	33	−0.4	−1.0
12	3332	− 38	0.5	−2.3	12	3253	91	−0.6	0.4	12	3309	− 18	−0.8	−3.9
1915					1919					1923				
1	3329	63	0.2	1.6	1	3322	60	−0.3	0.3	1	3407	− 1	−0.8	1.6
2	3305	68	0.1	−1.2	2	3327	85	−0.8	0.8	2	3360	18	−0.4	−1.3
3	3348	48	0.1	−1.4	3	3293	95	0.8	−1.2	3	3480	− 16	−0.1	3.6
4	3355	58	0.0	0.3	4	3300	77	1.2	−1.2	4	3354	52	0.2	0.0
5	3289	62	−0.3	−0.9	5	3307	56	0.3	0.6	5	3328	31	0.3	0.3
6	3293	22	0.6	0.9	6	3231	68	−0.2	−1.1	6	3182	111	0.5	−0.8
7	3270	3	0.2	−0.3	7	3273	27	0.0	1.5	7	3240	31	−0.2	−0.9
8	3179	− 82	1.3	−3.3	8	3247	11	0.4	0.4	8	3319	− 87	1.4	−0.5
9	3271	− 44	0.9	0.0	9	3202	11	1.0	−1.0	9	3220	7	0.8	−0.1
10	3245	− 23	1.7	−0.7	10	3191	39	0.6	−1.2	10	3249	− 1	0.4	−0.1
11	3280	42	0.5	2.7	11	3283	00	0.7	−0.1	11	3353	− 81	0.3	−1.3
12	3355	− 48	0.6	−1.2	12	3305	− 2	−0.1	−2.2	12	3455	−139	−0.4	−1.5

(to be continued)

(continued)

Date	L	$\Delta L''$	$\Delta T'$	$\Delta b'$	Date	L	$\Delta L''$	$\Delta T'$	$\Delta b'$	Date	L	$\Delta L''$	$\Delta T'$	$\Delta b'$
1924	mm				1928	mm				1932	mm			
1	3423	− 33	−0.2	1.0	1	3463	− 75	0.2	1.3	1	3441	− 33	0.6	3.8
2	3422	− 65	0.4	−2.1	2	3473	− 68	−0.2	0.9	2	3353	27	0.1	−0.1
3	3488	− 51	−0.5	1.1	3	3402	3	0.1	−0.7	3	3453	− 61	−0.2	−1.4
4	3406	3	1.0	1.0	4	3437	− 23	−0.1	0.3	4	3428	− 42	−0.5	−1.7
5	3393	− 56	0.0	−1.7	5	3435	− 75	0.5	0.6	5	3394	− 28	−0.2	0.9
6	3281	32	0.1	0.2	6	3362	− 51	−0.3	−0.3	6	3240	91	−0.8	1.3
7	3379	− 46	−0.7	3.3	7	3391	− 76	−1.8	0.8	7	3295	− 26	−0.6	−0.8
8	3360	−107	−0.3	−0.7	8	3211	57	−2.1	−1.4	8	3328	− 67	−0.2	0.6
9	3345	− 95	−0.8	0.0	9	3330	− 73	−0.4	1.0	9	3268	− 35	−0.5	−0.4
10	3288	− 14	−0.4	1.1	10	3315	− 48	−0.4	0.6	10	3262	− 17	−0.6	−0.7
11	3355	− 86	−0.7	−2.5	11	3359	− 43	−0.5	1.2	11	3285	− 13	−0.3	−1.3
12	3358	− 32	0.0	−0.4	12	3320	10	−0.5	−0.6	12	3398	− 69	0.4	0.8
1925					1929					1933				
1	3404	− 38	0.0	−0.6	1	3362	32	−1.4	0.1	1	3375	8	0.7	2.0
2	3477	− 65	−0.3	1.4	2	3373	24	−1.5	−1.0	2	3413	− 50	1.2	−0.2
3	3471	− 71	−0.4	−1.5	3	3484	− 54	−1.4	−0.3	3	3410	− 17	0.7	−0.4
4	3427	8	−0.4	1.6	4	3436	− 43	−0.1	−1.3	4	3418	− 12	0.8	1.2
5	3361	10	−0.5	0.4	5	3413	− 43	−0.6	0.2	5	3344	9	0.8	1.0
6	3304	7	−0.3	−0.3	6	3396	− 79	−0.4	0.1	6	3286	11	1.0	0.5
7	3326	− 9	−1.2	1.6	7	3324	− 32	−0.1	0.8	7	3328	− 40	0.3	1.5
8	3357	− 69	−1.1	1.1	8	3310	− 76	1.2	−0.6	8	3211	35	0.1	−0.2
9	3292	− 49	−0.1	0.2	9	3292	− 44	−1.2	−0.5	9	3245	− 18	−0.4	−0.7
10	3266	− 30	0.2	−1.1	10	3242	− 2	0.8	−0.2	10	3306	− 72	0.4	−0.5
11	3307	− 27	0.6	−0.4	11	3284	31	−0.8	0.8	11	3303	− 14	−0.1	0.3
12	3424	−136	0.4	−2.9	12	3374	− 31	0.1	1.0	12	3262	− 14	1.5	−4.2
1926					1930					1934				
1	3489	−118	0.5	0.3	1	3408	− 2	−0.9	2.1	1	3357	− 32	1.7	−1.4
2	3487	− 90	1.3	1.8	2	3405	− 5	−0.5	0.8	2	3366	− 54	2.4	−2.9
3	3478	− 86	1.1	−0.5	3	3480	− 43	−0.1	2.2	3	3411	− 52	1.1	−2.5
4	3464	−106	0.5	−3.3	4	3432	− 38	0.3	−0.2	4	3464	− 55	0.3	0.9
5	3412	− 31	0.0	1.7	5	3456	− 91	0.1	1.1	5	3445	− 68	−0.7	1.3
6	3351	− 20	−0.2	1.3	6	3281	14	0.4	−0.2	6	3345	− 34	−0.4	0.2
7	3333	− 42	−1.2	−0.4	7	3212	38	0.5	−1.1	7	3289	− 2	−1.7	−0.6
8	3223	− 57	−0.8	−0.2	8	3315	− 77	0.9	0.0	8	3362	− 68	−2.7	0.6
9	3354	−124	0.1	−0.6	9	3237	7	−0.1	0.9	9	3293	− 37	−2.1	−0.2
10	3329	− 89	−0.3	−1.4	10	3237	5	−0.4	−0.7	10	3278	11	−1.1	2.1
11	3371	− 80	0.2	0.1	11	3318	− 30	−0.6	−0.3	11	3283	− 7	−0.5	−1.2
12	3332	− 36	0.5	−2.1	12	3376	− 32	−1.2	0.4	12	3353	− 12	1.2	2.6
1927					1931					1935				
1	3465	−108	1.0	−0.3	1	3372	15	−1.2	0.4	1	3340	− 9	1.8	−1.0
2	3459	− 65	0.1	0.4	2	3386	35	−1.6	1.4	2	3383	− 10	2.0	1.4
3	3470	− 38	0.1	1.4	3	3376	38	−0.6	−0.1	3	3356	10	1.8	−1.3
4	3451	− 27	0.1	1.2	4	3446	− 54	−0.8	−1.5	4	3423	− 15	0.3	0.8
5	3438	− 87	0.3	−0.3	5	3405	− 30	−1.1	0.7	5	3335	11	0.1	−0.3
6	3442	−121	−0.4	0.4	6	3395	−103	0.8	0.0	6	3291	39	−1.7	0.3
7	3371	− 90	0.0	0.1	7	3320	− 37	−2.1	−1.3	7	3209	96	−2.5	0.0
8	3352	−113	0.3	−1.1	8	3361	− 80	−0.7	1.7	8	3214	57	−2.8	−1.2
9	3291	− 49	−1.5	−1.3	9	3325	− 74	−0.9	0.6	9	3184	60	−1.6	−0.6
10	3273	− 15	0.0	0.3	10	3279	− 15	−0.5	0.8	10	3255	− 26	0.1	−1.2
11	3313	− 51	0.2	−2.1	11	3300	12	−0.5	1.5	11	3316	− 2	0.0	2.2
12	3436	−149	0.3	−3.0	12	3361	− 32	−0.4	0.1	12	3360	− 42	0.0	−0.4

(to be continued)

(continued)

Date	L	$\Delta L''$	$\Delta T'$	$\Delta b'$	Date	L	$\Delta L''$	$\Delta T'$	$\Delta b'$	Date	L	$\Delta L''$	$\Delta T'$	$\Delta b'$
1936	mm				1940	mm				1944	mm			
1	3353	− 15	0.0	−2.1	1	3279	41	−0.8	−4.3	1	3341	88	0.0	4.2
2	3363	− 7	0.0	−2.0	2	3374	27	−0.5	0.9	2	3293	125	0.0	2.1
3	3440	3	−0.6	2.1	3	3364	16	−0.2	−2.3	3	3299	116	−0.5	−0.5
4	3376	25	−1.1	−1.1	4	3379	12	−0.2	−1.0	4	3429	− 19	−1.2	−1.1
5	3349	29	−0.2	1.8	5	3392	− 40	−0.4	−0.3	5	3400	− 36	−0.9	−0.5
6	3268	69	−1.4	1.1	6	3312	1	−0.1	0.7	6	3374	− 67	−0.5	−0.8
7	3268	5	−0.7	−0.6	7	3215	68	−0.2	0.6	7	3327	− 41	−0.7	−0.2
8	3286	− 26	−1.3	−0.5	8	3220	61	−0.5	1.8	8	3217	37	0.0	−0.3
9	3235	2	−0.2	0.2	9	3174	56	−0.6	−0.7	9	3169	37	0.5	−2.0
10	3257	− 25	−0.2	−1.3	10	3251	7	0.0	0.9	10	3243	− 5	0.1	−1.1
11	3259	46	−0.5	1.0	11	3263	27	0.6	1.0	11	3240	37	−0.1	−1.3
12	3317	2	0.8	0.5	12	3243	46	0.4	−2.2	12	3265	90	−0.6	1.2
1937					1941					1945				
1	3372	00	0.9	1.4	1	3298	94	0.5	1.9	1	3289	69	−1.0	−2.2
2	3421	− 47	1.3	0.7	2	3377	116	0.1	2.9	2	3338	65	−1.8	−0.8
3	3371	− 4	1.2	−1.8	3	3317	100	0.5	0.4	3	3453	− 9	−0.1	2.1
4	3352	74	0.6	2.5	4	3341	59	−0.2	−0.9	4	3432	− 27	−0.2	−0.5
5	3214	106	−1.0	−1.4	5	3289	67	−0.4	−0.6	5	3324	18	−1.1	−2.4
6	3228	132	−2.0	2.3	6	3327	− 23	−0.7	−1.2	6	3260	71	−1.4	0.1
7	3184	125	−2.8	0.0	7	3157	95	−1.5	−3.6	7	3369	− 78	−2.2	−1.4
8	3195	116	−2.0	2.6	8	3096	140	−1.4	−3.1	8	3339	− 40	−0.9	2.2
9	3199	44	−0.5	0.4	9	3186	47	−1.5	−2.0	9				
10	3237	20	−0.2	0.6	10	3266	1	−0.1	0.9	10				
11	3235	35	0.3	−0.8	11	3250	42	0.1	0.0	11				
12	3293	− 28	0.3	−4.1	12	3292	46	0.1	0.6	12				
1938					1942					1947				
1	3337	89	0.8	1.6	1	3276	129	−0.1	2.3	1				
2	3378	− 33	0.3	−2.5	2	3291	141	−0.9	2.3	2				
3	3402	9	0.3	0.6	3	3388	37	0.9	1.7	3	3442	− 15	−1.1	−0.2
4	3329	37	−0.1	−2.7	4	3413	5	0.5	1.2	4	3476	− 59	−0.ε	−2.3
5	3285	56	−0.1	0.8	5	3291	49	−0.1	−1.5	5	3381	− 31	0.9	0.2
6	3216	71	0.0	−1.2	6	3221	72	0.1	−1.3	6	3386	− 77	0.5	0.4
7	3220	77	−1.8	0.1	7	3132	136	0.1	−0.8	7	3376	−104	1.5	0.9
8	3214	67	−0.7	1.7	8	3136	65	0.9	−3.1	8	3322	− 66	2.0	1.9
9	3112	111	−0.6	−1.2	9	3215	− 13	1.1	−1.6	9	3168	36	1.0	−1.7
10	3172	70	−0.1	−0.4	10	3192	42	0.8	−0.7	10	3164	80	0.4	−1.1
11	3216	57	−0.3	−1.2	11	3242	57	0.1	0.5	11	3287	− 16	1.1	−0.5
12	3269	41	−0.2	−1.2	12	3293	46	−0.3	0.3	16	3322	− 15	0.7	−1.5
1939					1943					1948				
1	3308	82	−0.8	1.0	1	3364	61	−0.4	3.5	1	3334	− 11	2.6	−1.2
2	3387	14	−0.5	0.9	2	3364	69	−0.4	3.1	2	3290	51	3.3	−0.4
3	3360	33	−0.3	−1.4	3	3344	63	−0.5	−1.1	3	3437	− 32	2.4	1.7
4	3391	36	−0.8	1.1	4	3385	46	−1.0	0.7	4	3386	− 5	2.2	0.1
5	3286	65	−0.5	−0.5	5	3289	60	−0.4	−1.1	5	3427	− 68	1.2	0.6
6	3272	36	−1.0	−0.6	6	3291	8	−0.2	−1.1	6	3262	− 6	2.3	−1.8
7	3273	− 5	0.9	0.6	7	3300	− 33	−1.2	−2.2	7	3230	− 13	3.5	−1.2
8	3214	39	−0.3	−0.1	8	3253	− 10	0.2	−0.9	8	3208	− 4	2.5	−1.6
9	3207	11	0.0	−0.9	9	3217	− 26	2.1	−1.5	9	3172	34	1.9	−0.6
10	3195	47	0.5	0.2	10	3229	− 2	0.8	−1.2	10	3206	18	1.7	−0.5
11	3246	29	0.5	−0.2	11	3309	− 2	0.1	1.1	11	3289	1	1.6	1.4
12	3303	49	−0.3	1.9	12	3325	146	0.1	3.3	12	3301	12	2.3	1.0

(to be continued)

(continued)

Date	L	$\Delta L''$	$\Delta T'$	$\Delta b'$
1949	mm			
1	3286	42	2.6	−0.8
2	3268	37	2.1	−4.3
3	3367	6	2.0	−1.2
4	3314	49	1.8	−1.7
5	3314	7	1.9	−1.0
6	3314	− 15	0.8	−0.1
7	3262	− 15	2.2	−0.3
8	3200	27	2.7	0.4
9	3244	− 12	0.3	−0.2
10	3171	61	0.5	−1.1
11	3189	116	0.5	1.4
12	3211	83	0.5	−2.3
1950				
1	3278	− 20	0.9	−2.3
2	3385	− 14	1.1	−0.3
3	3411	− 11	0.9	−0.2
4	3321	45	2.7	−0.5
5	3255	49	3.8	−0.3
6	3166	80	3.7	−1.2
7	3248	24	4.0	−0.2
8	3148	17	3.5	−2.9
9	3146	55	2.3	−0.5
10	3185	68	0.6	0.5
11	3178	101	0.9	−0.9
12	3293	− 4	0.6	−2.4
1951				
1	3326	27	2.2	0.6
2	3311	47	2.3	−0.1
3	3333	29	2.8	−1.2
4	3352	30	1.7	−0.1
5	3260	53	2.5	−1.0
6	3168	84	2.0	−2.4
7	3266	− 15	1.6	−0.6
8	3197	28	2.7	0.2
9	3054	173	0.0	−0.9
10	3118	106	0.9	−1.2
11	3231	30	0.5	−1.9
12	3318	− 13	−0.3	−2.3
1952				
1	3328	− 5	2.4	−1.4
2	3279	75	3.1	0.4
3	3251	110	1.9	−2.2
4	3335	38	2.3	−0.4
5	3321	11	1.7	−0.3
6	3261	− 8	2.2	−2.2
7	3211	13	1.8	−2.4
8	3099	100	3.3	−1.1
9	3104	90	1.5	−1.9
10	3146	84	0.9	−0.9
11	3133	126	2.0	−0.5
12	3203	82	3.1	−0.4

Date	L	$\Delta L''$	$\Delta T'$	$\Delta b'$
1953	mm			
1	3203	110	2.9	−1.7
2	3333	63	2.4	2.9
3	3340	14	2.3	−2.3
4	3316	63	2.2	−0.1
5	3302	23	2.5	−0.1
6	3191	63	2.0	−2.3
7	3210	32	1.3	−1.6
8	3087	124	1.7	−1.8
9	3090	122	0.8	−1.2
10	3116	118	1.0	−0.5
11	3142	125	1.4	−0.5
12	3242	70	2.7	1.3
1954				
1	3164	147	3.9	−0.8
2	3315	22	3.6	−0.4
3	3330	52	2.5	0.0
4	3315	25	3.3	−1.9
5	3313	5	1.8	−1.3
6	3167	112	1.2	−1.2
7	3160	83	0.7	−2.1
8	3138	63	2.9	−1.4
9	3190	− 9	1.9	−2.5
10	3061	169	0.5	−1.3
11	3169	91	1.2	−1.3
12	3210	79	2.3	−0.8
1955				
1	3226	105	2.4	−0.8
2	3257	39	2.9	−4.2
3	3289	102	2.2	0.4
4	3320	49	2.3	−0.7
5	3184	102	2.8	−2.7
6	3215	39	2.5	−1.8
7	3173	38	3.3	−1.9
8	3136	65	2.5	−1.8
9	3162	64	0.4	−0.6
10	3208	44	0.2	0.1
11	3197	149	−0.2	3.8
12	3164	136	2.3	0.0
1956				
1	3259	94	2.4	0.8
2	3313	69	1.1	0.5
3	3360	93	1.7	4.6
4	3337	80	1.5	2.1
5	3345	35	1.2	2.8
6	3179	110	2.6	1.0
7	3117	129	2.2	−0.4
8	3185	41	1.6	−0.8
9	3217	31	0.6	1.3
10	3160	106	0.7	1.6
11	3149	137	1.4	0.9
12	3266	27	2.0	0.8

Date	L	$\Delta L''$	$\Delta T'$	$\Delta b'$
1957	mm			
1	3289	65	2.2	0.7
2	3275	84	3.3	1.0
3	3286	71	2.4	−2.0
4	3325	56	3.0	0.9
5	3286	60	1.3	0.3
6	3184	110	1.2	−0.1
7	3167	79	1.1	−1.4
8	3238	− 2	2.2	0.5
9	3187	16	2.6	−0.1
10	3164	110	0.1	−1.4
11	3222	73	1.1	1.3
12	3221	58	2.4	−1.5
1958				
1	3357	19	1.0	1.1
2	3348	17	2.2	0.3
3	3333	42	2.2	−0.8
4	3385	6	2.0	0.7
5	3237	93	2.4	0.2
6	3193	84	2.9	0.4
7	3216	31	1.5	−1.0
8	3229	24	1.2	0.8
9	3146	65	0.2	−1.9
10	3220	60	−0.4	1.6
11	3180	128	0.4	1.5
12	3247	54	1.6	−0.7
1959				
1	3262	86	1.1	−0.8
2	3358	44	2.4	3.3
3	3336	75	2.4	2.1
4	3289	79	3.1	0.0
5	3299	30	2.5	0.2
6	3149	134	1.9	−0.2
7	3125	113	1.9	−1.3
8	3112	99	1.6	−2.0
9	3099	151	1.1	−0.9
10				
11				
12				

Table 3, b. Hososima

Date	L	$\Delta L''$	$\Delta T'$	$\Delta b'$	Date	L	$\Delta L''$	$\Delta T'$	$\Delta b'$	Date	L	$\Delta L''$	$\Delta T'$	$\Delta b'$
1900	mm				1904	mm				1908	mm			
1	2572	140	0.5	0.3	1	2716	40	−1.1	1.2	1	2685	51	−0.5	0.6
2	2714	12	0.4	0.9	2	2701	31	−0.3	0.3	2	2651	57	0.7	0.0
3	2734	− 37	0.7	−0.1	3	2660	48	−0.4	−0.9	3	2667	50	0.1	0.5
4	2602	57	0.7	−0.1	4	2667	10	0.6	1.1	4	2678	− 30	1.3	0.0
5	2579	21	−0.3	−1.5	5	2617	− 26	0.8	−0.5	5	2663	− 52	−0.1	−0.4
6	2535	26	−0.1	1.4	6	2552	− 6	0.2	0.7	6	2586	− 70	0.9	−0.5
7	2448	65	−0.6	−0.9	7	2422	67	0.8	−0.6	7	2404	107	−0.7	−1.2
8	2331	105	0.2	−0.7	8	2415	1	1.3	−0.5	8	2457	− 4	−0.6	−0.7
9	2441	13	0.1	−0.1	9	2423	15	0.4	−0.8	9	2430	44	−0.8	0.1
10	2552	− 48	−0.2	0.9	10	2477	− 1	0.2	−0.6	10	2556	− 72	−0.4	−0.9
11	2540	41	−0.2	−0.6	11	2630	− 58	0.6	−0.1	11	2605	− 7	−1.1	−0.7
12	2649	24	0.4	0.7	12	2627	50	−0.1	0.2	12	2671	64	−3.1	0.1
1901					1905					1909				
1	2657	34	0.9	−0.7	1	2592	40	2.3	−3.0	1	2681	62	−2.0	−1.1
2	2703	28	−1.3	−1.3	2	2683	− 23	2.3	−1.2	2	2764	− 10	−2.0	−0.6
3	2718	3	0.6	1.6	3	2663	38	1.0	0.7	3	2689	50	−1.0	0.5
4	2570	74	0.9	−0.9	4	2618	22	1.5	−0.3	4	2580	75	0.2	−1.1
5	2533	67	0.3	−0.6	5	2591	17	0.9	0.9	5	2639	− 25	0.0	0.0
6	2502	20	−0.1	−1.6	6	2559	− 71	1.6	−1.6	6	2610	− 99	0.7	−1.2
7	2442	71	−0.8	−1.2	7	2548	− 66	1.5	−0.1	7	2507	10	1.0	1.8
8	2403	51	0.5	1.1	8	2452	10	−0.7	−0.1	8	2370	39	−0.3	−3.5
9	2475	− 19	−0.5	−0.8	9	2456	25	0.0	1.8	9	2447	− 1	−0.3	−1.3
10	2455	3	0.2	−2.0	10	2457	38	−0.4	−0.1	10	2554	− 55	−0.5	0.1
11	2640	− 40	−0.8	−0.1	11	2510	102	−0.8	0.8	11	2583	1	−0.3	−0.5
12	2724	− 13	−1.7	0.4	12	2543	98	1.1	−0.7	12	2812	−111	−0.7	1.1
1902					1906					1910				
1	2736	− 5	−1.0	−0.5	1	2668	42	0.6	0.4	1	2707	− 2	−0.8	−2.2
2	2788	− 32	0.3	3.0	2	2693	13	−0.9	−2.6	2	2807	− 88	−0.5	−1.0
3	2703	− 10	0.6	−0.5	3	2640	63	0.4	−0.1	3	2764	− 25	−1.4	−0.1
4	2683	1	−0.5	0.0	4	2642	12	1.0	0.0	4	2725	− 23	−1.4	0.0
5	2556	53	−0.3	−0.8	5	2552	52	0.3	−0.3	5	2611	− 12	0.5	−0.4
6	2494	22	0.0	−1.9	6	2552	− 20	−0.1	−0.8	6	2644	−102	−0.4	−0.5
7	2531	− 18	−0.4	−0.6	7	2461	− 11	0.4	−4.2	7	2534	− 40	0.1	−1.3
8	2460	0.0	−0.9	−0.5	8	2493	− 57	0.3	−0.5	8	2355	73	0.0	−1.6
9	2395	60	−1.3	−2.1	9	2470	− 12	0.5	0.8	9	2494	− 36	−0.5	−0.7
10	2494	27	−1.0	1.0	10	2448	− 1	1.8	−0.4	10	2466	24	−0.5	−0.6
11	2581	16	−0.4	0.3	11	2510	79	0.2	0.6	11	2651	− 64	−0.3	−0.3
12	2532	89	0.9	−2.5	12	2772	− 95	−0.9	−1.0	12	2737	− 37	−0.8	0.9
1903					1907					1911				
1	2681	40	−0.7	−0.8	1	2696	18	−0.4	−0.9	1	2765	− 43	−0.8	−0.9
2	2701	21	0.9	1.4	2	2679	48	−0.4	−0.2	2	2828	− 64	−0.4	2.6
3	2620	60	0.8	−1.8	3	2700	11	−0.3	−0.5	3	2651	47	0.1	−0.9
4	2641	28	0.4	0.2	4	2742	− 60	−0.4	0.0	4	2680	− 10	−0.2	−0.6
5	2587	40	0.0	1.0	5	2687	− 95	0.3	−1.2	5	2684	− 56	0.1	1.2
6	2468	55	−0.1	−1.5	6	2590	− 44	−0.7	−0.7	6	2563	− 29	0.0	−0.5
7	2426	102	−0.9	−0.2	7	2522	− 17	−0.9	−2.0	7	2508	8	0.1	0.4
8	2489	− 18	0.4	2.3	8	2444	− 28	0.0	−2.5	8	2474	− 28	−0.5	−1.0
9	2455	− 2	0.6	0.6	9	2394	− 14	−0.3	−1.9	9	2435	37	0.0	1.1
10	2427	42	0.2	−1.1	10	2447	42	−0.5	−0.7	10	2482	7	−0.5	−0.7
11	2596	4	−0.8	−0.1	11	2565	63	−2.3	−0.2	11	2606	− 16	−0.1	0.2
12	2638	67	−1.6	0.1	12	2736	3	−3.0	0.5	12	2688	7	−0.1	1.6

(to be continued)

(continued)

Date	L	$\Delta L''$	$\Delta T'$	$\Delta b'$	Date	L	$\Delta L''$	$\Delta T'$	$\Delta b'$	Date	L	$\Delta L''$	$\Delta T'$	$\Delta b'$
1912	mm				1916	mm				1920	mm			
1	2720	18	−0.6	0.6	1	2702	5	1.0	0.7	1	2788	− 79	−0.3	−1.1
2	2661	44	0.3	−0.8	2	2675	− 1	0.6	−2.7	2	2765	− 25	0.1	1.5
3	2688	9	0.2	−0.8	3	2723	− 4	−0.4	−0.1	3	2757	− 22	−0.3	1.3
4	2726	− 39	0.1	1.1	4	2654	31	−0.1	0.7	4	2760	− 81	0.2	0.7
5	2641	− 33	−0.1	−0.6	5	2572	27	0.6	−0.2	5	2572	− 16	0.2	−4.1
6	2513	− 50	2.2	−2.6	6	2508	5	1.2	−0.3	6	2589	− 64	0.0	−1.2
7	2571	− 61	−0.2	−0.5	7	2492	4	0.7	−0.2	7	2521	− 5	0.1	0.4
8	2458	8	−0.7	0.2	8	2325	75	0.6	−2.8	8	2508	− 98	−0.3	−3.4
9	2416	33	−0.2	−0.9	9	2490	− 38	0.9	1.0	9	2480	− 15	−0.6	−0.3
10	2546	− 41	−0.8	0.1	10	2455	26	0.7	0.5	10	2500	− 31	0.4	−0.8
11	2639	− 37	−0.6	0.4	11	2430	138	0.8	−0.1	11	2626	− 61	0.8	−0.3
12	2585	111	0.1	2.0	12	2577	68	1.2	−0.2	12	2657	12	0.3	0.2
1913					1917					1921				
1	2666	67	−0.2	0.8	1	2648	85	−0.6	0.2	1	2785	− 57	−0.1	0.6
2	2667	63	−0.4	0.0	2	2748	− 24	−1.0	−1.4	2	2759	− 49	0.0	−0.9
3	2722	− 5	−0.4	−0.2	3	2813	− 85	−0.4	0.6	3	2770	− 69	0.1	−0.7
4	2664	− 10	0.6	−0.6	4	2758	−106	−0.1	−1.8	4	2698	− 24	0.3	0.4
5	2604	− 16	0.5	−1.2	5	2706	− 90	−0.5	−0.6	5	2627	− 42	0.4	−1.6
6	2491	30	0.0	−1.5	6	2580	− 24	−0.9	−0.2	6	2549	− 10	−0.9	−1.5
7	2492	17	−0.4	−0.9	7	2590	− 78	0.7	1.0	7	2508	2	0.7	0.8
8	2351	66	0.1	−2.3	8	2474	− 36	0.2	−0.5	8	2462	− 48	0.7	−1.6
9	2473	7	−0.9	0.4	9	2529	− 67	0.3	0.8	9	2524	− 61	−0.3	0.0
10	2485	− 19	−0.1	−1.8	10	2524	− 56	0.0	−1.5	10	2497	− 2	−0.7	−0.5
11	2621	− 18	0.0	1.4	11	2662	− 50	−0.8	0.7	11	2715	− 82	−1.8	0.9
12	2763	− 80	−0.1	0.7	12	2767	− 95	−1.0	−1.5	12	2718	− 17	−0.8	1.0
1914					1918					1922				
1	2816	− 85	−0.4	0.4	1	2852	−111	−1.3	−0.2	1	2790	− 36	−1.4	0.6
2	2718	9	−0.3	−0.1	2	2786	− 24	−0.6	2.1	2	2719	0.0	−0.5	−1.0
3	2613	81	0.3	−0.9	3	2815	− 99	0·2	0.6	3	2750	− 25	−0.6	0.1
4	2656	9	−0.2	−1.0	4	2777	−100	0.2	0.5	4	2674	14	−0.7	0.0
5	2586	29	0.2	0.4	5	2713	− 92	−0.4	−0.1	5	2575	5	1.5	−0.3
6	2539	5	−0.3	−0.2	6	2684	−118	−0.9	0.5	6	2508	− 6	1.3	−1.0
7	2496	− 31	2.0	−0.6	7	2579	− 89	−0.5	−2.5	7	2487	37	−0.1	0.7
8	2445	− 30	0.8	−1.4	8	2539	− 69	−0.6	0.7	8	2461	− 25	0.7	0.1
9	2404	42	0.8	0.4	9	2420	21	0.0	−1.2	9	2450	26	0.1	1.6
10	2498	16	−0.5	1.2	10	2507	− 12	0.0	0.5	10	2537	− 54	0.0	−0.4
11	2558	28	0.0	0.1	11	2560	37	0.2	1.2	11	2568	29	−0.6	0.0
12	2677	− 6	−0.2	−0.4	12	2669	5	0.1	0.3	12	2715	− 26	−0.8	0.1
1915					1919					1923				
1	2666	61	−0.1	0.5	1	2702	10	−0.1	−0.6	1	2757	11	−1.6	1.4
2	2620	62	0.6	−2.1	2	2662	63	−0.3	−0.2	2	2704	12	−0.9	−1.8
3	2635	72	0.1	−0.2	3	2646	35	1.1	−0.7	3	2744	− 48	−0.9	−2.6
4	2597	73	0.2	0.0	4	2647	20	0.1	−0.4	4	2634	43	0.0	0.2
5	2604	7	−0.3	−0.7	5	2642	− 27	0.5	0.8	5	2555	40	0.2	−1.1
6	2489	69	−0.3	0.8	6	2517	− 14	0.6	−2.0	6	2478	55	0.0	−0.6
7	2532	− 21	0.1	0.0	7	2524	− 4	0.0	0.5	7	2522	− 6	−0.3	−0.2
8	2403	− 26	0.9	−4.1	8	2483	− 29	−0.6	−0.5	8	2508	− 60	0.4	0.5
9	2413	8	0.7	−1.6	9	2555	− 93	−0.6	−0.5	9	2381	36	0.2	−2.7
10	2459	− 13	1.0	−1.7	10	2543	− 56	−0.4	−0.7	10	2449	25	0.1	−0.9
11	2534	51	1.0	1.5	11	2596	− 40	1.0	−0.7	11	2640	− 48	−0.8	−0.7
12	2689	− 33	0.6	−0.3	11	2730	− 57	0.3	0.5	12	2715	− 6	−0.8	1.6

(to be continued)

(continued)

Date	L	$\Delta L''$	$\Delta T'$	$\Delta b'$	Date	L	$\Delta L''$	$\Delta T'$	$\Delta b'$	Date	L	$\Delta L''$	$\Delta T'$	$\Delta b'$
1924	mm				1928	mm				1932	mm			
1	2762	− 34	−0.3	0.3	1	2772	− 65	0.8	0.4	1	2694	12	2.1	2.3
2	2750	− 36	−0.5	−1.4	2	2741	0.0	−0.1	1.3	2	2615	74	1.9	0.1
3	2758	9	−1.5	1.9	3	2671	11	0.9	−0.9	3	2740	− 49	1.1	0.1
4	2667	17	−0.5	0.0	4	2614	41	0.8	−0.2	4	2727	− 62	−0.1	−0.8
5	2613	− 20	0.0	−1.6	5	2617	− 28	1.0	−0.4	5	2630	− 2	−0.3	0.6
6	2475	55	0.1	−0.7	6	2519	− 3	0.6	−1.0	6	2438	109	0.1	0.6
7	2516	27	0.5	3.0	7	2505	− 8	0.6	−0.3	7	2501	15	0.1	0.4
8	2340	72	0.2	−2.5	8	2316	54	1.2	−4.2	8	2419	13	−0.4	−1.9
9	2492	− 17	−0.5	0.6	9	2441	− 7	1.1	−0.1	9	2466	− 18	0.2	−0.4
10	2450	48	−0.4	0.1	10	2502	− 38	1.0	−0.3	10	2501	− 17	0.4	0.3
11	2569	47	−1.8	−0.4	11	2602	− 32	1.2	0.7	11	2562	− 2	0.9	−0.5
12	2626	82	−1.4	0.6	12	2626	17	1.8	0.5	12	2612	37	1.6	0.7
1925					1929					1933				
1	2641	70	−0.3	−1.0	1	2718	− 29	1.5	0.1	1	2687	13	1.7	1.2
2	2694	59	−0.8	1.1	2	2744	− 47	1.2	−0.1	2	2722	− 13	0.4	−0.4
3	2763	− 32	−0.9	0.1	3	2761	− 70	1.1	0.1	3	2652	49	0.1	−0.7
4	2692	30	−1.1	2.0	4	2727	− 62	0.3	−0.2	4	2648	28	0.1	0.3
5	2577	52	−1.1	−0.5	5	2632	− 17	−0.4	−0.5	5	2585	41	0.0	0.9
6	2533	− 1	−0.2	−1.0	6	2546	− 28	0.4	−1.1	6	2519	5	0.7	−0.2
7	2508	10	0.1	0.5	7	2533	− 11	0.1	0.8	7	2540	− 32	1.0	1.1
8	2440	4	−0.3	−0.8	8	2457	− 23	0.6	−0.2	8	2404	26	0.5	−0.7
9	2365	75	0.0	−1.3	9	2455	− 9	0.2	−0.5	9	2426	12	0.9	−0.1
10	2440	39	0.0	−0.7	10	2453	33	−0.8	−1.4	10	2492	− 26	1.1	0.0
11	2539	49	−0.4	−0.4	11	2596	62	−3.2	0.7	11	2521	45	0.8	−0.2
12	2746	− 55	−0.9	0.1	12	2653	10	0.2	−0.4	12	2534	68	1.8	−2.6
1926					1930					1934				
1	2819	− 59	−1.3	1.2	1	2760	− 34	0.0	0.6	1	2722	− 19	0.9	0.2
2	2784	− 25	−0.6	1.9	2	2700	26	−0.6	−0.6	2	2687	9	0.5	−1.2
3	2743	− 10	−0.7	0.5	3	2692	41	−0.7	0.5	3	2732	− 42	0.0	−1.7
4	2731	− 32	−2.1	−1.3	4	2646	31	−0.8	−1.0	4	2702	− 7	−0.7	0.5
5	2596	45	−1.2	0.2	5	2677	− 20	−1.7	0.7	5	2677	− 41	−0.5	0.9
6	2514	40	−0.2	0.7	6	2550	134	−2.2	−0.1	6	2604	− 49	−0.3	0.6
7	2568	− 40	−0.2	0.8	7	2464	60	−1.1	−0.8	7	2574	− 78	1.0	0.2
8	2513	− 52	0.2	1.2	8	2463	− 1	−1.3	−1.0	8	2635	−175	0.5	1.6
9	2455	− 19	1.2	0.2	9	2530	− 19	−1.8	1.4	9	2539	− 93	0.3	−0.4
10	2563	− 82	−0.1	−0.7	10	2474	38	−2.0	−1.2	10	2521	− 13	0.0	1.5
11	2641	− 35	−0.6	0.7	11	2598	24	−1.3	0.8	11	2661	− 81	0.2	−0.1
12	2661	24	−0.7	−0.1	12	2685	6	−0.5	0.7	12	2646	17	0.9	0.7
1927					1931					1935				
1	2723	4	−0.9	−0.7	1	2718	− 14	−0.2	−1.4	1	2711	− 42	1.6	−1.3
2	2752	− 19	−0.5	0.1	2	2713	12	−0.7	−0.8	2	2723	− 13	0.8	0.3
3	2716	6	−0.3	0.3	3	2691	42	−1.1	−0.1	3	2700	− 13	0.5	−1.1
4	2678	− 11	0.7	0.5	4	2697	10	−1.9	−0.4	4	2654	26	−0.5	−0.3
5	2653	− 41	0.1	0.0	5	2608	51	−2.0	0.4	5	2568	45	−0.1	−0.2
6	2609	− 69	0.1	0.1	6	2550	127	−2.6	−1.2	6	2547	− 9	0.0	−0.2
7	2599	− 97	1.2	1.0	7	2588	− 20	−3.3	−0.8	7	2503	14	−0.2	0.0
8	2506	− 69	0.4	−0.3	8	2499	− 13	−1.3	0.8	8	2454	− 38	0.2	−2.2
9	2479	− 31	−0.3	−1.1	9	2508	− 57	0.5	0.3	9	2355	77	−0.2	−2.2
10	2452	41	0.3	0.8	10	2475	4	0.9	0.7	10	2558	− 91	0.4	−0.7
11	2566	− 32	1.5	−1.6	11	2493	60	1.6	0.0	11	2602	− 18	0.8	1.1
12	2711	− 94	2.1	−1.0	12	2599	43	2.1	0.9	12	2696	− 26	0.7	0.9

(to be continued)

(continued)

Date	L	$\Delta L''$	$\Delta T'$	$\Delta b'$	Date	L	$\Delta L''$	$\Delta T'$	$\Delta b'$	Date	L	$\Delta L''$	$\Delta T'$	$\Delta b'$
1936	mm				1940	mm				1944	mm			
1	2762	− 58	0.7	0.0	1	2756	− 96	1.3	−2.4	1	2668	28	1.9	1.2
2	2689	7	0.2	−1.7	2	2819	− 79	0.0	1.4	2	2639	54	1.5	0.1
3	2764	− 6	−0.2	3.2	3	2751	− 67	0.0	−2.1	3	2615	72	0.4	−1.3
4	2665	7	−0.7	−1.3	4	2735	− 52	−0.5	−0.1	4	2619	39	0.4	−0.6
5	2639	13	−1.3	0.9	5	2727	− 94	−0.6	0.5	5	2639	− 30	0.4	0.2
6	2538	32	−0.9	0.8	6	2661	− 93	−0.7	1.0	6	2592	− 50	0.1	0.2
7	2563	− 23	−1.4	−0.1	7	2554	− 16	0.0	1.9	7	2516	4	0.7	1.2
8	2607	−108	−2.1	0.6	8	2499	− 29	0.0	1.6	8	2488	− 20	−0.1	1.3
9	2471	1	−0.5	0.4	9	2445	− 12	0.3	−1.4	9	2386	56	0.6	−0.2
10	2384	76	0.6	−1.2	10	2515	− 49	1.1	0.0	10	2388	70	1.3	−0.3
11	2505	53	1.8	0.7	11	2586	− 32	1.9	0.5	11	2439	105	1.5	−1.7
12	2614	15	2.2	0.1	12	2647	− 18	2.0	−0.2	12	2564	73	1.9	0.2
1937					1941					1945				
1	2698	− 21	1.9	−0.2	1	2723	− 42	1.6	−1.1	1	2679	39	0.1	−1.1
2	2759	− 83	1.7	−0.9	2	2752	− 42	1.2	0.9	2	2624	102	−0.6	−0.4
3	2712	− 62	1.6	−2.3	3	2673	14	1.0	−0.4	3	2677	60	0.1	2.3
4	2662	16	0.8	1.5	4	2705	− 46	0.5	−0.4	4	2656	21	0.6	0.1
5	2566	25	0.6	−0.8	5	2621	4	−0.5	0.1	5	2540	56	−0.3	−1.6
6	2483	67	0.0	0.7	6	2591	− 37	−0.8	−0.2	6	2443	102	−0.4	−0.1
7	2444	34	1.1	−1.0	7	2426	88	−1.5	−2.2	7	2432	71	−0.2	−0.9
8	2493	− 6	0.3	3.3	8	2332	117	−1.0	−1.5	8	2419	95	−0.7	1.7
9	2497	− 33	0.1	0.7	9	2418	62	−1.3	−0.2	9	2465	18	0.4	0.5
10	2495	− 13	0.3	0.0	10	2577	− 55	−0.6	1.7	10	2435	60	0.4	−0.8
11	2583	− 51	2.1	−0.9	11	2571	7	0.1	−0.4	11	2523	57	0.7	−0.5
12	2729	− 92	1.0	−1.1	12	2598	47	1.1	−0.4	12	2636	32	0.0	−1.1
1938					1942					1946				
1	2751	− 34	1.1	1.6	1	2662	29	0.9	−0.7	1	2696	23	−0.2	0.0
2	2792	− 95	0.5	−1.1	2	2593	127	0.3	0.3	2	2609	101	0.6	0.2
3	2734	− 36	0.3	−0.6	3	2651	63	0.5	0.9	3	2579	143	0.1	1.1
4	2702	− 52	0.3	−1.4	4	2694	2	0.0	1.7	4	2677	14	−0.6	0.6
5	2604	5	0.4	0.2	5	2521	100	−0.9	−0.8	5	2391	172	3.1	−0.3
6	2563	− 52	0.6	−1.4	6	2427	140	−1.5	−0.3	6	2347	225	−0.1	1.1
7	2561	− 45	−0.1	0.0	7	2380	151	−0.5	0.6	7	2391	68	1.3	−1.9
8	2433	12	−0.6	−1.2	8	2327	102	0.0	−1.5	8	2362	68	0.3	−1.0
9	2440	10	0.0	−0.5	9	2447	19	−0.3	0.2	9	2406	54	0.0	0.2
10	2482	− 34	1.2	−1.2	10	2458	11	1.0	0.1	10	2471	28	0.0	0.8
11	2636	− 67	1.0	0.3	11	2587	− 35	1.7	0.1	11	2491	17	0.9	−1.0
12	2711	− 36	0.2	0.5	12	2659	− 26	1.5	−0.7	12	2630	30	−0.2	−1.0
1939					1943					1947				
1	2710	17	0.0	0.7	1	2770	− 71	1.3	0.5	1	2692	9	−0.1	−1.2
2	2803	− 78	0.5	1.0	2	2697	22	0.9	1.1	2	2721	− 27	0.8	−0.7
3	2737	− 53	0.2	−1.8	3	2613	52	1.1	−1.9	3	2740	− 33	0.7	0.9
4	2676	3	0.0	0.4	4	2630	52	0.4	1.2	4	2719	— 32	−1.0	−0.3
5	2619	− 8	−0.1	−0.4	5	2558	39	0.6	−0.4	5	2544	86	−1.0	−0.1
6	2525	13	−0.3	−0.7	6	2527	19	−0.3	−0.1	6	2504	64	−1.5	0.0
7	2497	26	−0.1	0.6	7	2448	58	−0.2	−0.8	7	2534	8	−1.0	0.9
8	2415	2	0.6	−1.5	8	2460	8	−0.5	0.7	8	2521	− 5	−1.3	3.3
9	2505	− 59	0.5	−0.1	9	2480	− 15	−0.2	0.3	9	2427	10	0.4	−0.7
10	2462	11	0.4	−0.5	10	2483	− 10	0.5	−0.4	10	2384	94	0.8	0.7
11	2560	− 3	1.2	−0.3	11	2616	− 44	1.1	0.7	11	2546	15	1.3	1.2
12	2636	46	1.5	3.0	12	2629	45	1.4	2.3	12	2632	19	1.1	1.2

(to be continued)

(continued)

Date	L	$\Delta L''$	$\Delta T'$	$\Delta b'$	Date	L	$\Delta L''$	$\Delta T'$	$\Delta b'$	Date	L	$\Delta L''$	$\Delta T'$	$\Delta b'$
1948	mm				1952	mm				1956	mm			
1	2672	32	0.3	−0.4	1	2699	20	−0.8	−1.1	1	2618	82	−0.1	−1.5
2	2649	49	0.7	−0.5	2	2657	92	−0.9	0.7	2	2670	50	−0.5	−0.9
3	2598	110	0.6	0.8	3	2602	98	−0.2	−1.2	3	2683	75	−0.5	2.7
4	2618	36	0.9	0.1	4	2584	75	0.1	−1.0	4	2598	95	−0.1	1.3
5	2606	14	0.1	0.8	5	2570	38	−0.5	−1.2	5	2499	173	−1.0	2.9
6	2469	58	0.1	−0.7	6	2488	45	−1.4	−2.7	6	2453	147	−0.4	3.9
7	2433	93	−0.2	0.9	7	2387	94	−0.9	−3.8	7	2447	108	0.2	3.5
8	2376	69	−0.4	−0.7	8	2349	64	−0.2	−3.0	8	2429	19	0.3	0.4
9	2384	40	2.1	0.9	9	2353	69	−0.1	−2.8	9	2450	20	−0.2	0.7
10	2329	133	1.2	0.1	10	2419	39	0.2	−1.9	10	2420	76	0.2	0.9
11	2536	30	1.7	1.4	11	2410	115	1.0	−3.0	11	2470	139	0.0	2.0
12	2614	24	1.6	0.1	12	2563	102	0.6	0.4	12	2661	28	1.0	2.8
1949					1953					1957				
1	2598	77	1.7	−0.7	1	2633	84	−0.7	−1.1	1	2644	41	1.7	0.1
2	2632	29	1.4	−2.5	2	2649	119	−0.9	2.1	2	2615	96	1.8	1.8
3	2668	22	1.1	0.0	3	2597	75	0.3	−2.6	3	2596	100	1.2	0.6
4	2572	117	−0.4	0.5	4	2589	86	−0.5	−0.7	4	2672	− 5	1.3	1.4
5	2559	58	−0.2	−0.1	5	2462	131	−0.6	−2.5	5	2530	63	1.3	0.4
6	2445	80	−0.2	−1.5	6	2446	63	−1.1	−4.1	6	2461	54	1.3	0.0
7	2467	71	−1.0	0.4	7	2503	− 9	−1.1	−3.1	7	2477	19	0.7	−0.2
8	2279	161	−0.2	−1.0	8	2374	13	0.4	−4.1	8	2422	15	0.4	−0.3
9	2398	63	0.2	0.6	9	2277	121	0.3	−4.0	9	2338	138	−1.0	−0.1
10	2368	112	0.2	−0.3	10	2403	17	0.7	−4.1	10	2507	− 20	0.2	0.2
11	2418	162	0.6	0.5	11	2513	20	0.9	−2.6	11	2566	24	0.5	1.1
12	2541	78	1.9	−1.2	12	2596	45	1.0	−0.8	12	2622	33	0.7	−0.2
1950					1954					1958				
1	2639	37	0.1	−3.0	1	2554	79	1.0	−4.9	1	2737	− 38	1.9	1.4
2	2697	19	−0.1	−0.6	2	2652	26	0.7	−2.3	2	2667	15	2.1	0.1
3	2649	48	0.6	−0.2	3	2688	65	0.4	3.7	3	2629	40	2.4	0.3
4	2493	146	1.5	−0.4	4	2638	58	0.5	2.4	4	2723	− 69	1.8	1.1
5	2433	134	2.0	−0.6	5	2628	31	−0.6	2.5	5	2592	22	0.4	0.6
6	2430	84	1.1	−0.4	6	2430	153	−0.8	2.0	6	2429	88	1.4	0.3
7	2401	83	0.4	−1.6	7	2459	116	−1.2	2.9	7	2487	− 16	2.3	0.2
8	2238	167	0.5	−2.6	8	2434	83	−0.7	4.1	8	2523	56	0.2	1.7
9	2288	157	0.2	−0.6	9	2407	65	−0.1	1.0	9	2417	26	0.7	0.0
10	2423	62	−0.1	−0.4	10	2342	198	−0.5	3.2	10	2496	7	0.3	1.6
11	2404	160	0.0	−1.6	11	2490	176	−2.9	1.8	11	2524	39	1.7	0.9
12	2615	42	−1.1	−2.8	12	2567	139	0.5	3.3	12	2675	− 39	1.9	0.1
1951					1955					1959				
1	2666	34	−0.1	−1.5	1	2669	91	−0.1	3.0	1	2740	− 45	1.3	0.2
2	2613	95	−0.3	−1.5	2	2626	88	−0.2	−0.9	2	2717	− 35	2.7	1.0
3	2612	87	0.1	−0.8	3	2635	105	0.4	2.7	3	2718	− 27	2 7	2.4
4	2590	98	−0.5	0.9	4	2603	103	0.2	2.7	4	2657	− 22	2.0	0.0
5	2493	126	−0.6	−0.5	5	2546	97	−0.2	1.9	5	2587	5	1.5	0.6
6	2396	142	−0.6	−1.1	6	2523	84	−0.8	3.8	6	2467	26	2.1	−0.5
7	2410	96	−1.1	−2.2	7	2492	76	−0.5	3.4	7	2445	40	1.6	0.3
8	2429	10	−0.6	−1.7	8	2460	59	−0.6	4.4	8	2474	− 61	1.0	−1.2
9	2308	131	−0.9	−2.7	9	2478	35	−0.4	3.6	9	2516	− 70	0.2	−0.5
10	2384	74	0.0	−2.3	10	2483	20	0.3	1.6	10				
11	2598	− 43	0.0	−2.3	11	2610	22	−0.5	2.8	11				
12	2685	− 19	−1.3	−2.4	12	2585	84	0.5	0.5	12				

Table 3, c. Wazima

Date	L	$\Delta L''$	$\Delta T'$	$\Delta b'$	Date	L	$\Delta L''$	$\Delta T'$	$\Delta b'$	Date	L	$\Delta L''$	$\Delta T'$	$\Delta b'$
1900	mm				1904	mm				1908	mm			
1	1891	108	−0.7	1.3	1	2038	− 36	−1.2	0.9	1	2009	1	−1.2	1.5
2	1994	66	−0.9	0.9	2	2071	− 16	−0.6	0.9	2	2042	1	−0.6	0.0
3	2011	45	−0.3	−0.5	3	2126	− 56	−0.3	0.5	3	2055	15	−0.4	0.4
4	2028	39	−0.2	1.1	4	2121	− 50	0.1	1.8	4	2116	− 34	−1.0	1.2
5	1921	28	−0.2	−2.1	5	2041	− 70	−0.5	−0.8	5	2001	− 23	−0.8	−0.7
6	1976	− 74	0.1	1.7	6	1854	15	0.7	−0.1	6	1879	− 5	−0.3	−1.0
7	1827	− 31	0.0	−1.3	7	1795	0.0	1.4	0.4	7	1825	− 2	−1.4	−1.0
8	1742	11	−0.5	0.1	8	1741	− 9	0.8	0.1	8	1779	− 20	−1.2	−0.4
9	1838	− 50	0.7	0.7	9	1752	28	−0.3	−1.2	9	1819	2	−1.5	0.4
10	1869	− 6	−0.1	1.0	10	1851	− 2	−0.5	−0.5	10	1921	− 67	−0.6	−0.3
11	1910	− 45	0.0	0.0	11	1841	16	−1.1	−2.0	11	1863	− 7	−1.4	−2.4
12	1930	− 12	0.2	0.9	12	1931	− 20	−0.3	−0.2	12	1998	− 59	−1.0	1.0
1901					1905					1909				
1	2040	− 66	0.7	1.2	1	1974	− 54	1.8	−1.5	1	2033	− 37	−0.9	0.8
2	2000	− 25	0.5	−3.8	2	2074	− 65	0.5	−1.2	2	2045	− 18	−0.9	−1.6
3	2108	− 41	0.5	1.3	3	2218	−119	0.0	3.1	3	2111	− 20	−0.8	1.5
4	2111	− 53	0.4	1.2	4	2091	− 23	−0.5	0.8	4	2029	15	−0.4	−0.9
5	2007	− 48	0.5	−0.5	5	1993	− 10	−0.3	0.3	5	2011	− 27	−0.6	0.0
6	1925	− 65	0.3	−1.3	6	1915	− 36	−0.8	−1.2	6	1948	− 69	−0.5	−0.8
7	1845	− 35	−0.6	−1.0	7	1852	− 43	0.0	−0.3	7	1866	− 13	−0.4	2.5
8	1699	49	0.5	0.9	8	1734	36	−2.1	−0.7	8	1806	− 97	0.9	−1.5
9	1834	− 63	0.7	−0.6	9	1729	102	−1.4	1.3	9	1815	− 8	−1.2	−0.3
10	1913	− 74	−0.1	−0.8	10	1771	66	0.5	−0.2	10	1869	− 3	−1.0	0.1
11	1885	− 26	−0.6	−1.2	11	1859	33	−0.7	1.1	11	1893	− 22	−1.0	−0.8
12	1919	4	−1.0	−0.2	12	1886	14	0.7	0.2	12	1991	− 67	−0.7	1.0
1902					1906					1910				
1	2025	− 42	−1.0	−0.3	1	1975	5	−0.2	0.5	1	2044	− 84	−0.4	−1.3
2	2129	− 56	−0.6	2.3	2	2034	− 21	−0.3	−1.9	2	2114	− 95	−0.7	−1.8
3	2104	− 52	0.1	−0.3	3	2002	44	−0.3	−1.3	3	2104	− 46	−0.5	−0.6
4	2088	− 37	−0.3	−0.2	4	2003	45	−0.5	−0.7	4	2161	− 78	−1.0	1.3
5	1953	22	−0.6	−0.7	5	1985	1	−0.7	0.0	5	2033	− 31	−1.2	0.6
6	1908	− 43	0.1	−1.1	6	1951	− 63	−0.8	−0.5	6	1919	− 48	−0.4	−1.4
7	1869	− 45	−1.6	−1.1	7	1854	− 77	−0.7	−3.6	7	1859	− 47	−0.7	−1.0
8	1825	− 44	−2.2	0.1	8	1822	− 66	−1.7	−1.2	8	1675	56	−0.8	−2.0
9	1800	− 32	−0.1	−1.9	9	1791	38	−1.8	0.6	9	1860	− 31	−2.1	0.2
10	1873	− 4	−0.3	1.2	10	1944	13	−0.8	−0.3	10	1963	−103	−0.3	0.5
11	1979	− 95	−0.2	1.2	11	1929	− 26	−1.1	1.5	11	1933	−138	3.8	−0.5
12	1957	− 79	0.6	−1.6	12	1936	− 41	−1.1	−2.4	12	1968	− 72	1.0	0.3
1903					1907					1911				
1	2030	− 78	0.6	−0.6	1	2036	− 45	−1.0	0.3	1	2072	− 99	0.6	1.0
2	2103	− 71	1.0	1.2	2	2047	− 13	−0.5	−0.5	2	2132	− 75	1.1	3.2
3	2138	− 86	1.0	0.8	3	2126	− 61	−0.5	−0.1	3	2086	− 42	1.1	0.3
4	2085	− 38	1.1	1.2	4	2144	− 75	−0.5	0.9	4	2061	− 21	0.1	−0.5
5	1983	0.0	0.1	0.8	5	1998	− 63	0.2	−2.7	5	2084	− 69	−0.9	2.0
6	1880	− 18	0.0	−1.5	6	1954	− 81	−0.1	−0.8	6	1911	− 26	−0.5	−0.4
7	1787	44	−1.4	−0.4	7	1886	− 84	0.0	−0.8	7	1794	11	0.7	0.3
8	1772	23	−1.8	1.6	8	1763	− 52	−0.2	−2.7	8	1800	− 69	0.8	0.0
9	1871	− 71	0.1	0.8	9	1885	− 74	−1.4	−0.2	9	1742	54	0.7	1.3
10	1891	16	−3.8	−0.3	10	1871	− 7	−1.0	−0.1	10	1782	24	1.3	−1.6
11	1909	− 34	−0.9	−0.4	11	1901	− 26	−0.4	0.2	11	1869	− 30	1.6	0.0
12	1922	− 9	−0.9	−0.8	12	1929	− 3	−1.3	−0.3	12	1923	− 10	1.2	1.8

(to be continued)

(continued)

Date	L	$\Delta L''$	$\Delta T'$	$\Delta b'$	Date	L	$\Delta L''$	$\Delta T'$	$\Delta b'$	Date	L	$\Delta L''$	$\Delta T'$	$\Delta b'$
1912	mm				1916	mm				1920	mm			
1	2003	− 44	1.4	0.9	1	1994	− 74	4.0	1.2	1	1913	− 42	4.5	−1.9
2	1988	2	1.7	−1.1	2	2017	− 57	2.5	−2.4	2	2031	− 12	2.6	2.2
3	2056	− 31	1.7	−0.4	3	2003	69	−1.9	−1.3	3	2135	− 42	0.3	3.0
4	2043	− 1	0.6	0.2	4	2033	60	−1.7	1.2	4	2108	− 46	0.4	1.5
5	2002	− 38	0.1	−0.6	5	1949	73	−3.1	−0.2	5	2003	− 68	−0.8	−3.2
6	1913	− 51	−0.5	−2.1	6	1845	65	−2.5	−1.0	6	1951	− 40	−2.5	−0.9
7	1871	− 64	−0.4	−1.0	7	1764	99	−3.6	−0.7	7	1816	41	−1.9	1.0
8	1801	− 49	−0.2	0.4	8	1753	− 73	2.1	−2.2	8	1837	− 80	−2.7	−2.4
9	1822	− 18	−1.0	−0.3	9	1795	− 28	2.3	1.1	9	1868	− 29	−2.2	0.9
10	1926	− 55	−0.9	0.6	10	1903	− 65	1.4	1.0	10	1897	− 51	−0.3	−0.5
11	1899	− 6	−1.5	0.2	11	1965	− 96	1.5	2.2	11	1920	− 73	1.1	0.0
12	1892	105	−3.1	2.8	12	1891	− 28	3.0	0.3	12	1942	− 33	1.2	1.5
1913					1917					1921				
1	1949	− 1	2.1	1.0	1	1880	7	3.3	−2.1	1	2012	− 53	1.1	0.5
2	1996	− 14	2.4	−0.8	2	2015	− 78	3.4	−3.0	2	2042	− 43	1.3	−1.0
3	2075	− 68	2.4	−0.8	3	2102	− 95	3.5	0.5	3	2026	5	0.6	−1.3
4	2122	−113	3.1	0.8	4	2093	−148	5.1	−1.5	4	2027	48	−0.5	1.4
5	2013	− 95	2.4	−1.2	5	2002	−119	4.2	−1.7	5	2004	− 16	−1.6	−0.9
6	1861	− 53	3.2	−1.6	6	1941	−110	3.0	−0.1	6	1990	− 57	−3.3	−0.2
7	1811	− 47	2.7	−0.3	7	1857	− 53	1.5	1.2	7	1830	69	−4.2	1.3
8	1734	− 47	1.7	−2.2	8	1745	− 36	1.8	−0.4	8	1810	− 14	−3.8	−0.8
9	1837	− 42	0.3	0.7	9	1774	9	2.0	1.1	9	1826	26	−3.2	0.6
10	1931	−116	0.9	−1.4	10	1870	1	−2.4	−1.0	10	1891	− 30	−1.1	−0.4
11	1967	− 93	0.8	1.7	11	1842	56	−2.5	−0.6	11	1868	2	−1.0	−0.9
12	2001	−110	0.9	−0.2	12	1834	77	−3.1	−3.7	12	1942	− 10	−0.1	1.6
1914					1918					1922				
1	2020	− 79	1.2	−0.7	1	1974	34	−3.5	−1.5	1	2005	− 16	−0.2	1.2
2	2129	−106	1.5	1.1	2	2049	59	−2.5	2.6	2	2025	22	0.3	0.7
3	2043	− 35	2.8	−0.3	3	2077	− 2	−0.1	1.1	3	2046	11	0.3	0.3
4	2062	− 64	2.3	−1.0	4	2065	− 46	2.6	1.0	4	2047	23	−0.7	0.7
5	1993	− 62	3.0	0.5	5	1997	−103	4.4	−0.5	5	2001	1	−1.3	0.5
6	1868	− 41	2.9	−0.5	6	1930	−103	3.1	−0.3	6	1857	29	−1.3	−1.3
7	1757	− 13	3.4	−1.0	7	1838	− 71	1.8	−1.2	7	1763	78	−1.0	0.8
8	1702	− 4	1.8	−1.2	8	1765	− 46	2.3	1.0	8	1710	45	−0.9	−0.3
9	1719	60	1.7	1.2	9	1739	− 4	2.6	−1.0	9	1746	72	−0.3	1.7
10	1785	51	1.0	0.4	10	1805	9	2.8	0.9	10	1816	34	−0.6	−0.6
11	1866	− 35	1.8	−0.3	11	1798	44	2.1	0.9	11	1697	155	0.0	−1.0
12	1925	− 39	0.6	−1.0	12	1915	− 20	2.2	1.7	12	1861	33	−0.3	−1.5
1915					1919					1923				
1	1937	25	0.8	0.4	1	1904	34	2.1	0.2	1	1923	75	−0.4	1.6
2	1997	− 18	1.7	−2.0	2	1959	47	2.1	0.6	2	2013	− 12	0.5	−1.8
3	1986	11	2.5	−1.5	3	1985	7	3.3	−0.8	3	2059	35	0.3	3.1
4	2044	− 39	3.1	0.5	4	1947	25	4.1	−0.7	4	1988	56	−0.3	0.0
5	1969	− 43	2.2	−0.9	5	1954	− 64	5.4	0.4	5	1935	48	−1.1	−0.7
6	1862	− 31	3.3	0.3	6	1839	− 67	5.2	−1.8	6	1843	53	−1.5	−0.8
7	1832	− 91	4.4	0.1	7	1861	−101	4.4	1.5	7	1789	52	−1.9	−0.2
8	1729	−115	4.7	−3.9	8	1795	− 90	2.6	0.3	8	1715	57	−1.4	0.4
9	1827	−103	3.6	−0.6	9	1839	−114	3.7	−0.4	9	1781	− 6	−0.7	−2.1
10	1859	− 49	1.5	−1.0	10	1817	− 57	4.1	−1.5	10	1793	54	−0.7	−1.0
11	1880	1	0.8	2.2	11	1890	− 93	3.7	−0.5	11	1823	52	−1.7	−1.4
12	1930	− 58	2.2	−0.1	12	1930	− 88	3.8	−0.3	12	1908	19	0.0	1.4

(to be continued)

(continued)

Date	L	$\Delta L''$	$\Delta T'$	$\Delta b'$	Date	L	$\Delta L''$	$\Delta T'$	$\Delta b'$	Date	L	$\Delta L''$	$\Delta T'$	$\Delta b'$
1924	mm				1928	mm				1932	mm			
1	1978	− 4	0.2	0.5	1	1736	237	0.4	0.9	1	2033	− 4	−0.9	3.3
2	2004	7	−0.2	−1.9	2	1768	261	0.9	1.0	2	2031	13	−0.7	−0.1
3	2086	4	−0.5	1.8	3	1740	300	0.6	−0.6	3	2072	− 6	−1.3	−1.0
4	2051	8	−0.3	0.4	4	1791	267	−0.1	0.7	4	2041	5	−0.8	−1.2
5	1993	− 24	−1.0	−1.7	5	1781	211	−1.5	−0.4	5	1942	23	1.0	0.6
6	1873	19	−1.0	−0.5	6	1730	180	−2.5	−0.8	6	1868	6	0.9	0.5
7	1805	43	0.4	3.2	7	1703	169	−3.7	0.0	7	1791	7	1.1	0.2
8	1746	− 31	0.7	−1.3	8	1622	155	−4.3	−2.7	8	1738	− 14	2.0	−0.2
9	1894	− 91	−0.3	0.5	9	1708	119	−1.9	0.5	9	1847	− 55	−0.1	−0.1
10	1888	− 19	−0.7	0.7	10	1773	82	−0.3	0.3	10	1818	34	−0.5	−0.3
11	1832	21	−1.3	−2.5	11	1839	35	0.0	0.8	11	1803	61	−0.6	−0.8
12	1939	− 9	−0.8	0.6	12	1806	116	−0.1	1.0	13	1920	30	−0.9	2.0
1925					1929					1933				
1	1974	− 1	−0.5	−0.4	1	1712	272	−0.4	0.5	1	2001	16	−1.5	1.7
2	2058	1	−0.6	1.2	2	1937	87	0.0	−0.7	2	2041	29	−2.4	−0.2
3	2055	5	−1.0	−1.1	3	2039	21	−0.2	−0.1	3	2083	24	−2.9	0.1
4	2061	37	−1.3	2.1	4	2027	22	−0.7	−0.9	4	2073	22	−1.8	1.2
5	1958	29	−1.2	−0.5	5	2010	− 2	−1.9	0.2	5	1945	37	0.0	0.6
6	1894	− 2	−1.6	−1.2	6	1915	− 1	−2.6	−0.8	6	1872	− 10	1.4	0.2
7	1891	− 33	−1.8	1.1	7	1806	64	−2.8	0.8	7	1813	− 33	3.2	1.5
8	1761	− 2	−1.2	−0.3	8	1640	129	−2.2	−0.8	8	1671	23	2.6	−0.5
9	1787	3	−0.2	−0.3	9	1773	48	−2.1	−0.4	9	1709	61	1.3	0.0
10	1868	− 29	0.1	−0.5	10	1899	− 42	−0.8	−0.3	10	1822	22	0.2	−0.1
11	1846	4	0.4	−0.6	11	1876	13	−0.7	0.9	11	1841	41	−0.8	0.3
12	1832	29	1.2	−2.1	12	1916	10	0.7	2.2	12	1825	64	−0.7	−2.4
1926					1930					1934				
1	1949	7	0.9	0.1	1	2049	− 40	−0.4	2.4	1	1917	66	−1.7	−1.1
2	2023	12	1.2	1.7	2	1981	52	0.7	0.9	2	1988	48	−1.9	−2.1
3	2017	19	0.9	−0.5	3	1927	144	0.9	2.1	3	1996	66	−2.4	−2.7
4	2007	17	−0.4	−2.4	4	1898	156	0.2	0.6	4	2093	12	−2.2	1.5
5	1974	34	−1.6	0.6	5	1827	175	−0.9	1.0	5	2012	− 9	−1.0	0.9
6	1913	13	−1.9	1.0	6	1688	232	−2.3	0.0	6	1862	7	0.8	0.0
7	1812	17	−0.9	0.1	7	1642	211	−2.9	−0.6	7	1809	− 13	1.1	0.0
8	1644	112	−0.7	0.0	8	1688	108	−3.6	−0.5	8	1756	6	−0.2	1.1
9	1695	81	0.7	−0.2	9	1794	3	1.1	1.8	9	1739	50	−0.1	−0.3
10	1823	5	−0.3	−1.9	10	1761	66	0.8	−0.6	10	1894	− 7	−0.6	2.2
11	1890	1	−1.0	0.7	11	1721	154	−0.6	0.0	11	1816	61	−1.4	−0.8
12	1844	52	0.1	−0.8	12	1742	215	−1.2	2.1	12	1967	14	−1.4	3.7
1927					1931					1935				
1	1952	− 2	0.8	−0.5	1	1988	8	−1.4	0.2	1	1939	45	−1.5	−0.8
2	1997	33	0.4	0.3	2	2073	8	−2.0	1.1	2	2032	47	−1.9	1.1
3	2004	69	0.1	1.3	3	2039	47	−1.3	0.5	3	2043	24	−1.2	−0.8
4	2040	46	−0.8	1.8	4	2015	48	−1.3	−0.5	4	2053	14	−0.6	0.6
5	1926	74	−1.9	−0.4	5	1952	41	−0.6	0.6	5	1901	54	0.6	−0.7
6	1868	64	−3.2	−0.2	6	1906	− 26	−0.2	−0.4	6	1839	33	1.3	0.8
7	1774	107	−3.8	0.4	7	1876	− 74	0.2	−0.6	7	1778	19	1.2	0.3
8	1729	52	−3.3	−1.2	8	1742	17	0.2	1.4	8	1759	− 43	0.7	−1.2
9	1754	85	−4.0	−1.2	9	1806	− 7	0.2	0.8	9	1775	5	0.0	−0.8
10	1688	185	−1.7	−0.1	10	1860	12	0.1	1.4	10	1821	7	0.4	−1.0
11	1807	46	−0.5	−1.4	11	1863	28	−0.6	1.2	11	1927	− 34	0.1	2.3
12	1831	51	0.5	−1.3	12	1911	25	−0.4	1.5	12	1957	− 33	−0.2	0.9

(to be continued)

(continued)

Date	L	$\Delta L''$	$\Delta T'$	$\Delta b'$	Date	L	$\Delta L''$	$\Delta T'$	$\Delta b'$	Date	L	$\Delta L''$	$\Delta T'$	$\Delta b'$
1936	mm				1940	mm				1944	mm			
1	1932	41	−1.5	−1.7	1	1907	44	−1.5	−3.8	1	1990	24	−1.3	1.6
2	2014	39	−2.5	−1.6	2	2073	14	−1.8	1.4	2	1956	90	−1.7	−1.3
3	2106	28	−2.6	2.5	3	2055	2	−1.5	−2.4	3	1987	61	−1.3	−2.5
4	2068	4	−2.1	−0.9	4	2031	20	−0.8	−1.3	4	2040	23	−1.7	−1.2
5	2026	− 29	−0.5	1.1	5	1991	− 31	0.8	−0.5	5	2014	− 39	−0.2	−0.3
6	1906	− 26	0.6	0.6	6	1887	− 7	0.9	0.5	6	1957	−101	1.3	−0.5
7	1816	− 16	0.7	−0.1	7	1775	50	1.8	1.2	7	1810	− 16	2.1	0.3
8	1746	− 10	0.3	−0.2	8	1723	27	1.2	1.5	8	1726	3	1.7	0.8
9	1736	40	0.9	0.0	9	1897	−105	0.0	−0.4	9	1679	83	1.6	−0.4
10	1750	74	0.4	−1.3	10	1899	− 48	0.5	0.4	10	1831	12	0.4	0.0
11	1802	90	−0.9	0.9	11	1886	− 22	0.9	0.6	11	1848	1	−0.1	−1.5
12	1914	28	−1.1	1.1	12	1869	18	1.0	−0.8	12	1883	16	−0.8	−1.9
1937					1941					1945				
1	2010	7	−1.8	1.2	1	1883	43	0.6	−2.7	1	1974	4	−2.3	−2.4
2	2125	− 66	−1.5	0.0	2	2072	− 12	−0.3	1.5	2	2012	71	−3.2	−0.4
3	2081	− 30	−0.8	−1.6	3	2014	32	−0.1	−1.2	3	2085	42	−2.6	1.4
4	2064	31	−0.9	2.3	4	2027	14	−0.3	−1.1	4	2065	5	−1.4	−0.2
5	1910	52	−0.3	−1.4	5	1962	5	0.6	0.1	5	1941	24	−1.4	−2.6
6	1862	37	0.3	1.6	6	1906	− 31	0.3	−0.3	6	1877	8	−0.8	−0.9
7	1772	7	1.7	−0.5	7	1789	3	0.2	−1.5	7	1812	6	−0.9	−0.9
8	1736	3	2.6	2.8	8	1722	33	−1.2	−0.8	8	1745	22	0.2	1.8
9	1786	− 12	1.6	0.6	9	1815	6	−1.2	0.6	9	1807	− 11	0.5	0.5
10	1826	12	0.9	0.3	10	1892	− 27	0.0	1.1	10	1887	− 35	0.2	0.2
11	1882	− 34	0.4	−0.8	11	1947	− 71	0.0	0.7	11	1818	58	−1.2	−1.0
12	1842	− 57	−0.5	−2.5	12	1937	− 29	0.7	0.7	12	1904	30	−0.7	−2.9
1938					1942					1946				
1	1997	31	−1.8	1.7	1	1913	39	−0.6	−2.3	1	1990	− 12	−2.0	0.1
2	2055	− 3	−2.7	−2.4	2	2011	40	−0.8	0.2	2	2049	18	−1.5	0.4
3	2119	− 25	−1.8	0.0	3	2125	− 40	−0.2	1.7	3	2065	44	−1.5	1.7
4	2004	35	−0.7	−2.1	4	2081	− 14	0.0	1.2	4	2028	30	−0.4	−0.2
5	1919	45	0.9	−0.1	5	2006	− 33	−0.1	−0.4	5	1906	73	−0.3	0.2
6	1875	− 25	1.3	−0.3	6	1861	9	0.4	−0.5	6	1818	93	−1.6	0.1
7	1857	− 44	0.8	0.5	7	1724	56	1.8	−0.4	7	1747	42	0.6	−1.4
8	1782	− 56	1.4	−0.1	8	1711	− 10	1.7	−1.3	8	1678	45	1.0	−0.6
9	1735	22	1.7	−0.9	9	1777	− 4	1.0	−0.2	9	1660	117	0.9	−0.2
10	1863	4	−1.2	−0.5	10	1831	4	0.7	−0.2	10	1816	5	2.7	0.9
11	1858	− 4	0.5	−0.7	11	1866	− 14	−0.3	−1.5	11	1950	−107	1.4	−0.2
12	1901	23	0.0	0.7	12	1920	− 22	−0.6	−1.7	12	1878	65	0.3	−3.3
1939					1943					1947				
1	1972	44	−1.2	1.5	1	2005	− 13	−1.9	−0.8	1	2040	− 44	−0.8	0.7
2	2081	− 4	−1.1	1.5	2	2063	8	−1.9	0.4	2	2002	20	−1.5	−2.7
3	2094	− 33	−0.8	−1.2	3	2085	− 7	−1.8	−0.9	3	2071	4	−1.5	−0.6
4	2068	13	−0.6	1.2	4	2072	19	−1.4	1.3	4	2077	− 31	−1.1	−1.9
5	1983	− 10	0.2	−0.3	5	1998	− 17	−0.3	0.0	5	2033	− 37	−0.9	0.2
6	1815	39	0.8	−1.6	6	1918	− 37	0.2	0.0	6	1923	− 22	−1.2	−0.4
7	1801	− 7	2.3	1.0	7	1889	− 75	0.8	0.9	7	1831	14	−0.2	0.6
8	1776	− 67	2.0	−0.6	8	1824	− 95	1.7	0.8	8	1756	10	0.6	2.1
9	1735	17	2.2	−0.7	9	1818	− 52	1.6	−0.1	9	1719	49	0.9	−0.9
10	1834	− 13	1.8	−0.2	10	1893	− 69	0.9	−0.8	10	1783	52	0.1	0.1
11	1837	13	1.0	−0.3	11	1923	− 50	−0.3	0.1	11	1822	61	−0.6	0.6
12	1909	53	−0.1	3.4	12	1875	67	−0.4	1.8	12	1898	45	−1.6	0.3

(to be continued)

(continued)

Date	L	$\Delta L''$	$\Delta T'$	$\Delta b'$	Date	L	$\Delta L''$	$\Delta T'$	$\Delta b'$	Date	L	$\Delta L''$	$\Delta T'$	$\Delta b'$
1948	mm				1952	mm				1956	mm			
1	1965	27	−2.0	−1.1	1	1978	− 9	−0.4	−0.6	1	1917	24	−0.8	−3.2
2	2017	49	−1.7	0.1	2	2051	− 6	−0.8	−0.1	2	2020	− 1	−1.4	−2.8
3	2113	8	−1.5	1.8	3	2084	− 45	−0.9	−2.6	3	2111	− 21	−0.7	1.5
4	2071	− 9	−0.5	0.2	4	2005	44	0.3	0.4	4	2072	− 9	0.2	1.3
5	1941	31	0.6	0.3	5	2019	− 57	0.9	0.2	5	1974	4	1.5	2.2
6	1875	− 18	0.5	−0.9	6	1879	− 5	1.8	1.7	6	1866	19	2.0	2.7
7	1726	71	1.2	0.0	7	1801	19	1.8	2.8	7	1786	32	1.9	2.7
8	1752	− 34	1.3	−0.7	8	1717	63	1.1	4.1	8	1737	− 25	1.7	−0.3
9	1782	14	0.7	1.0	9	1644	168	1.2	3.1	9	1768	30	0.5	1.1
10	1829	32	0.4	1.2	10	1768	100	0.5	2.1	10	1856	3	0.4	1.4
11	1905	5	−0.3	2.7	11	1836	63	0.2	2.8	11	1822	63	0.0	1.5
12	1924	19	−0.2	2.1	12	1871	68	0.1	2.4	12	1878	49	−0.4	0.8
1949					1953					1957				
1	1863	77	−0.1	−2.4	1	1892	80	−1.0	−1.1	1	2011	− 6	−1.2	1.1
2	1946	41	0.3	−3.9	2	2039	62	−1.7	3.0	2	2034	31	−1.3	0.8
3	2069	− 1	−0.8	−0.2	3	2031	22	−0.4	−0.9	3	2021	38	−1.1	−1.3
4	1979	86	−1.2	−0.3	4	2050	20	0.3	2.0	4	2066	− 8	0.1	0.8
5	1947	15	0.2	−0.7	5	1954	36	1.1	2.6	5	1961	− 17	1.8	0.0
6	1922	− 58	0.6	−0.6	6	1813	70	1.2	1.6	6	1900	− 41	1.7	0.4
7	1880	− 60	0.3	0.9	7	1778	61	1.1	3.3	7	1775	0.0	1.5	−1.0
8	1728	− 22	1.8	−0.6	8	1697	72	1.2	3.4	8	1761	− 29	0.8	0.1
9	1795	− 25	1.7	0.5	9	1714	123	0.1	3.6	9	1845	− 36	−0.4	0.8
10	1790	38	0.7	−0.6	10	1792	87	−0.2	2.1	10	1812	30	0.1	−0.3
11	1843	58	−1.2	1.2	11	1843	64	−0.8	2.2	11	1894	− 13	0.3	1.6
12	1833	89	−1.5	−0.9	12	1930	32	−0.4	3.5	12	1872	26	0.5	−0.2
1950					1954					1958				
1	1936	27	−2.0	−3.0	1	1940	39	−0.6	−0.1	1	1999	− 15	−0.6	0.3
2	2068	− 25	−0.9	−0.4	2	2046	6	−0.6	0.7	2	2052	− 6	−0.6	0.2
3	2065	− 3	−0.8	−0.7	3	2095	1	−0.1	2.7	3	2050	− 2	−0.2	−1.0
4	2050	8	0.0	0.7	4	2057	− 2	1.4	2.2	4	2100	− 53	0.6	0.6
5	1915	24	1.7	−0.5	5	2019	− 47	1.7	2.0	5	1996	− 61	2.3	−0.1
6	1862	− 2	0.4	−1.1	6	1909	11	0.0	2.9	6	1841	− 1	2.8	0.3
7	1799	− 25	0.4	−2.4	7	1851	− 7	0.1	2.5	7	1783	− 28	3.2	−0.4
8	1708	− 36	0.8	−4.5	8	1811	− 21	0.4	4.0	8	1768	− 37	1.5	0.9
9	1740	26	0.6	−1.1	9	1851	− 49	0.6	1.6	9	1764	14	0.6	−0.2
10	1863	− 24	0.3	−0.3	10	1824	63	−0.1	2.8	10	1875	− 4	−0.4	1.2
11	1850	− 7	0.1	−1.5	11	1885	16	−0.2	2.5	11	1938	− 42	−0.8	1.4
12	1902	− 27	−0.1	−2.7	12	1877	63	0.1	2.5	12	1944	− 32	0.1	0.4
1951					1955					1959				
1	2020	− 41	−0.8	−0.3	1	1934	60	−1.0	0.5	1	1976	− 11	−0.7	−1.3
2	2049	− 31	−0.9	−2.3	2	1958	41	−0.5	−3.2	2	2155	− 78	−0.2	3.1
3	2039	1	−0.3	−1.7	3	2104	− 7	−0.1	2.8	3	2124	− 51	0.4	1.7
4	2040	2	0.1	−0.4	4	2072	2	0.7	2.8	4	2006	8	1.4	−0.9
5	1923	11	1.1	−1.7	5	1946	43	0.0	1.1	5	1986	− 53	2.3	−0.2
6	1774	52	1.6	−2.3	6	1867	1	2.6	2.2	6	1837	− 6	2.4	−0.8
7	1780	− 16	1.2	−2.2	7	1759	33	4.0	3.4	7	1696	71	2.1	−0.8
8	1720	− 32	2.1	−1.6	8	1748	8	2.4	3.9	8	1738	− 33	0.6	−2.2
9	1601	154	1.2	−1.2	9	1842	− 19	0.8	3.4	9	1669	114	0.2	−0.4
10	1786	17	1.3	−1.8	10	1979	−115	−0.2	1.0	10				
11	1831	− 4	0.7	−2.0	11	1903	− 8	−0.6	1.5	11				
12	1905	− 19	0.4	−1.2	12	1879	17	0.1	−0.8	12				

Table 3, d. Osyoro

Date	L	$\Delta L''$	$\Delta T'$	$\Delta b'$	Date	L	$\Delta L''$	$\Delta T'$	$\Delta b'$	Date	L	$\Delta L''$	$\Delta T'$	$\Delta b'$
1906	mm				1910	mm				1914	mm			
1	1658	− 25		0.8	1	1698	− 73	0.9	1.0	1	1644	− 34	0.1	−0.8
2	1696	− 31		0.2	2	1653	− 47	0.7	−3.6	2	1691	− 6	0.8	2.4
3	1646	7		−1.2	3	1682	− 38	0.2	−1.7	3	1647	16	1.1	0.5
4	1631	8		−1.0	4	1741	− 68	0.6	2.1	4	1649	− 1	0.4	0.0
5	1612	− 21		0.0	5	1629	− 25	0.2	1.1	5	1589	− 16	1.7	0.1
6	1623	− 66	0.0	1.4	6	1565	− 61	0.9	−1.9	6	1557	− 39	0.5	−1.1
7	1550	− 81	0.7	−0.8	7	1541	− 52	0.3	0.3	7	1458	0.0	0.5	−1.8
8	1537	−100	1.2	−0.3	8	1494	− 32	−0.1	0.5	8	1450	− 1	0.1	−0.3
9	1526	− 36	0.0	0.3	9	1514	− 32	0.0	−0.3	9	1473	26	0.3	1.2
10	1578	− 28	−0.2	0.7	10	1645	− 71	0.6	3.2	10	1512	27	0.4	0.3
11	1610	− 26	−0.9	1.7	11	1629	− 84	−0.1	−0.6	11	1551	8	−0.4	0.2
12	1613	− 73	−0.2	−3.0	12	1641	− 40	−1.3	0.6	12	1582	− 7	−1.1	−1.1
1907					1911					1915				
1	1669	− 10	1.1	3.7	1	1739	− 59	−1.9	2.8	1	1601	63	−1.6	1.8
2	1692	− 26	0.7	0.9	2	1788	− 68	−1.9	2.8	2	1621	32	−0.4	−1.0
3	1733	− 64	0.5	0.5	3	1657	58	−1.9	2.0	3	1590	49	0.7	−1.6
4	1718	− 49	0.8	2.0	4	1710	− 37	−1.8	0.1	4	1604	50	0.3	0.4
5	1578	− 60	2.4	−3.5	5	1702	− 78	−1.3	1.4	5	1581	17	−0.3	0.3
6	1576	− 43	0.2	−0.3	6	1580	− 38	−1.0	−0.6	6	1509	21	0.1	−0.6
7	1575	− 75	0.1	1.0	7	1506	3	−1.8	0.1	7	1498	− 2	−0.8	−0.1
8	1485	− 70	2.4	−0.9	8	1522	− 26	−3.0	0.6	8	1437	− 17	−0.3	−2.8
9	1576	− 73	0.8	2.0	9	1474	44	−1.8	0.9	9	1513	− 29	1.0	0.7
10	1558	− 15	−0.7	−0.3	10	1549	− 6	−2.6	−1.9	10	1542	− 22	1.3	−0.3
11	1629	− 49	−0.3	1.9	11	1590	− 11	−2.0	0.2	11	1608	− 20	−0.2	2.6
12	1646	− 85	−0.6	−1.8	12	1600	− 3	−0.4	1.1	12	1573	− 9	−0.2	−1.2
1908					1912					1916				
1	1667	7	−0.2	3.5	1	1669	− 36		0.8	1	1598	38	0.7	1.7
2	1678	− 13	0.2	0.4	2	1690	− 32	0.4	0.0	2	1700	− 49	0.5	−0.4
3	1704	− 18	−0.3	1.1	3	1695	− 34	0.3	−0.3	3	1739	− 99	−0.2	−2.3
4	1747	− 66	0.6	2.7	4	1666	− 28	−0.3	−1.3	4	1673	7	−0.5	1.7
5	1672	− 54	−1.7	0.6	5	1641	− 52	0.1	−0.1	5	1574	22	−0.1	0.3
6	1588	− 54	0.0	−0.4	6	1552	− 32	0.6	−0.9	6	1530	− 13	1.3	−0.5
7	1537	− 37	−0.4	0.6	7	1519	− 53	0.6	−1.1	7	1495	− 16	1.6	0.7
8	1513	− 72	1.5	0.3	8	1522	− 48	0.0	1.5	8	1479	− 56	2.7	−0.1
9	1541	− 45	1.1	1.7	9	1542	− 51	−0.4	0.1	9	1512	− 38	1.0	−0.1
10	1576	− 45	0.7	0.0	10	1618	− 47	−1.5	1.1	10	1609	− 46	−0.2	1.7
11	1585	− 83	−0.4	−4.0	11	1597	− 23	−2.2	−0.2	11	1692	− 86	0.4	4.4
12	1641	− 58	−0.4	0.1	12	1640	20	−2.4	4.2	12	1647	− 48	0.0	1.6
1909					1913					1917				
1	1756	− 59	−1.4	4.5	1	1684	− 13	−1.9	2.1	1	1590	3	0.0	−2.2
2	1695	− 55	−1.0	−2.5	2	1665	− 5	−0.9	−0.9	2	1659	− 57	2.0	−2.9
3	1736	− 29	−0.2	2.8	3	1688	− 33	−1.1	−1.9	3	1776	− 90	0.4	1.7
4	1658	− 7	0.7	0.5	4	1712	− 43	0.3	1.5	4	1727	− 91	−0.1	−1.3
5	1632	− 62	1.8	−0.1	5	1645	− 70	−0.1	−1.3	5	1600	− 47	−0.4	−3.2
6	1599	− 91	2.4	−0.3	6	1551	− 31	−0.5	−1.9	6	1596	− 63	−0.6	−1.0
7	1552	− 56	1.4	1.8	7	1534	− 18	−2.1	0.3	7	1538	− 37	−0.1	0.9
8	1523	− 85	1.4	0.0	8	1459	− 16	−1.6	−2.2	8	1446	− 8	1.0	−0.4
9	1521	− 50	1.3	0.0	9	1561	− 47	−2.6	−0.1	9	1514	− 14	0.4	1.4
10	1599	− 70	−0.3	−1.0	10	1645	− 87	−1.6	0.1	10	1571	− 41	0.0	−0.7
11	1621	− 78	−1.3	−1.8	11	1666	− 73	−2.1	1.3	11	1557	− 25	−0.7	−2.1
12	1642	− 47	−0.9	0.5	12	1711	−118	−1.3	0.0	12	1499	− 5	0.8	−5.7

(to be continued)

(continued)

Date	L	$\Delta L''$	$\Delta T'$	$\Delta b'$	Date	L	$\Delta L''$	$\Delta T'$	$\Delta b'$	Date	L	$\Delta L''$	$\Delta T'$	$\Delta b'$
1918	mm				1922	mm				1926	mm			
1	1556	− 1	1.5	−3.8	1	1700	− 65	−0.2	0.8	1	1618	− 28	1.8	−0.9
2	1682	− 5	1.3	2.3	2	1765	− 55	−0.2	3.5	2	1671	− 16	1.0	0.3
3	1699	− 32	0.5	0.4	3	1736	− 64	−0.8	−0.4	3	1663	− 26	1.0	−1.5
4	1724	− 43	0.4	2.5	4	1690	− 17	0.0	1.6	4	1606	− 8	−0.4	−4.4
5	1632	− 58	0.0	−1.3	5	1607	3	−0.3	1.2	5	1629	− 10	−0.7	1.5
6	1541	− 24	−0.2	−1.8	6	1513	10	0.0	−1.2	6	1554	− 1	−0.8	0.4
7	1484	− 2	−0.5	−0.9	7	1463	32	−0.2	0.4	7	1471	10	−0.8	−1.2
8	1443	21	0.1	0.8	8	1425	8	−0.3	−1.8	8	1406	46	−1.3	−1.3
9	1375	92	0.1	−1.4	9	1449	53	0.0	1.2	9	1450	26	−0.3	−1.0
10	1496	51	0.4	0.9	10	1542	− 19	0.6	−0.7	10	1507	7	−1.3	−3.0
11	1516	54	−0.1	1.3	11	1505	19	1.3	−1.0	11	1562	− 5	−1.4	−0.8
12	1569	28	0.2	1.6	12	1521	− 3	1.1	−3.6	12	1528	21	−0.1	−2.3
1919					1923					1927				
1	1592	35	−0.5	−0.1	1	1652	− 21	0.5	1.1	1	1618	− 18	0.7	−1.0
2	1652	42	−0.7	1.8	2	1695	− 40	0.5	−0.1	2	1679	− 12	−0.8	−0.3
3	1621	32	−0.2	−1.3	3	1709	− 10	0.8	3.0	3	1674	21	−0.9	1.3
4	1587	52	0.1	−0.9	4	1641	12	−0.2	−0.1	4	1705	4	−0.2	4.2
5	1572	20	−0.1	0.0	5	1602	− 2	−0.1	0.6	5	1598	− 12	−0.6	−0.9
6	1500	20	0.2	−1.3	6	1528	12	−0.8	−0.6	6	1561	− 17	−1.4	−0.8
7	1545	− 42	0.9	1.9	7	1493	− 14	−0.6	−1.2	7	1496	− 4	−1.0	−0.5
8	1530	− 64	−0.3	0.7	8	1449	9	−0.8	−0.6	8	1450	− 33	1.5	−1.5
9	1514	− 30	0.1	−0.1	9	1486	− 16	−0.1	−1.3	9	1504	− 20	−0.5	−0.6
10	1526	− 5	0.6	−0.8	10	1530	2	−0.8	−1.8	10	1443	91	0.2	−0.2
11	1557	− 7	0.8	0.5	11	1509	9	0.2	−2.4	11	1498	27	0.6	−1.5
12	1615	− 48	0.2	−0.7	12	1597	− 16	0.9	1.0	12	1570	− 21	0.6	−1.7
1920					1924					1928				
1	1602	− 20	1.0	−2.2	1	1632	1	0.5	1.3	1	1618	14	0.7	1.4
2	1745	− 39	0.8	4.0	2	1647	− 16	−0.2	−2.5	2	1674	− 10	0.3	0.4
3	1814	− 92	1.0	4.9	3	1713	− 12	−1.1	1.6	3	1644	15	0.7	−0.1
4	1763	− 90	1.4	2.8	4	1678	− 1	−0.4	1.6	4	1653	12	1.1	1.9
5	1674	−105	1.0	−0.8	5	1613	− 47	−0.4	−2.2	5	1594	− 12	0.5	−0.2
6	1606	− 87	1.0	−0.7	6	1559	− 11	−0.2	0.5	6	1550	− 12	−0.2	−0.2
7	1517	− 46	2.3	0.7	7	1453	49	0.2	1.2	7	1517	− 2	−0.5	1.6
8	1522	−110	2.4	−1.1	8	1457	− 17	0.9	−0.3	8	1453	7	0.2	0.6
9	1584	− 85	0.7	1.6	9	1535	− 47	−0.1	0.1	9	1494	− 16	1.3	0.5
10	1616	− 68	−1.1	−0.2	10	1577	− 32	−0.2	0.3	10	1551	− 5	1.0	1.4
11	1601	− 41	−0.3	0.4	11	1525	− 22	−0.1	−3.8	11	1555	− 2	0.6	0.6
12	1663	− 42	−0.6	2.7	12	1572	7	0.7	0.7	12	1528	54	−0.4	0.0
1921					1925					1929				
1	1708	− 65	−0.5	1.1	1	1607	6	0.7	−0.1	1	1585	36	−0.6	−0.6
2	1703	− 33	−0.6	−1.1	2	1693	− 15	−0.4	0.9	2	1637	15	−0.7	−1.4
3	1677	− 29	0.2	−1.4	3	1663	− 10	−0.8	−1.8	3	1681	− 23	−0.2	−0.9
4	1678	− 1	0.7	2.5	4	1680	8	−0.4	2.4	4	1652	− 7	−0.1	−0.6
5	1637	− 55	1.2	0.3	5	1589	14	0.1	1.0	5	1647	− 30	−0.4	1.7
6	1621	− 79	0.7	0.8	6	1524	− 2	0.2	−1.1	6	1583	− 37	−0.5	0.1
7	1500	− 5	1.5	1.8	7	1533	− 19	0.0	2.0	7	1489	9	−0.6	0.2
8	1486	− 54	1.3	−0.5	8	1474	− 9	0.1	0.9	8	1382	47	0.0	−1.9
9	1563	− 60	0.8	2.0	9	1504	− 15	0.2	0.4	9	1484	14	−0.7	0.3
10	1594	− 37	1.0	2.2	10	1552	− 33	0.6	−1.0	10	1562	− 18	0.3	0.6
11	1561	− 64	0.9	−3.4	11	1566	− 34	0.6	−1.0	11	1593	− 19	0.4	2.0
12	1632	− 53	0.5	0.5	12	1526	− 4	1.6	−2.9	12	1686	− 47	0.2	4.8

(to be continued)

(continued)

Date	L	$\Delta L''$	$\Delta T'$	$\Delta b'$	Date	L	$\Delta L''$	$\Delta T'$	$\Delta b'$	Date	L	$\Delta L''$	$\Delta T'$	$\Delta b'$
1930	mm				1934	mm				1938	mm			
1	1730	22	−1.3	3.4	1	1601	63	0.9	−1.4	1	1610	93	0.9	1.6
2	1728	52	−0.3	3.4	2	1618	70	0.5	−2.9	2	1650	29	0.7	−3.4
3	1744	44	0.1	3.9	3	1604	78	0.4	−3.9	3	1714	36	0.9	1.7
4	1721	23	0.5	2.1	4	1669	70	−0.4	1.0	4	1587	84	0.5	−3.4
5	1639	31	−0.1	0.6	5	1626	50	−0.3	0.9	5	1567	86	0.8	0.1
6	1533	74	−0.1	−0.2	6	1548	54	0.3	−0.3	6	1531	61	0.5	−0.8
7	1454	104	0.0	0.0	7	1517	51	0.2	0.9	7	1551	28	−0.1	1.5
8	1440	79	0.2	−0.2	8	1509	39	−1.7	0.4	8	1519	27	0.7	2.3
9	1505	71	0.2	1.7	9	1471	99	−0.9	0.3	9	1434	82	1.1	−2.1
10	1499	100	0.9	0.0	10	1604	50	−0.7	2.8	10	1566	48	0.4	0.7
11	1512	94	0.3	−1.0	11	1504	86	0.0	−2.4	11	1566	38	0.6	−0.8
12	1599	19	0.1	2.2	12	1623	82	0.2	4.5	12	1598	46	0.0	−0.3
1931					1935					1939				
1	1661	53	−0.6	1.1	1	1634	47	0.3	−0.6	1	1649	64	−0.9	0.8
2	1719	55	−0.9	2.4	2	1658	77	0.9	1.0	2	1705	43	−1.1	0.3
3	1664	73	−0.4	−0.4	3	1643	60	0.8	−2.0	3	1707	19	−0.3	−1.1
4	1636	70	−0.4	−1.5	4	1677	64	−0.9	1.4	4	1687	65	−0.5	1.8
5	1580	94	−0.9	0.2	5	1561	86	−0.5	−1.5	5	1622	39	0.0	0.0
6	1591	49	−2.0	0.7	6	1509	93	−0.4	−0.8	6	1519	76	0.1	−1.0
7	1566	28	−2.6	0.5	7	1451	109	−0.2	0.0	7	1495	72	−0.1	0.6
8	1465	95	−2.5	0.6	8	1459	74	−1.4	−0.5	8	1507	16	0.0	−0.1
9	1498	85	−1.4	0.8	9	1481	93	−0.9	0.6	9	1482	44	1.3	−1.1
10	1524	86	0.4	0.4	10	1494	79	0.7	−2.1	10	1532	81	0.7	0.9
11	1543	97	0.6	1.9	11	1611	32	1.0	2.4	11	1579	32	0.6	−0.3
12	1608	61	0.3	1.8	12	1637	28	−0.1	1.2	17	1578	93	0.8	2.4
1932					1936					1940				
1	1664	71	1.3	4.4	1	1580	63	0.0	−3.6	1	1579	47	1.0	−4.2
2	1667	72	1.0	1.4	2	1581	106	1.1	−2.5	2	1677	50	0.9	0.4
3	1653	45	1.0	−2.2	3	1681	77	0.4	1.8	3	1653	59	1.0	−1.1
4	1620	77	0.4	−1.6	4	1656	65	−0.3	−0.3	4	1656	53	−0.2	−1.1
5	1542	110	0.4	−0.4	5	1629	57	−0.4	1.6	5	1597	39	0.0	−1.9
6	1527	106	0.7	2.4	6	1543	65	0.0	−0.1	6	1566	51	−0.5	0.2
7	1481	76	0.1	0.0	7	1488	59	−0.1	−0.9	7	1449	102	0.3	−0.3
8	1470	70	−1.1	0.3	8	1458	64	−0.6	−0.7	8	1473	82	−0.6	1.8
9	1555	29	−1.0	1.3	9	1472	85	0.3	0.3	9	1564	10	−0.5	0.9
10	1469	15	−0.1	−2.0	10	1446	127	0.2	−2.6	10	1584	34	0.0	0.7
11	1485	115	0.8	−1.0	11	1490	142	−0.5	0.3	11	1571	48	1.1	0.7
12	1576	85	1.2	2.0	12	1552	117	0.1	1.7	12	1567	50	1.4	−1.1
1933					1937					1941				
1	1682	47	0.4	3.1	1	1652	79	−0.9	2.2	1	1600	− 4	0.9	−1.2
2	1695	49	−1.0	0.1	2	1781	− 18	−0.5	1.9	2	1679	− 8	0.7	1.3
3	1713	58	−1.4	1.3	3	1705	9	−0.4	−2.1	3	1642	2	0.4	−1.5
4	1697	66	−0.6	2.6	4	1657	108	−0.2	3.1	4	1621	17	−0.1	−1.1
5	1608	75	−0.5	1.2	5	1520	123	−0.5	−1.8	5	1600	− 3	0.3	0.7
6	1542	68	0.3	0.3	6	1553	94	−0.4	2.6	6	1610	− 67	−0.6	−0.2
7	1505	58	1.3	1.5	7	1455	82	1.4	−0.4	7	1503	− 9	−0.6	0.0
8	1425	89	1.2	0.2	8	1436	91	1.5	1.5	8	1456	23	−1.9	0.4
9	1436	105	0.5	−0.7	9	1524	46	−0.1	1.0	9	1505	− 4	−0.7	0.6
10	1563	52	−0.3	0.2	10	1534	84	−0.2	0.5	10	1579	− 35	−0.8	−0.3
11	1550	75	−0.3	0.0	11	1590	23	0.7	−0.1	11	1621	− 30	0.1	3.0
12	1564	51	0.3	−2.3	12	1532	63	0.0	−4.0	11	1654	− 63	0.6	1.5

(to be continued)

(continued)

Date	L	$\Delta L''$	$\Delta T'$	$\Delta b'$	Date	L	$\Delta L''$	$\Delta T'$	$\Delta b'$	Date	L	$\Delta L''$	$\Delta T'$	$\Delta b'$
1942	mm				1946	mm				1950	mm			
1	1618	− 25	0.0	−2.2	1	1629	− 2	0.8	0.2	1	1608	− 2	−0.8	−1.9
2	1649	32	−0.2	1.2	2	1678	− 17	0.4	−0.2	2	1696	− 37	0.5	0.2
3	1736	− 37	0.2	2.4	3	1722	− 13	−0.8	1.5	3	1672	− 24	0.7	−0.9
4	1675	− 31	−0.3	−0.8	4	1621	26	−0.2	−1.4	4	1692	− 24	2.0	2.9
5	1620	− 33	−0.3	−0.5	5	1562	16	−1.1	0.9	5	1566	− 12	2.7	−0.5
6	1555	− 26	−0.2	−0.8	6	1500	31	0.3	−1.1	6	1539	− 44	3.1	−0.7
2	1461	10	0.1	−1.1	7	1454	− 13	4.6	−0.3	7	1471	− 46	3.3	−2.0
8	1483	− 20	−1.0	−0.2	8	1399	53	1.3	0.3	8	1432	− 73	4.4	−3.5
9	1499	− 14	−0.7	−0.6	9	1491	− 29	0.9	−1.7	9	1506	− 57	1.5	−1.5
10	1579	− 41	−0.3	−0.3	10	1476	78	0.6	0.9	10	1597	− 45	−0.4	0.7
11	1552	− 46	0.1	−3.3	11				1.0	11	1588	− 35	−0.7	−0.5
11	1624	− 62	0.4	−0.9	12				−4.7	12	1600	− 37	−0.8	−1.8
1943					1947					1951				
1	1649	− 61	0.4	−1.8	1				2.0	1	1654	− 7	−0.7	1.3
2	1686	− 26	0.2	0.0	2	1642	− 2	0.0	−2.5	2	1695	− 18	−0.2	1.0
3	1687	− 22	0.3	0.0	3	1656	7	0.6	−0.7	3	1674	− 13	−0.1	−0.6
4	1682	− 18	−0.1	0.8	4	1619	− 14	0.3	−4.2	4	1663	− 11	0.8	0.6
5	1638	− 40	−0.3	0.3	5	1637	− 40	0.0	−0.4	5	1560	− 14	1.1	−2.5
6	1584	− 47	0.2	0.0	6	1576	− 6	−0.2	1.4	6	1459	26	1.5	−2.8
7	1581	− 71	0.5	2.1	7	1487	11	0.1	0.1	7	1500	− 36	1.2	−0.8
8	1530	− 83	1.3	0.7	8	1491	− 9	−0.3	1.1	8	1407	− 20	2.3	−3.1
9	1548	− 78	1.4	0.1	9	1473	15	−0.1	−0.7	9	1352	98	0.6	−2.2
10	1602	− 75	0.7	−0.3	10	1517	54	−0.8	1.0	10	1503	35	−0.6	−0.6
11	1628	− 76	−0.3	−0.2	11	1495	57	−0.5	−1.2	11	1591	− 45	−0.9	−1.2
12	1602	− 4	−0.6	1.0	12	1551	34	−1.7	−1.7	12	1586	− 4	0.0	0.3
1944					1948					1952				
1	1656	− 4	−0.8	1.6	1	1548	− 19	2.2	−1.5	1	1646	− 20	−0.3	0.1
2	1645	5	−1.2	−1.9	2	1617	33	1.7	−0.3	2	1685	8	−1.2	1.4
3	1675	− 4	−0.2	0.1	3	1692	12	1.3	3.0	3	1716	− 28	−0.8	0.8
4	1688	− 28	−0.6	0.1	4	1660	− 12	2.8	1.2	4	1630	25	0.8	0.9
5	1643	− 58	0.2	−0.3	5	1589	− 19	2.6	−0.2	5	1617	− 54	1.7	−0.7
6	1606	− 84	0.0	−1.3	6	1529	− 30	2.4	−1.8	6	1515	− 37	2.5	−2.5
7	1515	− 44	0.7	−0.6	7	1434	8	2.9	−1.8	7	1473	− 36	2.4	−1.8
8	1475	− 21	0.3	0.3	8	1462	− 59	3.5	−1.7	8	1428	− 15	1.4	−1.9
9	1466	4	0.6	−0.6	9	1466	14	−0.5	−1.7	9	1385	65	0.6	−2.2
10	1601	− 53	0.2	1.0	10	1547	0.0	0.3	0.1	10	1487	40	0.4	−0.6
11	1604	− 61	0.1	−0.6	11	1616	− 41	0.2	1.8	11	1554	43	−1.2	2.4
12	1599	− 49	−0.8	−2.8	12	1624	− 1	0.3	2.8	12	1611	24	−2.4	2.3
1945					1949					1953				
1	1622	5	−1.1	−2.2	1	1548	33	1.3	−2.2	1	1582	36	−0.8	−1.0
2	1561	− 2	−0.7	−2.2	2	1612	− 3	2.1	−2.2	2	1650	50	−0.4	2.6
3	1710	− 14	−1.0	0.4	3	1651	− 6	0.6	−1.2	3	1684	− 26	0.6	−0.2
4	1646	1	−0.3	−1.6	4	1609	34	0.5	−0.2	4	1650	− 3	1.1	0.5
5	1588	− 15	−1.0	−2.5	5	1543	− 1	1.7	−2.3	5	1567	18	1.5	0.8
6	1558	17	−1.7	0.5	6	1591	− 42	2.4	2.8	6	1505	− 1	1.7	−1.2
7	1553	− 20	−2.3	0.7	7	1533	− 63	1.7	0.1	7	1477	− 22	1.3	−1.4
8	1492	− 19	−2.2	1.7	8	1456	− 47	1.8	−1.9	8	1432	− 13	1.0	−1.8
9	1553	− 46	−0.4	0.5	9	1473	− 20	1.1	−1.6	9	1454	18	0.1	−1.0
10	1633	− 53	−0.2	1.9	10	1522	− 7	0.7	−1.2	10	1517	16	0.3	−0.2
11	1577	− 30	0.0	−1.2	11	1555	27	−0.7	1.7	11	1547	7	−1.0	−0.7
12	1558	− 16	−0.4	−3.8	12	1565	17	−0.7	−0.3	12	1596	31	−0.7	3.1

(to be continued)

(continued)

Date	L	$\Delta L''$	$\Delta T'$	$\Delta b'$	Date	L	$\Delta L''$	$\Delta T'$	$\Delta b'$	Date	L	$\Delta L''$	$\Delta T'$	$\Delta b'$
1954	mm				1956	mm				1958	mm			
1	1607	27	0.3	1.1	1	1589	− 34	0.2	−4.9	1	1604	18	1.1	0.9
2	1670	− 4	0.4	0.6	2	1633	− 54	0.4	−6.0	2	1663	20	1.3	2.7
3	1716	− 27	0.3	1.8	3	1700	− 52	1.3	−0.4	3	1609	26	0.8	−1.8
4	1678	− 41	1.4	0.1	4	1605	− 31	1.5	−4.6	4	1658	− 5	0.6	0.6
5	1599	− 47	1.2	−1.9	5	1539	− 41	2.5	−4.9	5	1567	− 7	1.6	−1.0
6	1594	− 44	0.9	1.6	6	1517	− 21	1.8	−1.7	6	1500	2	3.2	−0.1
7	1557	− 76	0.9	0.2	7	1483	− 14	0.6	−0.9	7	1450	− 13	3.6	−0.8
8	1530	− 80	−0.8	−1.0	8	1463	− 19	−0.2	−0.9	8	1472	− 25	1.8	1.0
9	1526	− 65	0.0	−1.9	9	1483	12	0.4	1.0	9	1482	− 2	0.3	−0.2
10	1523	39	−1.2	0.7	10	1539	24	0.4	2.1	10	1584	− 8	−0.7	2.2
11	1562	18	−0.9	1.4	11	1496	78	0.1	1.7	11	1613	− 20	−0.4	2.8
12	1582	26	0.0	2.3	12	1530	41	−0.1	−0.6	12	1635	− 47	−0.1	0.7
1955					1957					1959				
1	1603	30	0.1	0.9	1	1606	20	0.3	0.5	1	1641	− 21	−0.9	−0.9
2	1567	47	1.0	−2.8	2	1647	33	0.7	2.0	2	1739	− 39	1.3	4.0
3	1677	13	0.9	2.4	3	1614	18	0.4	−2.4	3	1746	− 54	1.6	3.2
4	1663	− 21	0.9	0.0	4	1620	13	1.3	−0.3	4	1603	8	1.9	−1.5
5	1598	− 19	1.1	0.0	5	1566	− 4	2.2	−0.3	5	1565	− 13	2.8	−0.6
6	1513	− 24	1.9	−2.2	6	1521	− 3	2.3	0.4	6	1517	− 16	3.5	0.1
7	1446	− 34	3.5	−2.8	7	1470	− 25	3.1	−0.6	7	1405	30	2.7	−1.7
8	1453	− 52	2.6	−1.8	8	1473	− 43	1.7	−0.4	8	1475	− 48	1.1	−1.1
9	1583	−101	0.0	−0.3	9	1498	− 12	−0.3	−0.2	9	1444	22	0.7	−0.9
10	1615	−101	−0.4	−2.2	10	1487	36	−0.6	−1.7	10				
11	1578	− 54	−0.5	−2.6	11	1554	24	−0.2	1.8	11				
12	1531	− 28	0.4	−5.4	12	1577	− 5	−0.1	−0.5	12				

Table 3, e. Kôti

Date	L	$\Delta L''$	$\Delta T'$	$\Delta b'$	Date	L	$\Delta L''$	$\Delta T'$	$\Delta b'$	Date	L	$\Delta L''$	$\Delta T'$	$\Delta b'$
1951	mm				1954	mm				1957	mm			
1	2992	− 36	0.6	−2.2	1	2892	73	0.6	−1.5	1	3004	− 11	0.2	0.1
2	2978	− 35	0.7	−4.3	2	3004	10	0.9	1.3	2	3018	18	−0.5	1.1
3	2995	− 64	0.1	−4.1	3	3033	− 15	0.2	2.6	3	2926	47	−0.2	−1.3
4	2999	−71	−0.2	−3.0	4	3003	− 33	0.2	0.6	4	2964	− 12	0.6	−0.2
5	2872	−42	0.3	−3.7	5	2975	− 80	0.4	1.4	5	2880	− 11	−0.1	−1.3
6	2743	0.0	−0.3	−3.9	6	2780	41	−1.1	0.9	6	2792	− 36	0.6	−1.5
7	2788	− 7	−1.2	−2.7	7	2799	24	−0.9	0.9	7	2790	− 31	0.3	−2.5
8	2734	8	−0.2	−2.2	8	2772	28	−0.1	2.3	8	2798	− 49	−0.6	−2.2
9	2634	70	−0.1	−2.8	9	2738	14	−0.5	0.3	9	2674	71	−1.4	−1.4
10	2752	− 8	0.5	−1.4	10	2675	130	−0.4	2.0	10	2795	− 31	−0.3	−1.0
11	2986	−130	0.1	−1.2	11	2839	35	0.3	0.4	11	2913	− 46	0.0	−0.5
12	3084	−131	−0.7	−0.6	12	2931	33	0.3	1.5	12	2890	29	0.3	−1.9
1952					1955					1958				
1	3115	− 88	−1.0	1.1	1	3006	34	−0.4	2.9	1	3070	− 64	0.5	1.5
2	3039	11	−1.0	1.6	2	2979	22	−0.1	−1.0	2	2999	− 2	0.9	0.0
3	3009	− 13	−0.6	−0.1	3	2965	45	0.1	1.9	3	2940	25	0.6	−0.9
4	2988	− 31	−0.5	−1.3	4	2964	18	0.4	1.8	4	2995	− 38	0.4	−0.1
5	2917	− 39	0.1	−0.3	5	2861	26	0.5	0.9	5	2906	− 40	0.2	−1.2
6	2863	− 49	−0.1	1.7	6	2884	− 77	0.7	2.5	6	2757	5	0.9	−0.7
7	2725	82	−0.1	0.7	7	2850	− 39	0.8	2.2	7	2753	− 2	1.6	−1.4
8	2661	141	0.4	3.1	8	2811	− 14	0.0	2.2	8	2804	− 42	−0.1	−0.6
9	2650	101	1.7	3.1	9	2860	− 88	0.2	2.7	9	2690	9	1.1	−1.6
10	2775	21	−0.1	1.7	10	2847	− 69	−0.1	0.3	10	2829	− 47	−0.1	0.6
11	2752	123	0.1	0.2	11	2959	− 53	−0.6	0.9	11	2798	53	0.7	−0.8
12	2929	39	0.1	1.6	12	2990	− 59	0.0	−1.4	12	2944	− 47	1.4	−1.4
1953					1956					1959				
1	2987	20	−0.4	0.4	1	3010	− 32	0.1	−1.1	1	3079	− 96	0.4	−0.4
2	3026	25	−0.6	2.2	2	3072	− 62	−0.4	−0.7	2	3096	− 79	0.7	1.3
3	3014	− 22	−0.3	0.0	3	3044	− 34	−0.2	1.5	3	3014	− 21	0.8	1.5
4	2937	63	−0.4	2.1	4	2957	8	0.2	0.2	4	2904	36	0.5	−1.2
5	2834	81	−0.6	1.6	5	2870	36	−0.3	1.3	5	2844	− 2	1.5	−1.2
6	2739	77	−0.8	0.9	6	2729	66	1.1	2.1	6	2759	− 21	1.3	−2.0
7	2800	36	−0.6	2.3	7	2742	44	1.5	1.2	7	2730	14	1.3	−2.3
8	2687	103	0.4	2.2	8	2773	− 34	0.2	−2.0	8	2777	− 51	−0.4	−3.7
9	2649	111	0.4	2.1	9	2773	− 23	−0.7	−0.1	9	2807	−115	1.3	−1.9
10	2740	60	0.0	2.1	10	2803	− 25	−0.4	−0.1	10				
11	2860	22	0.6	1.4	11	2799	81	−0.3	0.1	11				
12	2961	4	0.7	2.1	12	2971	1	−0.8	0.7	12				

Table 3, f. Kainan

Date	L	$\Delta L''$	$\Delta T'$	$\Delta b'$	Date	L	$\Delta L''$	$\Delta T'$	$\Delta b'$	Date	L	$\Delta L''$	$\Delta T'$	$\Delta b'$
1953	mm				1956	mm				1959	mm			
1					1	2743	− 63	−0.4	−3.6	1	2741	8	−1.0	0.8
2	2772	23	0.0	2.5	2	2794	− 58	−1.4	−3.6	2	2824	− 46	1.1	2.5
3	2855	−105	0.2	−1.2	3	2789	− 32	−0.4	−1.4	3	2764	27	0.8	2.6
4	2741	16	−1.2	0.3	4	2695	12	0.4	−1.6	4	2677	60	−0.1	0.1
5	2641	− 4	0.3	−0.2	5	2626	17	0.2	0.1	5	2573	66	0.7	0.4
6	2474	31	−0.1	−1.2	6	2482	25	0.6	−0.2	6	2472	44	0.2	0.0
7	2545	− 22	−0.5	−0.2	7	2469	11	1.4	−1.2	7	2423	104	0.1	0.8
8	2462	39	−0.6	−0.8	8	2496	7	0.8	0.9	8	2512	− 11	−0.6	−0.8
9	2410	87	0.4	0.1	9	2521	− 9	1.0	2.0	9	2533	− 21	−0.6	0.1
10	2496	29	0.6	0.0	10	2544	6	0.8	2.1	10				
11	2621	− 2	0.1	0.0	11	2542	102	0.4	2.2	11				
12	2727	− 28	0.4	0.9	12	2726	25	−1.6	2.5	12				
1954					1957									
1	2636	49	1.0	−1.6	1	2743	0.0	−0.2	1.4					
2	2765	− 14	0.7	0.0	2	2753	52	−0.7	2.4					
3	2784	− 4	0.6	1.5	3	2737	57	−1.4	0.2					
4	2759	− 28	0.4	0.2	4	2763	− 8	−0.3	1.2					
5	2728	− 70	−0.3	0.6	5	2633	35	−0.7	0.9					
6	2515	47	−1.4	1.6	6	2507	21	−0.1	0.5					
7	2540	25	−1.5	1.8	7	2475	54	−0.1	0.7					
8	2512	− 13	0.0	−0.3	8	2496	14	0.1	0.7					
9	2510	− 39	0.1	−2.2	9	2421	112	−1.0	1.1					
10	2428	121	−0.7	0.3	10	2548	− 5	0.0	0.7					
11	2600	0.0	0.6	−0.9	11	2647	− 8	0.2	1.6					
12	2677	7	1.0	0.5	12	2613	77	−0.1	−0.4					
1955					1958									
1	2718	24	−0.1	1.4	1	2768	− 9	−0.3	2.4					
2	2713	5	0.7	−2.5	2	2773	− 3	0.6	1.3					
3	2726	44	1.0	0.5	3	2719	52	0.1	0.3					
4	2712	6	0.5	0.0	4	2719	− 3	0.2	1.1					
5	2597	19	0.6	−1.5	5	2626	15	0.6	0.4					
6	2618	−121	0.9	−0.6	6	2463	48	1.1	0.7					
7	2562	− 67	0.7	−0.9	7	2470	45	1.2	1.2					
8	2548	− 51	−0.1	−0.6	8	2512	4	0.8	1.9					
9	2610	−118	−0.3	−1.1	9	2391	102	0.9	0.4					
10	2653	−152	−0.5	−3.1	10	2546	28	−0.5	2.4					
11	2694	− 94	−1.1	−2.9	11	2536	98	0.2	1.2					
12	2720	− 74	0.1	−3.4	12	2662	30	0.5	0.5					

Table 3, g. Asamusi

Date	L	$\Delta L''$	$\Delta T'$	$\Delta b'$	Date	L	$\Delta L''$	$\Delta T'$	$\Delta b'$	Date	L	$\Delta L''$	$\Delta T'$	$\Delta b'$
1954	mm				1956	mm				1958	mm			
1					1	2908	− 9	0.6	−2.3	1	2948	− 9	0.2	0.4
2					2	2952	− 11	0.0	−2.0	2	2999	− 23	0.2	0.9
3					3	3062	− 29	0.0	1.8	3	2970	13	0.0	−2.0
4					4	2997	13	−0.1	−0.8	4	3027	− 29	0.3	−1.0
5					5	2932	44	−0.3	0.2	5	2946	− 20	0.1	−1.0
6	2972	− 32	−0.8	2.0	6	2870	27	0.7	0.3	6	2870	1	0.3	−2.1
7	2929	− 39	−1.3	1.7	7	2846	8	0.3	0.6	7	2813	− 22	1.1	−3.3
8	2866	− 12	−1.2	2.2	8	2792	− 20	0.4	−2.3	8	2802	− 25	0.7	−1.6
9	2872	− 12	−0.8	0.9	9	2816	15	0.2	−0.2	9	2795	17	−0.3	−2.2
10	2850	51	−0.5	2.2	10	2881	− 7	0.4	1.1	10	2909	− 30	−0.4	0.6
11	2900	6	−0.4	1.0	11	2851	32	0.2	−0.1	11	2927	− 35	−0.1	0.3
12	2933	− 21	0.2	2.5	12	2847	35	−0.8	−0.8	12	2943	4	0.1	0.3
1955					1957					1959				
1	2939	13	−0.2	0.9	1	2953	8	−0.6	1.2	1	2961	− 32	−0.1	−0.7
2	2914	37	0.2	−1.0	2	3004	− 3	−0.3	2.3	2	3112	− 95	0.8	4.6
3	3046	3	0.3	3.3	3	2956	− 90	−0.2	−3.0	3	3094	− 74	0.7	1.6
4	3031	− 5	0.1	0.9	4	3005	− 4	−0.2	−1.3	4	2972	1	0.7	−2.4
5	2955	28	−1.0	0.1	5	2928	− 4	0.0	−1.2	5	2960	− 46	0.6	−1.4
6	2881	25	−0.4	−0.2	6	2888	− 16	0.4	−1.9	6	2899	− 32	0.5	−2.2
7	2794	63	0.6	1.1	7	2831	− 29	0.4	−3.2	7	2775	14	0.5	−4.1
8	2776	42	1.3	2.1	8	2800	− 25	0.5	−2.0	8	2787	− 38	0.9	−3.5
9	2853	− 25	2.1	1.5	9	2807	2	0.0	−2.1	9	2759	25	0.6	−3.4
10	2914	− 59	0.5	−0.2	10	2816	15	−0.4	−3.0	10				
11	2907	− 24	0.1	−0.2	11	2889	− 10	0.0	−0.6	11				
12	2871	− 10	0.2	−1.4	12	2879	− 11	0.5	−0.5	12				

Table 3, h. Kasiwazaki

Date	L	$\Delta L''$	$\Delta T'$	$\Delta b'$	Date	L	$\Delta L''$	$\Delta T'$	$\Delta b'$	Date	L	$\Delta L''$	$\Delta T'$	$\Delta b'$
1955	mm				1957	mm				1959	mm			
1					1	2615	− 4	0.0	1.1	1	2573	12	0.1	−0.7
2					2	2645	16	−0.4	0.8	2	2758	− 93	1.2	3.0
3					3	2625	38	−0.8	−1.5	3	2722	− 46	1.3	1.9
4					4	2687	− 9	−0.6	0.3	4	2613	26	0.6	−1.3
5					5	2581	20	−0.5	−0.4	5	2593	− 9	0.1	−0.9
6	2510	− 6	0.8	0.6	6	2525	− 27	−0.5	−1.4	6	2469	2	0.3	−2.4
7	2405	7	2.7	2.8	7	2418	− 19	−0.2	−1.6	7	2327	56	1.2	−1.1
8	2382	− 13	2.8	2.1	8	2388	− 31	1.0	−0.9	8	2347	− 25	1.1	−3.5
9	2480	− 19	0.5	1.4	9	2460	− 20	−0.1	−1.0	9	2326	84	1.1	−1.8
10	2559	− 60	−0.2	0.3	10	2435	46	−0.1	−1.0	10				
11	2525	3	−1.6	1.0	11	2509	− 10	0.4	1.1	11				
12	2552	− 26	−1.5	−0.8	12	2440	37	1.9	−0.5	12				
1956					1958									
1	2519	54	−0.7	−2.6	1	2655	− 52	0.7	1.4					
2	2622	− 13	−0.6	−3.3	2	2666	− 32	0.9	0.3					
3	2732	− 44	0.2	1.5	3	2655	5	0.7	0.0					
4	2698	− 44	0.5	−0.2	4	2701	− 36	0.0	0.0					
5	2616	− 6	0.3	1.3	5	2598	− 15	0.2	−0.9					
6	2490	32	−0.2	0.8	6	2480	1	0.7	−1.2					
7	2428	− 17	−0.6	−1.1	7	2400	− 6	0.8	−0.8					
8	2385	− 24	0.5	−1.2	8	2377	− 14	1.2	−0.2					
9	2412	40	−0.3	−0.3	9	2383	39	0.2	−2.0					
10	2481	14	0.4	0.7	10	2479	39	−0.9	0.9					
11	2437	51	1.2	1.3	11	2536	− 31	0.3	1.5					
12	2462	77	−0.5	1.3	12	2561	− 55	0.8	0.3					

Table 3, i. Nezugaseki

Date	L	$\Delta L''$	$\Delta T'$	$\Delta b'$	Date	L	$\Delta L''$	$\Delta T'$	$\Delta b'$	Date	L	$\Delta L''$	$\Delta T'$	$\Delta b'$
1955	mm				1957	mm				1959	mm			
1					1	2167	− 21	−0.9	1.7	1	2093	23	0.3	0.5
2					2	2196	47	0.2	2.0	2	2318	− 37	0.7	5.3
3	2291	− 41	0.8	2.3	3	2132	80	−0.8	−2.1	3	2277	− 31	1.0	2.2
4	2268	− 8	0.6	1.1	4	2228	31	−0.7	−0.2	4	2162	63	1.7	−0.5
5	2155	5	0.4	0.2	5	2137	20	−0.3	−0.7	5	2169	− 17	1.2	0.4
6	2085	9	−0.1	0.6	6	2094	− 18	−0.6	−1.3	6	2056	11	0.4	−1.0
7	1979	9	2.0	1.9	7	1979	− 17	−0.8	−2.7	7	1900	61	0.8	−1.3
8	1944	33	1.5	2.6	8	1983	− 31	−0.4	−1.1	8	1932	− 2	−0.5	−2.9
9	2047	− 23	0.5	1.3	9	2010	− 5	−0.6	−1.2	9	1890	67	1.2	−3.1
10	2122	− 64	−0.2	0.2	10	1986	49	−0.2	−1.5	10				
11	2092	− 22	−1.2	1.4	11	2059	− 14	1.0	1.3	11				
13	2062	− 25	0.0	−0.7	12	2003	25	1.1	−0.3	12				
1956					1958									
1	2103	− 29	0.2	−2.7	1	2068	49	0.6	0.9					
2	2198	− 8	−0.5	−2.7	2	2236	− 9	0.3	0.8					
3	2307	− 58	−0.3	1.1	3	2190	18	0.3	−1.4					
4	2254	− 9	0.3	−0.3	4	2260	− 14	−0.1	−0.6					
5	2186	− 12	0.5	1.4	5	2170	− 26	0.4	−1.0					
6	2075	11	0.6	0.7	6	2051	5	1.0	−1.2					
7	2010	2	−1.2	0.7	7	1963	− 3	0.2	−1.9					
8	1958	− 4	−1.0	−1.6	8	1943	27	−1.2	−0.5					
9	1983	26	0.1	−0.2	9	1929	60	−0.5	−2.3					
10	2048	16	0.3	1.2	10	2054	30	−0.9	1.6					
11	1972	85	0.3	1.5	11	2097	− 16	0.0	3.0					
12	1982	90	−1.0	1.0	12	2070	− 7	0.6	1.9					

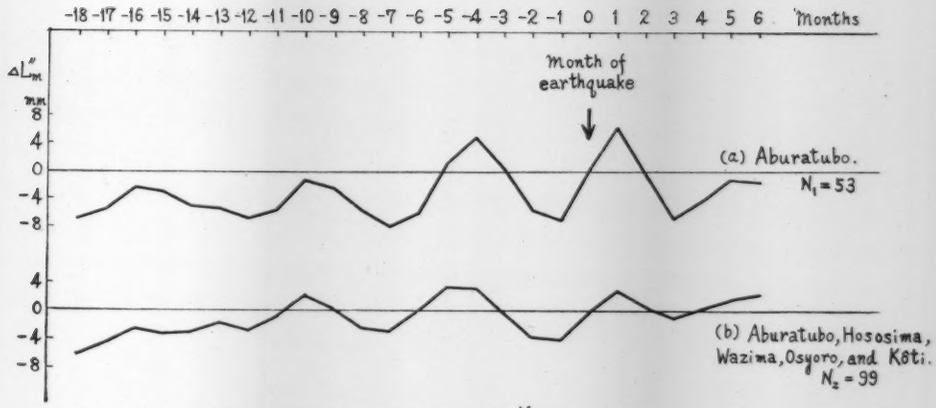

Fig. 2, a, b. The average change of $\Delta L''_m$ for different earthquakes with magnitude M, greater than 7.

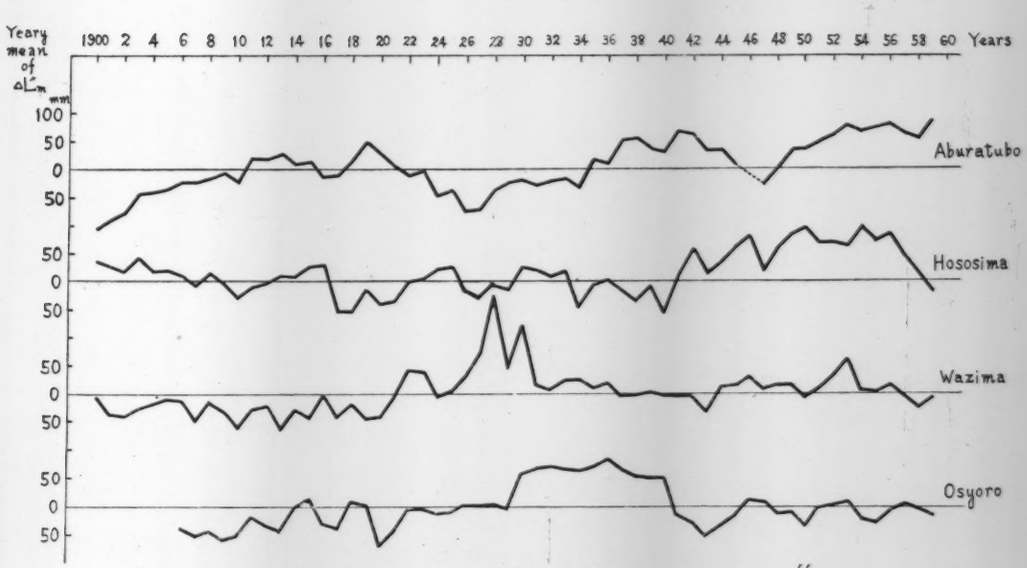

Fig. 3. Yearly mean sea-levels, calculated from $\Delta L''_m$.

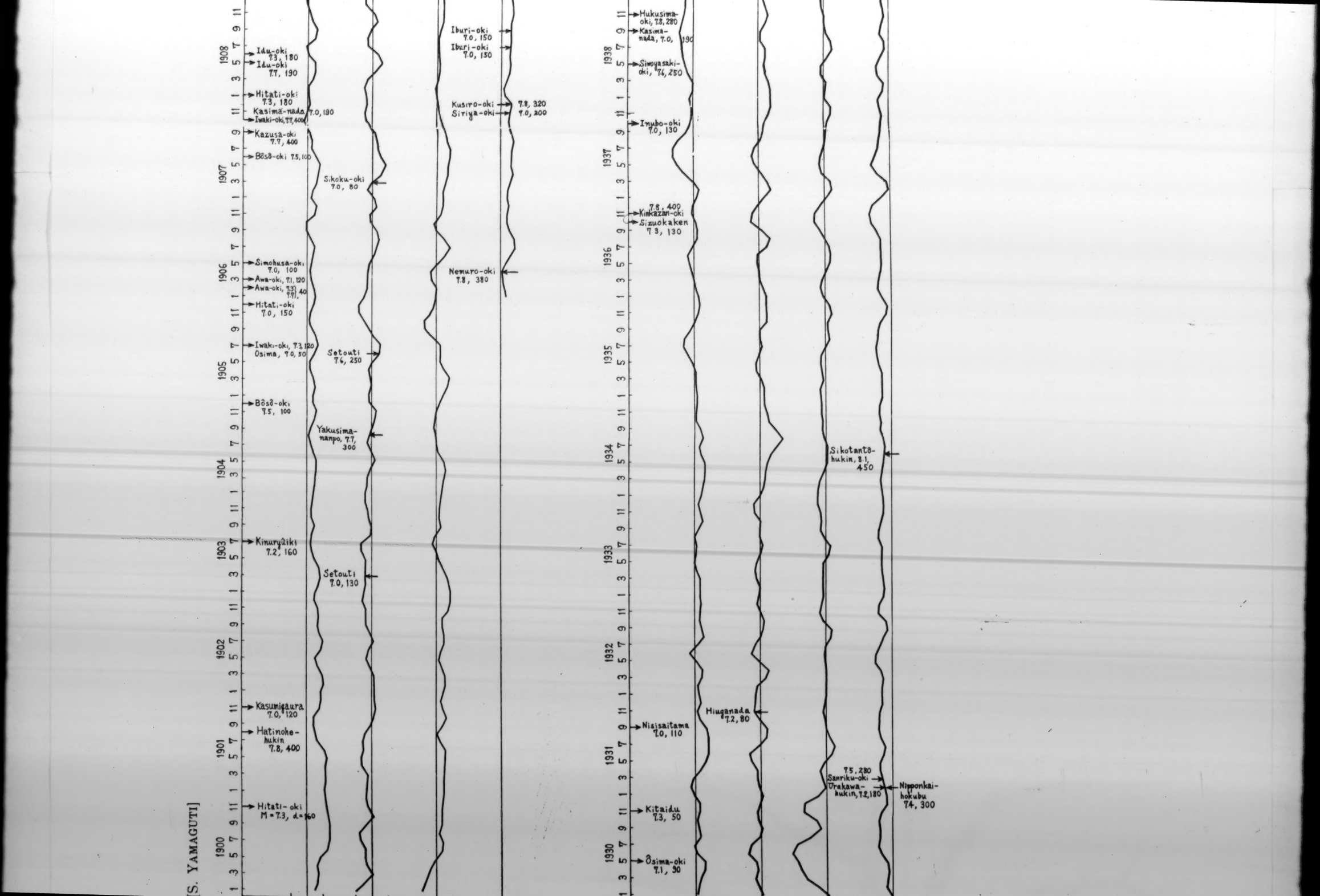
Idu-oki 7.3, 180
Idu-oki 7.7, 190
Hitati-oki 7.3, 180
Kasima-nada 7.0, 190
Iwaki-oki, 7.7, 400
Kazusa-oki 7.7, 400
Bôsô-oki 7.5, 100
Sikoku-oki 7.0, 80
Simohusa-oki 7.0, 100
Awa-oki, 7.1, 120
Awa-oki, 7.3, 7.1, 40
Hitati-oki 7.0, 150
Iwaki-oki, 7.3, 120
Ôsima, 7.0, 30
Setouti 7.6, 250
Bôsô-oki 7.5, 100
Yakusima-nanpo, 7.7, 300
Kinuryûiki 7.2, 160
Setouti 7.0, 130
Kasumigaura 7.0, 120
Hatinohe-hukin 7.8, 400
Hitati-oki M=7.3, d=160
Iburi-oki 7.0, 150
Iburi-oki 7.0, 130
Kusiro-oki 7.8, 320
Siriya-oki 7.0, 200
Nemuro-oki 7.8, 380
Hukusima-oki, 7.8, 280
Kasima-nada, 7.0, 190
Simoyasaki-oki, 7.6, 250
Inubo-oki 7.0, 130
7.8, 400
Kinkazan-oki
Sizuokaken 7.3, 130
Hiuganada 7.2, 80
Nisisaitama 7.0, 110
Kitaidu 7.3, 50
Ôsima-oki 7.1, 90
Sikotantô-hukin, 8.1, 450
7.5, 280
Sanriku-oki
Urakawa-hukin, 7.2, 180
Nipponkai-hokubu 7.4, 300
1900
1901
1902
1903
1904
1905
1906
1907
1908
1930
1931
1932
1933
1934
1935
1936
1937
1938

[S. YAMAGUTI]

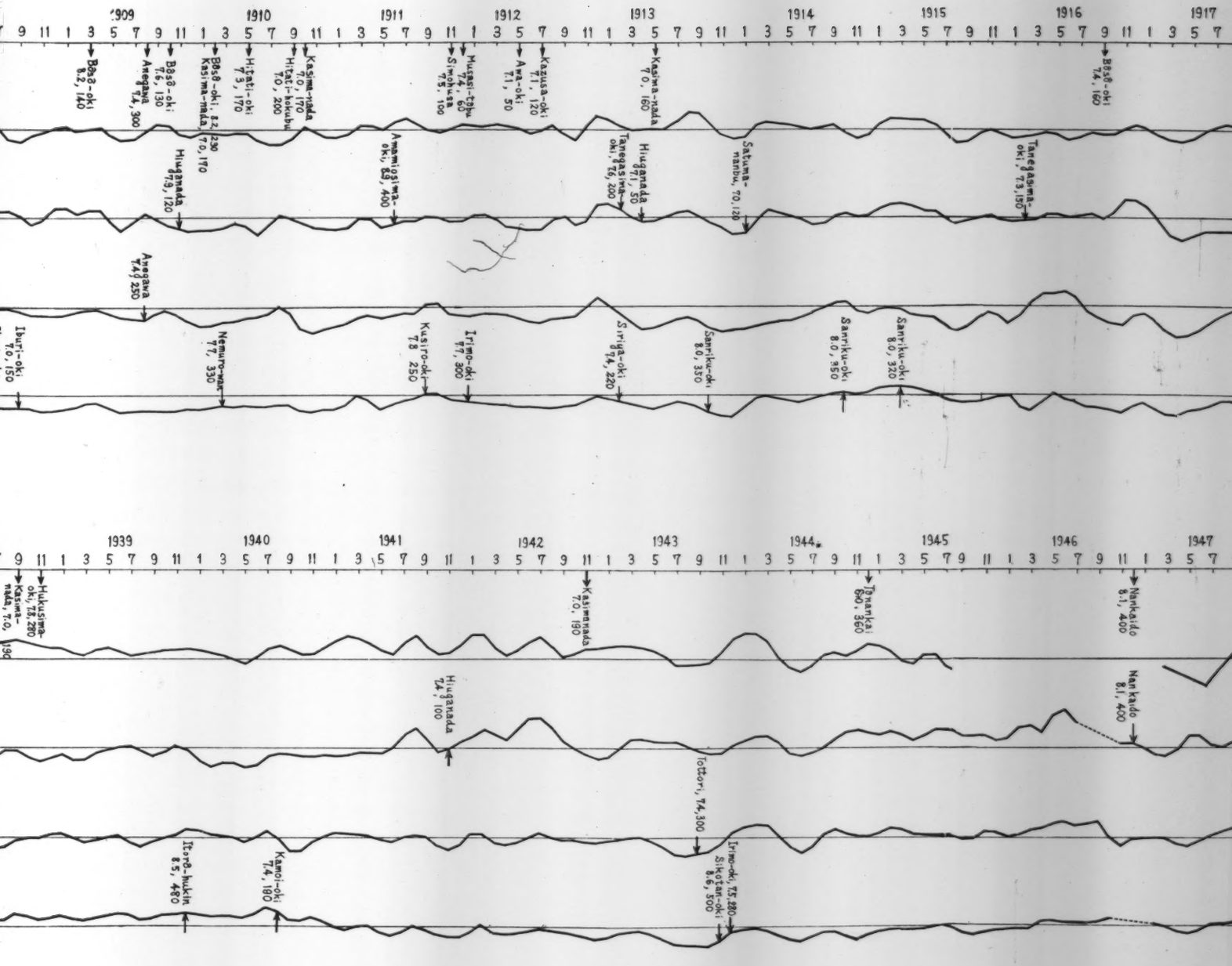

Fig. 1, a. Monthly mean sea-levels, corrected and smoothed. Great earthquak

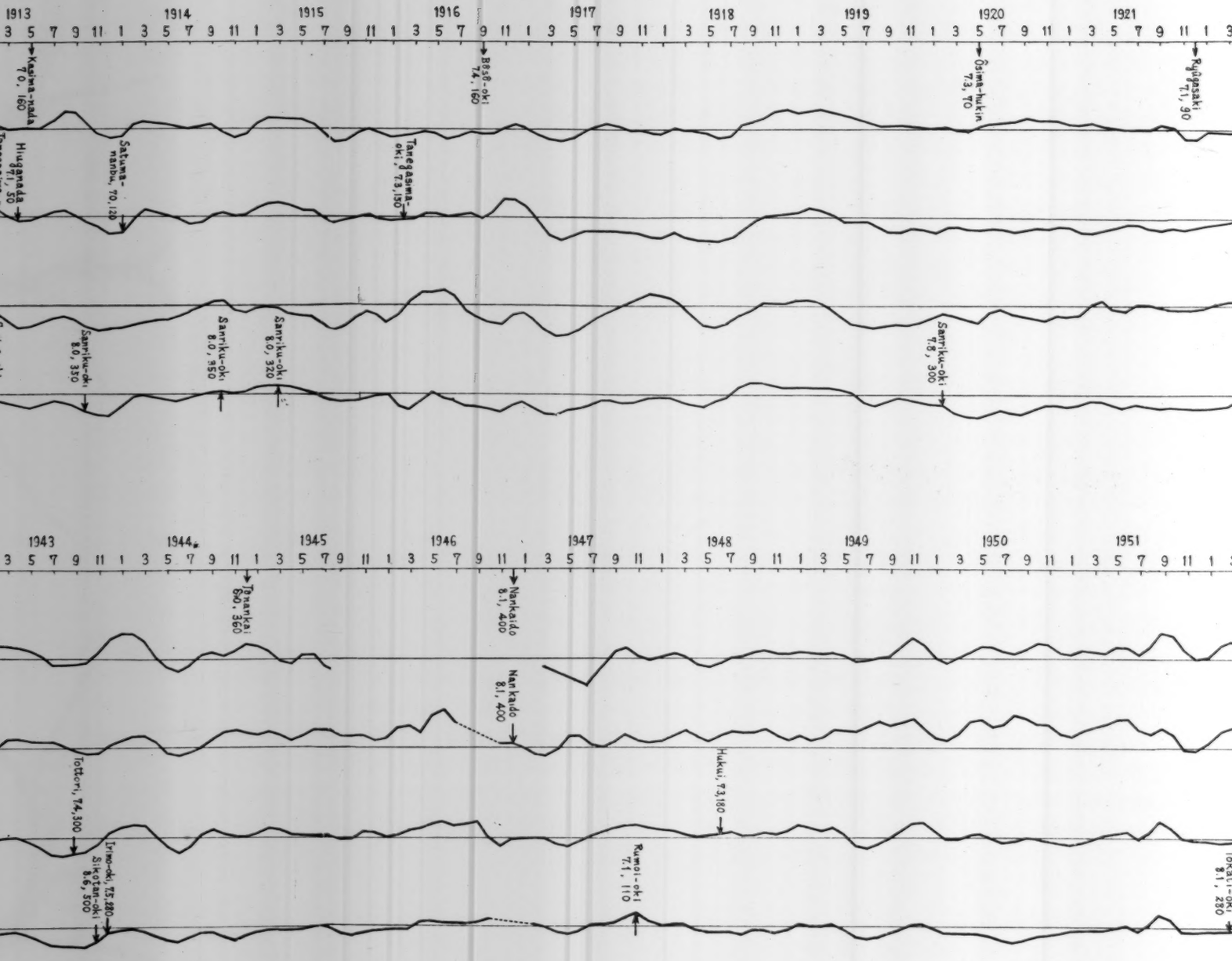

Monthly mean sea-levels, corrected and smoothed. Great earthquakes of magnitude greater than 7 are indicated by arrows.

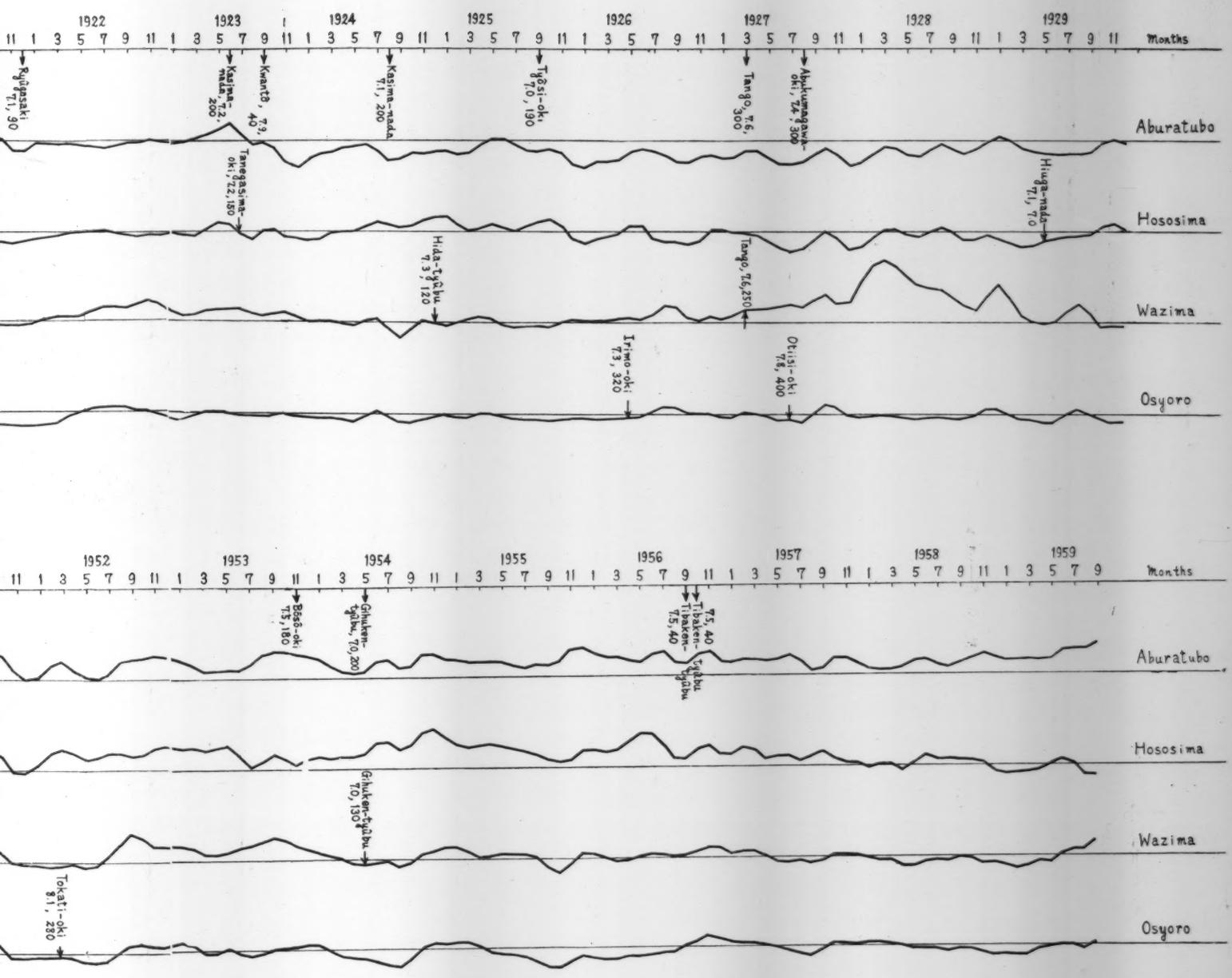
1922
1923
1924
1925
1926
1927
1928
1929
Months
Ryūgasaki 7.1, 90
Kasima-nada, 7.2, 200
Kwantō, 7.9, 40
Kasima-nada 7.1, 200
Tyōsi-oki 7.0, 190
Tango, 7.6, 300
Abukumagawa-oki, 7.4, 300
Aburatubo
Tanegasima-oki, 7.2, 150
Hiuga-nada 7.1, 7.0
Hososima
Hida-tyūbu 7.3, 120
Tango, 7.6, 250
Wazima
Irimo-oki 7.3, 320
Otiisi-oki 7.8, 400
Osyoro
1952
1953
1954
1955
1956
1957
1958
1959
Months
Bōsō-oki 7.5, 180
Gihuken-tyūbu, 7.0, 200
Tibaken-tyūbu 7.5, 40
7.5, 40
Aburatubo
Hososima
Gihuken-tyūbu 7.0, 130
Wazima
Tokati-oki 8.1, 280
Osyoro

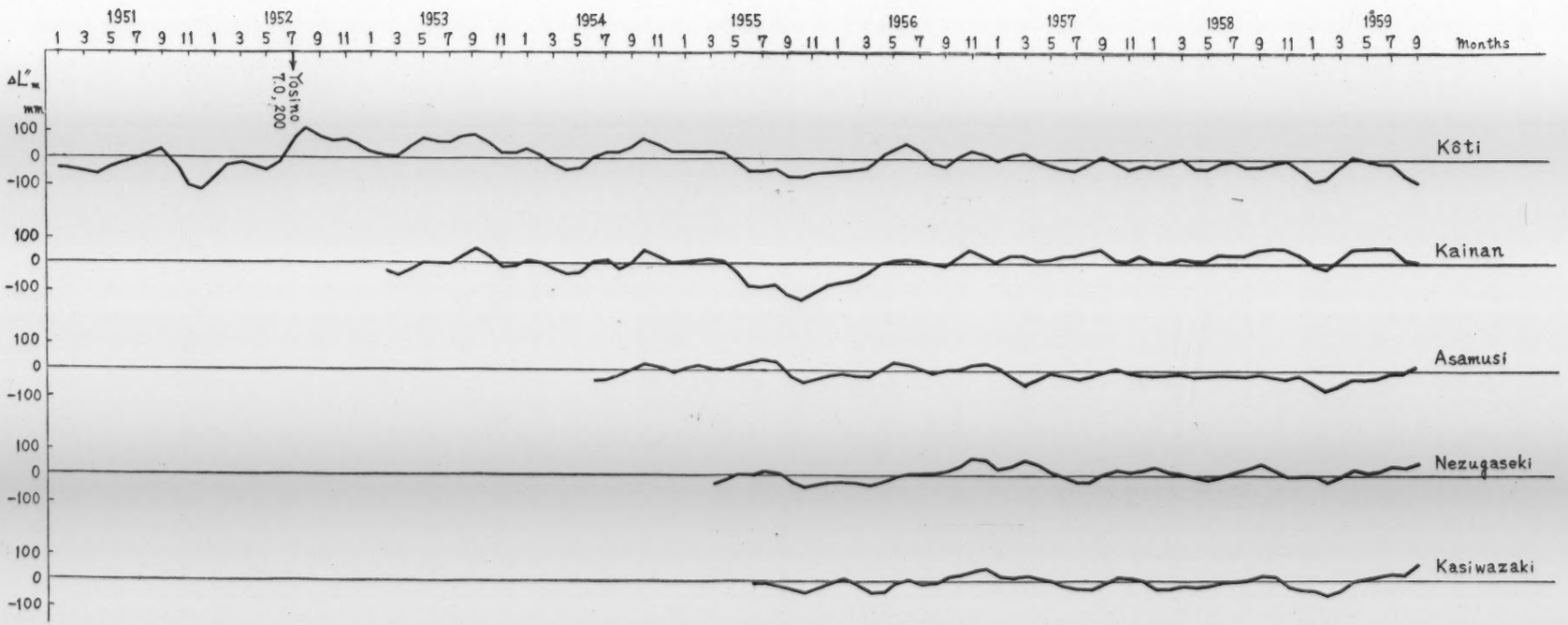

Fig. 1, b. Monthly mean sea-levels, corrected and smoothed. Great earthquakes of magnitude greater than 7 are indicated by arrows.

（震研彙報 第三十八号 図版 山口）

昭和35年3月25日印刷
昭和35年3月30日発行

東京都文京区本富士町一番地
東京大学構内
編纂兼
発行者　東京大学地震研究所

東京都新宿区山吹町一八四番地
印刷者　笠井康頼

東京都新宿区山吹町一八四番地
印刷所　株式会社国際文献印刷社

売捌所
東京都中央区日本橋通二丁目六番地
丸善株式会社

Sold by Maruzen Co., Ltd., Nihonbashi-dôri, Chûô-ku, Tôkyô.
Price of this copy: 531 Yen. (Postage exclusive.)